



UNIVERSITAT
POLITÈCNICA
DE VALÈNCIA

DEPARTMENT OF BIOTECHNOLOGY

Ph.D. Thesis

**Liquid Biopsy in non-small cell lung
cancer: exosomes as a tool for the study
of biomarkers.**

ELENA DURÉNDEZ SÁEZ

Supervisors:

Dr. Carlos Camps Herrero

Dr. Eloísa Jantus Lewintre

Valencia, Enero 2024.



VNIVERSITAT
ED VALÈNCIA

CARLOS CAMPS HERRERO, Dr. por la Universidad de Valencia,
Catedrático del Departamento de Medicina de la Universidad de Valencia y
Jefe del Servicio de Oncología del Hospital General Universitario de Valencia.

CERTIFICA:

Que Dña. Elena Duréndez Saéz, Graduada en Biotecnología, ha
realizado bajo mi dirección la Tesis Doctoral que lleva por título ***“Liquid
Biopsy in non-small cell lung cancer: exosomes as a tool for the study of
biomarkers”***. Dicha tesis reúne todos los requisitos necesarios para su juicio
y calificación para optar al título de Doctor por la Universidad Politécnica de
Valencia.

En Valencia, 31 de Octubre de 2023

Dr. Carlos Camps Herrero

D.N.I.: 22517012N



FUNDACIÓ
INVESTIGACIÓ
HOSPITAL GENERAL
UNIVERSITARI
VALÈNCIA



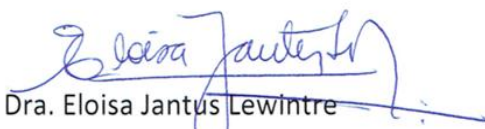
UNIVERSITAT
POLITÈCNICA
DE VALÈNCIA

ELOISA JANTUS LEWINTRE, Dra. por la Universidad de Valencia, Jefa del Laboratorio de Oncología Molecular de la Fundación del Hospital General Universitario de Valencia y Profesora Titular del Departamento de Biotecnología de la Universidad Politécnica de Valencia.

CERTIFICA:

Que Dña. Elena Duréndez Saéz, Graduada en Biotecnología, ha realizado bajo mi dirección la Tesis Doctoral que lleva por título ***“Liquid Biopsy in non-small cell lung cancer: exosomes as a tool for the study of biomarkers”***. Dicha tesis reúne todos los requisitos necesarios para su juicio y calificación para optar al título de Doctor por la Universidad Politécnica de Valencia.

En Valencia, 31 de Octubre de 2023.


Dra. Eloisa Jantus Lewintre
D.N.I: 24474835Y

«La ciencia no sabe de países, porque el conocimiento le pertenece a la humanidad y es la antorcha que ilumina al mundo. La ciencia es el alma de la prosperidad de las naciones y la fuente de todo progreso».

Louis Pasteur

AGRADECIMIENTOS

Quiero empezar este apartado dando las gracias a los pacientes y a sus familiares, que con gran valentía y generosidad cedieron sus muestras haciendo posible que la investigación avance y que el sol pueda brillar a pesar de la tormenta. También dar las gracias a la Asociación Española contra el Cáncer (AECC Valencia), que apostó por nuestras capacidades y me brindó la oportunidad de llevar a cabo esta formación predoctoral.

A mis directores, el Dr. Carlos Camps y la Dra. Eloisa Jantus, por hacer posible este proyecto. Carlos, gracias por haberme dado la oportunidad de entrar en un grupo como el tuyo. Me acogiste desde el primer momento y siempre has tenido para mí buenas palabras y gestos. He aprendido mucho de tu sabiduría y tu calidad humana, solo espero que este no sea el fin de tantos éxitos a tu lado. Nunca podré agradecerte lo suficiente todo tu apoyo durante estos años.

Eloisa, eres un ejemplo para las mujeres que buscan alcanzar el éxito en este duro y caótico mundo llamado ciencia. Como docente, debo decir que eres una de esas personas que hipnotiza a quien te escucha. Tu forma de explicar las cosas de manera clara, concisa y didáctica hace que lo difícil parezca fácil.

A la Dra. Silvia Calabuig, una grandísima profesional y mejor persona. Creo que nunca te he agradecido lo suficiente todo lo que has hecho por mí durante mi etapa predoctoral, has sido mi roca. He aprendido mucho de ti, has sido mi impulso para mejorar y, aunque a veces te dieran ganas de mandarme a paseo, siempre has estado ahí para todo. Gracias por tanto cariño y apoyo, soy afortunada de seguir teniéndote en mi vida tras este largo camino.

Marais, Susana, Andrea, no se qué hubiese sido de mí sin vosotras. Quiero seguir celebrando juntas cada cumpleaños, cada amigo invisible, cada derrota y cada victoria. Sois maravillosas en todos los sentidos. Parte de este trabajo también es vuestro. Gracias por estar siempre a mi lado, no me faltéis nunca.

A todos los que fueron o son miembros del laboratorio de Oncología Molecular FIHGUV, gracias por tan buenos momentos. Sandra, Eva, Macarena, Alejandro, Ester, Borja, Mari Luz... durante años hemos compartido mucho, nos hemos ayudado y apoyado y nuestros momentos de risas han hecho que todo fuese más fácil de afrontar.

Y por supuesto, al Dr. Rafael Sirera, por su disponibilidad, ayuda y consejo siempre que lo he necesitado, gracias.

Franklin y Héctor, mis chicos favoritos, mis hermanos de otra madre, por muchos años más que sigamos compartiendo aventuras. Bruno, Clara, Sara, nunca olvidaré estos años a vuestro lado. Soy feliz de haber estado rodeada de tan grandes personas durante esta etapa.

También quiero dar las gracias a los Drs. Jesús Paramio, Cristian Suárez, Julián Carretero, Eva Serna y Carolina Martínez-Ciarpaglini por su contribución a este trabajo, además de su amabilidad y ganas de ayudar en todo momento.

Estaré siempre agradecida al Profesor Christian Rolfo, por permitirme formar parte de su equipo durante mi estancia de investigación. Tú fuiste hogar para todos nosotros el tiempo que estuvimos fuera de casa. Solo hay una cosa capaz de superar tu larga trayectoria profesional, y es tu generosidad. Conocer a alguien con una mente y un corazón tan brillante es un auténtico privilegio.

A mi Pablito Reclusa, el mejor compañero de piso y guía turístico que alguien pueda imaginar. Gracias por coger un vuelo siempre que te he necesitado.

También quiero dar las gracias a mi equipo actual, al que tan afortunada me siento de pertenecer: el grupo de Investigación en Oncología del IIS INCLIVA, liderado por el Dr. Andrés Cervantes. Cuanto he aprendido y sigo aprendiendo de vuestro talento.

Paco, mi gran descubrimiento, ha sido genial trabajar a tu lado durante estos 3 últimos años. No tengo duda de que con tu conocimiento y tu forma de ser llegarás muy lejos, teniendo un grupo propio al que liderar.

Vero, Belén, Manu, Lucía, Blanca, Raquel, Andrea, Alba... gracias Lab 3 por aguantarme cada día. Nuestras risas, escape rooms, meriendas y viajes me han dado mucha vida.

Pepa ha sido un lujo poder tratar de cerca con alguien como tú. Tu vocación, experiencia, dedicación y bondad son admirables, gracias por abrirnos siempre las puertas de tu casa.

Noelia gracias por haberme dado la oportunidad de entrar en este gran grupo, me quedo con todos los buenos momentos que hemos vivido juntos.

Brenda me alegro mucho de haberte conocido, no pierdas nunca esa fuerza, sonrisa y amabilidad.

A todas las chicas del Lab 2, las mejores vecinas que uno puede tener. En especial a Iris, Anna y Sandra, gracias por vuestra ayuda, consejos y las largas charlas de campana. Sois estupendas.

Tampoco puedo pasar sin mencionar a mis "Predocs AECC". Empezamos siendo un grupo de 5 desconocidos, pero os habéis convertido en amigos. Gracias por vuestro apoyo, alegría y quedadas, me habéis aportado mucho.

A mis padrinos, Teresa y Luis, quienes se tomaron muy en serio la tarea que mis padres les otorgaron hace 31 años, porque a día de hoy seguís sin soltarme de la mano. Gracias por tanto. En general a la familia Duréndez y a los Sáez, por cuidarme y quererme tanto, sin importar si era la mayor o la más pequeña. A mis abuelos: Rosario, Manolo, Teresa y Evaristo, que son y serán las estrellas de mi universo. Vosotros me enseñasteis que el éxito no va sobre logros profesionales o personales, sino que trata sobre la huella que uno deja en los demás a su paso por este mundo. Os llevo siempre en mi corazón.

A mi otra familia, los Prado Jácome, que me acogieron como a una hija, hermana, sobrina y nieta desde el primer día, gracias por estar siempre y hacerme sentir tan querida.

A mi marido Ronny, quiero darle las gracias por celebrar mis logros, pero también por secar mis lágrimas, porque esta etapa no ha estado exenta de ninguno de estos dos elementos. El sacrificio que ha conllevado esta tesis también ha sido tuyo. Gracias por demostrarme cada día ese amor, respeto y orgullo, que te aseguro es mutuo. Quiero seguir luchando a tu lado por una vida llena de sueños cumplidos.

Por último, pero primerísimos en mi vida, quiero dedicar este trabajo a mi núcleo inquebrantable, mi red de seguridad, a mis padres Elena y Evaristo. Gracias de corazón por estar a mi lado a cada paso del camino, con paciencia, amor y apoyo incondicional. Vosotros me habéis enseñado a superarme, a luchar por mis objetivos y a dar siempre lo mejor sin esperar nada a cambio. Espero poder algún día, devolveros todo lo bueno que me habéis dado. Ojalá que os sintáis tan orgullosos de mí como yo lo estoy de ser vuestra hija.

ABSTRACT

Despite recent advancements in lung cancer treatment, its incidence and mortality rates remain high worldwide. Specifically, non-small cell lung cancer (NSCLC) accounts for nearly 85% of all lung cancers, with a 5-year survival rate of 20%. Given this scenario, the primary objective of this study is to comprehensively characterize the exosomes secreted by NSCLC cells. These microvesicles are known to be involved in numerous tumoral processes, potentially containing a wealth of information about the molecular characteristics of the disease.

To achieve this, primary cultures and cell lines, along with peripheral blood samples obtained from NSCLC patients were used. An initial screening in exosomes secreted *in vitro* allowed the identification of a significant number of mRNAs and miRNAs, related to various biological processes and signaling pathways. Moreover, some genes such as *FDFT1* and *SNAI1* stood out due to their overexpression in exosomes derived from cells grown in tumorspheres formation (3D models), which are enriched in cancer stem cell population. Additionally, markers found within these microvesicles were associated with two of the most common histological subtypes: adenocarcinoma (LUAD) and squamous cell carcinoma (LUSC).

Subsequently, to validate the findings seen in exosomes, the most significant markers were analyzed *in silico* in an NSCLC tissue cohort from the TCGA database. These results revealed an association between the expression of *SNAI1* and patient survival (OS and RFS, $p < 0.05$). Furthermore, *XAGE1B*, *SEPP1*, and *TTF-1* expression (previously identified in exosomes) maintained a significant relationship with the LUAD group, while *CABYR*, *RIOK3*, and *CAPRIN1* remained overexpressed in LUSC patients (Mann-Whitney test, $p < 0.05$). These markers were also analyzed in a cohort of 186 NSCLC patients from the University General Hospital of Valencia. The association of *SNAI1* expression and the survival of early-stage patients (RFS in LUAD patients, $p < 0.05$) was confirmed, as well as the overexpression of *CABYR* and *RIOK3* in LUSC patients, and of *XAGE1B* and *TTF-1* in LUAD.

Furthermore, exosomes present in blood samples of the advanced-stage cohort, allowed the identification of other biomarkers associated with clinically relevant characteristics of the patients. Moreover, exosomal cargo was also used to detect gene mutations related to the clinical management of NSCLC.

In summary, the results obtained in this thesis highlight the potential of exosomes as a source of biomarkers for the study of the different stages of NSCLC development. These microvesicles offer a comprehensive and real-time view of the disease's molecular features and can be obtained repeatedly and in a minimally invasive way.

RESUMEN

A pesar de los nuevos avances en el tratamiento del cáncer de pulmón, su tasa de incidencia y mortalidad siguen en cabeza en todo mundo. Concretamente, el cáncer de pulmón no microcítico (CPNM) representa casi el 85% de todos los cánceres de pulmón, siendo su supervivencia a 5 años muy reducida. En base a dicho escenario, el objetivo principal de este trabajo es el de caracterizar de manera exhaustiva los exosomas secretados por las células del CPNM. Se sabe que estas microvesículas están involucradas en números procesos celulares, por lo que pueden contener gran cantidad de información acerca de las características moleculares del tumor.

Para ello se han empleado cultivos primarios y líneas comerciales crecidas en diferentes condiciones, así como muestras de sangre periférica obtenida de los pacientes con CPNM. Un primer screening llevado a cabo en los exosomas secretados *in vitro*, ha permitido obtener un gran número de mRNAs y miRNAs relacionados con diferentes procesos biológicos y vías de señalización. Además, algunos genes como *FDFT1* y *SNAI1* han destacado por su sobreexpresión en exosomas procedentes de las células crecidas en formación de tumoresferas (modelos 3D), las cuales están enriquecidas en población de células madre tumorales. A su vez, otros marcadores presentes en el interior de estas microvesículas, se han mostrado relacionados con dos de los subtipos histológicos más frecuentes: adenocarcinoma (LUAD) y carcinoma escamoso (LUSC).

Posteriormente, para validar los hallazgos obtenidos en exosomas, los marcadores más significativos fueron analizados *in silico* en una cohorte de muestras de tejido, compuesta por 661 pacientes con CPNM (TCGA database). Estos resultados han revelado una asociación entre la expresión del gen *SNAI1* y la supervivencia de estos pacientes (OS y RFS $p < 0.05$). Además, los genes *XAGE1B*, *SEPP1* y *TTF-1* (previamente determinados en exosomas), mantienen una relación significativa con el grupo de pacientes LUAD; mientras que *CABYR*, *RIOK3* y *CAPRIN1* se mantienen sobreexpresados

en LUSC (Mann-Whitney test $p < 0.05$). Estos marcadores también se han analizado en una cohorte de 186 pacientes con CPNM procedentes del Hospital General Universitario de Valencia, donde se corroboró la asociación de *SNAI1* con la supervivencia de los pacientes en estadios tempranos (RFS en pacientes LUAD, $p < 0.05$), así como la sobreexpresión de *CABYR* y *RIOK3* en pacientes LUSC, y de *XAGE1B* y *TTF-1* en LUAD.

Por otra parte, el aislamiento de los exosomas presentes en la sangre periférica de pacientes en estadios avanzados, ha permitido identificar otros marcadores asociados a características clínico-patológicas relevantes. A su vez, el contenido de estas microvesículas ha sido empleado para la detección de mutaciones génicas ligadas al manejo clínico del CPNM.

En resumen, los resultados obtenidos en este trabajo ponen de manifiesto el potencial de los exosomas como fuente de biomarcadores para el estudio de las diferentes etapas de desarrollo del CPNM. Estas microvesículas ofrecen una visión completa y en tiempo real, de las características de la enfermedad, pudiendo ser aisladas de forma repetida y mediante técnicas mínimamente invasivas.

RESUM

A pesar dels avanços recents en el tractament del càncer de pulmó, les seues taxes d'incidència i mortalitat continuen sent altes a nivell mundial. Concretament, el càncer de pulmó de cèl·lules no petites (CPNM) representa gairebé el 85% de tots els càncers de pulmó, amb una taxa de supervivència a 5 anys molt limitada. Donat aquest escenari, l'objectiu principal d'aquest estudi és caracteritzar de manera exhaustiva els exosomes secretats per les cèl·lules de CPNM. Aquestes microvesícules estan involucrades en nombrosos processos tumorals i poden contenir una gran quantitat d'informació sobre les característiques moleculars de la malaltia.

Per aconseguir-ho, es van utilitzar cultius primaris i línies cel·lulars (cultiu en diferents condicions), juntament amb mostres de sang perifèrica obtingudes de pacients amb CPNM. Un cribratge inicial en exosomes secrets *in vitro* va permetre identificar una quantitat significativa de mARNs i miARNs relacionats amb diversos processos biològics i vies de senyalització. A més, alguns gens com *FDFT1* i *SNAI1* van destacar per la seua sobreexpressió en exosomes derivats de cèl·lules creixuts en formació de tumorsferes (models 3D), que estan enriquides en poblacions de cèl·lules mare tumorals. A més, s'han trobat marcadors en aquestes microvesícules associats amb dos dels subtipus histològics més comuns: adenocarcinoma (LUAD) i carcinoma escamós (LUSC).

Posteriorment, per validar els resultats obtinguts en exosomes, es van analitzar *in silico* els marcadors més significatius en una cohort de teixit de CPNM de la base de dades TCGA. Aquests resultats van revelar una associació entre l'expressió del gen *SNAI1* i la supervivència dels pacients (OS i RFS, $p < 0,05$). A més, l'expressió dels gens *XAGE1B*, *SEPP1* i *TTF-1* (prèviament identificats en exosomes) va mantenir una relació significativa amb el grup LUAD, mentre que *CABYR*, *RIOK3* i *CAPRN1* van continuar sobreexpressats en els pacients de LUSC (prova de Mann-Whitney, $p < 0,05$). Aquests marcadors també es van analitzar en una cohort de 186 pacients amb CPNM de l'Hospital General Universitari de València, on es va confirmar l'associació de l'expressió de *SNAI1* i la supervivència dels pacients en estadi

precoç (RFS en pacients de LUAD, $p < 0,05$), així com la sobreexpressió de *CABYR* i *RIOK3* en pacients de LUSC, i de *XAGE1B* i *TTF-1* en LUAD.

D'altra banda, els exosomes presents en mostres de sang de la cohort d'estadis avançats van permetre la identificació d'altres biomarcadors associats a característiques clíniques rellevants dels pacients. A més, la càrrega exosomàtica també es va utilitzar per detectar mutacions genètiques relacionades amb el tractament clínic del CPNM.

En resum, els resultats obtinguts en aquesta tesi destaquen el potencial dels exosomes com a font de biomarcadors per a l'estudi de les diferents etapes del desenvolupament del CPNM. Aquestes microvesícules ofereixen una visió completa i en temps real de les característiques moleculars de la malaltia i poden ser obtingudes de manera repetida i amb una mínima invasió.

TABLE OF CONTENTS

LIST OF ABBREVIATIONS AND ACRONYMS.....	XXII
LIST OF FIGURES	XXIX
LIST OF TABLES	XXXIII
I. INTRODUCTION	1
1. CANCER.....	3
1.1. CONCEPT.....	3
1.2. MOLECULAR FEATURES OF CANCER CELLS	3
1.3. EPIDEMIOLOGY	5
2. LUNG CANCER.....	7
2.1. EPIDEMIOLOGY AND RISK FACTORS	7
2.2. PHYSIOLOGY OF THE LUNG	11
2.3. DIAGNOSIS, STAGING AND PROGNOSIS	12
2.3.1. DIAGNOSIS	12
2.3.2. STAGING AND PROGNOSIS	14
2.4. HISTOPATHOLOGICAL CLASSIFICATION	17
2.4.1. SMALL CELL LUNG CANCER (SCLC).....	18
2.4.2. NON-SMALL CELL LUNG CANCER (NSCLC).....	19
2.4.2.1. Lung adenocarcinoma - LUAD	19
2.4.2.2. Lung squamous cell carcinoma - LUSC	20
2.4.2.3. Large cell carcinoma - LCC	22
2.4.3. NEUROENDOCRINE TUMORS (NETS)	22

2.5. MOLECULAR CLASSIFICATION OF LUNG CANCER.....	23
2.5.1. MOLECULAR CLASSIFICATION OF SCLC	24
2.5.2. MOLECULAR CLASSIFICATION OF NSCLC.....	24
2.5.2.1. LUAD genomic alterations	25
2.5.2.2. LUSC genomic alterations.....	26
2.5.2.3. Alterations common to both NSCLC subtypes ...	27
2.6. NSCLC TREATMENT	28
3. CELLULAR CLONALITY AND TUMOR HETEROGENEITY	31
3.1. MODELS OF TUMOR HETEROGENEITY.....	31
3.2. CSC PROPERTIES AND TUMOR MICROENVIRONMENT.....	33
3.3. 3D <i>IN VITRO</i> MODELS	34
4. LIQUID BIOPSY	38
4.1. EXTRACELLULAR VESICLES.....	40
4.1.1. GENERAL FEATURES, CLASSIFICATION AND NOMENCLATURE	40
4.1.1.1. Exosomes	41
4.1.2. BIOGENESIS AND SECRETION	42
4.1.3. EXOSOMES CARGO	45
4.2. EXOSOMES IN CANCER.....	48
4.2.1. EXOSOMES AS A REGULATORS OF TME	50
4.2.1.1. Exosomes role in tumor angiogenesis.....	52
4.2.2. EXOSOMES IN METASTATIC NICHES	53

4.2.3. EXOSOMES IN TUMOR PROLIFERATION AND CHEMORESISTANCE	55
4.3. NSCLC-DERIVED EXOSOMES	57

II. OBJECTIVES AND HYPOTHESIS61

III. MATERIALS & METHODS65

1. MATERIALS 67

1.1 RECRUITED PATIENTS..... 67

1.1.1. TISSUE SAMPLES 67

1.1.2. BLOOD SAMPLES 68

1.2 ESTABLISHMENT OF PRIMARY CELL CULTURES..... 68

1.3 COMMERCIAL NSCLC CELL LINES 69

2. METHODS 71

2.1 CELL CULTURE GROWTH CONDITIONS 71

2.2 EXOSOMES CHARACTERIZATION 71

2.2.1. EXOSOME ISOLATION FROM CELL CULTURES 71

2.2.2. EXOSOMES ISOLATION FROM PLASMA SAMPLES 72

2.2.3. NANOPARTICLE TRACKING ANALYSIS (NTA)..... 73

2.2.4. NEGATIVE-STAINING AND TRANSMISSION ELECTRON MICROSCOPY OF EXOSOMES 74

2.2.5. IMMUNOBLOTTING 75

2.2.6. FLOW CYTOMETRY ANALYSIS 76

2.3. NUCLEIC ACIDS ISOLATION.....	77
2.3.1. RNA ISOLATION AND INTEGRITY.....	77
2.3.1.1. Exosomes from cell cultures.....	77
2.3.1.2. Exosomes from plasma.....	77
2.3.1.3. Fresh tissue from NSCLC cohort.....	78
2.3.2 DNA ISOLATION FROM CELL CULTURES/PLASMA-DERIVED EXOSOMES.....	78
2.4. DETERMINATION OF THE MUTATIONAL STATUS.....	79
2.4.1 EXOSOMAL MUTATIONAL STATUS FROM ESTABLISHED NSCLC CULTURES.....	79
2.4.1.1. Mutational status determination by BEAMing digital PCR.....	79
2.4.1.2. Detection of ALK rearrangements by RT-qPCR...	80
2.4.2 EXOSOMAL MUTATIONAL STATUS FROM BLOOD SAMPLES OF NSCLC PATIENTS.....	80
2.5. GENE EXPRESSION ANALYSIS.....	82
2.5.1. WHOLE MRNA EXPRESSION PROFILING OF EXOSOMES DERIVED FROM CELL CULTURES.....	82
2.5.2. DEGS VALIDATION USING RT-QPCR.....	84
2.5.3. GENE EXPRESSION PANEL IN PLASMA-DERIVED EXOSOMES.....	86
2.5.3.1 Data Normalization and Analysis.....	88
2.6. IMMUNOFLUORESCENCE ANALYSIS.....	89
2.7. IMMUNOHISTOCHEMICAL ANALYSIS.....	89
2.8. IN SILICO DATASET VALIDATION.....	90

2.9. STATISTICAL ANALYSIS	91
2.10. OTHER STATISTICAL METHODS.....	91

IV. RESULTS AND DISCUSSION.....93

CHAPTER 1: CELL CULTURES 95

1.1. CHARACTERIZATION OF EXOSOMES DERIVED FROM NSCLC CELL CULTURES	95
1.2. MUTATIONAL STATUS OF EXOSOMES DERIVED FROM CELL CULTURES	107
1.3. DIFFERENTIAL EXPRESSION PROFILES OF TUMOR CELL CULTURES-DERIVED EXOSOMES	108
1.3.1. DEGS IN EXOSOMES FROM 2D VS 3D MODELS	109
1.3.1.1. Differential expressed miRNAs in exosomes from 2D vs 3D	113
1.3.2. DEGS IN EXOSOMES FROM LUAD and LUSC.....	115
1.3.2.1. Differential expressed miRNAs in exosomes from LUAD and LUSC.....	120
1.3.3. DEGS IN EXOSOMES FROM CELL LINES VS PRIMARY CULTURES.....	126
1.4. DEGs VALIDATION IN TUMOR CELL CULTURES-DERIVED EXOSOMES	128
1.4.1. DEGs VALIDATION IN EXOSOMES FROM 3D vs 2D CULTURES.....	128
1.4.2. DEGs VALIDATION IN EXOSOMES FROM LUAD AND LUSC CULTURES	133

1.5. IN-SILICO VALIDATION OF EXOSOMAL BIOMARKERS IN NSCLC	142
1.6. VALIDATION OF EXOSOMAL BIOMARKERS IN A RESECTED NSCLC COHORT.....	146
CHAPTER 2: PLASMA	155
2.1. CHARACTERIZATION OF EXOSOMES DERIVED FROM NSCLC PLASMATIC SAMPLES.....	155
2.2. MUTATIONAL STATUS DETERMINATION THROUGH LIQUID BIOPSY ELEMENTS	158
2.3. ANALYSIS OF PLASMA EXO-mRNA FOR BIOMARKERS DETECTION	166
V. INTEGRATION OF RESULTS	179
VI. CONCLUSIONS	187
VII. REFERENCES	191
VIII. ANNEXES	229
A. SUPPLEMENTARY MATHERIAL	231
B. FUNDING	240
C. COMMUNICATIONS TO NATIONAL AND INTERNATIONAL CONFERENCES	240

D. AWARDS.....	243
E. PUBLICATIONS DURING THE DOCTORAL THESIS	244
F. APPROVAL FROM THE INSTITUTIONAL ETHICAL AND SCIENTIFIC REVIEW BOARD.	246
G. INFORMED CONSENT DOCUMENT.....	249

LIST OF ABBREVIATIONS AND ACRONYMS

2D: two-dimensional

3D: three-dimensional

95%CI: 95% confidence interval

ABC: avidin-biotin-peroxidase complexes

AC: atypical carcinoid

ADC: adenocarcinoma

AIS: adenocarcinoma in situ

AKT1: v-akt murine thymoma viral oncogene homolog 1

Alix: ALG-2 interacting protein

ALIX: ALG-2-interacting protein X

ALK: anaplastic lymphoma kinase

Amp: amplification

ANOVA: analysis of variance

APC: allophycocyanin

ARID1A: AT-rich interactive domain 1A

ATCC: american type culture collection

BAC: bronchoalveolar carcinoma

BEAMING: beads, emulsions, amplification, and magnetics

bFGF: basic fibroblast growth factor

BRAF: v-raf murine sarcoma viral oncogene homolog B1

BSA: bovine serum albumin

CABYR: calcium binding tyrosine phosphorylation regulated

CAF: cancer associated fibroblast
CAPRN1: cytoplasmic activation/proliferation-associated protein-1
CCD: charge-coupled device
CDKN2A: cyclin-dependent kinase inhibitor 2A
cfDNA: cell-free DNA
CI: confidence interval
ctDNA: circulant tumor-DNA
CIOMS: biomedical research involving human subjects
CTA: cancer testis antigens
CSC: cancer stem cells
CS-LC: cells similar to cancer cells
CT: computed tomography
CTC: circulant tumor cell
ctDNA: circulating tumor DNA
CTLA-4: cytotoxic T-lymphocyte associated protein 4
DDR2: discoidin domain receptor tyrosine kinase 2
DE: differential expression
DEG: differential expressed genes
DEL: deletion
DFS: disease-free survival
dPCR: digital PCR
EBUS: endobronchial ultrasound
EDTA: ethylenediaminetetraacetic acid
EGF: epidermal growth factor

EGFR: epidermal growth factor receptor
EML4: echinoderm microtubule-associated protein-like 4
ESCRT: endosomal sorting complex required for transport
EUS: endoscopic ultrasound
EV: extracellular vesicle
FasL: fas ligand
FBS: fetal bovine serum
FC: flow cytometry
FC: fold change
FDA: food and drug administration
FDFT1: farnesyl-diphosphate farnesyltransferase 1
FFPE: formalin-fixed paraffin-embedded
FGFR1: fibroblast growth factor receptor 1
FSC: forward scatter
GEO: gene expression omnibus
GM: gangliosides
GO: gene ontology
GOBP: gene ontology biological process
H&E: hematoxylin and eosin
HCUV: hospital clínico universitario de Valencia
HER2: human epidermal growth factor receptor 2
HGUV: hospital general universitario de Valencia
IB: immunoblot
IF: immunofluorescence

IHC: immunohistochemistry
ILV: intraluminal vesicle
IMA: invasive mucinous adenocarcinoma
JSI: jaccard similarity index
KEAP1: kelch-like ECH-associated protein 1
KRAS: kirsten rat sarcoma viral oncogene homolog
LCC: large cell carcinoma
LCINS: lung cancer in never smokers
LCNEC: large-cell neuroendocrine carcinoma
lincRNA: long intergenic RNA
lncRNA: long non-coding RNA
LUAD: lung adenocarcinoma
LUSC: lung squamous cell carcinoma
MAP2K1/ MEK1: mitogen-activated protein kinase kinase 1
MB: mutant beads
MET: mesenchymal epithelial transition factor proto-oncogene
MF: mutant fraction
mi: minimally invasive carcinoma
MICA: MHC class I chain related-protein A
miRNA: micro RNA
ML: milliliters
MRI: magnetic resonance imaging
mRNA: messenger RNA
MUT: mutation

MVB: multivesicular body
MYC: myelocytomatosis oncogene
NCAM1: neural cell adhesion molecule 1
NCBI: national center for biotechnology information
NET: neuroendocrine tumor
NF1: neurofibromin 1
NGS: next generation sequencing
NRF2: nuclear factor erythroid 2-related factor 2
NRG1: neuregulin 1
NSCLC: non-small cell lung cancer
NTA: nanoparticle tracking analysis
NTRK1: neurotrophic tyrosine kinase receptor type 1
OS: overall survival
PBS: phosphate-buffered saline
PC: phosphatidylcholine
PCA: principal component analysis
PD-1: programmed cell death protein 1
PDGFRA: platelet derived growth factor receptor alpha
PD-L1: programmed death-ligand 1
PDX: patient-derived xenograft
PE: phosphatidylethanolamine
PE: phycoerythrin
PET-CT: positron-emission tomography with computed tomography
PI: phosphatidylinostol

PIK3CA: phosphatidylinositol-4,5-bisphosphate 3-kinase, catalytic subunit alpha

PS: performance status

PS: phosphatidylserine

PVDF: polyvinylidene difluoride

RB1: retinoblastoma 1

RFA: radiofrequency ablation

RIOK3: RIO kinase 3

RMA: robust multiple-array average

ROS1: reactive oxygen species proto-oncogene 1

RT: room temperature

RT-qPCR: reverse transcription quantitative real-time PCR

SBRT: stereotactic body radiotherapy

SCLC: small cell lung cancer

SD: standard deviation

SDS: sodium dodecyl sulfate

SEM: standard error of the mean

SEPP1: selenoprotein P plasma 1

SMARCA4: SWI/SNF related matrix associated, actin-dependent regulator of chromatin, subfamily A, member 4

SNPs: single nucleotide polymorphisms

SOX2: SRY-box transcription Factor 2

SqCC: squamous cell carcinoma

SQS: squalene synthase

SS: superficial spreading tumor.

SSC: side scatter

STK11: serine/threonine kinase 11

TC: typical carcinoid

TCGA: the cancer genome atlas program

TEM: tetraspanin-enriched microdomain

TEP: tumor educated platelet

TFR: transferrin receptor

TGF: transforming growth factor

TNF: tumor necrosis factor

TRAIL: TNF-related apoptosis-inducing ligand

TSG101: tumor susceptibility gene 101

TTF-1: transcription termination factor 1

WHO: world health organization

WNT5A: wntless-type MMTV integration site family, member 5A

WT: wild type

XAGE1: x antigen family member 1

XPD: xeroderma pigmentosum group D

LIST OF FIGURES

Figure 1. The hallmarks of cancer.

Figure 2. Most commonly diagnosed tumours worldwide.

Figure 3. Top cancer sites per country associated with estimated number of deaths in both sexes (all ages, excluding non-melanoma skin cancer).

Figure 4. Physiological anatomy of the respiratory system.

Figure 5. Reference diagram representing the 8th edition of TNM staging classification of lung cancer.

Figure 6. Cytologic and histologic features of SCLC.

Figure 7. Cytologic and histologic features of NSCLC adenocarcinoma.

Figure 8. Cytologic and histologic features of NSCLC squamous cell carcinoma.

Figure 9. Cytologic and histologic features of LCNEC.

Figure 10. Genomic alterations in lung cancer.

Figure 11. Different models of tumor heterogeneity.

Figure 12. Representation of the process of biogenesis and secretion of different extracellular vesicles, including exosomes.

Figure 13. Composition and cargo of exosomes.

Figure 14. Exosomes as a key element in liquid biopsy for cancer study.

Figure 15. Graphic scheme of the methodology used in the isolation of exosomes secreted *in vitro*.

Figure 16. Graphical scheme of the operation of the Nanosight instrument.

Figure 17. BEAMING dPCR operation scheme.

Figure 18. Graphic scheme of the methodology used to carry out the whole genome gene expression microarrays.

Figure 19. Representation of the workflow required for the analysis of plasmatic EV samples using an nCounter panel.

Figure 21. Plots of concentration and size distribution obtained using a NanoSight NS300 instrument in cell cultures-derived exosomes.

Figure 22. Representative transmission electron microscopic images of exosomes isolated from 2D (a) and 3D (b) NSCLC cell cultures.

Figure 23. Immunoblotting analysis for the exosomal surface markers.

Figure 24. Flow cytometry analysis of the surface markers in exosomes isolated from cell cultures.

Figure 25. Flow cytometry controls for validation of signal detection in exosome samples.

Figure 26. *EGFR* and *KRAS* genes mutations analysis by BEAMing technology.

Figure 27. Microarray transcriptomic analysis of exosome cargo from different growth conditions.

Figure 28. miRNAs analysis in exosomes from 2D and 3D cultures.

Figure 29. Transcriptomic microarray analysis of exosomal cargo from histological subtypes comparisons.

Figure 30. Pathological processes enrichment of differentially expressed genes between LUAD and LUSC-derived exosomes.

Figure 31. Transcriptomic microarray analysis of exosomal cargo from primary cell cultures and commercial cell lines.

Figure 32. Validation of *FDFT1* and *SNAI1* expression in tumor-derived exosomes from 2D and 3D cell cultures.

Figure 33. Validation of *WNT5A* expression in tumor-derived exosomes from 2D and 3D cell cultures.

Figure 34. Validation of *XAGE1B* and *CABYR* expression in tumor-derived exosomes from 2D cell cultures.

Figure 35. Analysis of *TTF-1* and *SEPP1* expression in tumor-derived exosomes from 2D cell cultures.

Figure 36. Analysis of *RIOK3* and *CAPRIN1* expression in tumor-derived exosomes from 2D cell cultures.

Figure 37. Validation of *XAGE1B* expression in cell cultures-derived exosomes from both models (2D-monolayer and 3D-tumorspheres).

Figure 38. Immunofluorescent staining of *CABYR* and *XAGE1* in primary cultures.

Figure 39. Prognostic value of *SNAI1* in the TCGA NSCLC cohort.

Figure 40. Mann–Whitney U-test of the histology-related biomarkers in TCGA cohort.

Figure 41. Kaplan–Meier plots for OS according to the relative expression of *SNAI1* in the global HGUV cohort (a) and LUAD group (b).

Figure 42. Mann–Whitney U-test of the histology-related biomarkers in HGUV cohort.

Figure 43. Median of relative expression of *XAGE1B* (a) and *CABYR* (b) in tumor tissue from HGUV NSCLC resected cohort vs. its expression in NAT (normal adjacent tissue) obtained by Mann Whitney test.

Figure 44. Prognostic value of *XAGE1B* in the HGUV NSCLC cohort.

Figure 45. Plot of size distribution obtained using a NanoSight NS300 instrument in plasma-derived exosomes.

Figure 46. Representative TEM images of multiple exosomes isolated from NSCLC plasma samples.

Figure 47. Flow cytometry analysis of the surface markers CD63 and CD81 in exosomes isolated from NSCLC patients' plasma.

Figure 48. Comparison of different methods to detect *EGFR* alterations in a patient with a low mutant fraction.

Figure 49. Comparison of dPCR-3D results on exosomal sample with low mutant fraction isolated from 1ml of plasma (a) and serum (b).

Figure 50. Quantification and integrity of RNA obtained from plasma exosomes by bioanalyzer.

Figure 51. Hierarchical cluster analysis of probes that have amplified within the plasma exosome cohort.

Figure 52. Mann–Whitney U-test of the exosomal biomarkers in plasma cohort.

Figure 53. Kaplan-Meier plot for RFS according to *MICA* expression levels of the LUSC group (TCGA cohort).

Figure 54. Integration of results encompassed in this thesis.

Figure S1. Flow cytometry control serial dilutions for validation of signal detection in exosome samples.

Figure S2. Kaplan-Meier plots for survival according to clinicopathological variables for the TCGA cohort.

Figure S3. Kaplan-Meier plots for survival according to clinicopathological variables for the HGUV cohort.

Figure S4. Mann–Whitney U-test in HGUV cohort. Non-significant p-values for SEPP1 (a) and CAPRIN1 (b).

Figure S5. Prognostic value of CABYR in the HGUV NSCLC cohort.

LIST OF TABLES

Table 1. Summary of descriptors of the TNM Classification System 8th Edition.

Table 2. Clinicopathological characteristics of the patients employed for the primary cell cultures establishment.

Table 3. Main characteristics of the cell lines included in the study.

Table 4. List of antibodies used for immunoblot (IB), immunofluorescence (IF) and flow cytometry (FC) analyses.

Table 5. TaqMan® Assays used in dPCR for mutational status determination.

Table 6. TaqMan® Gene Expression Assays used in RT-qPCR expression analysis.

Table 7. Summary of the probes collected in the nCounter panel for their analysis in the plasmatic exosomal RNA samples.

Table 8. Biological pathway enrichment in 3D (a) vs. 2D exosomes (b).

Table 9. Exosome-derived miRNAs with most increased differential expression between LUAD and LUSC.

Table 10. Clinicopathological characteristics of the patients included in HGUV NSCLC cohort.

Table 11. Mutational analysis in cfDNA and exosomal DNA using different dPCR-based methods.

Table 12. Comparative summary of exosomal DNA features isolated from NSCLC serum and plasma samples.

Table 13. Clinicopathological characteristics of the patients included in NSCLC plasma cohort.

Table S1. The definition of descriptors of the TNM Classification System 8th Edition.

Table S2. Molecular alterations detected in cell cultures-derived exosomes with different histologies.

Table S3. Enrichment of GOBP categories according to the target genes of exo-miRNAs secreted from 2D and 3D cell cultures.

Table S4. Enrichment analysis of pathological processes and its associated pathways based on the number of DEGs overlapped.

Table S5. Clinicopathological characteristics of the patients included in the *in silico* cohort (TCGA database).

Table S6. Results of survival analysis in the TCGA validation cohort, based on the expression of exosomal biomarkers found in plasma cohort.

Table S7. Results of survival analysis in the TCGA validation cohort, based on exosomal expression of CD24 and MICA (previously detected in plasma cohort).

I. INTRODUCTION

1. CANCER

1.1. CONCEPT

The term *cancer* encompasses a broad spectrum of diseases that can affect different types of cells and tissues, all of which share the uncontrolled growth of neoplastic cells [1]. Tumorigenesis is a multi-step process involving dynamic changes in the genome. These changes cause cancer cells to stop carrying out the homeostatic mechanisms that regulate normal and controlled proliferation, giving them a greater capacity for growth and promoting changes at histopathologic and molecular level different from those of normal cells. Cancer cells acquire the ability to migrate from the tissue of origin to other tissues and organs, a process known as metastasis [2].

These newly acquired characteristics confer great complexity to tumors, as cancer cells are able to recruit different cell types (immune cells, tumor stem cells, endothelial cells, and cancer-associated fibroblasts) to serve as active helpers, creating a tumor microenvironment in which proliferation and invasion are favored [1].

1.2. MOLECULAR FEATURES OF CANCER CELLS

Hanahan and Weinberg postulated in 2000 a unifying model that proposed six characteristics or alterations in cell physiology shared by all tumor cell types, essential for the development of cancer (called *Hallmarks*

Introduction

of Cancer). These alterations are defined as functional capacities acquired by tumor cells, through different mechanisms and at different steps during the course of tumorigenesis, which confer a series of evolutionary advantages upon the cells [1].

Eleven years later, the same authors proposed four new properties, thus constituting the 10 distinctive characteristics of cancer that we know today:

1. Unlimited replicative potential
2. Self-sufficiency in growth signals
3. Insensitivity to growth inhibitors
4. Evasion of apoptosis
5. Inducing angiogenesis
6. Capacity for invasion and metastasis
7. Genomic instability and mutations
8. Reprogramming energy metabolism
9. Pro-inflammatory capacity
10. Evasion of the immune system

Furthermore, the authors posit that tumor biology cannot be understood simply by enumerating cancer hallmarks, but must also encompass the contribution of the tumor microenvironment [3].

In this last year, a new review published by Hanahan introduced several prospective new hallmarks and enabling characteristics, which might eventually be integrated as core components of the conceptualization of

Introduction

cancer hallmarks. These parameters are: unlocking phenotypic plasticity, non-mutational epigenetic reprogramming, polymorphic microbiomes and senescent cells (Figure 1) [4].

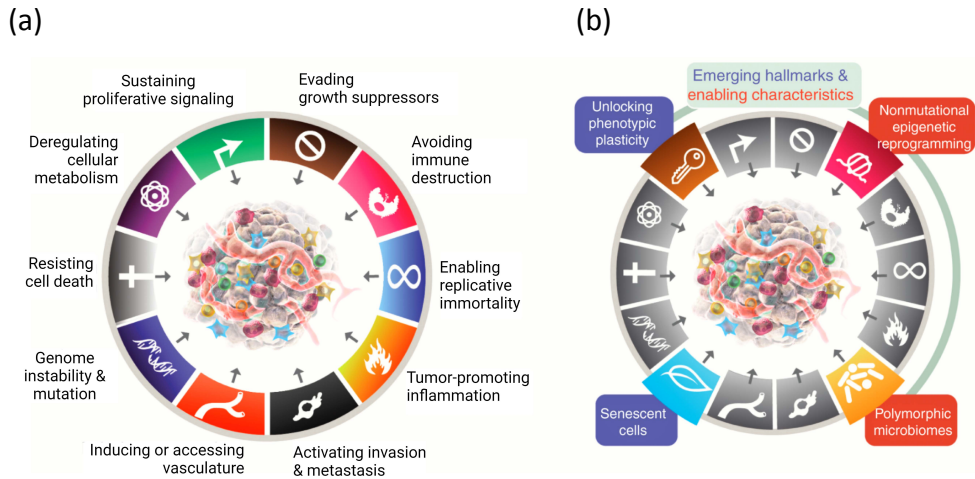


Figure 1. The hallmarks of cancer. This illustration represents the capabilities of cancer cells as proposed by Hanahan and Weinberg in 2011 **(a)**. The hallmarks previously postulated together with the additional proposed emerging hallmarks and enabling characteristics in 2022 **(b)** [4].

1.3. EPIDEMIOLOGY

Cancer remains a leading cause of morbidity and mortality worldwide. The International Agency for Research on Cancer estimates that approximately 18.1 million cancer cases were diagnosed worldwide in 2018. The same agency has estimated that in 2020, approximately 19.3 million new cases will be diagnosed in the world (latest data available worldwide, estimated within the GLOBOCAN project) [5]. However, we know that the COVID-19 pandemic affected the number of cancer diagnoses in many

Introduction

countries, so the actual number of cancers diagnosed in 2020 is likely to have been lower. Global estimates also indicate that the number of new cases will increase over the next two decades, reaching 28.4 million new cases per year in 2040 [5].

The most commonly diagnosed tumors worldwide in 2020 will be those of the lung, breast, colon and rectum, prostate, and stomach, all with more than one million cases (Figure 2) [6].

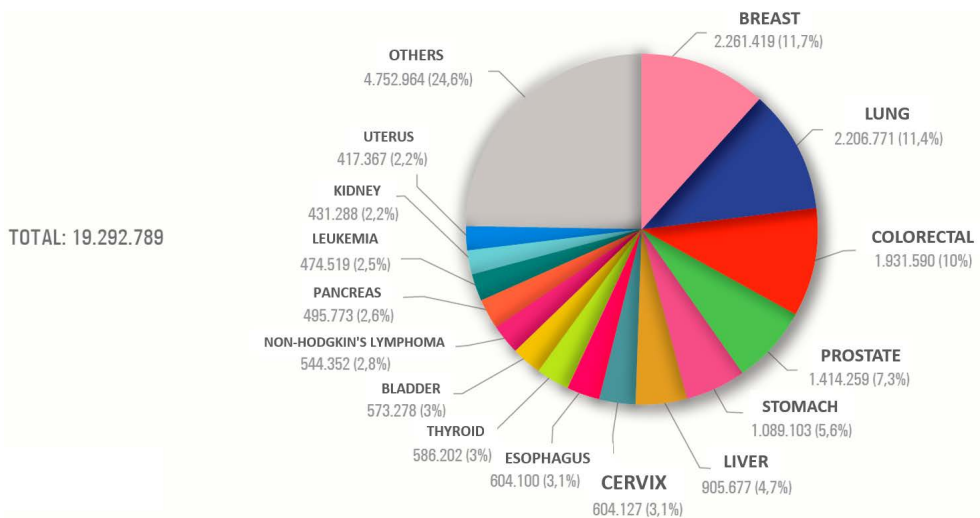


Figure 2. Most commonly diagnosed tumours worldwide. Estimate for the year 2020, both sexes. Adapted from [6]

Cancer is also one of the main causes of morbidity and mortality in Spain. The number of cancers diagnosed in Spain in 2023 is estimated to reach 279,260 cases (according to REDECAN calculations), a number very similar to that of the year 2020. However, as in the world, the reality may be slightly different as this estimate does not include the possible effect of COVID-19 [7].

2. LUNG CANCER

2.1. EPIDEMIOLOGY AND RISK FACTORS

Lung cancer is currently estimated to cause 2.2 million new cases and 1.8 million deaths worldwide, making it the second most commonly diagnosed cancer and the leading cause of cancer death in 2020. Lung cancer is the leading cause of cancer morbidity and mortality in men, while in women it ranks third in incidence and second in mortality after breast cancer [8]. Incidence and mortality rates are approximately two times higher in men than in women, although the sex ratio varies widely by region. Moreover, incidence and mortality rates are three to four times higher in developed countries when compared to emerging countries (Figure 3) [9]. Nevertheless, this pattern may undergo transformation as the tobacco epidemic evolves, considering that over 80% of smokers aged ≥ 15 years reside in low- and middle-income countries. The survival rate of lung cancer patients at 5 years after diagnosis is only 10% to 20% in most countries (diagnosed between 2010 and 2014). [9].

Introduction

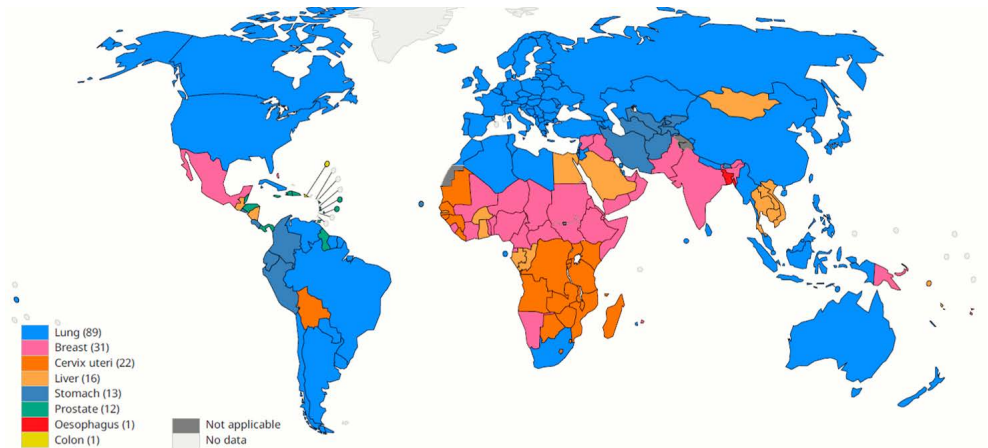


Figure 3. Top cancer sites per country associated with estimated number of deaths in both sexes (all ages, excluding non-melanoma skin cancer). Data Source: GLOBOCAN 2020, graph production: IARC [5].

Low-dose computed tomography (LDCT) screening of high-risk individuals (current and former smokers) can help diagnose the disease at an early stage, when treatment has a higher success rate [10].

The efficacy of annual LDCT screening in reducing lung cancer mortality has been validated in various independent international randomized clinical trials [11]. Despite these promising results, translating this benefit to the broader population has presented challenges, hindering the implementation of lung cancer screening as a vital component of a comprehensive strategy to alleviate the burden of this disease in the short term [12].

Cigarette smoking continues to be the single most important risk factor, with over 90% of lung cancer cases attributed to smoking [13]. In addition, the

Introduction

cancer risk increases with the duration of exposure, the number of cigarettes smoked per day, and the degree of inhalation [14–16]

Tobacco smoke contains approximately 5,000 chemicals, including at least 69 that are considered carcinogenic [17,18]. The carcinogenic potential of these substances is related to the secondary products formed during their metabolism. All of them are metabolized by cytochrome P450, which is largely involved in the response to xenobiotics and their detoxification. The accumulation of some of these by-products, which have the ability to react with DNA to form double-stranded adducts, favors the appearance of mutations that can affect genes relevant to the development of this neoplasia, such as *TP53* [19,20].

An area of increasing interest and incidence is lung cancer in never smokers (LCINS). LCINS has been recognised as a distinct disease entity from that in ever-smokers, and its significant impact has been indicated by being ranked in the most common cause of cancer death worldwide [21–23]. LCINS primarily occurs in women and younger patients, with adenocarcinoma (the most common histologic subtype) which start in the cells that would normally secrete substances such as mucus. [24]. Numerous risk factors have been suggested for the development of LCINS. Environmental or occupational exposure to certain carcinogens such as arsenic, asbestos, radon gas (among others) has also been proposed as a possible modulator of risk in the development of lung cancer. Other risk factors associated with this type of cancer are: diet rich in saturated fats, poor diet, air pollution,

Introduction

infectious agents, female hormonal factors and other diseases such as diffuse cystic fibrosis [25–29].

In addition to all the previously discussed external agents, genetic factors such as epigenetic alterations (including DNA methylation, histone modifications, and non-coding RNA expression), and previous diseases, have been widely reported in the literature to play an important role in the genesis of lung cancer [30]. Additionally, the presence of some single nucleotide polymorphisms (SNPs) in the human genome have been studied for their relationship with the risk of suffering from this neoplasia. Different studies have shown that patients with certain polymorphic variants present in specific regions of the genome were more likely to suffer from lung cancer compared to disease-free smokers or healthy individuals [31,32].

Other groups have based their studies on demonstrating that punctual mutations in genes related to DNA repair mechanisms, such as the *XPD* gene (related to the NER-nucleotide excision repair pathway), were associated with an increased risk of lung cancer [33]. Additionally, mutations in cytochrome P450, which is related to the metabolism of drugs and carcinogens, occur more frequently in smokers and significantly elevate the risk of developing this disease. [34,35].

In addition to this genetic background, the presence of other respiratory diseases is also considered a risk factor. Some pathologies such as asthma or pulmonary fibrosis have also been linked to an increased risk of lung cancer

[36,37]. The sum of these elements, along with late diagnosis, is what contributes to the overall poor prognosis of this type of cancer.

2.2. PHYSIOLOGY OF THE LUNG

The thoracic cavity contains two lungs, distinguished as the right lung and the left lung. Each lung is partitioned into distinct lobes, each further divided into independent segments. Within this anatomical arrangement, every segment (and consequently, each lobe) possesses its own dedicated vascular and lymphatic network. This unique organization ensures that the removal of a specific segment or lobe does not disrupt the vascular or lymphatic patterns in neighboring lung segments (Figure 4). Additionally, tumors originating in one segment typically follow an individual drainage pattern [38]. This characteristic enables the surgical removal of subunits of each lung, specifically targeting affected segments, without compromising the overall viability of the entire lung. Consequently, a comprehensive understanding of pulmonary architecture proves essential in effectively managing lung cancer.

The development of lung cancer involves several stages, constituting a multistep process. Certain subtypes exhibit distinct premalignant precursor lesions [39]. Prior to acquiring invasiveness, the lung epithelium undergoes morphological transformations, encompassing hyperplasia, metaplasia, dysplasia, and carcinoma in situ. Among these, dysplasia and carcinoma in situ are recognized as the primary premalignant lesions due to their higher

Introduction

likelihood of progressing to invasive cancer and lower tendency to regress spontaneously [40].

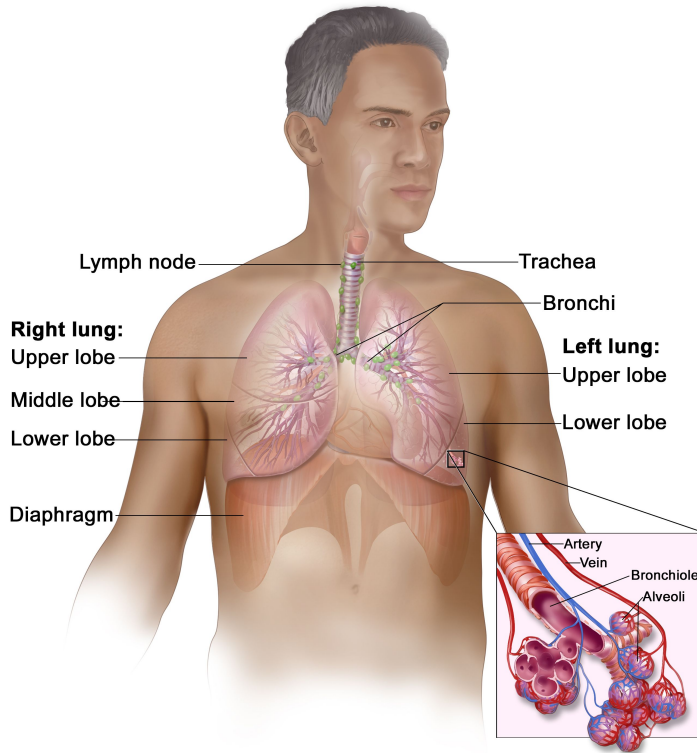


Figure 4. Physiological anatomy of the respiratory system [40].

2.3. DIAGNOSIS, STAGING AND PROGNOSIS

2.3.1. DIAGNOSIS

Frequently, the diagnosis of lung cancer is challenging due to insufficient detection programs and the delayed onset of clinical symptoms. Patients are typically initially diagnosed by the presence of symptoms such as persistent cough, hemoptysis, dyspnea, chest pain, weight loss, among

Introduction

others [41]. Consequently, 70-75% of lung cancer patients are diagnosed with advanced disease, and 50% present with distant metastases at the time of diagnosis, which hinders the possibility of curative surgery [42].

Subsequently, The National Lung Screening Trial (NLST) found that annual LDCT scanning over three years led to a 20% decrease in lung cancer mortality compared to chest radiography. The trial involved 53,454 high-risk individuals, with 59% being men. A subsequent analysis suggested a notable difference between genders, with women experiencing a greater screening benefit [43]. A few years later, a clinical trial called NELSON emerged as the second-largest randomized controlled trial focused on reducing lung cancer mortality through LDCT screening for high-risk individuals. NELSON reported that approximately 50% of cancers diagnosed in the screening group were at an early stage, with 65% to 70% classified as stages IA to II. In contrast, about 70% of cancers in the control group were diagnosed at stage III/IV. Overall, LDCT scanning resulted in a 26% reduction in mortality for high-risk men and an impressive 61% reduction for high-risk women over a 10-year period [43,44].

Simultaneously, histologic confirmation of the disease is essential for an accurate diagnosis, necessitating tissue examination. Patients with suspected resectable lung cancer may be diagnosed at the time of surgery. However, in patients who cannot tolerate surgery or when advanced disease is suspected, tissue from a biopsy may be obtained. It is essential to note that fresh samples are the preferred choice for molecular testing. Tissue samples preserved in paraffin blocks, despite optimal conditions, may alter

Introduction

the sample's microenvironment. Therefore, in cases of recurrence or before making any changes in treatment decisions, it is advisable to opt for new biopsies. Consequently, a re-biopsy should be considered when deemed necessary for the benefit of the patient.

In these cases, bronchoscopic techniques and endoscopic ultrasound (EUS) or endobronchial ultrasound (EBUS) are commonly used to obtain tumor biopsies [45,46].

2.3.2. STAGING AND PROGNOSIS

Lung cancer staging is based on the tumor-node-metastasis (TNM) system established by the American Joint Committee on Cancer (AJCC). The system is based on the spread of the primary tumor (T), the extent of lymph node involvement (N), and the presence or absence of metastases (M) (Figure 5). The latest revised version of the malignant tumor classification (8th TNM) was published in December 2016 and has been in effect since January 2017 [47]. The Staging and Prognostic Factors Committee is in charge of the process of proposing new recommendations. The newly established database consisted of 124,581 cases and their analysis are expected to provide proposals for changing the TNM classification toward the ninth edition, which is scheduled to be in use in January 2024 [48]. The combination of T, N, and M determines the specific stage of the disease (Table 1 and S1). Each of these has specific treatment and prognostic

Introduction

implications, so it is critical to have a good classification of tumors before making any therapeutic decision.

Table 1. Summary of descriptors of the TNM Classification System 8th Edition. Adapted from [49]

T/M	N0	N1	N2	N3
	STAGE			
T1a	IA1	IIB	IIIA	IIIB
T1b	IA2	IIB	IIIA	IIIB
T1c	IA3	IIB	IIIA	IIIB
T2a	IB	IIB	IIIA	IIIB
T2b	IIA	IIB	IIIA	IIIB
T3	IIB	IIIA	IIIB	IIIC
T4	IIIA	IIIA	IIIB	IIIC
M1a	IVA	IVA	IVA	IVA
M1b	IVA	IVA	IVA	IVA
M1c	IVB	IVB	IVB	IVB

Introduction

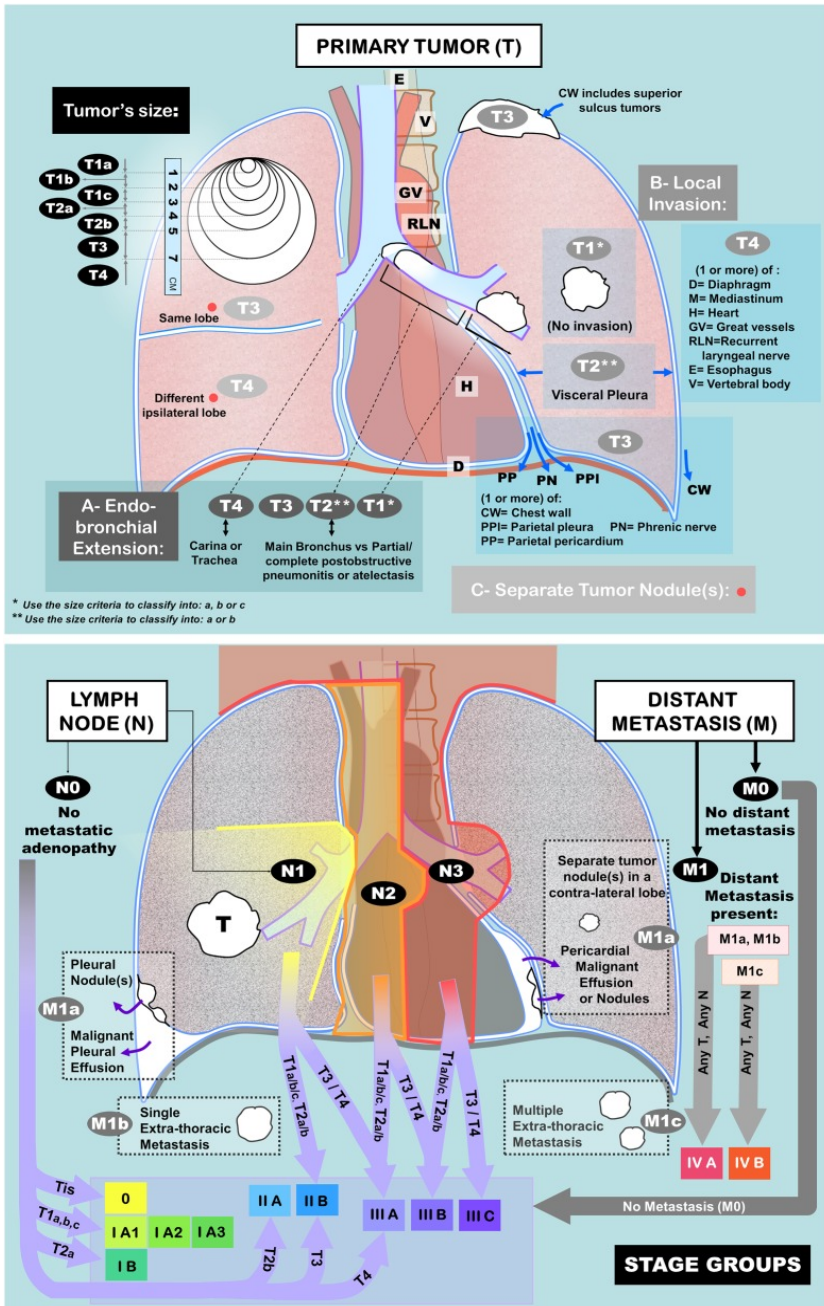


Figure 5. Reference diagram representing the 8th edition of TNM staging classification of lung cancer. The upper part of the diagram classifies the different T categories through a comparison of the possible tumor dimensions. Subsequently, for a more efficient

Introduction

classification, it is necessary to consider additional criteria for the invasion/extent of the primary tumor, if applicable. The invasion/extent criteria (endobronchial extension (A), local invasion (B), and separate tumor nodule(s) (C)) will be used exclusively to elevate, not decrease, the T classification. Finally, the lower diagram is necessary to determine the N and M classifications, combining them with the T category to establish the corresponding stage. The lower illustration outlines N1, N2, N3, and separate tumor nodule(s) of M1a based on a right-sided primary neoplasm (indicated by the letter T). For a left-sided lung neoplasm, mirror the image accordingly [50].

The importance of TNM also lies in the fact that it provides important prognostic and therapeutic information. Those tumors with a certain location and histology and with the same TNM classification have, in principle, the same behaviour [51]. The prognostic information of TNM is associated with stage, with overall survival (OS) decreasing as tumor stage increases [52].

2.4. HISTOPATHOLOGICAL CLASSIFICATION

To date, the anatomo-pathological classification of lung cancer is based on histological and pathological techniques. Histological evaluation and diagnosis is performed on tumor biopsy or cytological samples, obtained by different procedures according to the 2021 WHO Classification and the results of specific markers determined by immunohistochemistry (IHC) [53].

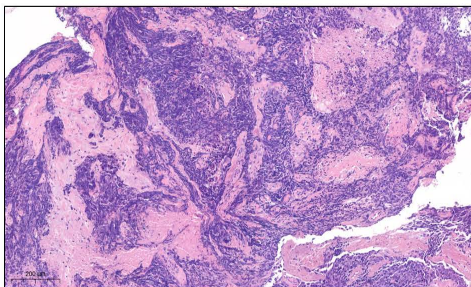
The histological classification of lung cancer can be used to predict the prognosis of patients, as well as to personalize their treatment. They are generally recognized two fundamental subtypes of lung cancer based on the

histopathological characteristics: small cell lung cancer and non-small cell lung cancer [54].

2.4.1. SMALL CELL LUNG CANCER (SCLC)

SCLC is a high-grade neuroendocrine carcinoma that accounts for approximately 15% of lung cancers. It receives this name because of the size of its cells (Figure 6), characterized by a rounded oval morphology and scant cytoplasm. It tends to be located in the central area of the lung and can compress vessels or organs at that level. SCLC is closely associated with smoking and is characterized by a high mitotic rate and frequent extensive necrosis. Therefore, its rapid growth and aggressiveness are usually associated with a poor prognosis. [55]. Thus, by the time of diagnosis, the majority of the tumors cannot be resected as they have already spread, being chemotherapy the most frequent treatment option [56–58].

(a)



(b)

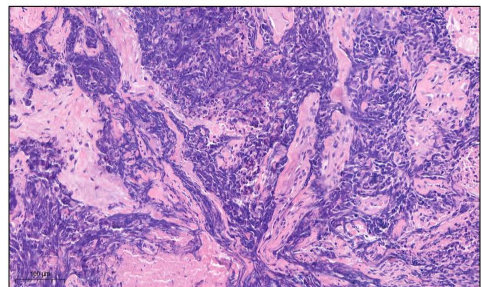


Figure 6. Cytologic and histologic features of SCLC. High-power field view of a formalin-fixed paraffin-embedded (FFPE), hematoxylin and eosin (H&E)-stained slide at 20X. Scale bar 200 μm **(a)**. IHC H&E staining at 40X. Scale bar 100 μm **(b)**. — Images provided by the Pathology Department of the Hospital Clínico Universitario de Valencia (HCUV).

2.4.2. NON-SMALL CELL LUNG CANCER (NSCLC)

NSCLC tumor cells are larger than normal epithelial lung cells (hence the name) and the location is usually peripheral or central. This is a slow-growing tumor that usually originates from the bronchial epithelium. The recommended initial treatment for early stage (I-III A) NSCLC is surgery; however, due to the highly variable clinical manifestations at these stages, in 50% of cases diagnosed, the disease is already advanced, leaving the patient with no surgical option [59].

In addition, NSCLC is a group that includes several histologic subtypes, with adenocarcinoma, squamous cell carcinoma and large cell carcinoma being the most common.

2.4.2.1. Lung adenocarcinoma - LUAD

LUAD is the most common histologic subtype of NSCLC accounting for more than 40% of cases. It originates from bronchoalveolar cells, is usually found in the peripheral areas of the lung and is more likely to be surgically resected. When the tumor is well differentiated (commonly referred to as low grade), it resembles the normal glandular structure with an acinar, papillary, micropapillary, lepidic or solid pattern. In contrast, poorly differentiated (high-grade) ADCs have lost the glandular morphology. It is characterized as a carcinoma with acinar/tubular structure or mucin production, positive for TTF-1 (NKX2-1) (Figure 7) and/or napsin A by IHC [60,61].

Introduction

The sub-classification of lung adenocarcinomas has remained practically unchanged since its last modification in 2015, in which terms such as bronchoalveolar carcinoma (BAC) or the mixed subtype were excluded. In addition, new concepts such as adenocarcinoma in situ (AIS), minimally invasive carcinoma, invasive non-mucinous adenocarcinoma, invasive mucinous adenocarcinoma (IMA), colloid adenocarcinoma, fetal adenocarcinoma or enteric-type adenocarcinoma were introduced [53].

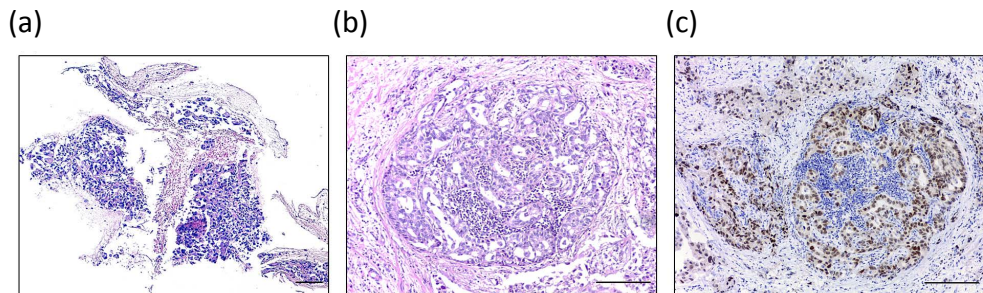


Figure 7. Cytologic and histologic features of NSCLC adenocarcinoma. High-power field view of an NSCLC FFPE piece, H&E-stained of a cancerous lesion and their adjacent non-tumor tissue (10X) **(a)**. IHC of H&E staining of the lung lesion (20X) **(b)**. IHC staining of TTF-1 reveals positivity corresponding to LUAD (20X) **(c)**.

Scale bar 200 μ m. — Images provided by the Pathology Department of the Hospital Clínic Universitario de Valencia (HCUV).

2.4.2.2. Lung squamous cell carcinoma - LUSC

LUSC or the epidermoid subtype accounts for approximately 30% of all NSCLC and is associated with smoking habits and is more common in men than in women. It originates from the lining epithelium and is often found in the lobar or main bronchi. It is defined as carcinoma with keratinization or intercellular bridges with CK5/6, p40 and p63 positive staining by IHC. In 2015, the WHO revised the classification to recognize three variants of SCC

Introduction

based on histological examination (Figure 8). These three variants are: keratinizing, non-keratinizing, and basaloid [60–62].

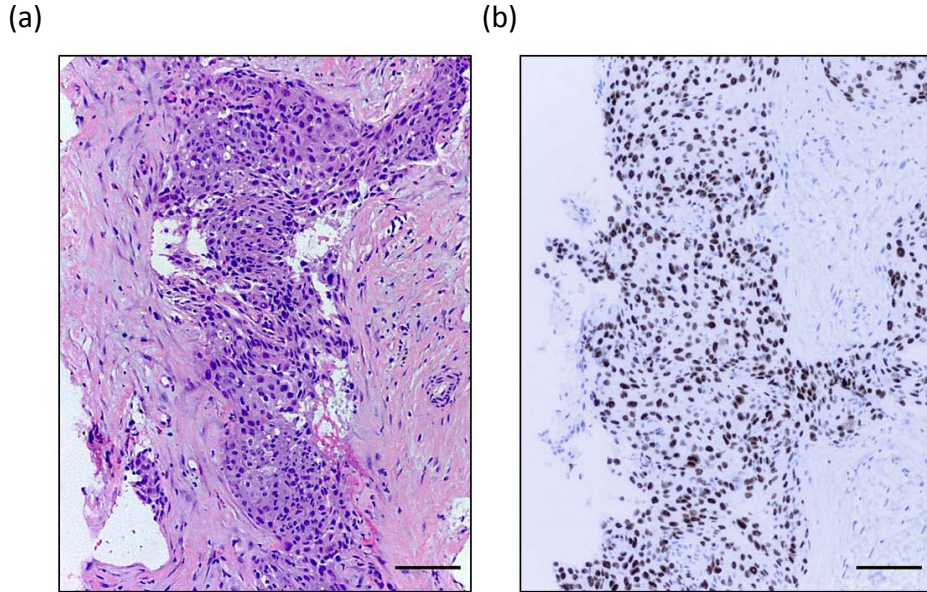


Figure 8. Cytologic and histologic features of NSCLC squamous cell carcinoma. High-power field view of an NSCLC FFPE specimen, H&E-stained, depicting a cancerous lesion and its adjacent non-tumor tissue. (10X) **(a)**. IHC staining of P63 reveals positivity corresponding to LUSC (10X) **(b)**. Scale bar 200 μm . — [Images provided by the Pathology Department of the Hospital Clínico Universitario de Valencia \(HCUV\).](#)

2.4.2.3. Large cell carcinoma - LCC

LCC is the least frequent among the NSCLC, representing around 10% of lung cancers. This subtype consists of tumors that lack the cytological, architectural, and immuno-histochemical characteristics necessary for classification into other subtypes. Typically, it arises from undifferentiated lung epithelial cells and can be located in either the lung's periphery or centrally. On macroscopic examination, these tumors often exhibit a more

aggressive clinical course due to their rapid growth and propensity to metastasize [61].

2.4.3. NEUROENDOCRINE TUMORS (NETS)

Neuroendocrine tumors (NETs) of the lung comprise a heterogeneous population of tumors, including a spectrum of tumors from the low-grade typical carcinoid (TC) and intermediate-grade atypical carcinoid (AC) to the high-grade large-cell neuroendocrine carcinoma (LCNEC) and small-cell carcinoma [63].

LCNEC are most often situated within the periphery of the upper lobes and many times show extraparenchymal tumor extension and broad zones of tumor necrosis (Figure 9) [64]. Unlike SCLC, this subtype can be determined using traditional neuroendocrine immunohistochemical markers widely used in pathology practice including synaptophysin, chromogranin A and CD56 (NCAM1) [65].

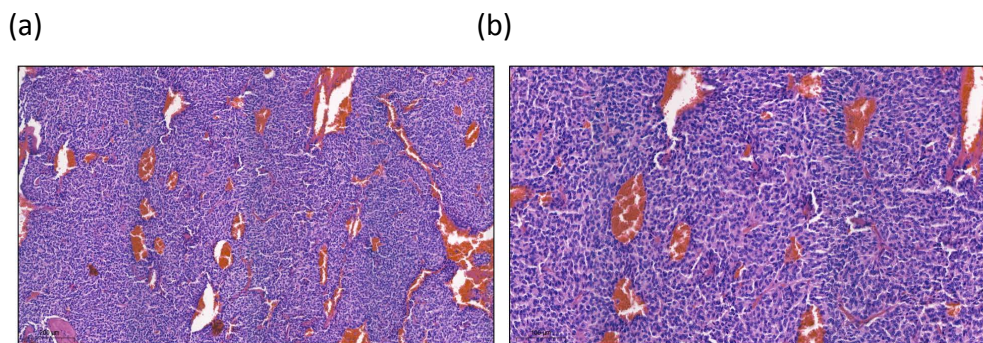


Figure 9. Cytologic and histologic features of LCNEC. High-power field view of a FFPE, H&E-stained slide 20X (scale bar 200 μm) **(a)** and 40X (scale bar 100 μm) **(b)**. This tumor shows different foci of necrosis (red-orange areas) within nests of carcinoid tumor cells. — [Images](#)

Introduction

provided by the pathological anatomy service of the Hospital Clínico Universitario de Valencia (HCUV).

NSCLC accounts for approximately 85% of all lung cancers. Therefore, given its high incidence among patients with lung neoplasia, it is the primary focus of our research development.

2.5. MOLECULAR CLASSIFICATION OF LUNG CANCER

Lung cancer is a molecularly heterogeneous disease, and a profound understanding of its biology is crucial for the development of effective therapies. Accumulation of mutations in different oncogenes and tumor suppressors is ultimately the cause of tumorigenesis for almost all lung cancers. Tumors are composed by cell subpopulations or clones with different molecular characteristics, which give rise to intratumoral heterogeneity.

2.5.1. MOLECULAR CLASSIFICATION OF SCLC

The most striking alterations found at the individual gene level in SCLC are the nearly uniform loss of function of the tumor suppressors *TP53* and *RB1*. Inactivating mutations in *TP53* and *RB1* have been shown to affect up to 90% and up to 65% of SCLC, respectively, indicating that the loss of these genes is an important event in the onset of SCLC development. Loss of

functional *TP53* would therefore allow for genomic instability, which could be the basis for the further accumulation of driver mutations [66]. Other recurrent genetic aberrations have been identified in SCLC, among which *MYC* family genes, stand out as oncogenic drivers that may constitute novel therapeutically tractable targets [67].

2.5.2. MOLECULAR CLASSIFICATION OF NSCLC

Continuing with the various genomic alterations given in lung cancer, it should be noted that NSCLC is one of the most genomically diverse tumors, and therefore, there are a variety of molecularly defined subsets of patients characterized by specific sets of driver gene mutations (Figure 10).

Introduction

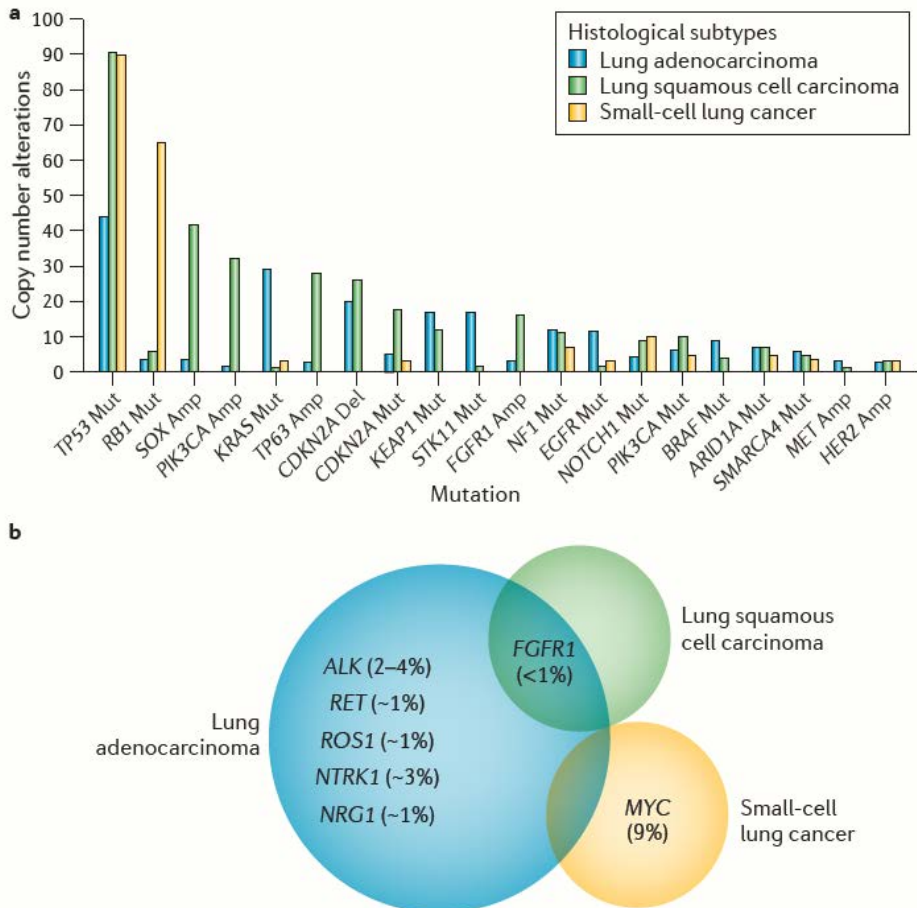


Figure 10. Genomic alterations in lung cancer. The most common mutations (Mut), gene copy number variations (Amplifications or Deletions) (a) and translocations (b) according to histological subtypes [68].

2.5.2.1. LUAD genomic alterations

EGFR and *KRAS* mutations, along with *EML4-ALK* fusions, represent the three most prevalent driver alterations in LUAD. From a clinical perspective, *EGFR* mutations are more frequently observed in female never-

Introduction

smokers and are linked to a more favorable prognosis. In contrast, *KRAS* mutations are associated with a poorer outcome, primarily because, until recently, there were no approved therapeutic agents available for *KRAS*-mutant tumors [69].

Other driver genes preferentially mutated in LUAD, but at a significantly lower frequency (1–5%) include *HER2* and *MAP2K1/MEK1* which are mutually exclusive of *PIK3CA*, *BRAF*, *EGFR* and *KRAS* mutations [70].

Also, oncogenic rearrangements leading to targetable gene fusions are well-established cancer driver events in lung adenocarcinoma [71]. Less than 10% of LUADs harbor *ALK* rearrangements in Caucasian populations. Histological morphology of *ALK* rearranged LUAD is typically solid with few foci of signet ring cells [72]. Other cancer driver fusion genes in LUAD are *ROS1*, *RET*, *NTRK1* and *NRG1*. The resulting chimeric proteins also are therapeutic targets [73,74].

2.5.2.2. LUSC genomic alterations

Fewer actionable alterations have been identified in LUSC, and as a result, targeted therapies for these alterations have not yet been approved for clinical use. Recurrent alterations characteristic of LUSC include amplification of *SOX2*, *PIK3CA*, *PDGFRA* and *FGFR1*, and mutation of *DDR2*, *AKT1* and *NRF2*. Despite the high frequency of *SOX2* and *PIK3CA* amplification (20-30% of cases), no drugs are currently available to target these alterations [75].

2.5.2.3. Alterations common to both NSCLC subtypes

Many alterations are observed at similar frequencies in both LUAD and LUSC, including *TP53*, *BRAF*, *PIK3CA*, *MET* and *STK11* mutations, loss of *PTEN* expression and amplification of *MET* with *BRAF*, *PIK3CA*. *TP53* mutation is the most common mutation in both subtypes, occurring in more than 50% of samples, but targeting *TP53* is inherently difficult due to the wide range of mutant proteins that exist and the multitude of complex protein-protein interactions [76].

The molecular characterization of lung tumors has revealed that many of these mutations are typically present in the initiating clones, underscoring their role in tumor initiation [70]. This discovery makes them attractive targets for therapeutic intervention. In essence, our understanding of the tumor's molecular biology, coupled with the identification of alterations that drive oncogenic signaling, has prompted about a transformative shift in the treatment of this disease. It has paved the way for new therapies tailored to target specific mutations, offering not only improved quality of life and life expectancy for patients but also deeper insights into the various mechanisms of oncogenic resistance to antineoplastic treatments.

In summary, NSCLC exhibits significant genomic diversity, impacting treatment and prognosis. For this reason, our study is centered on NSCLC.

2.6. NSCLC TREATMENT

The treatment of NSCLC hinges on a multitude of factors, including the patient's functional status (PS: performance status), histologic type, lung functionality, and the various molecular alterations present in the tumor cells [77]. Treatment options encompass conventional methods such as surgery, radiation, or chemotherapy, as well as more recent therapeutic approaches like targeted therapies and immunotherapy.

For patients in the early stages (stages I-II and select cases in stage IIIA), the primary curative treatment is complete surgical tumor resection. In specific cases, alternatives include radiofrequency ablation (RFA) or stereotactic body radiation therapy (SBRT) for stage I or II patients with a limited medical justification for surgery [78]. Nonetheless, there is a non-negligible percentage of patients who relapse. Neoadjuvant or adjuvant chemotherapy or radiotherapy can improve local control and is recommended for patients with resectable NSCLC [79].

The evolution of advanced NSCLC treatment represents a significant milestone, transitioning from conventional non-specific regimens to personalized therapy tailored to the distinct characteristics of each patient's tumor. For advanced NSCLC patients with a favorable performance status, platinum-based doublet chemotherapy has traditionally served as the standard first-line treatment [80]. Pemetrexed maintenance demonstrated additional survival benefits if tumors had been at least stable after 4 to 6 cycles of platinum-based dual therapy [81].

Introduction

Other strategies involve the utilization of anti-angiogenesis monoclonal antibodies targeting vascular endothelial growth factor (VEGF) and its receptor (VEGFR). These approaches have demonstrated additional survival benefits when combined with first-line platinum-based double chemotherapy (bevacizumab) [82,83] or docetaxel second-line (ramucirumab or nintedanib) [84,85].

Thanks to a better understanding of tumor biology, mutational genomic alterations, cancer immunology and the tumor microenvironment, treatment paradigms for NSCLC patients have evolved along two main routes: (i) targeted molecular therapies based on different driver oncogenes in cancer cells and (ii) immune checkpoint inhibitors, which use monoclonal antibodies against specific ligands to reverse the immunosuppressive effects caused by tumor cells [86].

Targeted molecular therapy is now the first-line treatment for patients with NSCLC whose tumors harbor targetable oncogene driver mutations due to its high efficacy and reduced toxicity [87,88]. Over the past decade, treatments for advanced NSCLC have evolved dramatically, allowing for more individualized selection of treatment options. Molecular profiles and immunologic status help determine treatment options.

For example, patients with *EGFR* mutations, *ALK* rearrangement, *ROS1* rearrangements, *BRAF* mutations and *NTRK* mutations should receive FDA-approved targeted therapy as first-line treatment [89]. Other oncologic

Introduction

driver mutations such as *RET*, *MET*, and *HER2* in NSCLC are also targets for treatment [90,91].

Under normal biological circumstances, the immune system can identify and eliminate cancer cells and other microorganisms through a carefully controlled mechanism that involves a balance of activating and inhibitory signals. Nevertheless, tumor cells possess the ability to interfere with this process, enabling the immune system to evade this surveillance [86].

Immunotherapy (particularly immunologic blockades to checkpoints such as PD-1/PD-L1 axis, and CTLA-4) has opened new horizons significantly improving clinical outcomes in patients with NSCLC advanced without mutations in target genes. Roughly, it can be said that immunotherapy is based on the modulation of the function of the immune system by increasing its effectiveness in attacking cancer cells and stopping or delaying their growth [92,93]. Immune checkpoints blockers (ICBs) have been approved as a second-line therapy for patients with advanced NSCLC whose tumors progress to platinum-based chemotherapy or targeted therapies, as well as in the first-line NSCLC setting [94].

However, while immunotherapy and targeted therapies have resulted in extended survival for certain patients, their effectiveness is not always uniformly consistent across all tumors. Resistance to treatment typically arises from the intricate nature of tumors, which comprise diverse cell populations and a microenvironment that facilitates their growth and expansion. This implies that treatments can affect different subclones of the

same tumor in diverse ways [95]. For this reason, it is necessary to use experimental models that allow us to obtain more information about the different cellular subpopulations that coexist within the tumour and their role in the biological processes involved in the progression of the disease.

3. CELLULAR CLONALITY AND TUMOR HETEROGENEITY

It is crucial to consider that tumors are made up of a variety of cell types. Alongside tumor cells, there are cancer stem cells, stromal cells, endothelial cells, immune system cells, among others, collectively constituting the "tumor microenvironment". This environment favors cell proliferation and invasion, exhibiting high heterogeneity that results in genetic diversity that can serve as a substrate for natural selection and tumor evolution [96].

3.1. MODELS OF TUMOR HETEROGENEITY

In tumor tissue, we can identify subpopulations of cancer stem cells (CSC) or cancer stem-like cells (CS-LC), which have been widely associated with chemoresistance and tumor recurrence [97]. CSC/CS-LC were initially described as a rare subpopulation of cancer cells with unlimited self-renewal capacity and the ability to differentiate and repopulate the entire tumor. The classical CSC model proposed a hierarchical organization, based on the

Introduction

existence of a cell within the tumor tissue with stem cell properties, capable of proliferating and maintaining itself indefinitely thanks to its self-renewal capacity [98,99]. In this model, only the CSC population has the capacity to generate and maintain the tumor, unlike the rest of the cells that form it, which do not have this capacity. However, subsequent experimental evidence suggests that cancer cells have great plasticity in their stemness, so cells that are not CSCs can also generate CSCs (Figure 11) [100,101].

The stochastic model or model of clonal evolution of cancer, postulates that one or several cells of the tissue acquire a mutation and from this and through an uncontrolled division process, new genetic alterations are accumulating. Through the selection of the most suitable clones, they reach the stage of tumor cell, finally giving rise to the tumor [102]. According to this model, any resulting tumor cells would be capable of maintaining and expanding the tumor, as well as giving rise to new tumors (Figure 11). However, both models are not exclusive and have been proposed as a unified model by some authors [103].

The ability to move from one cell compartment to another or between differentiated states of somatic and stem cells, is called cell plasticity [104]. According to this principle, the idea that there is a clear distinction between stochastic and hierarchical models is inaccurate. This is because stochastic events have the potential to generate new populations with hierarchical organization. Consequently, depending on the genotype and the communication within the microenvironment, groups of cancer stem cells

Introduction

(CSC) can evolve to regain the capacity for long-term repopulation [105]. This capacity for dedifferentiation can be inherited (hierarchical theory) or acquired through mutations that lead to a permissive capacity similar to that of stem cells (stochastic theory) (Figure 11) [106]. Understanding these mechanisms can aid in the development of new tools for the diagnosis and treatment of tumors.

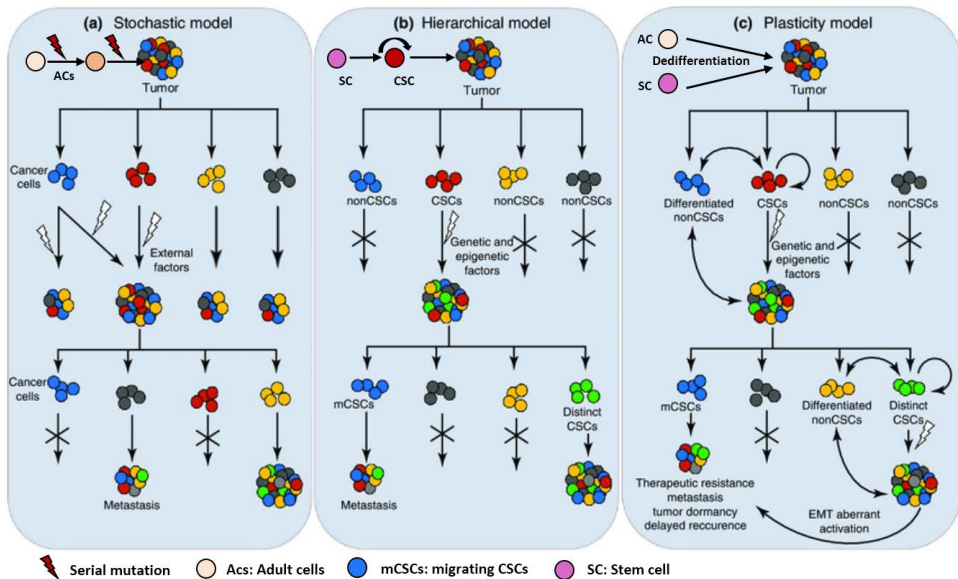


Figure 11. Different models of tumor heterogeneity. Stochastic model, in which every cell in the tumor has tumorigenic potential (a). Hierarchical model, only cells with stem cell-like characteristics (i.e., CSC) have important role in tumor progression (b). Plasticity model, both CSCs and non-CSCs have important roles in tumorigenesis (c). Adapted from [107]

3.2. CSC PROPERTIES AND TUMOR MICROENVIRONMENT

The host microenvironment surrounding cancer stem cells (CSCs) or progenitor cells can significantly influence the initial tumorigenic potential of these cells [106]. Specific microenvironmental conditions may promote

the survival and growth of the most resilient clone, enabling it to evolve hierarchically and generate a substantial tumor mass. On the contrary, the same CSC or progenitor cell placed in an unfavorable environment may not contribute to tumor growth [108].

In this context, a 'niche' refers to a distinct anatomical, molecular, and cellular microenvironment within a tumor. As a result, multiple niches can coexist within a tumor, leading to the development of multiple distinct CSC populations and increasing overall cellular diversity [109].

3.3. 3D *IN VITRO* MODELS

In the past decade, monolayer (2D) cell cultures and animal models have served as standard tools for cancer research. However, today, we are increasingly recognizing the various limitations associated with these models.

Animal models offer an *in vivo* environment into which human cancer cells or small tumor fragments can be transplanted, promoting graft growth (xenografts) [110]. Nevertheless, these models come with significant drawbacks, including high costs and limitations related to maintenance, reproducibility, and experimental design flexibility. Notably, the major limitation in cancer research, such as PDX (patient-derived xenograft) models, is the absence of a functional immune system, a common issue in all xenograft models [111]. Moreover, promoting the welfare of

Introduction

experimental animals encourages the use or development of alternative methods that reduce the necessity for *in vivo* experiments [112].

On one hand, 2D cell cultures offer a simple, cost-effective, and well-standardized approach for studying the mechanisms and behavior of tumor cells. However, they inherently lack the ability to replicate the intricate complexity of *in vivo* tumor tissue for several reasons. Cells grown in 2D cultures fail to mimic many of the biological, chemical, and mechanical signals present in tissues. This is attributed to their limited adhesion in the x-y plane, forced apical-basal polarity, absence of soluble gradients, and unrestricted proliferation, among other factors [113].

Conversely, three-dimensional (3D) cultures are extensively utilized to explore the biology of epithelial tissues because they can faithfully replicate the 3D organization and functionality of cells within tissues. Significantly, 3D assays excel in replicating the *in vivo* conditions of specific cell populations within the tumor, thereby fostering the growth of a subpopulation of cancer cells with stem cell-like properties. This characteristic proves to be a substantial advantage in the exploration of potential cancer treatments. Utilizing 3D models to study CSCs can substantially enhance our comprehension of tumorigenesis, metastasis, and the various mechanisms that drive tumor recurrence and progression [114].

In this context, 3D models offer the distinct advantage of providing solute gradients and allowing adhesion distribution across all three spatial dimensions, without enforced polarity. If the phenotypes of CSC-derived 3D

Introduction

cultures can be controlled by adjusting the culture conditions, these cultures become valuable tools for investigating the relationship between CSC maintenance and differentiation induced by the tumor microenvironment. To achieve this, it's essential to experiment with well-characterized CSCs under the appropriate conditions [115–117].

As a result, these 3D cultures have emerged as promising platforms for various applications, including the development of innovative drug delivery methods, the study of self-renewal and pluripotency, the establishment of primary cultures from patients, and the analysis of interactions between tumor cells and their microenvironment to identify novel biomarkers.

In recent years, several techniques have been developed for the 3D culture of CSCs. The most common methods for creating tumorspheres include scaffold-free techniques or suspension cultures (using ultra-low binding plates), the hanging drop method, or organoid formation (embedding cells in a droplet of extracellular matrix). Additionally, there are approaches using scaffolds that enable co-culture with other cell populations, such as immune system cells or connective tissue cells (like cancer-associated fibroblasts, or CAFs) [118–120].

Tumorspheres are primarily generated by suspending single cells in a medium that is supplemented with several growth factors and without fetal bovine serum (FBS). Within this environment, a subset of tumor cells can survive and subsequently proliferate. As they continue to expand clonally, they form spheroids and acquire stem cell-like characteristics [121]. In

Introduction

general, CSCs need specific conditions to support their self-renewal and specialized divisions, with hypoxia playing a particularly pivotal role. As tumorspheres grow and exceed several hundred microns in diameter, the cells on the outermost layer start consuming a significant amount of oxygen and nutrients. This, coupled with increased cell adhesion in the core, results in growth arrest or even necrosis in the innermost layers due to a lack of oxygen and sustenance [122,123]. Different studies show that hypoxia in tumor cells can cause an alteration in the gene expression profile, thus promoting different phenomena such as metabolic alteration and angiogenesis amongst others. So unlike 3D cultures, 2D cultures cannot generate this hypoxic environment and mimic the *in vivo* scenario as 3D cultures do [124–126].

Extensive characterization of CSC properties in tumorspheres derived from any cancer cell line or tissue should be performed to ensure that the generated tumorspheres are truly enriched in the CSC population [127]. The formation of these tumorspheres is currently used for research in various types of tumors such as those of the colon, liver, breast, prostate and lung, among others [128].

The use of these *in vitro* experimental models in the present study represents a powerful tool for investigating NSCLC, enabling us to unravel relevant biological information about the behavior and mechanisms of this type of tumors.

4. LIQUID BIOPSY

In recent years, there has been a growing demand for alternative sources of diagnostic, prognostic, and therapeutic response biomarkers to complement the clinical gold standard of tissue-based biopsies. These biomarkers support clinical decisions after tumor classification. Issues such as inadequate sample quality or insufficient tumor material can impede the establishment of a complete molecular profile of the tumor in many cases, leading to clinical delays [129]. Often, the urgency to initiate treatment outweighs the necessity for a comprehensive diagnostic assessment, especially in cases where prompt treatment is critical. Consequently, any technique that facilitates a safe, convenient, and expedited diagnostic process is of great benefit and can be readily integrated into routine clinical practice.

Unfortunately, a significant proportion of patients present with advanced disease (stage III/IV) and surgery may not be indicated. In such cases, the only tissue that may be available for molecular profiling are small needle core biopsies or cytology specimens, which is not always sufficient due to lack of tumor material. This would need a further re-biopsy, which carries a complication risk [130]. Furthermore, biopsies in many cases are not feasible outright or at re-biopsy due to tumor location or patient's performance status [131,132].

In this line, liquid biopsy is emerging as a new minimally invasive approach (through biological fluids) for the detection of relevant tumor characteristics in clinical practice. The liquid biopsy is composed of different analytes such

Introduction

as circulating tumor cells (CTCs) or macromolecular tumor products including circulating cell-free DNA (cfDNA), circulating tumor DNA (ctDNA), circulating miRNA, extracellular vesicles (EVs), tumor educated platelets (TEPs) among others; which can provide information about the cells from which they were secreted during the different processes of the disease. [133]

Moreover, considering the intratumoral spatial and temporal heterogeneity, the diverse components integrated into liquid biopsies can offer a more comprehensive representation of tumor cell populations and their molecular characteristics, including the tumor microenvironment. Liquid biopsies prove particularly valuable in scenarios requiring serial sampling, such as monitoring disease progression or detecting the emergence of resistance mutations to current targeted therapies. They also hold promise in identifying patients at risk of relapse after treatment and could potentially serve as a vital component of future screening protocols.

Given the potential that liquid biopsy holds as a tool for the clinical management of this disease, it is vital to focus on the development and standardization of protocols for the isolation and processing of these analytes. This is to ensure that they can be routinely implemented in clinical practice in the near future. This thesis is based on addressing many of these aspects and needs related to the use of exosomes as a multidisciplinary approach.

4.1. EXTRACELLULAR VESICLES

4.1.1. GENERAL FEATURES, CLASSIFICATION AND NOMENCLATURE

Extracellular vesicles (EVs) are structures released by cells through active or passive regulation, or as a consequence of cell death [134]. These membrane-bound vesicular structures contain substantial amounts of biologically active information acquired from their origin cells, which can be transported to other cells or organs in homeostasis or disease conditions [135]. Likewise, they can be classified into different groups based on their size, morphological features, cellular origin or content. Some of the best-known EVs will be highlighted below.

In the first place, there are the so-called apoptotic bodies, which originate when cells enter apoptosis and as a consequence are subdivided into vesiculated bodies that have a size between 800-5000 nanometers (nm). Then, in a smaller size range we find the microvesicles (from 100 to 1000 nm), which are released into the cellular environment by outpouching of the plasma membrane [136]. Finally, and as a subtype within microvesicles, there are exosomes that can have a size between 40-160 nm and whose biogenesis and release take place through a highly regulated process at the cellular level [135].

In terms of nomenclature, the International Society of Extracellular Vesicles (ISEV) endorses the use of the term 'extracellular vesicle' as a generic term for particles naturally released from cells, enclosed by a lipid bilayer, and

Introduction

lacking a functional nucleus (i.e., non-replicative). As there is still no consensus on specific markers for distinguishing between EV subtypes, such as 'exosomes' (of endosomal origin) and 'ectosomes' (of plasma membrane origin), assigning an EV to a particular biogenesis pathway remains a challenging task. One exception is when EVs are captured during the process of release using live imaging techniques. Therefore, it is imperative to clearly and prominently define the chosen term at the outset of any publication [137].

Throughout the development of this thesis project, we will use the term 'exosome.' Despite our inability to confirm its precise mechanism of secretion, 'exosome' is the term most commonly used to refer to this particular subtype of microvesicles.

4.1.1.1. Exosomes

Exosomes are very small vesicles (40-160nm), spherical in shape and composed of a lipid bilayer, which are secreted by most cell types. Its existence was first discovered in 1987 [138]. Initially, they were considered to be mere containers of cellular waste, but evidence began to emerge that they act as carriers of important information to distant tissues of the body and are able to modulate their physiology. They have been shown to act as messengers of biological information belonging to the cells from which they were secreted, both under normal conditions and in pathological processes [139].

Introduction

In addition, they are also related to various cellular processes, proliferation, toxicity, control of cell activity, among others. For example, some studies pointed out that these vesicles are important modulators of the immune response, with great relevance for the spread or protection against diseases such as cancer or the infectivity of certain parasites [140,141].

They would also be key elements in the differentiation of stem cells (of different origins) and in regenerative processes. Various studies have confirmed their presence in most biological fluids such as plasma, urine, tears, saliva, gastric juices, among others [142–144]. For these reasons, they are excellent candidates for disease progression biomarkers in liquid biopsies.

4.1.2. BIOGENESIS AND SECRETION

The biogenesis of exosomes commences with the formation of a structure known as the early endosome (Figure 12). This endosome comprises a vesicle containing an intraluminal space created by the invagination of the cellular plasma membrane. It resides within the cell's cytosolic compartment. Subsequent invaginations of the membrane generate additional intraluminal vesicles (ILVs), which will become future exosomes. These ILVs remain contained within the intraluminal cavity of the endosome, forming what is referred to as a multivesicular body (MVB) [145].

Introduction

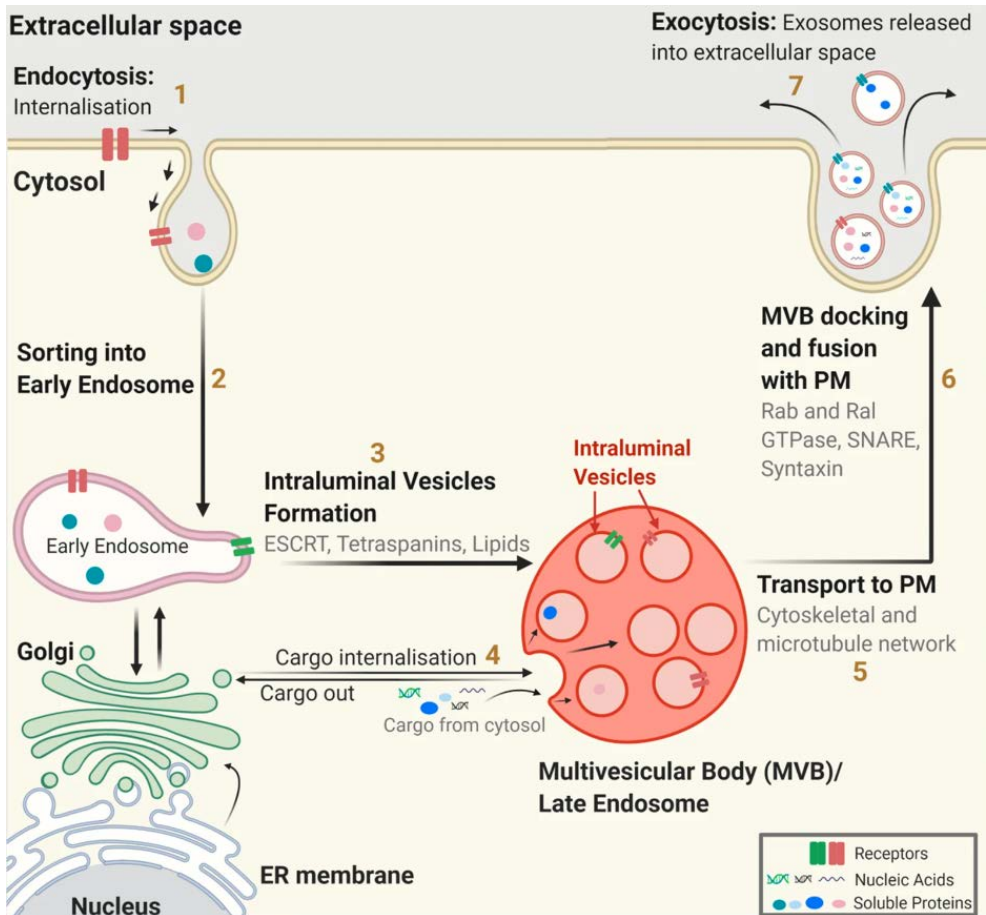


Figure 12. Representation of the process of biogenesis and secretion of different extracellular vesicles, including exosomes. [146] ER: Endoplasmic Reticulum; MVB: Multivesicular Bodies; PM: Plasma membrane.

Two main molecular regulation mechanisms for its formation have been described. The main mechanism involves ESCRT proteins. Endosomal Sorting Complex Required for Transport (ESCRT) machinery is involved in the formation of ILVs, through the formation of different protein complexes that lodge or interact with the membrane of the early endosome, inducing its invagination [147]. ESCRT consists of four complexes plus associated

Introduction

proteins: ESCRT-0 is responsible for cargo clustering in an ubiquitin-dependent manner, ESCRT-I and ESCRT-II induce bud formation, ESCRT-III drives vesicle scission, and the accessory proteins (especially the VPS4 ATPase) allow dissociation and recycling of the ESCRT machinery [148].

Alternatively, there is another pathway for sorting exosomal cargo into multivesicular bodies (MVBs) that operates independently of the ESCRT system. This pathway appears to rely on raft-based microdomains for the lateral segregation of cargo within the endosomal membrane [149]. Proteins, including tetraspanins, also play a role in exosome biogenesis and cargo loading. Tetraspanin-enriched microdomains (TEMs) are specialized membrane platforms found throughout the cell membrane, serving as compartments for the organization of receptors and signaling proteins [149].

Different specialized mechanisms ensure the specific sorting of bioactive molecules in exosomes, either through the ESCRT-dependent or independent mechanism (involving tetraspanins and lipids); which can act differently depending on the type of cell of origin [150]. Many of these proteins have been described and used as specific markers of exosomes, with Alix, CD9, CD63, CD81 and TSG101 as most relevant examples [151].

Once the multivesicular body (MVB) is formed, it needs to fuse with the cellular membrane to release the exosomes. This fusion process is tightly regulated by a series of specific proteins (Figure 12). Among the first regulators identified were members of the Rab family of proteins, specifically Rab27a and Rab27b. Some authors noted that inhibiting these

proteins or their effectors resulted in a reduction in the tumor cells' ability to release exosomes [152].

Another secretion regulation mechanism, especially interesting due to its relationship with cancer, is the one mediated by *TP53*. There is evidence that one of the transcriptional targets of this gene (*TSAP6*) is activated in response to DNA damage, favoring the secretion of exosomes [153]. Likewise, the action of some enzymes or the modulation of certain factors, such as the concentration of calcium ions or the pH; have also been related to the release of exosomes [154–156].

4.1.3. EXOSOMES CARGO

One of the most interesting aspects in the study of exosomes is that their content does not seem to be an exact reflection of the biological information of the cells of origin [157]. It appears that the specific biological information carried by exosomes may have a biological purpose directed towards the recipient cells into which they will be internalized [158].

The composition of its lipid membrane is clearly distinguishable from the cell membrane. In exosomes, a special enrichment of saturated lipids (sphingomyelin, phosphatidylserine, ceramides and cholesterol) has been reported, which are related to the presence of the so-called "lipid rafts" [159,160]. We can identify various proteins in their cargo, including those linked to the cytoskeleton (like actin and tubulin), enzymes involved in

Introduction

energy metabolism, proteins associated with vesicle transport (such as the Rab family), molecules responsible for cell adhesion (like tetraspanins), and those involved in the creation of exosomes (such as ESCRT complex proteins) (Figure 13).

Several members of the tetraspanin protein family, including CD9, CD63, and CD81, are highly concentrated on the lipid bilayer surface of exosomes. Interestingly, transmembrane integrins and other proteins present on the exosome surface play a crucial role in determining the target cell type, contributing to organ-specific homing [161], or conversely, serving as a signature of the parental cells from which they originated [162]. Some of these adhesion molecules, such as CD9 and CD81, can facilitate direct membrane fusion between exosomes and recipient cells, allowing for the transfer of exosomal cargo (Figure 13). Other molecules, like CD55 and CD59, serve to protect exosomes from complement-mediated attacks, increasing their stability in circulation. Moreover, high levels of CD47 expression on the exosome surface may enhance their resistance to phagocytosis by monocytes and macrophages [163].

Introduction

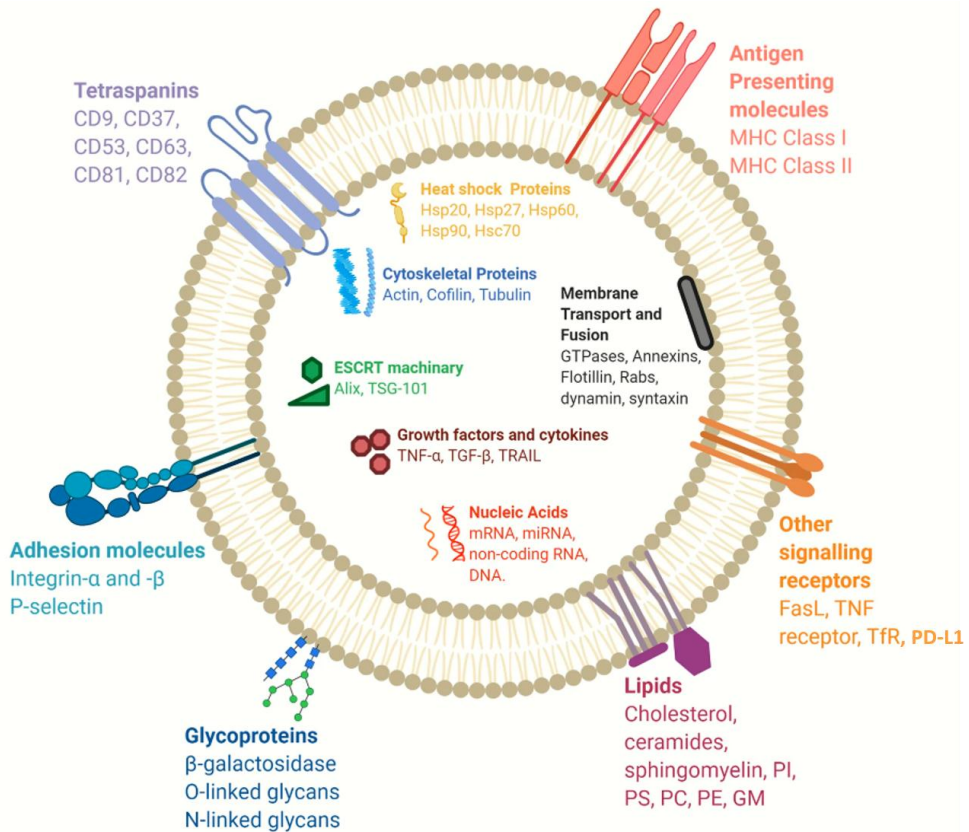


Figure 13. Composition and cargo of exosomes. Adapted from [146].

Hsp: Heat shock proteins, PI: Phosphatidylinositol, PS: Phosphatidylserine, PC: Phosphatidylcholine, PE: Phosphatidylethanolamine, GM: Gangliosides, TSG: Tumor susceptibility gene, TNF: Tumor necrosis factor, TGF: Transforming growth factor, TRAIL: TNF-related apoptosis-inducing ligand, FasL: Fas ligand, TfR: Transferrin receptor. PD-L1: Programmed death-ligand 1.

Furthermore, exosomes contain abundant and diverse nucleic acids such as DNA, messenger RNAs (mRNAs), and microRNAs (miRNAs), being the last one the most abundant cargo and consequently, the focus of most exosomes' biomarker research and functional studies [164,165].

Other types of RNAs, such as long non-coding RNAs (lncRNAs), long intergenic RNAs (lincRNAs), and circular RNAs, are also present [166–168].

The fact that exosomes exhibit such an extensive and diverse content, capable of traveling through various biological fluids protected from degradation, and being able to internalize into target tissues different from where they originated, makes their study particularly interesting for understanding the functioning of various biological processes. This is why exosomes have been chosen (from among all the elements offered by liquid biopsy) as the focus of study in the present work.

4.2. EXOSOMES IN CANCER

As mentioned earlier, exosomes are microvesicles that play a pivotal role in a wide range of biological processes. They have the ability to activate or inhibit various signaling pathways by transporting proteins, lipids, nucleic acids, and other substances to recipient cells. In the context of cancer, specifically, exosomes derived from cancer cells are involved in multiple aspects of tumor initiation and progression. This includes the formation of pre-metastatic niches, the development of the tumor microenvironment, angiogenesis, immune evasion, and the acquisition of aggressive characteristics.

Notably, it has been observed that cancer patients exhibit higher levels of exosomes in their bloodstream compared to healthy individuals. Unlike CTCs

Introduction

and ctDNA, exosomes can be produced in large quantities and remain stable as they circulate in different body fluids [169]. Over the past decade, several technologies have been developed for the isolation of exosomes from various biological fluids. As a result, real-time monitoring of changes in exosomal cargo holds the potential to offer valuable insights for the essential requirements of precision medicine, encompassing diagnosis, prognosis, and disease monitoring (Figure 14).

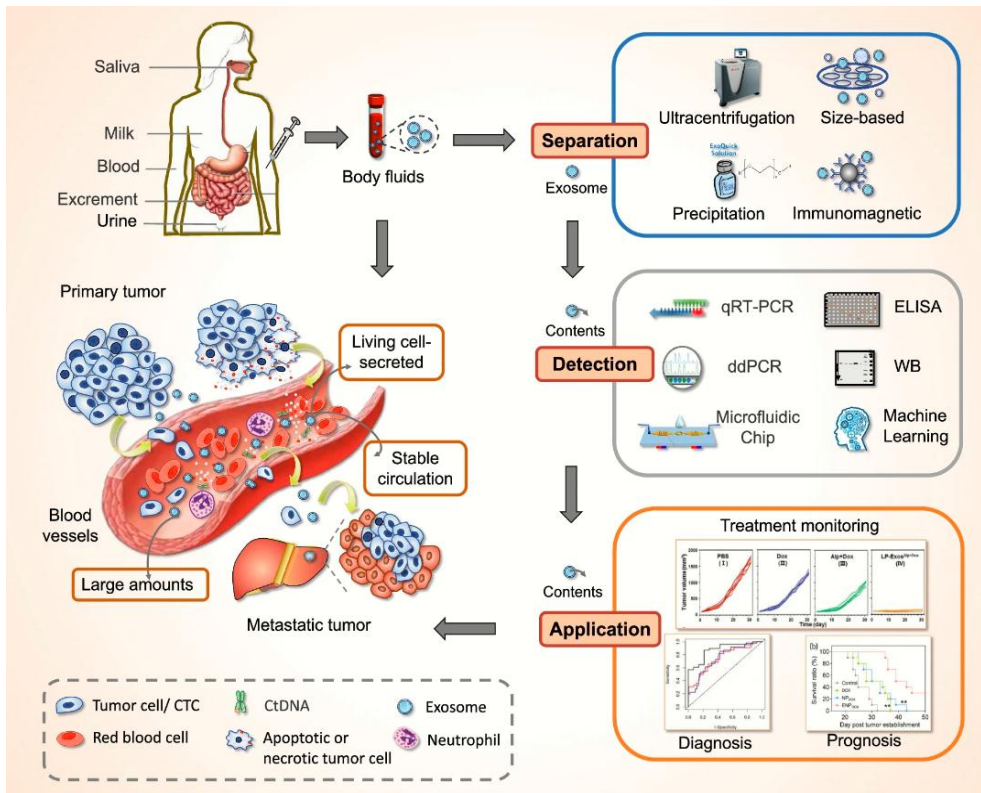


Figure 14. Exosomes as a key element in liquid biopsy for cancer study [170]. Exosomes are secreted by living cells and released into the bloodstream and various biological fluids. Isolation can be achieved through different techniques such as ultracentrifugation, precipitation, size-exclusion techniques, or immunomagnetic separation. Subsequently, their contents can be analyzed using various molecular biology approaches, and the interpretation of these results can provide valuable information about the diagnosis and prognosis of patients, as well as aid in monitoring the course of the disease.

All of these factors underscore the importance of investigating exosomes as a significant source of non-invasive and valuable biomarkers in the context of cancer [171–174].

4.2.1. EXOSOMES AS A REGULATORS OF TME

The term 'tumor microenvironment (TME)' encompasses the surroundings of a tumor, which include neighboring blood vessels, immune cells, stromal cells, signaling molecules, and the extracellular matrix [175].

The cells that make up the TME exchange information through various signalling pathways, ranging from juxtacrine interactions and cell-cell junctions to secreted factors such as cytokines, chemokines and extracellular vesicles [176]. TME is now known to play an indispensable role in tumour biology and is involved in tumourigenesis, progression and response to treatment [177]. Tumour cell-derived exosomes not only mediate cell-cell communication between tumour cells from different subpopulations with different clonal heterogeneity, but also remodel the tumour microenvironment by modulating the properties of different surrounding (non-tumour) cell types [178].

Within the tumor stroma, CAFs are the main cellular components of the TME in most solid cancers. Tumour cell-derived exosomes mediate the phenotypic change of fibroblasts into CAFs, being one of the key factors in oncogenic transformation [179]. CAF-derived exosomes (CDEs) promote cancer cell growth by inhibiting mitochondrial oxidative phosphorylation,

Introduction

thereby increasing glycolysis and glutamine-dependent reductive carboxylation in cancer cells [180]. CDEs can enhance cancer growth and spread through EMT. They can also mediate the interaction between tumour and immune cells to induce immunosuppression and immune tolerance [181].

Moreover, it's important to highlight that cancer cells can employ various strategies to evade the immune system. One major approach involves hindering the function of antigen-presenting cells or cytotoxic cells, directly preventing their recognition, and activating immunosuppressive cells. Some studies have shown that CSCs release exosomes containing RNA and proteins to participate in T-cell-mediated immune surveillance evasion [182]. Some researchers showed that CSC-Exos were rich in immunosuppressive proteins, such as programmed death ligand 1 (PD-L1). PD-L1 is highly expressed on the surface of tumour cells and binds to its surface receptor to inhibit T-cell activation, causing cancer cells to evade anti-tumour immunity [183].

In hypoxic conditions, tumor cells can release exosomes that carry transforming growth factor beta (TGF- β), potentially promoting Treg cell activity while inhibiting NK cell cytotoxicity, ultimately creating an immunosuppressive environment. Treg cells may impede antigen-presenting cell maturation by expressing CTLA-4 or by producing inhibitory cytokines, actively contributing to tumor development and progression [184–186].

4.2.1.1. Exosomes role in tumor angiogenesis

One of the fundamental processes that characterize cancer progression is the angiogenesis [187], which consists of the growth of new blood vessels [188]. Oxygen deprivation is a primary factor responsible for triggering tumor angiogenesis. The tumor's vascular microenvironment plays a significant role in stimulating the metabolism of tumor cells, prompting the release of crucial angiogenic growth factors. These growth factors are essential for activating the microvasculature [189]. The newly formed blood vessels supply the tumor with vital nutrients and oxygen, facilitating its growth and enabling cancer cells to detach from their primary site and disseminate through the bloodstream to distant organs [187].

Tumor cells actively generate, release, and harness exosomes to stimulate proliferation, migration, and angiogenesis. Exosomes derived from tumor cells are potent angiogenic regulators, as they transport specific proteins that can be taken up by endothelial cells, thereby influencing their angiogenic capabilities in response to the cargo carried by the exosomes they internalize [190–192].

4.2.2. EXOSOMES IN METASTATIC NICHES

Exosomes have been shown to play a prominent role in priming specific organs as premetastatic niches, favoring sites for future dissemination and metastatic seeding [193]. In addition, tumor-derived exosomes may contain specific integrins that determine their organotropism

Introduction

[194]. It has been shown that exposure to certain traditional cancer treatments can alter the content and function of exosomes concerning the pre-metastatic niche. In 2018, *Keklikoglou et al.* observed that extracellular vesicles released by breast cancer cells following exposure to chemotherapeutic drugs played a role in promoting the formation of a pre-metastatic niche in the lungs. This was achieved by the presence and transferring of exosomal annexin 6 to induce Ccl2 [195].

In the context of tumor heterogeneity, exosomes are pivotal components, as they govern interactions among subclones of cancer cells with varying metastatic potentials. In simpler terms, this means that exosomes derived from the most aggressive cells may have the ability to expedite tumor progression within a heterogeneous primary tumor by activating distinct signaling pathways in the recipient cells [196].

Notably, the process of EMT plays a crucial role in the initial phases of metastasis. It is characterized by the loss of cell polarity and cell-cell adhesion in epithelial cells, along with an increase in the migratory and invasive capabilities of mesenchymal stem cells [197]. Tumour-derived exosomes may promote the initiation and progression of metastasis by targeting EMT-related factors. Specifically, exosomes can trigger an EMT process through MAPK/ERK signalling [198].

This process can disrupt endothelial stability by causing the loss of VE-cadherin, leading to endothelial hyperpermeability. Inside the tumor, exosomes released by aggressive subclones play a role in accelerating tumor

Introduction

progression by spreading malignant properties. These properties affect both tumor cell plasticity and endothelial cell behavior. As a result, tumor cell-derived exosomes can enhance the metastatic process by not only promoting the formation of pre-metastatic niches that facilitate tumor growth at secondary sites but also by speeding up the initial stages of the metastatic cascade right within the primary tumor where these subclones coexist [196].

The above-mentioned findings highlight that exosomes are capable of carrying relevant information about the aggressiveness of a tumor. Potentially, this means that by studying these microvesicles, we could predict whether the disease will lead to a metastatic process or not, before it occurs. This predictive value as biomarkers makes exosomes key tools for the study and treatment of this type of cancer.

4.2.3. EXOSOMES IN TUMOR PROLIFERATION AND CHEMORESISTANCE

In order to proliferate rapidly, cancer cells require a significant amount of energy. Oxidative phosphorylation, although efficient, is too slow to meet the high energy demands of tumor cells. As a result, a metabolic shift from oxidative phosphorylation to glycolysis is initiated [199].

Exosomes have been found to enhance the growth rate of lung cancer cells by promoting glycolysis. In a study analyzing exosomes from irradiated lung cancer cells, researchers identified elevated levels of exosomal ALDOA and

Introduction

ALDH3A1, which were linked to the stimulation of glycolysis, ultimately leading to increased cell proliferation [200].

Furthermore, macrophages can release exosomes with tumor-promoting properties. *Wang et al.* (2020) demonstrated that macrophage-derived exosomes enhance glycolysis, contributing to the resistance of lung cancer cells to cisplatin chemotherapy. Molecular pathway analysis revealed that these exosomes contained high levels of specific miRNAs that reduced NEDD4L expression and stabilized c-Myc, further promoting glycolysis [201]. Moving on to a different aspect, the *STAT3* signaling pathway is considered oncogenic as it suppresses apoptosis, encourages cell cycle arrest, and promotes epithelial-mesenchymal transition (EMT), leading to increased growth and metastasis [202]. *STAT3* expression has been shown to be associated with a worse prognosis in patients with different types of cancer [203,204]. In addition, intercellular transfer of this marker through exosomes can contribute to the development of acquired drug resistance [205].

Chemoresistance has become a major obstacle in cancer treatment. An interesting point in this process is that exosomes may be involved in the inactivation of chemotherapeutic agents that initiate drug resistance [206]. Furthermore, exosomes can induce the egress of some molecules (such as cisplatin) from tumour cells under hypoxic conditions, demonstrating that they can prevent their internalisation. In this case, overexpression of *STAT3* under hypoxic conditions has been shown to be crucial for the release of

exosomes and the triggering of cisplatin resistance in some tumour types [207].

Moreover, exosomes can reduce effective drug utilisation by increasing their outflow. For this purpose, ATP-binding cassette (ABC) transporter proteins are ATP-driven pumps responsible for transferring drugs to the outside of the cell [208]. Some authors [209] found that chemoresistant breast cancer cells can transmit P-gp to sensitive cells via CSC-exosomes, making the sensitive cells resistant to chemotherapy. Diverse studies have shown that CSC-exosomes has the ability to horizontally transfer drug resistance by transmitting genetic material, which can cause sensitive cells to become resistant [210,211].

4.3. NSCLC-DERIVED EXOSOMES

Having discussed the role of exosomes in the primary processes of disease development, this section will now concentrate on their utility as diagnostic and prognostic biomarkers and their current application in clinical practice, particularly in lung cancer.

As previously mentioned, liquid biopsy involves the detection of tumor-related biomarkers extracted from bodily fluids, offering a minimally invasive and more comprehensive approach for early detection and investigation of the tumor's molecular profile. As a result, alternative diagnostic methods are currently under exploration.

Introduction

To date, the majority of exosomal biomarker studies in lung cancer are based on small RNAs such as miRNAs or lncRNA. Several publications in recent years have highlighted the role of some exosomal miRNAs as tools to discriminate between healthy patients and individuals with lung cancer [212–214]. In parallel, *Li et al.* (2019) postulated that low levels of the non-coding RNA GAS5 (growth arrest-specific transcript 5) detected in exosomes by liquid biopsy, can be used for the identification of NSCLC [215]. In many cases, these biomarkers, detected in blood with high sensitivity, can be detected at early stages of NSCLC. However, other type of biomarkers present in exosomes can provide valuable information for the clinical management of these patients. Some specific proteins detected in plasma exosomes, such as CD151, CD171 and tetraspanin 8, have been found to be higher in lung cancer patients irrespective of histological subtypes when compared to healthy controls [216].

Furthermore, exosomal biomarkers have been associated with some of the most common histologies in this type of cancer. For instance, a study by *Jin et al.* in 2017 revealed specific exosomal miRNAs in lung cancer patients, such as miR-181-5p, miR-30a-3p, miR-30e-3p, and miR-361-5p, which were linked to adenocarcinoma, as well as miR-10b-5p, miR-15b-5p, and miR-320b for patients with LUSC. These findings were identified through next-generation sequencing (NGS) and demonstrated diagnostic accuracy [217].

Regarding prognosis, certain exosomal biomarkers can predict treatment response. For instance, in *ALK*-positive NSCLC patients, reduced plasma exosome levels of Tim-3 and Galectin-9 are indicative of a positive response

Introduction

to first-generation *ALK*-TKIs [218]. In addition, it has also been shown that the presence of some exosomal markers in patients may be a potential clue for predicting the efficacy of immunotherapy in advanced NSCLC [219] or unexpected responses to radiotherapy, such as toxicity [220]. Meanwhile, downregulation of serum exosome miR-146a-5p indicates poor progression-free survival (PFS) and predicts the effect of cisplatin on NSCLC [221].

Moreover, some exosomal membrane-bound proteins such as NY-ESO-1, PLAP, EGFR, Alix and EpCam have been correlated with overall survival (OS) in NSCLC. These and other exosomal elements have been implicated in the prognosis of NSCLC patients in recent years [222–224].

Currently, research on biomarkers for NSCLC is primarily in the pre-clinical phase. While promising results are emerging, suggesting their potential use in screening programs and as prognostic/predictive biomarkers, several barriers hinder their clinical translation. Among the key challenges are the absence of reliable cut-off points and the significant variability between studies [225]. Moreover, a major obstacle is the lack of an approved tool for isolating exosomes from clinical samples up to this point.

To make the quantum leap, large-scale prospective clinical trials are needed to demonstrate their clinical utility. Clinical trials play a key role in the translational application of exosomes as a diagnostic, prognostic and therapeutic tool.

Introduction

A search carried out on <https://clinicaltrials.gov/ct2/search> in June 2023, shows about 13 trials that are related to exosomes in NSCLC.

It is probable that as more of these findings emerge and the aforementioned questions are addressed, exosomes (as part of liquid biopsy) will indeed emerge as a promising marker in the field of lung cancer in the near future.

II. HYPOTHESIS AND OBJECTIVES

Hypothesis & Objectives

The hypothesis proposed in this work is founded on several key premises:

Lung cancer remains the primary global cause of cancer-related mortality, exhibiting a disheartening 5-year survival rate of less than 15%. With advancements in clinical management, the demand for improved diagnostic, prognostic, and predictive biomarkers is crucial. Ideally, these biomarkers should provide non-invasive methods, enabling continuous patient monitoring throughout the disease. Liquid biopsy has emerged as a promising approach. Extracellular vesicles, and in particular exosomes, harbor essential genetic information and have the ability to transfer it to different parts of the body via internalization into neighboring cells. Beyond their role in cellular communication, exosomes actively participate in various tumor-related processes, including promoting malignancy, facilitating angiogenesis, and aiding immune system evasion.

Hypothesis: The study of exosomes secreted in NSCLC offers significant insights into the molecular characteristics of this disease, enabling the discovery of prognostic and predictive biomarkers. Their isolation from minimally invasive samples and high sensitivity render exosomes a valuable tool for diagnoses and monitoring lung cancer patients.

Main objective: The primary objective of this thesis work is to characterize and analyze NSCLC exosomes obtained from cell cultures and peripheral blood samples. This aims to advance our understanding of the disease

Hypothesis & Objectives

mechanisms and to identify potential biomarkers that could significantly improve the clinical management of NSCLC patients.

The **specific objectives** established are the following:

- 1) Evidencing the presence of exosomes in the supernatant of cell cultures and peripheral blood samples of NSCLC patients; quantification and morphological characterization of the obtained exosomes.
- 2) Detecting the presence of exosomal surface markers to validate the sample's nature and determine the most abundant in NSCLC.
- 3) Analyzing in these tumor exosomes the expression of relevant biomarkers and signaling pathways aiming to comprehend and identify the molecular mechanisms involved in modulating the disease.
- 4) Evaluating the association between the different markers obtained in exosomes with the clinicopathological NSCLC variables and patients' prognosis.
- 5) Determining the presence of the most frequent alterations of this pathology in exosomes.
- 6) Integrating the findings of the proposed exosomal markers and evaluating their clinical significance as potential biomarkers in the management of NSCLC.

III. MATERIALS AND METHODS

1. MATERIALS

1.1. RECRUITED PATIENTS

The study was conducted in accordance with the Declaration of Helsinki, and the protocol was approved by the Ethical Review Board of the General University Hospital of Valencia. Demographic and clinicopathologic characteristics were collected for all patients recruited for the study. Follow-up was performed according to the institutional standards for resected NSCLC.

Informed consent was obtained from each donor prior to sample collection. The study was approved by the Institutional Review Board of the General Hospital and was conducted in accordance with the International Code of Ethics for Biomedical Research Involving Human Subjects (CIOMS).

1.1.1. TISSUE SAMPLES

This study included 186 patients from the General University Hospital of Valencia who underwent surgery between 2004 and 2016. Lung tumor samples were obtained at the time of surgery and met the following eligibility criteria: candidate for surgical resection, untreated, older than 18 years, not pregnant, stage I-IIIa (according to the American Joint Committee on Cancer staging manual) with a histological diagnosis of NSCLC. A subset of patient tumor samples was processed immediately for primary culture establishment,

Materials & Methods

and the remainder were stored in RNAlater (Applied Biosystems, USA) at -80°C until further analysis.

1.1.2. BLOOD SAMPLES

Peripheral blood samples were collected from 50 patients with NSCLC in 10 ml EDTA K2 tubes (BD Vacutainer®, Plymouth, UK). Blood samples were delivered to the laboratory and immediately centrifuged at 2,000 x g for 10 min at room temperature (RT). The supernatant was collected and centrifuged at 1,500 x g for 10 min at RT to remove dead cells and debris (including platelets and fibrin). Cell-free plasma was used immediately or aliquoted into 2-4 ml vials and stored at -80°C until further processing.

1.2. ESTABLISHMENT OF PRIMARY CELL CULTURES

Surgical tumor specimens were washed and minced into small pieces. Tumor dissociation was carried out by enzymatic digestion (1 mg/ml collagenase type IV, 1 mg/ml dispase, and 0.001% DNase, Sigma, St. Louis, USA) for 3 h at 37 °C. Once tumor cells were successfully disaggregated, half of the cells were designated for monolayer culture, while the remaining half was seeded in suspension for the formation of tumorspheres (See section “2.1. *Tumor cell culture growth conditions*” of the Introduction). For this study, 4 well-established patient-derived lung cancer cultures were employed (Table 2).

Materials & Methods

Tumor profiling of each patient-derived culture was determined by next-generation sequencing (NGS) using OncoPrint Focus Assay (ThermoFisher Scientific, USA) and Ion GeneStudio S5 System (ThermoFisher Scientific, USA) to have a complete tumor profiling of each patient's sample.

Table 2. Clinicopathological characteristics of the patients employed for the primary cell cultures establishment.

Patient code ID	Gender	Age (years)	TNM stage	Histology	Smoking status	Progression & exitus	DFS (months)	Tumor mutational status
301	Male	71	IIB (T3N0M0)	LUSC	Former	No	75.50	<i>TP53</i> p.S261V*fs84, <i>PIK3CA</i> p.G118D
343	Female	60	IB (T2aN0M0)	LUAD	Former	Yes	7	<i>TP53</i> p.R158L
435	Male	70	IIB (T3N0M0)	LUAD	Current	No	24	<i>KRAS</i> p.G12C, <i>PIK3CA</i> p.H1047R
471	Female	83	IIA (T2BN0M0)	LUAD	Never	No	27	<i>PIK3CA</i> p.D538N

DFS: disease-free survival, LUAD: lung adenocarcinoma, LUSC: lung squamous cell carcinoma, WT: wild type.

1.3. COMMERCIAL NSCLC CELL LINES

Thirteen human NSCLC cell lines (A549, NCI-H1395, NCI-H1650, NCI-H1975, NCI-H2228, NCI-H358, NCI-H460, HCC-827, NCI-H520, NCI-H1703, LUDLU-1, SK-MES-1, PC9, and SW900) were used for the *in vitro* experiments. LUAD and the LUSC SW900 cell lines were purchased from American Type Culture Collection (ATCC, USA), whereas the rest of the LUSC cell lines were

Materials & Methods

kindly provided by Dr J. Carretero (University of Valencia, Spain) (Table 3). All cell cultures (primary and commercial) were tested for Mycoplasma before the initiation of the experiments and repeated periodically.

Table 3. Main characteristics of the cell lines included in the study.

Cell Line	Gender	Age (years)	Histology	Relevant mutations
NCI-H1650	Male	27	LUAD	<i>EGFR</i> p.E746_A750del
NCI-H1975	Female	UK	LUAD	<i>EGFR</i> p.L858R+ p.T790M, <i>PIK3CA</i> p.G118D, <i>TP53</i> p.R273H
NCI-H2228	Female	UK	LUAD	<i>EML4-ALK fusion</i> , <i>TP53</i> p.Q331*, <i>RB1</i> p.E204fs*10
NCI-H358	Male	UK	LUAD	<i>KRAS</i> p.G12C
A549	Male	58	LUAD	<i>KRAS</i> p.G12S
HCC-827	Female	39	LUAD	<i>EGFR</i> p. E746_A750del, <i>TP53</i> p.V218del
NCI-H1395	Female	55	LUAD	<i>BRAF</i> p.G469A
PC-9	Male	UK	LUAD	<i>EGFR</i> p.E746_A750del, <i>TP53</i> p.R248Q
SW900	Male	53	LUSC	<i>KRAS</i> p.G12V, <i>TP53</i> p.Q167*
NCI-H520	Male	UK	LUSC	<i>TP53</i> p.W146*
NCI-H1703	Male	54	LUSC	-
SKMES-1	Male	65	LUSC	<i>TP53</i> p.E298*
LUDLU-1	Male	72	LUSC	<i>TP53</i> p.R248W

LUAD: adenocarcinoma, LUSC: squamous cell carcinoma, UK: unknown.

2. METHODS

2.1. CELL CULTURE GROWTH CONDITIONS

Tumor cells growth in monolayer (2D cultures) were cultured in DMEM-F12 (primary cultures) or RPMI-1640 (commercial cells lines) containing 10% FBS, 200 µg/ml penicillin/streptomycin, 2 mM L-glutamine (for DMEM-F12), and 0.001% non-essential amino acids (for RPMI-1640). To generate tumorspheres (3D cultures), cells cultivated in a monolayer were trypsinized at 80% confluence using 0.05% trypsin-EDTA. These cells were then seeded at a low density in ultra-low attachment flasks (Corning, USA) containing serum-free medium (a mixture of DMEM-F12 and RPMI-1640) supplemented with 0.4% BSA, 50 µg/ml EGF, 20 µg/ml bFGF, 5 µg/ml ITS PREMIX, 2% B27, and 200 µg/ml penicillin/streptomycin (Gibco™, USA).

2.2. EXOSOMES CHARACTERIZATION

2.2.1. EXOSOME ISOLATION FROM CELL CULTURES

To isolate tumor-derived exosomes obtained from cell cultures, cells were grown in T175 cm² flask until 70-80% confluence during 72 hours, in 30 ml of FBS-depleted media (in case of monolayer cultures). After 72 hours, supernatant was differentially centrifuged at 500 g for 5 minutes, and then at 3,000 g for 20 minutes to eliminate cell detritus. Afterwards, the supernatant was filtered through a 0.2 µm filter (Corning, USA), and ultracentrifuged at

Materials & Methods

110,000 g for 1:45h (CP-NX, P50AT2 Rotor; Hitachi, Japan). A second ultracentrifugation was performed to wash the first pellet obtained; exosomes were resuspended in 30 ml of PBS. All centrifugations were performed at 4°C. Finally, exosomes were resuspended in a small volume (30-60 µl) of filtered-PBS and stored at -80°C until the corresponding analysis (Figure 15).

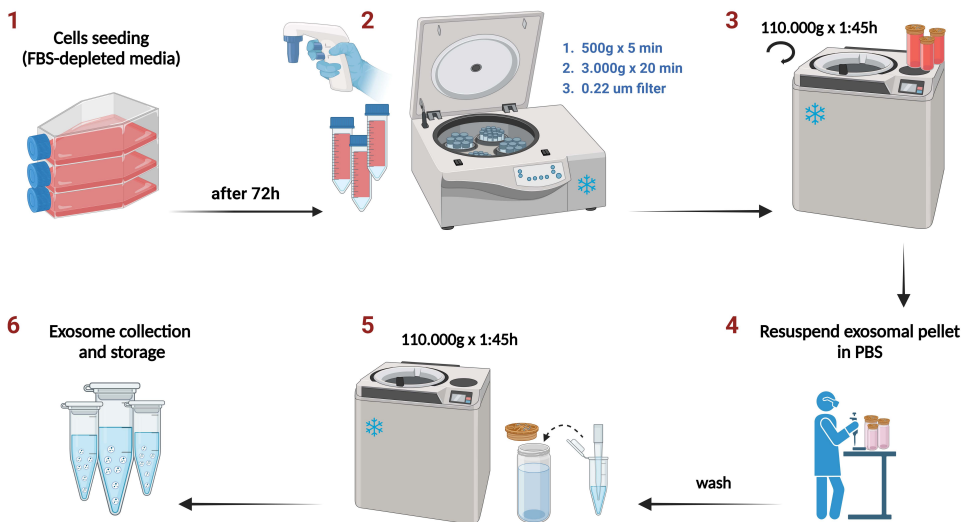


Figure 15. Graphic scheme of the methodology used in the isolation of exosomes secreted *in vitro*. (Own design created with BioRender.com)

2.2.2. EXOSOMES ISOLATION FROM PLASMA SAMPLES

Before isolation of exosomes, each aliquot of plasma was centrifuged at 3,000 g for 10 min at 4°C, discarding any type of sediment to ensure complete removal of cell debris and macrovesicles. Exosomes were isolated from 500-600 µl of NSCLC plasma by ExoGAG (Nasas Biotech, Spain). In this

case, plasma samples were incubated with 1-1.2 ml of ExoGAG reagent (NasasBiotech, Spain) during 5 min at 4°C. EVs were collected by centrifugation at 16,000 g during 15 min at 4°C (Eppendorf, Hamburg, Germany) and resuspended in PBS.

2.2.3. NANOPARTICLE TRACKING ANALYSIS (NTA)

Size distribution and concentration of isolated exosomes were measured using a NanoSight NS300 instrument (Malvern Instruments, Ltd., Malvern, UK). The instrument was calibrated using silica microspheres of different diameters prior to sample analysis. To perform the measurements, samples were diluted uniformly 10 to 100-fold in 0.1 µm-filtered PBS solution, to reduce the number of particles in the field of view to fewer than 100 per frame. This technique combines laser light scattering microscopy with a charge-coupled device (CCD) camera, which enables the visualization and recording of nanoparticles in solution (Figure 16).

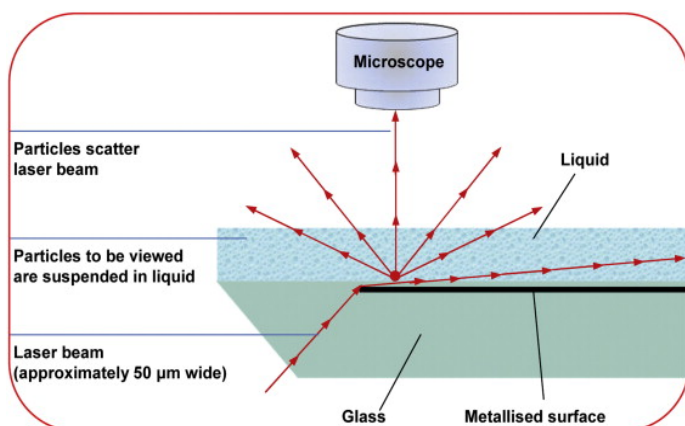


Figure 16. Graphical scheme of the operation of the Nanosight instrument [226].

Materials & Methods

The NTA software is then able to identify and track individual nanoparticles moving under Brownian motion and relates the movement to a particle size according to the following formula derived from the Stokes-Einstein equation [227]

$$\overline{(\mathbf{x}, \mathbf{y})^2} = \frac{2k_b T}{3R_h \pi \eta}$$

where k_b is the Boltzmann constant and $\overline{(\mathbf{x}, \mathbf{y})^2}$ is the mean-squared speed of a particle at a temperature T , in a medium of viscosity η , with a hydrodynamic radius of R_h .

Readings were taken 5 times during 60 seconds at 10 frames per second at room temperature. Approximately 3×10^8 particles/ml sample were conducted to assess the size distribution and concentration. Data was analyzed using nanoparticle tracking analysis software v3.1 with camera level set to 10 and detection threshold to 5 (Malvern Instruments Ltd. Amesbury, UK).

2.2.4. NEGATIVE-STAINING AND TRANSMISSION ELECTRON MICROSCOPY OF EXOSOMES

Six μl of exosomes resuspended in PBS were placed onto Formvar carbon-coated grids and contrasted with 2% uranyl acetate. Sample preparations were visualized using a FEI Tecnai G2 Spirit transmission electron microscope (FEI Europe, Netherlands). Imaging was performed using a Gatan

Materials & Methods

UltraScan US1000 CCD camera and data was analyzed with Digital Micrograph 1.8 (Gatan, Ametek, USA).

2.2.5. IMMUNOBLOTTING

Cell lines and isolated exosome pellets were lysed using a lysis buffer composed by: 50 mM Tris-HCl pH 7.5, 150 mM NaCl, 0.02% NaN₃, 0.1% sodium dodecyl sulfate (SDS), 1% NP40, 0.5% sodium deoxycholate, 2 mg/ml leupeptin, 2 mg/ml aprotinin, 1 mM phenylmethylsulfonyl fluoride (PMSF), and protease inhibitor cocktail (Roche, Switzerland). Bradford assay (Pierce, Rockford, USA) was employed to quantify the total protein concentration. 25 µg of total protein were separated on 10% SDS–polyacrylamide gel and electro-transferred to a 0.45 µm polyvinylidene difluoride (PVDF) membrane (Millipore, USA). The membrane was then blocked with 5% skim milk for 1 h and immunoblotted overnight at 4°C with CD9 anti-rabbit (Abcam, UK), TSG101 anti-mouse (Abcam, UK), Calnexin anti-rabbit (Abcam, UK), and β-actin anti-mouse (Sigma-Aldrich, USA). Afterwards, membranes were incubated with anti-IgG (whole molecule)-Peroxidase secondary antibodies (Sigma-Aldrich, USA; Thermo Fisher Scientific, USA) during 1h at room temperature (Supplementary Table 3). For chemiluminescent detection, the high sensitivity Amersham ECL Select™ detection reagent (GE Healthcare, USA) was used.

2.2.6. FLOW CYTOMETRY ANALYSIS

Isolated exosomes were incubated for 1h with human CD81-PE and human CD63-APC antibodies (Miltenyi Biotech, USA) (Table 4) in PBS. Negative control for background fluorescence was performed using the same antibodies incubated in PBS. After incubation, exosomes were acquired using FC500 MPL Flow Cytometer and CytExpert v2.3 software (Beckman-Coulter, Inc., USA). Finally, samples with positive staining for the antibodies of interest were treated with Triton 0.01% for 15 min at RT to lyse exosome's lipid bilayer. This point was performed to confirm that previously obtained signal mostly disappears, and could serve as a control to dismiss positivity due to cell debris.

Table 4. List of antibodies used for immunoblot (IB), immunofluorescence (IF) and flow cytometry (FC) analysis.

Antibody	Dilution	Catalog n°	Supplier	Technique
B-Actin Anti-Mouse mAb (Clone AC-15)	1:10.000	A5441	Sigma-Aldrich	IB
Calnexin Anti-Rabbit pAb	1:1000	Ab75801	Abcam	IB
CD9 Anti-Rabbit mAb (Clone EPR2949)	1:500	Ab92726	Abcam	IB
TSG101 Anti-Mouse mAb (Clone 4A10)	1:200	Ab83	Abcam	IB
Anti-Mouse IgG (whole molecule)- Peroxidase	1:2000	A9044	Sigma-Aldrich	IB
Anti-Rabbit IgG (whole molecule)- Peroxidase	1:2000	Sc-2313	Santa Cruz Biotec.	IB
XAGE1 Anti-Goat pAb	1:100	Ab27477	Abcam	IF
CABYR Anti-Rabbit pAb	1:100	Ab243417	Abcam	IF
Alexa Fluor 555 Anti-Rabbit IgG (H+L)	1:1000	A-31572	Thermofisher	IF
Alexa Fluor 488 Anti-Goat IgG (H+L)	1:1000	A-11078	Thermofisher	IF
CD63-APC (Clone REA1055)	1:50	130-118-151	Miltenyi Biotec.	FC
CD81-PE (Clone REA513)	1:50	130-118-481	Miltenyi Biotec.	FC

2.3. NUCLEIC ACIDS ISOLATION

2.3.1. RNA ISOLATION AND INTEGRITY

2.3.1.1. Exosomes from cell cultures

RNA from cell culture pellets and tumor frozen tissue samples was extracted using standard TRI Reagent® RNA Isolation Reagent, (Sigma-Aldrich, USA) method. Exosomal total RNA derived from cells cultures was isolated using the Total RNA Purification Kit (Norgen Biotek, Canada). RNA integrity and concentration were assessed with the Agilent 2100 Bioanalyzer (Agilent, USA), using RNA 6000 Nano and Pico Kit (Agilent, USA).

2.3.1.2. Exosomes from plasma

The exoRNeasy Midi Kit (Qiagen, Germany) was used to enrich for EVs from 600 µl plasma, according to the manufacturer's instructions. In the exosome purification stage, prefiltered sample (with particles larger than 0.2 µm excluded) is mixed with Precipitation Buffer and bound to an exoEasy membrane affinity spin column. The bound exosomes are washed and then lysed with QIAzol. In the RNA extraction step, chloroform is added to the QIAzol eluate, and the aqueous phase is recovered and mixed with ethanol. Total RNA, including miRNA, binds to the spin column, where it is washed three times and eluted.

To remove co-isolated DNA from the resuspended RNA, the DNA-free™ DNA Removal Kit (Thermo Fisher Scientific, USA), was used according to

Materials & Methods

manufacturer instructions. In short, 1 μ l DNase buffer and 0.5 μ l enzyme were added to 7.5 μ l RNA sample, followed by incubation at 37°C for 30 min and DNase removal.

2.3.1.3. Fresh tissue from NSCLC cohort

RNA isolation was carried out using Tri Reagent® (Invitrogen) according to the manufacturer's instructions. For tumor samples, a piece of 10-20 mg of tissue was dissected and 1 ml of Tri Reagent® was added. Samples were homogenized using TissueLyser (Qiagen) and 200 μ l of chloroform was added in order to separate the aqueous phase containing the RNA. Isopropanol was used to precipitate the nucleic acids and ethanol was used for washing. Total RNA was dissolved in nuclease-free water and stored at -80°C until further analysis.

2.3.2. DNA ISOLATION FROM CELL CULTURES/PLASMA-DERIVED EXOSOMES

DNA was extracted from exosomes using QIAamp DNA Micro kit (Qiagen, Germany) according to the manufacturer's instructions. DNA concentration was quantified using Qubit dsDNA high sensitivity assay, according to the manufacturer's protocol (Thermo Fisher Scientific, USA).

2.4. ANALYSIS OF THE MUTATIONAL STATUS

2.4.1. EXOSOMAL MUTATIONAL STATUS FROM ESTABLISHED NSCLC CULTURES

2.4.1.1. Mutational status determination by BEAMing digital PCR

For *EGFR*, *KRAS* and *BRAF* DNA mutation analysis, BEAMing digital PCR technique (Beads, Emulsions, Amplification, and Magnetics) (Sysmex Inostics, Inc., USA) was used (Figure 17).

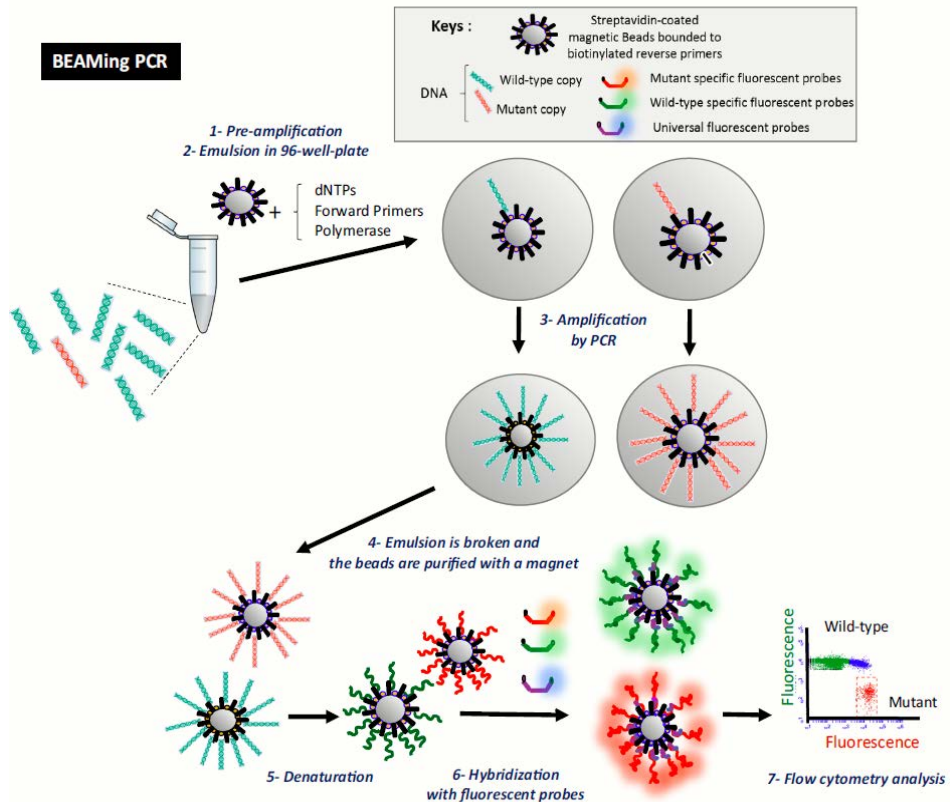


Figure 17. BEAMING dPCR operation scheme. Adapted from [228]. BEAMing is an emulsion PCR-based method. It involves the use of streptavidin-coated magnetic beads bounded to biotinylated reverse primers inside the compartments, to ensure that one strand of the PCR

Materials & Methods

product binds to the beads. After amplification, each compartment contains a bead coated with thousands of copies of the single DNA molecule originally present. A magnet can be used to retrieve these beads. BEAMing beads accurately reflect the diversity of DNA present in the template populations. The Universal Probe is used to distinguish between beads that contain PCR product and those that do not by binding to an amplicon outside the target region. Using this method, it is possible to identify what proportion of a DNA population contains a particular mutation. The signal-to-noise ratio of hybridization or enzymatic assays is extremely high because each bead contains thousands of molecules with an identical sequence. Finally, using flow cytometry, millions of beads can be analyzed in a matter of minutes, obtaining a digital PCR diagram where the different populations (wild type and mutant) are arranged. **PCR: polymerase chain reaction; dNTP deoxynucleotide triphosphate.**

2.4.1.2. Detection of *ALK* rearrangements by RT-qPCR

Starting from the exosomal RNA previously extracted, *ALK* gene rearrangements were determined by the *ALK* Gene Fusions and *ROS1* Gene Fusions Detection Kit (Amoy Diagnostics, China), mRNA was transcribed to cDNA at 42°C for 1 hour and the gene fusion was readily detected by quantitative real time PCR (RT-qPCR), according to the manufacturer's protocol.

2.4.2 EXOSOMAL MUTATIONAL STATUS FROM BLOOD SAMPLES OF NSCLC PATIENTS

To identify *KRAS* and *EGFR* mutations in human exosomal DNA, digital PCR was performed using Taqman SNP Genotyping assays (Table 5) on the Quantstudio 3D system (Thermofisher, USA) according to manufacturer's instructions. Samples concentration greater than 3 ng/μl of DNA was diluted

Materials & Methods

in elution buffer to ensure proper cluster separation during analysis. The functional abundance was calculated and reported as a percentage using the formula below [229]:

$$\text{Funct. Abundance (\%)} = \frac{\text{Total n}^{\circ} \text{ of mutant alleles}}{\text{Total n}^{\circ} \text{ of alleles}} - \text{Average false positive rate}$$

Table 5. TaqMan® Assays used in dPCR for mutational status determination.

Assay ID	Gene	COSMIC ID	Exon	Nucleotide mutation	Amino acid change	Genome location
Hs000000026_rm	<i>EGFR</i>	6224	21	c.2573T>G	p.L858R	chr.7 55191822 GRCh38
Hs000000029_rm	<i>EGFR</i>	6240	20	c.2369C>T	p.T790M	chr.7 55181378 GRCh38
Hs000000047_rm	<i>KRAS</i>	516	2	c.34G>T	p.G12C	chr.12 25245351 GRCh38
Hs000000056_rm	<i>KRAS</i>	532	2	c.38G>A	p.G13D	chr.12 25245347 GRCh38

The analysis of the digital PCR data was performed using QuantStudio 3D Analysis Suite, following manufacturer's instructions. The detection limit of the assay was determined using exosomal DNA extracted from cell lines. Also, DNA extracted from NSCLC cell lines and plasma cfDNA samples were used as reference (mutant DNA). False positive rate and threshold (intensity) limit for mutant alleles were determined using wild-type DNA at

Materials & Methods

concentrations representative of that of samples - 4 replicates at 0.1, 0.2 and 0.3 ng/ml for patients (total amounts of DNA = 0.65, 1.3, 1.95 ng, respectively), and 1 and 2 ng/ml for healthy donors (total DNA = 6.5 and 13 ng, respectively). The average false positive rate was calculated from all replicates, and used to calculate the reported functional abundance.

2.5. GENE EXPRESSION ANALYSIS

2.5.1. WHOLE mRNA EXPRESSION PROFILING OF EXOSOMES DERIVED FROM CELL CULTURES

Total RNA was extracted from exosomes derived from H1650, H1975, H2228, SW900, FIS 301, and FIS 343 cell cultures grown in both 2D and 3D conditions. Two distinct biological replicates were analyzed for each sample using the TRI Reagent® RNA Isolation Reagent (Sigma-Aldrich, USA). Subsequently, 13 ng of exosomal RNA underwent amplification, labeling, and hybridization utilizing the Clariom™ D Assay for human (ThermoFisher, USA), following the manufacturer's instructions. Briefly, the cDNA preparation and biotin labeling were conducted using the Affymetrix GeneChip WT Pico Kit. The arrays were then subjected to a 16-hour incubation at 45°C with 60 rpm rotation in an Affymetrix GeneChip 645 hybridization oven. Finally, scanning was performed using an Affymetrix® GeneChip Scanner 3000 7G at a 570nm wavelength excitation (Figure 18).

Materials & Methods

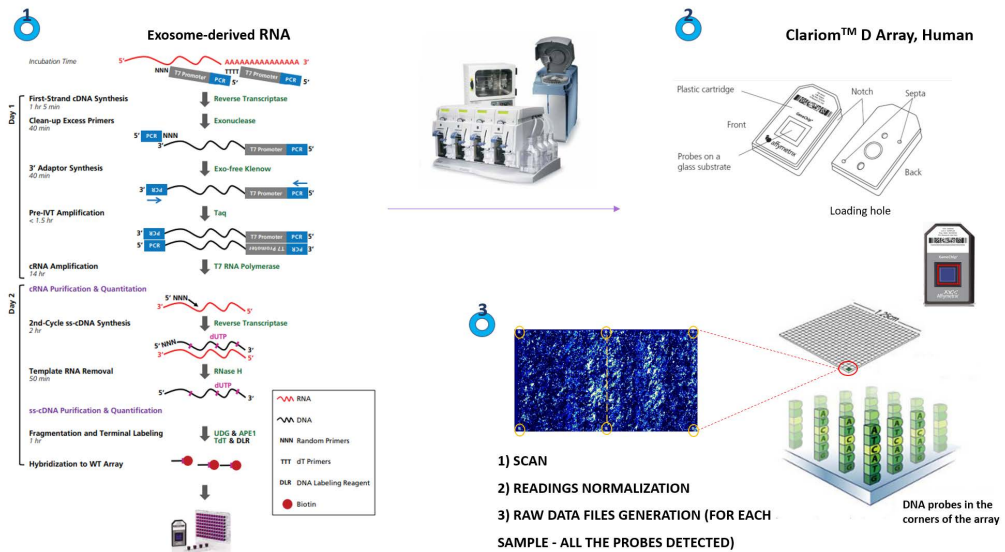


Figure 18. Graphic scheme of the methodology used to carry out the whole genome gene expression microarrays. Starting from exosomal RNA samples until obtaining the results for analysis (Own design).

Input files were normalized to eliminate systematic sources of variation that were not differences in expression (efficiency in colour marking, amount of RNA, and spatial effects of the chip, among others). The robust multiple-array average (RMA) algorithm was calculated using Affymetrix Expression Console and Transcriptome Analysis Console 4.0 software. CEL files were used to analyze significant changes in gene expression profiles and were statistically filtered using Partek Genomic Suite 6.6 software (Partek Inc., USA). Afterwards, a one-way ANOVA was performed and statistically significant genes were identified using a p-value < 0.05. Data are deposited in Gene Expression Omnibus (GEO) – NCBI database: GSE198238.

Materials & Methods

Pathway enrichment analysis was performed on the differentially expressed genes (DEGs) obtained by histology using Pathway Studio. The lists of pathological processes assigned to each of these gene sets were trimmed at approximately 100 lowest p-values ($p < 0.01$), being 4 the minimum of overlapped DEGs for each process. Data were rendered in a bubble plot using the Ggplot² package of R-Studio (RStudio, Inc.).

2.5.2. DIFFERENTIAL GENE EXPRESSION VALIDATION USING RT-QPCR

Reverse transcription–quantitative real time PCR was performed to validate the relative expression of the most significant differentially expressed genes in transcriptome microarrays and reference genes (Table 6). This step was done using a LightCycler®480 II system (Roche, Switzerland). Reverse transcription reactions were performed using 500 ng (cells and tissue samples) and 150 ng (exosomes samples) of total RNA, random hexanucleotides and the High-Capacity cDNA (complementary DNA) Reverse Transcription Kit (Applied Biosystems, USA), following the manufacturer's instructions. RT-qPCR was performed with assays based on hydrolysis probes using 1 μ l of cDNA, 2.5 μ l TaqMan Gene Expression Master Mix and 0.25 μ l TaqMan Gene Expression Assay (Applied Biosystems, USA) in a 5 μ l final reaction volume. To calculate the efficiency, random-primed qPCR Human Reference cDNA (Clontech, USA) was used. *ACTB*, *GUSB*, and *CDKN1B* were selected as endogenous controls using GeNorm software

Materials & Methods

(<https://genorm.cmgg.be/>) for tissue analysis, whereas *ACTB* and *GAPDH* were selected as an endogenous control for exosomes samples. Relative gene expression levels were expressed as the ratio of target gene expression and the geometric mean of the endogenous gene expressions according to *Pfaffl* formula [230].

Table 6. TaqMan® Gene Expression Assays used in RT-qPCR expression analysis.

Gene Symbol	Gene name	Assay ID
<i>ACTB</i> [‡]	Actin, Beta	Hs99999903_m1
<i>GAPDH</i> [‡]	Glyceraldehyde-3-phosphate dehydrogenase	Hs99999905_m1
<i>GUSB</i> [‡]	Glucuronidase, beta	Hs01558067_m1
<i>CDKN1B</i> [‡]	Cyclin-dependent kinase inhibitor 1B	Hs00153277_m1
<i>XAGE1B/E</i>	X Antigen Family Member 1B/E	Hs00220764_m1
<i>CABYR</i>	Calcium Binding Tyrosine Phosphorylation Regulated	Hs00201830_m1
<i>NKX2-1</i>	NK2 Homeobox 1	Hs00968940_m1
<i>SEPP1</i>	Selenoprotein P, plasma, 1	Hs01032845_m1
<i>CAPRN1</i>	Cell Cycle Associated Protein 1	Hs00195416_m1
<i>RIOK3</i>	RIO Kinase 3	Hs01566923_m1
<i>FDFT1</i>	Farnesyl-diphosphate farnesyltransferase 1	Hs00926054_m1
<i>SNAI1</i>	Snail family zinc finger 1	Hs00195591_m1
<i>WNT5A</i>	Wingless-type MMTV integration site family, member 5A	Hs00998437_m1

[‡] reference gene

2.5.3. GENE EXPRESSION PANEL IN PLASMA-DERIVED EXOSOMES

The nCounter[®] Low RNA Input Amplification Kit (NanoString Technologies, USA) was used to retrotranscribe and pre-amplify 4 µl EV-derived RNA from 36 NSCLC plasma samples, using 10 cycles. Retrotranscription was carried out in 0.5 ml tubes while pre-amplification, using primers targeting the genes included in the panel (NanoString Technologies). Reaction was performed in 384-well plates to prevent sample evaporation (NanoString Technologies). Subsequently, exo-cDNA was pre-amplified according to manufacturer instructions and samples were hybridized for 18 h at 65°C (Figure 19). A human custom panel consisting of 30 genes was used to analyze plasma-derived EVs, including biomarkers associated with CSCs population, immune and drug response, proliferation and cell cycle, and other genes associated with lung cancer presented in previous analysis (Table 7).

Materials & Methods

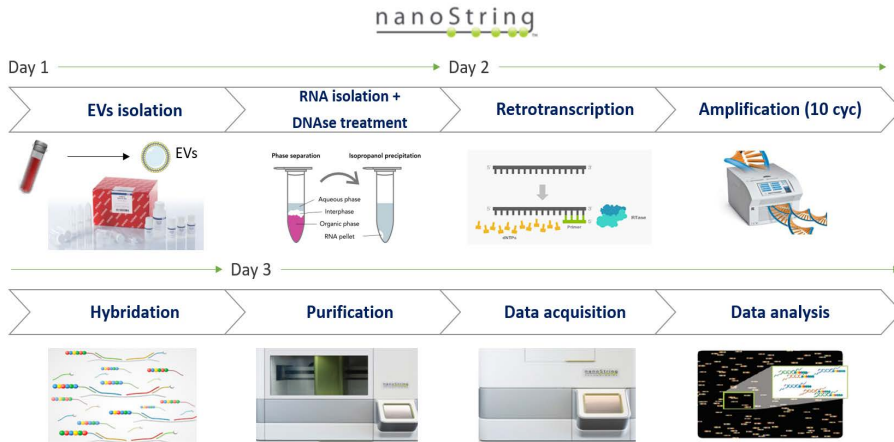


Figure 19. Representation of the workflow required for the analysis of plasmatic EV samples using an nCounter panel. Adapted from [231].

Table 7. Summary of the probes collected in the nCounter panel for their analysis in the plasmatic exosomal RNA samples.

Gene	Accession	Position
ACTB^z	NM_0011101.2	1011-1110
CABYR	NM_153769.2	524-623
CD24	NM_013230.2	1860-1959
CD274	NM_014143.3	502-601
CD44	NM_001001392.1	430-529
CDKN2A	NM_000077.4	560-659
CTNNB1	NM_001098210.1	1816-1915
CXCL8	NM_000584.2	26-125
CXCR2	NM_001557.2	2056-2155
EPCAM	NM_002354.1	416-515
FDFT1	NM_001287742.1	1696-1795
GAPDH^z	NM_001256799.1	387-486
IFITM1	NM_003641.3	483-582
LGALS3	NM_001177388.1	496-595
MICA	NM_000247.2	1064-1163
MMP13	NM_002427.2	952-1051
MMP9	NM_004994.2	1531-1630
NKX2-1	NM_003317.3	2012-2111

Materials & Methods

<i>RIOK3</i>	NM_003831.3	1921-2020
<i>RPL19</i>	NM_000981.3	316-415
<i>RPL7A</i>	NM_000972.2	67-166
<i>S100A2</i>	NM_005978.3	568-667
<i>SNAI1</i>	NM_005985.2	64-163
<i>SOX2</i>	NM_003106.2	152-251
<i>STAT1</i>	NM_007315.3	1796-1895
<i>STAT3</i>	NM_003150.3	2061-2160
<i>STK31</i>	NM_031414.2	2301-2400
<i>TP63</i>	NM_003722.4	1296-1395
<i>WNT5A</i>	NM_003392.3	476-575
<i>XAGE1B</i>	NM_001097604.2	401-500

≠ reference gene

2.5.3.1. Data normalization and analysis

Raw nCounter counts of expressed genes were normalized in R and R-studio v3.6.3 using the R package NanoStringNorm [232]. Normalization was performed following several steps: technical assay variability normalization using the geometric mean of the positive control probes, background correction using the mean plus two times standard deviation (SD) of the negative control probes, and sample content normalization using the total amount of counts for each sample. Normalized counts were \log^2 -transformed, and used for differential expression (DE) analysis. \log^2 fold change (FC) of each gene was calculated as the ratio of average \log^2 transformed counts of the cancer patient cohort vs. the housekeeping genes included. Heatmap was used to visualize \log^2 FC values of each gene included in the panel (on the y-axis), corresponding to the different patients analyzed (on the x-axis).

2.6. IMMUNOFLUORESCENCE ANALYSIS

Cells were fixed in 4% paraformaldehyde in PBS at room temperature for 15 min, washed with PBS, permeabilized with 0.4% Triton X-100 in PBS for 10 min, and washed again with PBS. Permeabilized cells were blocked with PBS containing 1% BSA for 1 h, and subsequently incubated with XAGE1 anti-goat [1:100] (Abcam, UK) and CABYR anti-rabbit [1:100] (Abcam, UK) antibodies in blocking buffer overnight at 4°C. Thereafter, cells were washed with PBS and incubated with Alexa-labelled IgG secondary antibodies (Table 4) for 1h. Slides were incubated with 4',6-diamidino-2-phenylindole for 3 min, mounted with Fluoromount Aqueous Mounting Medium (Sigma-Aldrich, USA), and analyzed using a Leica confocal microscope (Leica Microsystems, USA).

2.7. IMMUNOHISTOCHEMICAL ANALYSIS

Sections 4 µm thick were obtained from the most representative formalin-fixed, paraffin-embedded block of each NSCLC tumor for analysis. Immunohistochemical staining was performed using standard technique of antigen retrieval and development of avidin-biotin-peroxidase complexes (ABC). Briefly, 4-µm tissue sections were deparaffinised in xylene and mounted on Poly-L-lysine-coated slides. All slides were subjected to a heat-based antigen retrieval method using DAKO Target Retrieval Solution (Agilent, USA), containing 10 mM citrate buffer (pH 6) and a water bath (95–99°C) for

Materials & Methods

approximately 20 minutes before immunostaining. Primary antibody to TTF-1, DAKO clone 8G7G3/1 (Agilent, USA) at manufacturer's recommendation dilution (1:200) was used. Slides were counterstained with hematoxylin. Sections of TTF-1-positive LUAD were used as positive control. The primary antibody was replaced by diaminobenzidine (3,3'-diaminobenzidine) solution for the negative controls. TTF-1 nuclear staining was graded as negative (<5%), weak positive + (5–49%), and strong positive ++ (>50%) based on the percentage of tumor nuclei with unequivocal staining.

2.8. IN SILICO DATASET VALIDATION

In silico analysis was performed using different lung cancer datasets from The Cancer Genome Atlas (TCGA) consortium [233,234]. RNA-seq data and clinical information were downloaded from the ICGC Data Portal:

<https://dcc.icgc.org/releases/current/projects/LUAD-US>

<https://dcc.icgc.org/releases/current/projects/LUSC-US>.

Limma package from Bioconductor was used to obtain normalized RNA-seq data. Fit linear models for the genes were obtained before constructing the different contrast matrixes. Given the linear models, Empirical Bayes statistics were computed for differential expression analysis.

2.9. STATISTICAL ANALYSIS

Non-parametric Mann–Whitney U and Kruskal–Wallis tests were used to compare continuous variables; Spearman’s rank test was used to assess correlations between continuous variables, whilst the association between discrete variables was evaluated by the χ^2 test. Survival analyzes were performed using univariate Cox regression analysis and Kaplan–Meier (log-rank) test method with clinical pathological variables and gene expression levels dichotomized using median as a cut-off value. A probability of 95% ($p < 0.05$) was considered statistically significant for all analyzes. Statistical analysis was performed using the Statistical Package for the Social Sciences (SPSS, USA) version 15.0 and GraphPad Prism version 6.0.

2.10. OTHER STATISTICAL METHODS

DIANA mirPath online enrichment tool [235] was employed for the enrichment analysis of predicted miRNA targets. P-values were calculated using the hypergeometric test and adjusted with multiple Benjamini and Hochberg testing. Functional categories were considered as significantly enriched if at least 5 genes were assigned and the corrected p-value was lower than 0.05. Pathway enrichment analyzes were performed by online tool Enrichr [236]. DEGs were collected as an input gene sets and compared against the GO and KEGG libraries of annotated genes to identify which genes that significantly overlaps. The significance of overlapping between two gene sets was calculated by hypergeometric test.

IV. RESULTS AND DISCUSSION

CHAPTER 1: CELL CULTURES

1.1 CHARACTERIZATION OF EXOSOMES DERIVED FROM NSCLC CELL CULTURES

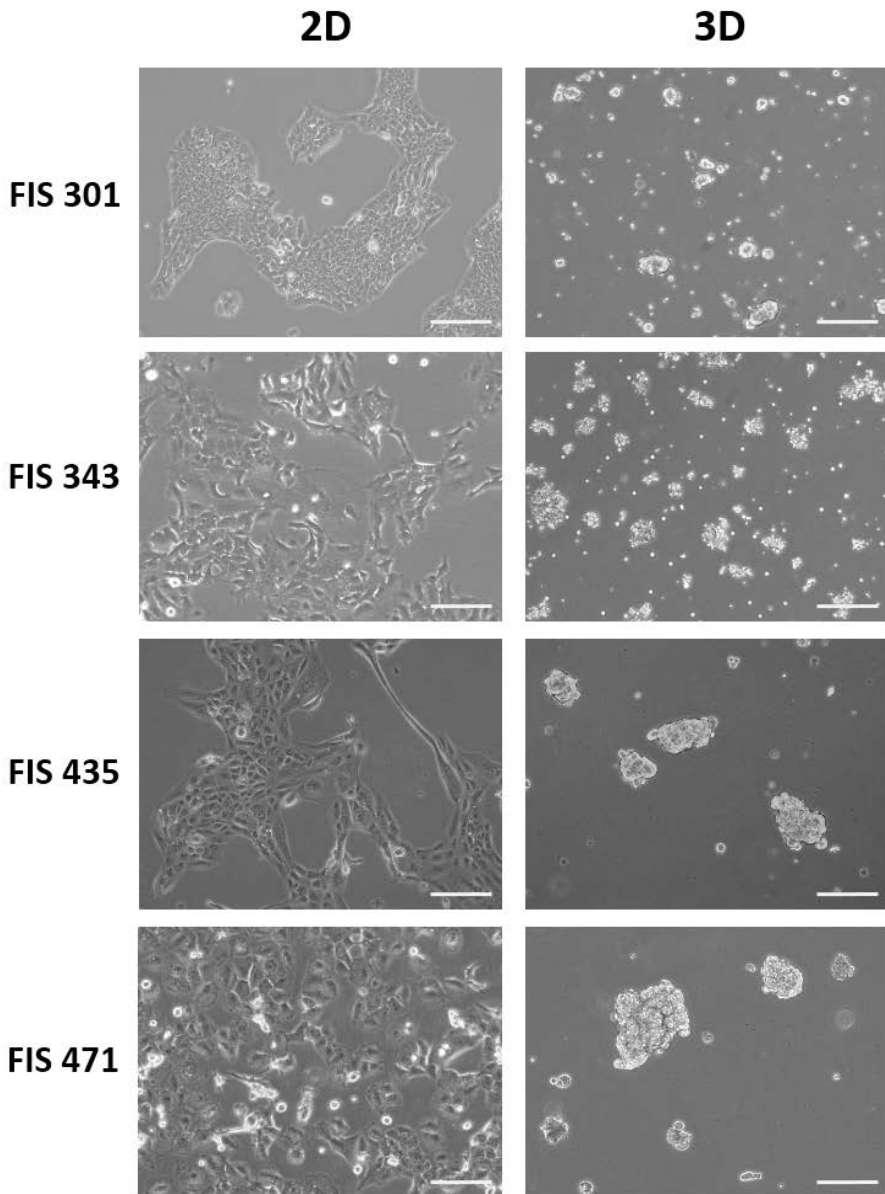
A total of 4 primary cell cultures from NSCLC patients and 13 lung cancer commercial cell lines grown in 2D-monolayer and 3D-tumorspheres conditions were used to characterize tumor-derived exosomes (Figure 20). To determine the efficiency of the methodology employed for the isolation of these exosomes, several techniques for their characterization were used.

The objective of initiating experiments with cell culture models is to conduct an initial global screening of exosome content exclusively originating from NSCLC tumor cells. As previously mentioned, exosomes are released into the body by various cell types, both in normal physiological conditions and during tumor processes (see section 4 of the Introduction). Consequently, exosomes in samples obtained through liquid biopsy will exhibit diverse origins and content. It is essential, prior to reaching this phase of the study, to have a thorough understanding of the characteristics of tumor-derived exosomes to identify their nature in the liquid biopsy samples.

Additionally, due to the lack of standardization in the methods employed for their isolation and characterization, it is imperative to establish a working protocol ensuring their proper handling for subsequent studies. The necessity to identify relevant biomarkers at different disease stages and the exploration of cellular subpopulations and molecular features of interest through these

biomarkers, make cell cultures a comprehensive and cost-effective strategy to fulfill these requirements.

(a)



(b)

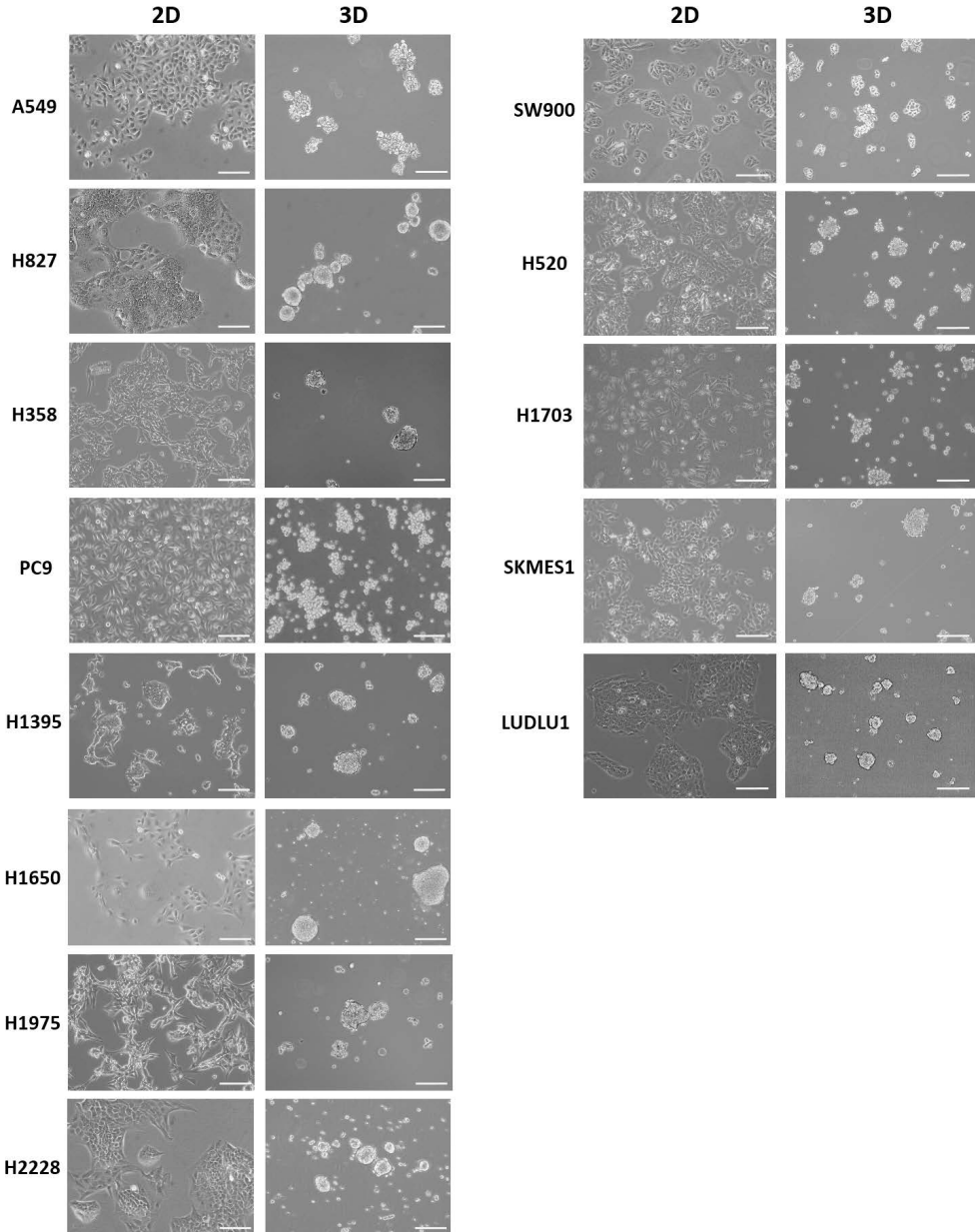


Figure 20. Representative images of primary patient-derived NSCLC cells cultures (a) and cell lines (b) in monolayer (2D) and tumorspheres formation (3D). Microscope images were taken at 10X magnification using a 200 μm scale bar.

Results & Discussion – Chapter 1

First, the diameter of isolated samples was determined by Nanoparticle Tracking Analysis (NTA) after calculating the average of 5 measurements over 60 seconds at 10 frames per second. The concentration obtained was 1×10^8 - 1×10^9 particles/ml (Figure 21a-c). The microvesicles had a diameter of 110 ± 156 nm (Figure 21d), which is consistent with the common diameter of exosomes, as we previously described (see section 4.1.1. of the Introduction).

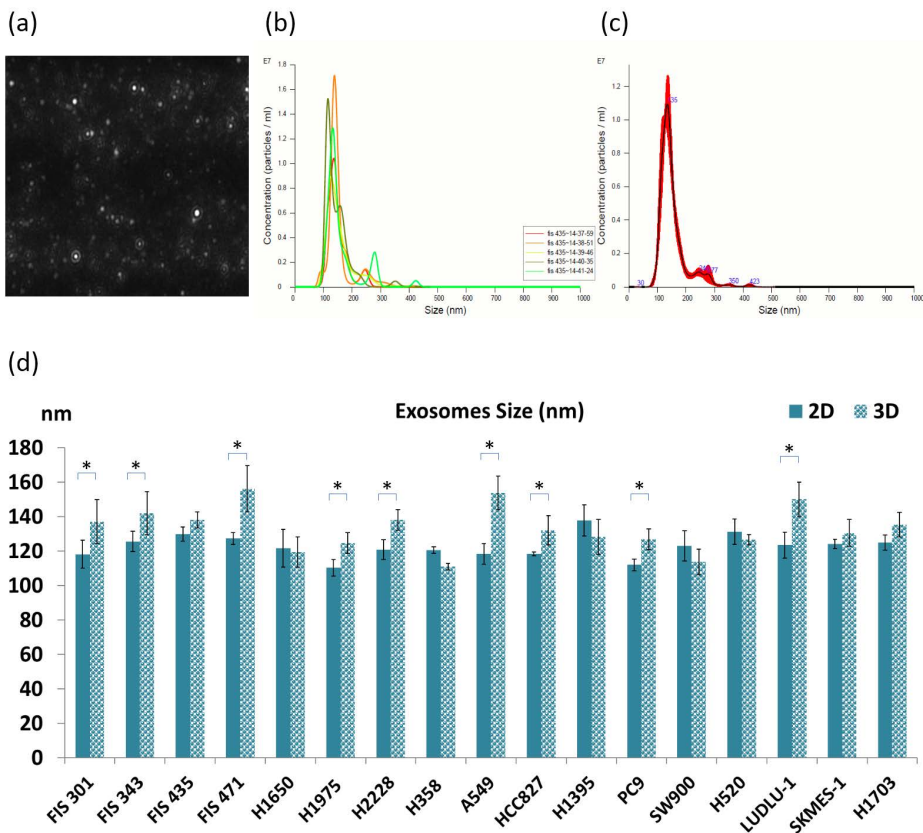


Figure 21. Plots of concentration and size distribution obtained using a NanoSight NS300 instrument in cell cultures-derived exosomes. According to the movement and speed of the particles through the fluid (a), measurements were taken five times over 60 seconds at 10 frames per second at room temperature (b). The average size (X-axis, nm) of all readings was calculated and is depicted in the red curve (Y-axis, concentration) (c). Mean size (nm) and standard deviation (SD) were calculated for 2D and 3D exosome samples (N=17). Asterisks correspond to a significance value ($p < 0.05$) between 2D and 3D size (d).

Subsequently, using images obtained by transmission electron microscopy (TEM), in order to know the real structure of the isolated particles, we were able to confirm that our samples exhibited a rounded and cup-shaped morphology. In many of them, we could distinguish the lipid bilayer that constitutes them, both in exosomes from 2D cell cultures (Figure 22a) and those secreted by 3D models (Figure 22b).

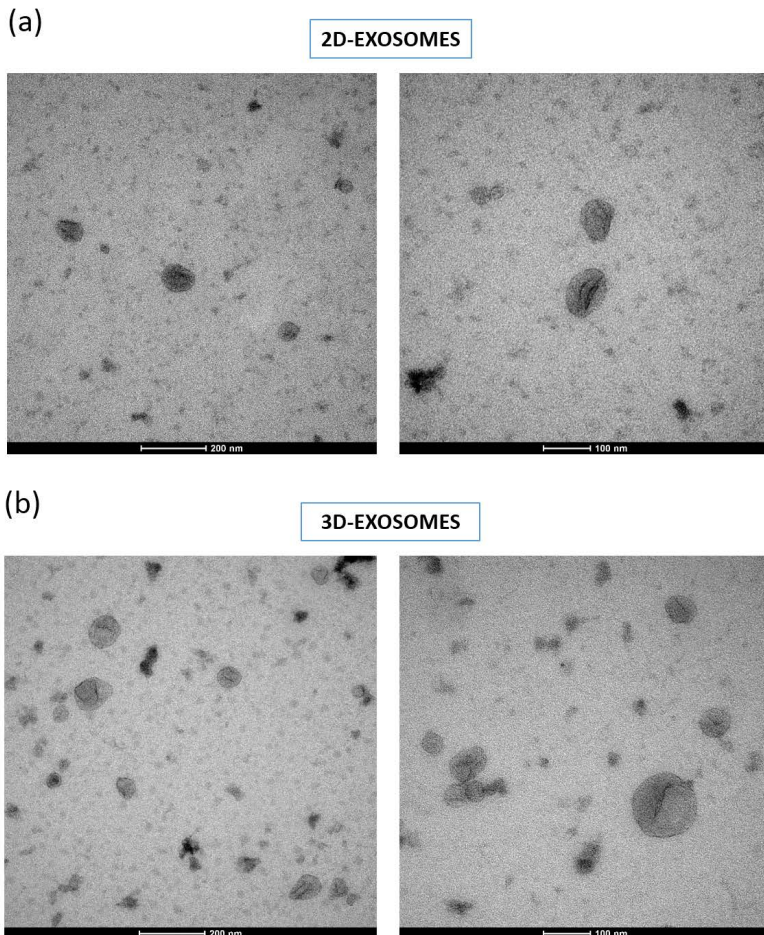


Figure 22. Representative transmission electron microscopic images of exosomes isolated from 2D (a) and 3D (b) NSCLC cell cultures. Scale bars at 200 nm (left side) and 100 nm (right side).

In addition, exosome-specific markers TSG101 (tumor susceptibility gene 101 protein), CD9, CD63 and CD81 were evaluated in tumor-derived exosomes through immunoblot and flow cytometry. On one hand, immunoblot analyzes revealed that some NSCLC exosomes co-expressed CD9 and TSG101 (Figure 23a). Exosomes tested negative for Calnexin, which was used as a control (endoplasmic reticulum marker). This demonstrates that no cellular debris was precipitated together with our exosomal samples (Figure 23b). Furthermore, β -Actin was used as a loading control to ensure that the observed expression differences between the exosomal surface markers were not due to lower protein loading but rather attributable to inherent expression differences among the samples.

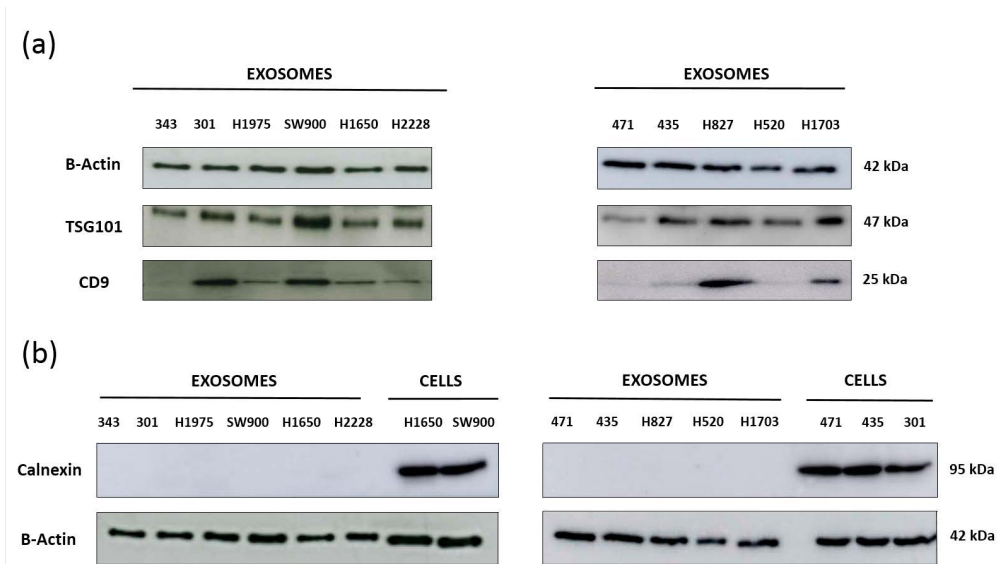


Figure 23. Immunoblotting analysis for the exosomal surface markers. TSG101 and CD9 protein expressions were determined across the 2D-exosome samples (a). Calnexin served as a negative control for exosome samples, while cells from H1650 and SW900 cell lines, as well as FIS 471, 435, and 301 primary cultures, were used as positive controls (b). β -Actin was utilized to evaluate equal protein loading, and a molecular weight marker was included to determine the size of the proteins.

Results & Discussion – Chapter 1

On the other hand, the positive expression of the exosomal surface markers CD63 and CD81 (tetraspanin superfamily of activation-linked cell surface antigens) was also detected by flow cytometry in samples from 2D (Figure 24a) and 3D-cell cultures (Figure 24b-c).

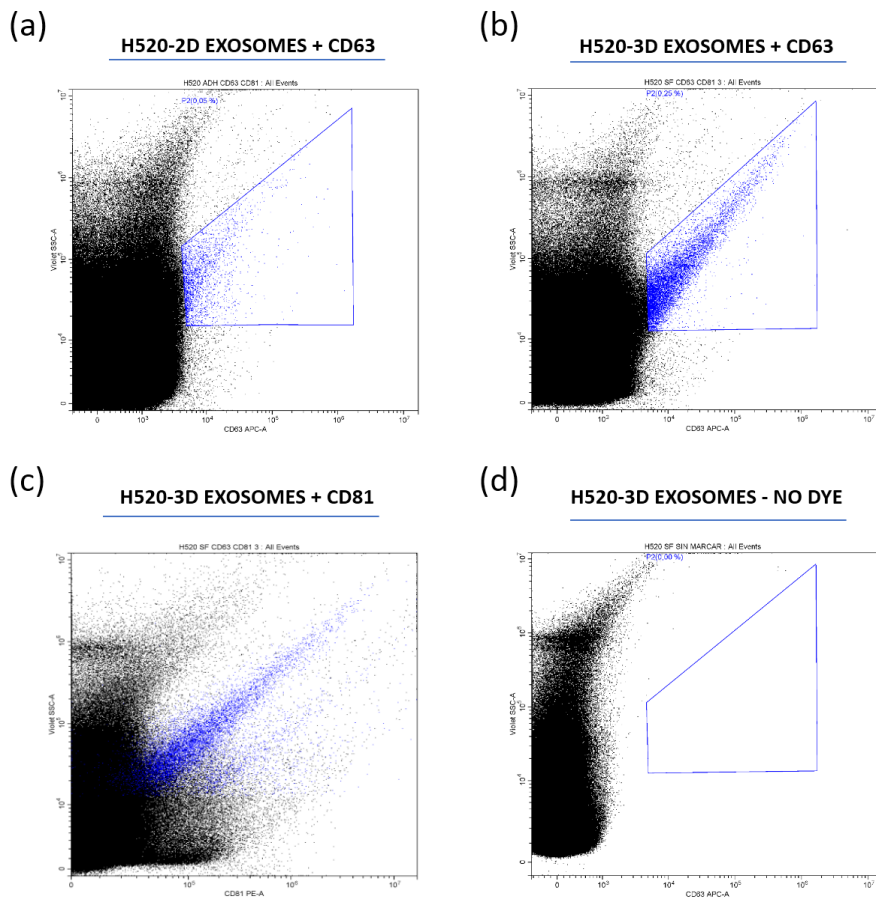


Figure 24. Flow cytometry analysis of the surface markers in exosomes isolated from cell cultures. Exosomes from the 2D-H520 cell line exhibited a CD63 positivity of 0.05% (a). Exosomes from 3D-H520 cell line showed a CD63 positivity of 0.25%, coexpressed with CD81 (b-c). Autofluorescence signals were not detected in samples, ensuring minimal interference with marker positivity (control 1) during analysis without the addition of any dye (d). The axes are displayed on a biexponential scale, where Y-axis corresponds to side scatter (SSC), and X-axis corresponds to forward scatter (FSC). In this case, CD63 was labeled with Allophycocyanin (APC), and CD81 was labeled with Phycoerythrin (PE).

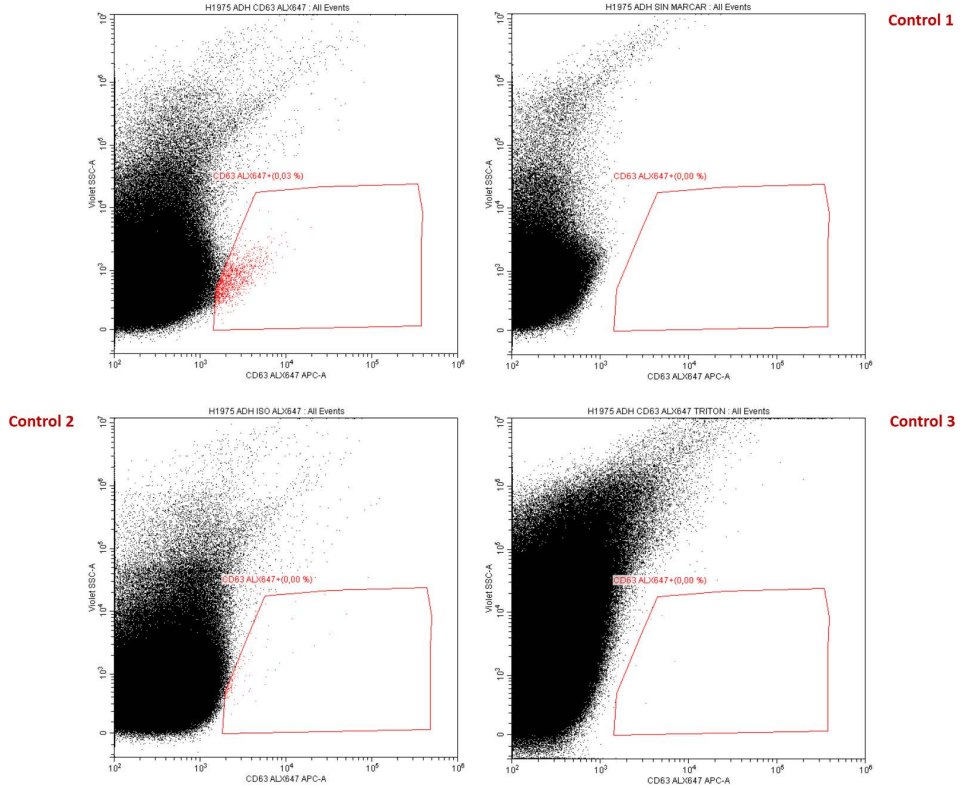
Moreover, three types of controls were randomly used on 2D and 3D-exosome samples to validate the signal intensity obtained with exosomal markers (Figure 25):

- Control 1 (autofluorescence control) refers to the analysis of the sample without the addition of any antibody (Figure 24d). Some cellular components are able to emit fluorescence on their own, masking the antigen-specific signal. In addition, this allows us to verify that there is no contamination from antibody residues between samples after the appropriate wash step.
- Control 2 (unwanted binding control) is based on the addition of a non-specific isoform. The antibodies used may bind to out-of-range epitopes present in the samples that are not the target of interest. Therefore, the sample is analyzed together with an antibody of the same isotype but not specific for CD63 or CD81.
- Control 3 (viability control) is based on the addition of a compound (TRITON) that destroys the lipid bilayer that makes up the exosomes, to which the molecules we want to detect are bound. Consequently, we should observe a total loss of signal.

Results & Discussion – Chapter 1

(a)

H1975-2D EXOSOMES CD63+



(b)

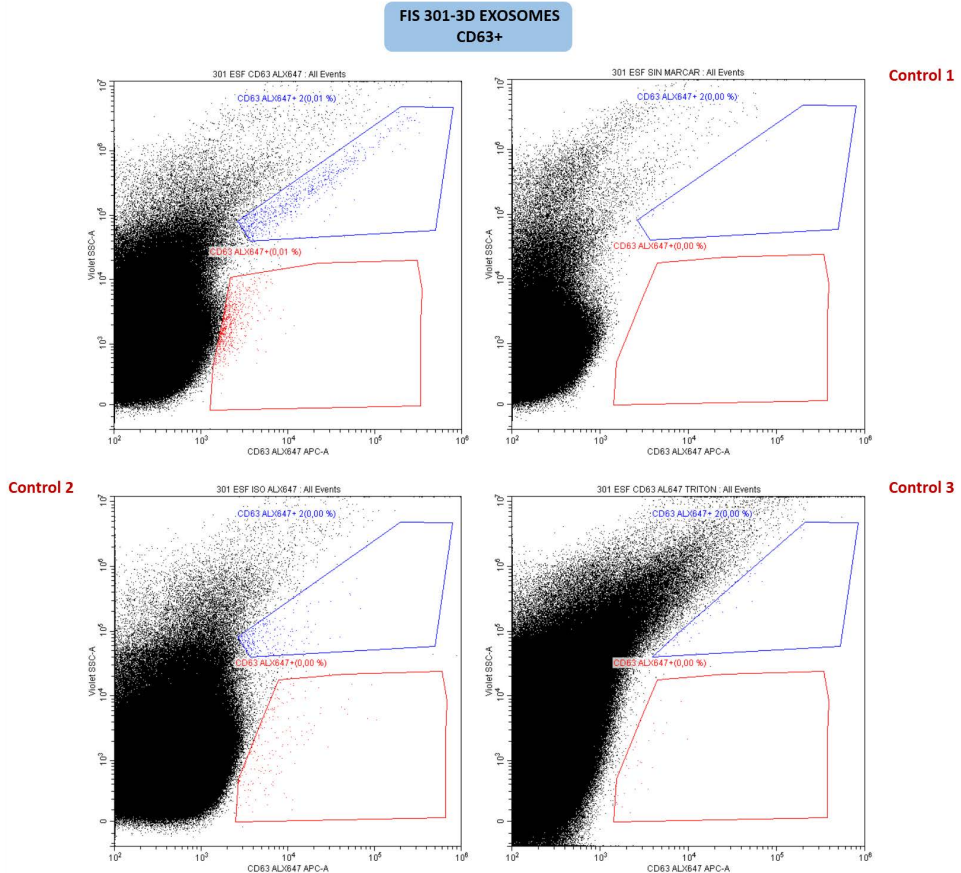


Figure 25. Flow cytometry controls for validation of signal detection in exosome samples. Controls 1, 2, and 3 were successfully conducted (0% positivity) on various samples from both 2D (a) and 3D-cultures (b), in which positivity for the markers of interest had been previously detected. The axes have a biexponential scale, where the Y-axis corresponds to side scatter (SSC), while the X-axis corresponds to forward scatter (FSC). In this case, CD63 was labeled with Alexa647-APC.

In cases where a minimum signal was detected in any of the samples during these 3 points, it was necessary to perform a compensation with respect to the signal obtained with the marker of interest. However, there were

generally no considerable deviations in the detection of these surface molecules on the NSCLC-derived exosomes. Moreover, to confirm that the signal obtained was in accordance with the amount of sample, a test was performed using serial dilutions of the same sample bound to the antibody. These measurements showed a loss of signal intensity proportional to the dilutions used (Figure S1).

After an exhaustive characterization of the different samples obtained, we can conclude that the methodology developed for the collection and isolation of exosomes from cell cultures is appropriate and efficient.

Using imaging techniques, no significant differences in morphology were observed between exosomes from cell lines and primary cultures, as well as between 2D and 3D cultures (Figure 22). Regarding size measurement, exosomes secreted from 3D cultures were generally larger in size compared to 2D-derived exosomes from the cell lines and primary cultures used (mean size 123.65nm-2D vs. 132.5nm-3D ($p=0.022$)) (Figure 21). In addition, surface marker such as CD63 showed higher expression on some exosome samples secreted from 3D cultures (Figure 24).

As previously described by various authors, the differences in the production of exosomes from cells in 3D vs. 2D models largely depend on the characteristics of the cells of origin and the methods used to establish the 3D cultures, among other factors [237]. In addition to those differences, some researchers have also found that cells in a 3D culture environment differ in

the expression of genes, proteins, and cell receptors from cells cultured in 2D [238,239].

Differential expression of genes and/or proteins in 2D and 3D-cell cultures is often the reason why cells growth in 3D systems behave differently in many cellular processes, including growth and proliferation, migration and invasion, and drug sensitivity, compared to cells cultured in 2D [240].

These transcriptional and translational changes have been associated with cell line adaptation when tumor cells are extracted from their native environment. When cells are taken away from the primary tumor and placed in a 2D culture system, they often lose many of their *in vivo* characteristics, including morphology, proliferation, and gene/protein expression. However, to some extent, these differences can be restored when the cells are reintroduced to an *in vivo* environment, such as an animal model, or when they are cultured within a reconstituted spatial structure that mimics the extracellular matrix (ECM) [241,242].

This information aligns with our observed findings regarding variations in size and the expression of certain surface proteins on exosomes from both models, suggesting that the differences may be attributed to variations in the cargo of these microvesicles. This intriguing point will be a subject of further investigation in our work.

1.2. MUTATIONAL STATUS OF EXOSOMES DERIVED FROM CELL CULTURES

In relation to the content of the exosomes from NSCLC, the DNA present in these microvesicles was analyzed in order to corroborate whether the presence of *EGFR*, *KRAS*, *BRAF* mutations, as well as *ALK* rearrangements, could be detected in exosomal cargo through digital PCR (dPCR). Mutation status correlated 100% (10 out of 10) between DNA obtained from culture cells and tumor-derived exosomes (Figure 26 and Table S2). These results corroborate the mutational status concordance among exosomes and matched cell cultures.

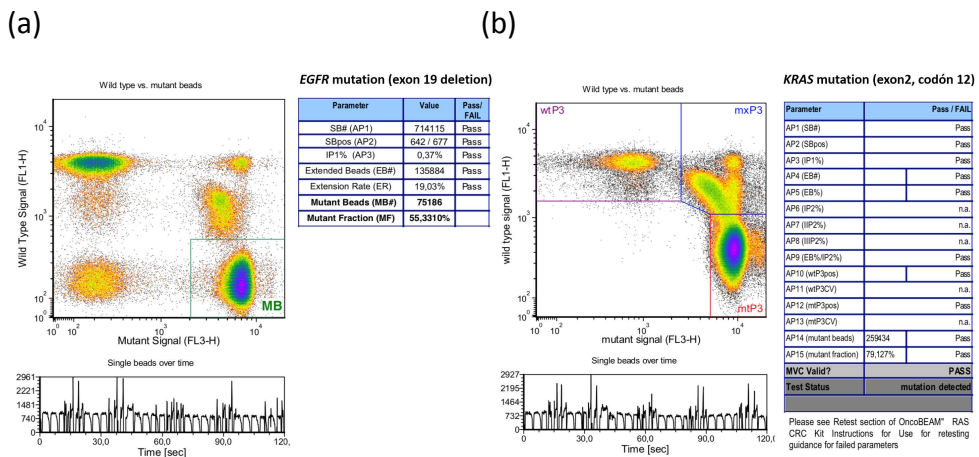


Figure 26. EGFR and KRAS genes mutations analysis by BEAMing technology. Mutant fraction (MF) of 55.33% for the EGFR exon 19 deletion was detected in exosomal DNA from H1650 cell line (a), whereas mutant fraction of 79.12% was present in SW900 exosomal DNA for a KRAS mutation (exon 2, codon 12) (b). The percentage of MF is calculated from the number of mutant beads (MB) or mutant particles (mtP3) represented in the lower right corner of the dot plot.

The presence of driver and targetable mutations in lung cancer, detected in the exosomes isolated from different cell cultures, leads us to draw different conclusions about the impact that exosomes may have at physiological and pathological levels. As previously mentioned, intratumoral molecular heterogeneity is well-documented in NSCLC. Studies have indicated a strong correlation between the proportion of cancer cells harboring *EGFR* mutations and the response to EGFR-TKI treatment. However, there are evidences demonstrating that exosomes originating from specific NSCLC clones, post-administration of first-line drugs, possess the ability to be internalized by other cell populations. This transfer results in the transmission of mutated nucleic acids, thereby inducing resistance to TKI therapy. Detecting and monitoring these mutations within components present in liquid biopsies could mark a significant advancement in the clinical management of these patients [243,244].

1.3. DIFFERENTIAL EXPRESSION PROFILES OF TUMOR CELL CULTURES-DERIVED EXOSOMES

To investigate the expression patterns of tumor cells-derived exosomes, we conducted a transcriptomic study using whole genome expression microarrays. For this initial approach, a selection was made of some primary cultures and cell lines (see section 2.5.1. of Materials & Methods), aiming to gather the main molecular characteristics of interest, including different histological types and molecular alterations. Additionally,

the secreted exosomes from these cell cultures originating from both growth models (2D and 3D) were analyzed.

Results obtained revealed the presence of a large number of mRNAs and small RNAs in exosomes. Through the supervised analysis of the microarray dataset, we were able to detect different expression profiles, grouping the samples into 3 main comparisons: 2D vs. 3D-derived exosomes, LUAD vs. LUSC and cell lines vs. primary cultures.

1.3.1. DIFFERENTIAL EXPRESSED GENES IN EXOSOMES FROM 2D VS 3D MODELS

In this part of the exosomal transcriptomic analysis, within all the probes composing the arrays used, the mRNAs were separated from small RNAs.

In the first instance, principal component analysis (PCAs) allowed us to obtain a global vision of the distribution of the samples among the different variables (Figure 27a). On the other hand, the heatmap represents the differentially expressed genes (DEGs) between the two groups for each comparison (Figure 27b). Arbitrary fold change (FC) cut-offs of >1 and significance p-values of ≤ 0.01 were used to perform this hierarchical clustering analysis on the data set. We found 81 genes overexpressed in exosomes from 3D cultures with a maximum fold change of 1.7, and 129 overexpressed in the 2D group with a maximum fold change of 1.52.

Among the most significant and interesting genes in this comparison (p -value ≤ 0.01), it is worth highlighting some such as *FDFT1* (with the highest FC in 3D group). *FDFT1* is a gene involved in cholesterol biosynthesis and metabolism, being this last one responsible for modulating the formation of lipid rafts in the cell membrane [245]. Changes in cholesterol biosynthesis are regarded as a hallmark of a variety of cancers [1]. Moreover, some genes related to the CSCs population such as *SNAI1* and *WNT5* (FC 1.2 and 1.3, respectively) [246,247] were overexpressed in 3D-exosomes group ($p \leq 0.01$).

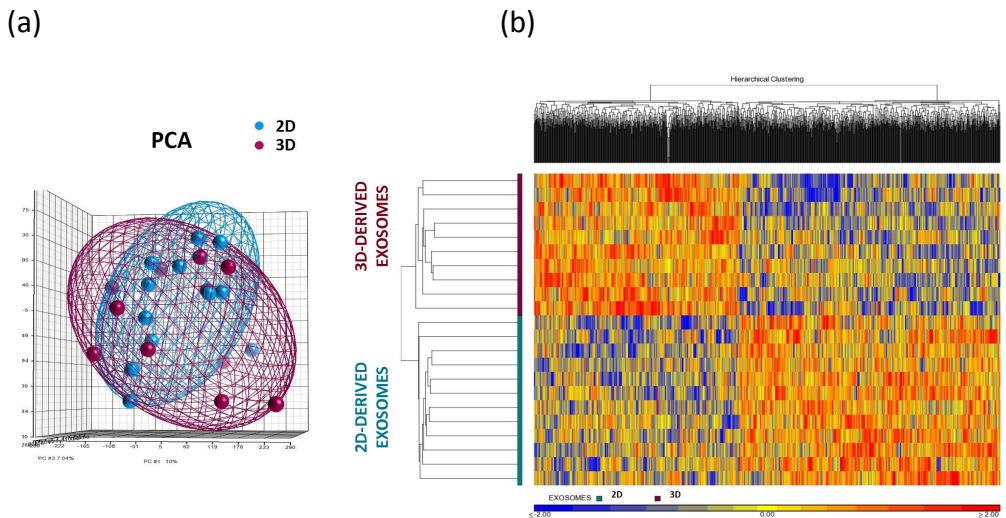


Figure 27. Microarray transcriptomic analysis of exosome cargo from different growth conditions. PCA plot of H1650, H1975, H2228, SW900, FIS 301 and FIS 343 exosomes samples in 2D and 3D conditions (two different biological replicates for each sample) (a). Hierarchical cluster analysis of differentially expressed genes between 3D and 2D exosomes (b). Red color represents overexpression and blue represents underexpression. Rows correspond to the exosome samples analyzed while the columns represent the probes detected throughout the samples.

After obtaining these results, pathway enrichment analysis was conducted from the DEGs observed in this microarray comparison to identify the main processes in which they are involved (Table 8).

Table 8. Biological pathway enrichment in 3D (a) vs. 2D exosomes (b).

(a) Pathways overexpressed in 3D-derived exosomes

METHOD	GO ID	DESCRIPTION	p-value
Enrichr	GO: 1905475	Regulation of protein localization to membrane	0.006
Enrichr	GO:0032148	Activation of protein kinase B activity	0.017
Enrichr	GO:0032731	Activation of Interleukin-1 beta production	0.018
Enrichr	GO:0051781	Stimulation of cell division	0.030

(b) Pathways overexpressed in 2D-derived exosomes

METHOD	GO ID	DESCRIPTION	p-value
Enrichr	GO:0034446	Substrate adhesion-dependent cell spreading	0.003
Enrichr	GO:0000904	Cell morphogenesis involved in differentiation	0.013
Enrichr	GO:0007229	Integrin-mediated signaling pathway	0.016
Enrichr	GO:0007187	G-protein coupled receptor signaling pathway	0.028

Regarding the impact that these enriched pathways may have in the group of samples belonging to 3D cultures, it should be noted that according to the Gene Ontology Resource database [248], the term GO:1905475 refers to "any process that modulates the frequency, rate, or extent of protein localization to the membrane". It is not surprising that genes overexpressed in 3D-derived exosomes are related to this pathway, since in 3D cultures there may be an enrichment of cells that have lost their epithelial characteristics, leading to EMT. Cells grown in a 3D conformation must rely on cell-cell and cell-ECM

interactions that cells from 2D cultures may have lost after adhering to the substrate in a single plane [249].

In addition, protein kinase B (PKB)/Akt is a central player in many cellular processes, including cell proliferation and differentiation, and plays an important role in survival when cells are exposed to various apoptotic stimuli. Constitutive activation of PKB/Akt has been described in many human cancers [250,251]. Genetic alterations also drive aberrant activation of the survival (Akt), which is observed with high frequency during malignant transformation and cancer progression [252]. So, the enrichment in the activation of this pathway observed in exosomes from 3D models (enhanced in CSCs population) (Table 8a), makes particular sense.

Moreover, Interleukin-1 β (IL-1 β) plays a pivotal role in promoting tumor growth and metastasis by inducing the production of growth factors such as VEGF, prostaglandin E2 and TGF- β . IL-1 β also serves as a key mediator in initiating inflammatory responses in pulmonary diseases, including chronic obstructive pulmonary disease and lung cancer [253]. The activation of these pathways, coupled with the stimulation of cell division (all of them enriched in exosomes from the 3D models) (Table 8a) may be associated with a more aggressive phenotype. So, the use of exosomes from these types of *in vitro* models better reflects the molecular characteristics of a relevant subset of NSCLC tumor cells.

In the context of pathways enriched in exosomes from 2D models (Table 8b), we observe substrate adhesion-dependent cell growth and a higher level of

global differentiation in the cultured cells. Additionally, there are interrelated pathways, including integrin signaling and G protein-coupled receptors, which are associated with processes like adhesion, polarity, and guidance, all of which are closely related to tumor cell biology [254,255]. However, these pathways are quite revealing regarding certain limitations that 2D models may have in studying tumor populations that exhibit greater dedifferentiation and a more aggressive phenotype.

1.3.1.1. Differential expressed miRNAs in exosomes from 2D vs 3D cultures

To further investigate the transcriptomic profile of exosomes from both cell culture models, expression analysis was performed by selecting only those probes corresponding to miRNAs (Figure 28). miRNAs are involved in various biological and pathological processes by regulating more than 30% of protein-coding genes [256]. However, most of the published knowledge on miRNA function comes from studies performed in 2D cell cultures, which lack the characteristics of the tumor microenvironment and the heterogeneous exposure to oxygen, metabolites and nutrients observed in the different layers of 3D cultures [257]. For this reason, we aimed to determine the transcriptomic profile of exo-miRNAs derived from 3D models and compare it with those obtained from 2D cell cultures.

A total of 28 differentially expressed miRNAs were identified in the analyzed exosomes samples. Hierarchical clustering revealed which of these biomarkers were overexpressed in each group (Figure 28a), and a further analysis was performed to determine their target genes. A total of 1080 genes were identified exclusively in the exosome-3D group and 616 in the 2D group, after excluding the 458 common genes (Figure 28b).

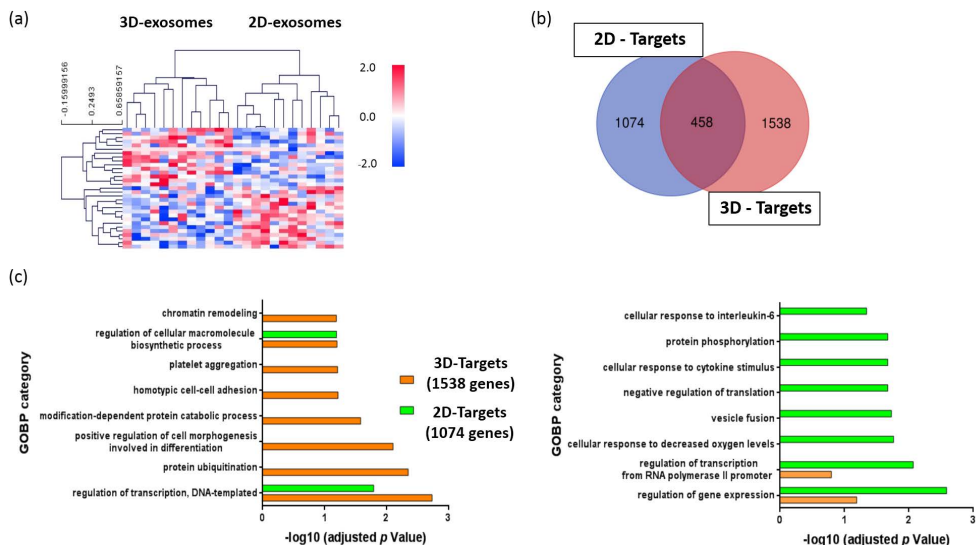


Figure 28. miRNAs analysis in exosomes from 2D and 3D cultures. Heatmap of the differentially expressed probes in both groups ($p \leq 0.01$) (a). Each miRNA was linked to a target gene (b), from which an enrichment analysis was performed to identify the major GOBP (Gene Ontology Biological Process) categories (c).

In addition, the GOBP categories enriched for each gene group were identified (Figure 28c) (Table S3). These results indicate that the reprogramming of miRNAs transcriptional profile can be followed by changes in the expression of relevant mRNA co-regulatory networks [258].

Similar analysis on exo-miRNAs and their targets, which may be involved in tumorigenicity, have been previously performed in other types of malignancies such as prostate cancer [259]. Although these predictions require further experimental validation, the enrichment and analysis of GO terms may yield a number of key related genes and pathways that contribute to the understanding of the molecular mechanisms of lung cancer and the discovery of potential targets for personalized therapies. Furthermore, the fact that these miRNAs are found inside exosomes, protected by their lipid bilayer, prevents their degradation in the bloodstream. Thus, exosomal miRNAs could serve as potential biomarkers for the management of NSCLC [260].

1.3.2. DIFFERENTIAL EXPRESSED GENES IN EXOSOMES FROM LUAD AND LUSC

According to the supervised analysis corresponding to the comparison of the two most common histological subtypes in NSCLC, PCA revealed a strong classification of samples between LUAD and LUSC (Figure 29a). To gain biological insights from the DEG sets according to histology, we further performed hierarchical clustering analyzes on the microarray dataset using arbitrary fold change (FC) cut-offs of >1 and significance p-values of ≤ 0.01 . We found 551 genes overexpressed in LUAD exosomes with a maximum fold change of 4.38, and 803 genes overexpressed in the LUSC group with a maximum fold change of 4.72 (Figure 29b). However, with the aim of focusing

the data collection on genes that exhibit a substantial difference compared to others, we restricted the FC cut-off to ≥ 1.5 . Using this criterion, we observed 46 genes overexpressed in LUAD and 293 overexpressed in LUSC samples.

After fine-tuning in more restrictive selection values, we can highlight some strongly expressed genes in LUAD (*XAGE1B* and *SEPP1*) and LUSC (*CAPRN1*, *RIOK3* and *CABYR*) derived exosomes for further validation (FC > 1.5), making an exception with *TTF-1* (*NKX2-1*) (FC < 1.5), which is an established LUAD marker routinely used for the determination of this histological subtype in NSCLC (among others types of tumors) [261].

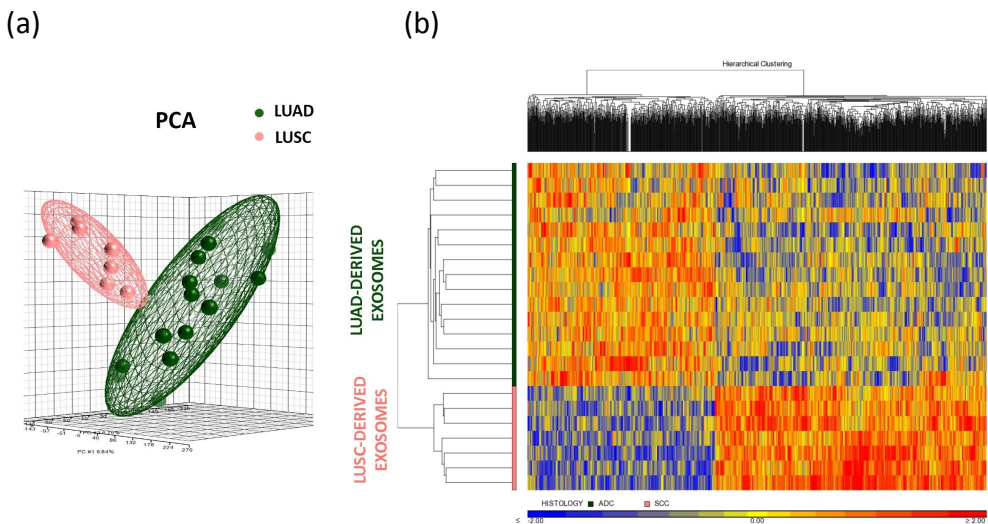


Figure 29. Transcriptomic microarray analysis of exosomal cargo from histological subtypes comparisons. PCA plot of H1650, H1975, H2228, SW900, FIS 301 and FIS 343 exosomes samples in 2D and 3D conditions (two different biological replicates for each sample) distributed according to histology (a). Hierarchical cluster analysis of differentially expressed probes between LUAD and LUSC (b). Red color represents overexpression and blue represents underexpression. Rows correspond to the exosome samples analyzed while the columns represent the probes detected throughout the samples. LUAD: lung adenocarcinoma; LUSC: lung squamous cell carcinoma.

After obtaining these results, pathway enrichment analysis was performed from the DEGs observed in the microarray histology comparison to identify the main processes in which they are involved. A total of 13 pathological processes were significantly enriched ($p \leq 0.03$). All these pathways obtained are related to the different hallmarks of cancer (Figure 30) (Table S4).

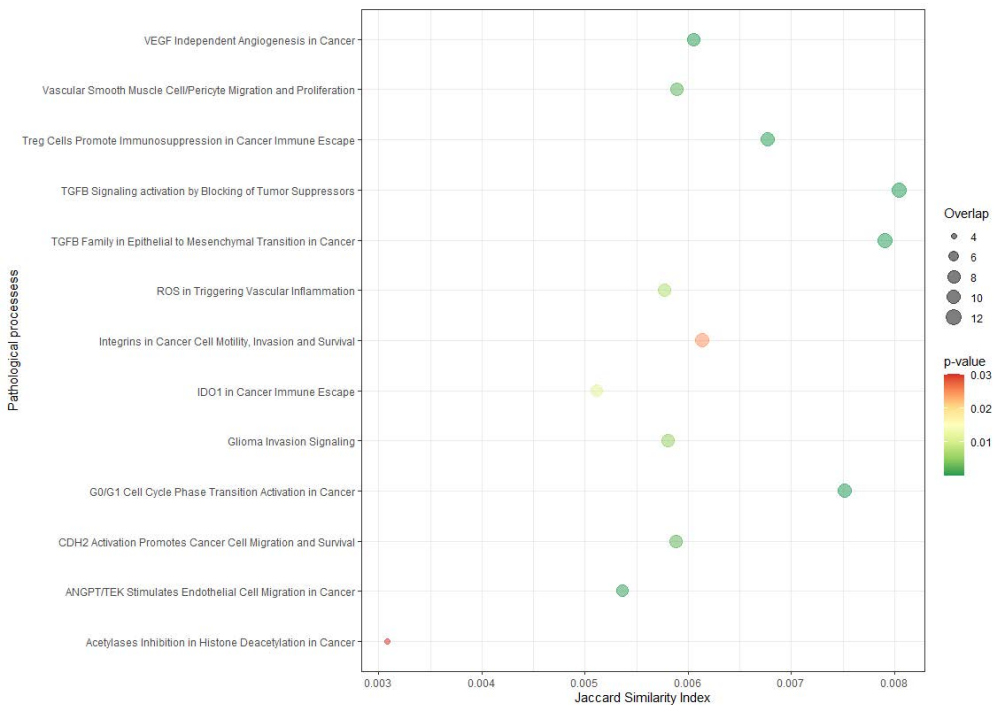


Figure 30. Pathological processes enrichment of differentially expressed genes between LUAD and LUSC-derived exosomes. Y-axis indicates the pathological process name and X-axis indicates the Jaccard similarity index (JSI). JSI measures the degree of similarity between two sets. It always takes values between 0 and 1, with 0 representing the least possible similarity between the two groups, and 1 indicating complete equality between the two comparisons. Bubble size indicates the number of overlapped genes for each process. The color bar indicates the p-value, representing in red the highest value (0.03), whereas values lower than 0.01 are represented in green. LUAD: lung adenocarcinoma; LUSC: lung squamous cell carcinoma.

Among the pathological processes that are most robustly distinguished in this enrichment analysis (from DEGs belonging to the histological comparison), some of them are related to the activation of TGF- β pathways. TGF- β is a family of cytokines involved in cellular processes such as haematopoiesis, proliferation, angiogenesis, differentiation, cell migration and apoptosis [262]. Several tumors, including those arising in the lung, express high levels of TGF- β [263–265], which has been correlated with tumour progression and clinical prognosis in these patients [266].

A study published by *Sato et al.* in 2021 showed that cells belonging to the tumor microenvironment, such as CAFs, are able to secrete TGF- β to induce a transition in histological patterns and tumour heterogeneity in lung adenocarcinoma [267]. In addition, other authors have also demonstrated the role of the TGF- β signalling pathway during the acquisition of invasion in lung adenocarcinoma tumours [268].

Besides this, TGF- β can also promote tumor invasion and metastasis by inducing EMT, which is often associated with the acquisition of stem-like characteristics [269]. In relation to these exosomes-enriched pathways, a study published in 2021 highlights the association between LUAD patients and TGF- β levels. High TGF- β -mediated EMT expression were associated with shorter survival and were predictive of poor prognosis in lung adenocarcinoma [270].

To continue with the review of these pathological processes, regulatory T cells (Tregs) are a subset of CD4⁺ T lymphocytes known to dampen the host

immune response against cancer cells. Within the tumor microenvironment, Tregs are potent mediators of immune tolerance, and a higher proportion of Tregs compared to cytotoxic T cells predicts a worse outcome in most solid tumors.

Results from a study published in 2013 [271] show that Tregs were present in all lung tissues examined, but with a significant enrichment in patients with LUAD. Differences in the amount of Tregs were found depending on the different tumor histologies, with a higher presence observed in LUAD compared to LUSC. This may result in a more permissive microenvironment for LUAD and may explain the aggressive patterns of tumor spread for this histology. Lung cancer patients with LUAD histology may benefit more from Treg-targeted therapy, so it is possible that histology is related to lymphocyte immune response.

Consistent with our findings in tumor tissue and exosome samples, another study demonstrated that patients with high levels of Treg had a significantly worse prognosis compared to those with low levels (5-year overall survival: 85.4 % vs. 93.0 %). Furthermore, CAFs from adenocarcinoma patients with high Treg levels expressed significantly higher mRNA levels of TGF- β and VEGF, both involved in Treg induction. This suggests that CAFs, by expressing immunoregulatory cytokines, may induce Tregs in the stroma, creating a tumor-promoting microenvironment in lung adenocarcinoma [272]. The proportion of Tregs in different locations of the tumor microenvironment can have variable prognostic impacts in NSCLC [273].

Continuing with these results (Figure 30), it is worth noting that angiogenesis, which is essential for tumor growth and metastasis, is regulated by various mechanisms and angiogenic factors like VEGF, TGF- β , and fibroblast growth factor. Some authors have reported a significant correlation between high levels of VEGF expression and the histological type in NSCLC, with LUAD patients showing higher VEGF expression. Furthermore, *in vitro* analysis of VEGF-A demonstrated distinct responses to hypoxic conditions between LUAD and LUSC cultures, indicating differences in angiogenic responses. These findings underscore the divergent responses between the major histological entities in NSCLC [274].

Our findings from tumor-derived exosomes (TEX) in NSCLC further support the hypothesis that these microvesicles have a significant role in the immune system and vascular tube formation [275]. Within the context of lung cancer, TEXs offer insights into the mechanisms underlying tumor metastasis and progression. Consequently, they hold potential as biomarkers for lung cancer diagnosis and therapy response assessment.

1.3.2.1. Differential expressed miRNAs in exosomes from LUAD and LUSC

After analyzing the expression of the different types of miRNAs present in the arrays, a total of 158 probes were observed in the histological comparison. Specifically, 86 were significantly overexpressed in LUAD-derived exosomes in comparison to 72 detected in LUSC samples ($p \leq 0.01$). Within this number of total probes, a selection of 4 miRNAs was made for each

histology according to their relevance and strength of expression in each group (Table 9).

Table 9. Exosome-derived miRNAs with most increased differential expression between LUAD and LUSC.

PUBLIC GENE ID	OFFICIAL SYMBOL	EXOSOMES SAMPLES
NR_030353	hsa-miR-623	Overexpressed in LUSC
NR_029680	hsa-miR-138	Overexpressed in LUSC
NR_029949	hsa-miR-18b	Overexpressed in LUSC
NR_029779	hsa-miR-200c	Overexpressed in LUSC
NR_029898	hsa-miR-339	Overexpressed in LUAD
NR_029503	hsa-miR-29a	Overexpressed in LUAD
NR_029507	hsa-miR-33a	Overexpressed in LUAD
NR_029505	hsa-miR-31	Overexpressed in LUAD

- miRNAs overexpressed in LUSC-derived exosomes:

The role of miR-623 as a suppressor of cell proliferation, migration and invasion through downregulation of cyclin-dependent kinases and

inhibition of phosphatidylinositol 3-kinase (PI3K)/Akt and Wnt/ β -catenin signaling pathways has been previously described in various cancers such as breast, hepatocellular carcinoma and pancreatic cancer [276–278]. This suggests that miR-623 may be a potential target for therapy in various tumor types. Specifically, downregulation of hsa-miR-623 was associated with poor clinical outcomes in NSCLC patients. Hsa-miR-623 behaved similarly to previous studies, suppressing cell proliferation, clonogenicity, migration and invasion *in vitro* and inhibiting xenograft growth and metastasis in animal models [279]. According to these previously described findings, and although its overexpression in a specific histological subtype remains to be confirmed, we believe the presence of this miRNA in exosomes is relevant as a potential biomarker in NSCLC.

MiR-138 has already been described in other studies to play an important role in the carcinogenesis of various types of tumors, acting as a tumor suppressor. It is well known that a single miRNA can target multiple genes. Specifically, miR-138 has been shown to inhibit *MYC* expression and suppress tumor growth in colorectal carcinoma and hepatocellular carcinoma cell lines [280]. In addition, the effects of miR-138 have also been identified as a promising prognostic biomarker and therapeutic target for oral squamous cell carcinoma with metastatic potential [281]. Specifically, in NSCLC it is possible that miR-138 plays a suppressive role in growth and metastasis [282,283]. In patient serum samples, this miRNA has already shown evidence of being a novel and valuable biomarker for the diagnosis of NSCLC [283]. However, the confirmation of their presence in NSCLC

exosomes by our work would mean that the biomarkers present in these microvesicles would have greater protection in the bloodstream. This would provide greater stability for the analysis of miRNAs present in cancer.

On the other hand, the stable overexpression of other small miRNAs, such as miR-18b, has been shown to be of great relevance in the development and progression of some types of tumors, such as melanoma or head and neck cancer [284,285]. There are findings regarding the presence of this miRNA in exosomes derived from CAFs in breast cancer, suggesting that these exosomes could induce EMT and promote the activation of the NF- κ B pathway through different target genes [286]. Although no publications exist on the role of miR-18b in NSCLC exosomes to support our findings, previous results in other tumors indicate the potential value of this marker in the study of the disease.

Finally, other members of our group in agreement with other publications, highlighted the presence of miRNA-200c in tissue samples from NSCLC tumors versus healthy tissue samples [287,288]. On the other hand, the presence of this miRNA has also been described in exosomes secreted by other types of tumors regardless of their histology [289,290]. However, in line with our results in NSCLC exosomes, there is previous evidence of the association of exo-miR-200c with head and neck squamous cell carcinoma [291,292].

- miRNAs overexpressed in LUAD-derived exosomes:

Aberrant expression of miR-339-5p has been shown to play a key role in several tumors, including hepatocellular carcinoma [293], breast cancer [294] and colorectal cancer [295]. miR-339-3p was found to be significantly upregulated in patients with NSCLC compared to healthy subjects, suggesting a diagnostic and predictive value for high-risk individuals [296]. In addition, the alteration of this miRNA has also been observed in patients with lung adenocarcinoma, revealing important effects on the development of this histology [297,298]. Although it is not regulated in the same sense in our exosome samples, the expression of miR-339 could be a potential biomarker for lung adenocarcinoma.

On the other hand, miR-29a has been shown to be present in NSCLC exosomes, but there is no study linking its presence in these EVs to a specific histologic subtype [220,299]. However, miR-29a-3p expression has been observed in lung adenocarcinoma cells. Studies have found that overexpression of miR-29a-3p is associated with cell proliferation, migration and invasion in LUAD cells [300]. These findings may be related to the observed overexpression of this biomarker in our LUAD-derived exosome samples.

The relative expression levels of miR-33a-5p have been positively correlated in tissue and serum of lung cancer patients compared to their expression in healthy controls [301,302]. Specifically, some authors have described that miR-33a-5p increases the sensitivity of lung adenocarcinoma cells to celastrol

(natural bioactive compound used as a treatment for multiple diseases) through regulation of mTOR signalling [303]. Therefore, the presence of this biomarker in LUAD exosomes could be related to specific pathways activated in this histology.

MiR-31 has previously been identified as one of the most oncogenic miRNA in LUAD. Several authors reported that miR-31 is specifically overexpressed in NSCLC, but not in SCLC or carcinoid, compared to normal lung tissue. Mechanistically, miR-31 alters distinct cell signaling programs within each histological subtype, resulting in phenotypic differences [304]. This suggests that there may be different functional roles for this miRNA in the different histological types of lung cancer. Other studies have confirmed that miR-31 is overexpressed in LUAD, and analysis of clinical data showed that high miR-31 expression was more common in patients with worse prognosis [305]. Additionally, separate studies have revealed the modulation of miRNAs within exosomes originating from tumor cells subjected to varying growth conditions, including hypoxia and normoxia. Notably, it was observed that the upregulation of exosomal miR-31-5p expression, triggered by intermittent hypoxia, directly initiated the activation of specific target genes, consequently promoting processes such as EMT. These findings underscore the pivotal role of exosomes as essential mediators in intercellular communication [306,307].

After reviewing the results, it is evident that miRNAs exhibit distinct functions depending on their specific cellular context. In some tissues, they may act as tumor suppressors, while in others, they promote oncogenesis, or they might

seem relatively inert in regulating cancer-related processes. Nonetheless, the precise role of miRNAs within different cell types in the same tissue and their collective contribution to oncogenesis remain under investigation. What is clear, however, is that exosomes derived from NSCLC tumor cells or other cells within the tumor microenvironment, such as CAFs, have the capacity to modulate the content and function of these miRNAs. This modulation can trigger diverse responses and signaling pathways during the tumor process. Consequently, these microvesicles are a valuable source of biomarkers for detecting and analyzing the disease.

1.3.3. DIFFERENTIAL EXPRESSED GENES IN EXOSOMES FROM CELL LINES VS PRIMARY CULTURES.

To investigate the impact of using primary cultures beyond the gold standard (commercial cell lines) for *in vitro* studies, differential expression analysis was performed between exosomes from both types of cell cultures. Hierarchical clustering analyzes on the microarray dataset was conducted using an arbitrary fold change (FC) cutoff of ≥ 1.5 and a p-value of ≤ 0.01 , considering a total of 142 probes in primary cultures (max FC 4.25) and 369 in cell lines (max FC 2.8) (Figure 31b).

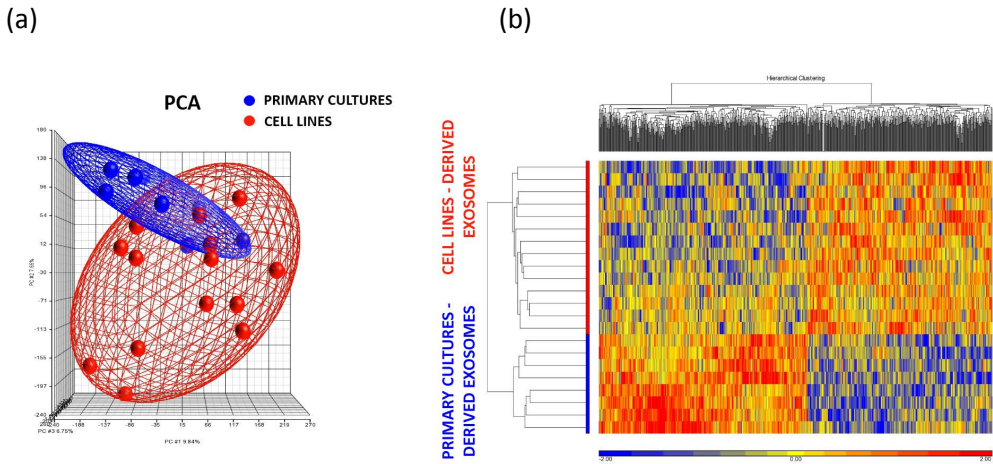


Figure 31. Transcriptomic microarray analysis of exosomal cargo from primary cell cultures and commercial cell lines. PCA plot of H1650, H1975, H2228, SW900, FIS 301 and FIS 343 exosomes samples in 2D and 3D conditions (two different biological replicates for each sample) distributed according to histology (a). Hierarchical cluster analysis of differentially expressed probes (b). Red color represents overexpression and blue represents underexpression. Rows correspond to the exosome samples analyzed while the columns represent the probes detected throughout the samples.

The clear distribution of the samples according to the origin of the cell cultures (Figure 31a), highlights the value of using primary cultures (established directly from the tumor of the follow-up patients) in the search for *in vitro* biomarkers in NSCLC. Other publications also emphasize the importance of using established primary cultures and animal models to study lung cancer [308,309]. For this reason, a larger validation cohort including more primary cultures will be used to validate the biomarkers obtained in the previous sections

1.4. DIFFERENTIAL EXPRESSED GENES VALIDATION IN TUMOR CELL CULTURES-DERIVED EXOSOMES

To confirm the findings obtained after the analysis of the expression microarrays, these candidate genes were examined in a larger number of exosome samples from NSCLC cell cultures (N=17), by RT-qPCR.

1.4.1. DIFFERENTIAL EXPRESSED GENES VALIDATION IN EXOSOMES FROM 3D vs 2D CULTURES

First, the relative gene expression of *FDFT1* was analyzed, which was the most overexpressed gene in the group of exosomes secreted by the 3D cultures. The results obtained showed that all exosome samples, with the exception of SW900, showed expression of this gene (16/17). In turn, all microvesicles from 3D cultures showed higher significant gene expression compared to monolayer cultures ($p=0.001$) (Figure 32a-b).

On the other hand, *SNAI1* also highlighted in the EVs-3D group in microarrays, demonstrated its presence in the exosomal cargo of 14/17 samples. At the same time, it has been confirmed that there is a predominant expression of this gene in exosomes from 3D cultures compared to adherent cultures (13/14) ($p=0.005$) (Figure 32c-d).

Results & Discussion – Chapter 1

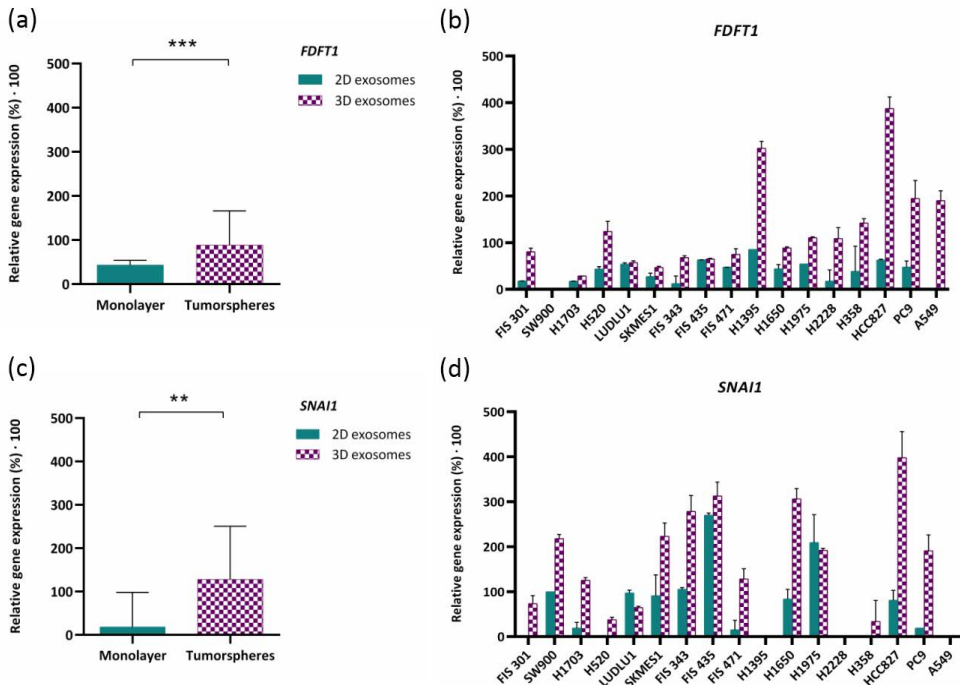


Figure 32. Validation of *FDFT1* and *SNAI1* expression in tumor-derived exosomes from 2D and 3D cell cultures. Median of relative gene expression of *FDFT1* and *SNAI1* measured by RT-qPCR in both groups (a-c). Mean with SD of de relative gene expression of *FDFT1* and *SNAI1* to reference genes *ACTB* and *GAPDH* analyzed in the complete group of cell cultures-derived exosomes (b-d). Error bars represent the standard error of the mean (SEM). Green bars correspond to 2D-derived exosomes while purple bars correspond to exosomes derived from 3D cultures. Significance values were ** $p \leq 0.01$, and *** $p \leq 0.001$.

Finally, the expression of *WNT5A* was also analyzed as a marker of interest that was overexpressed in the 3D exosome group. In this case, relative gene expression was found in only 4 of the 17 exosome samples used for validation ($p > 0.05$). The overexpression of *WNT5A* in these 4 samples could not be related to the mutations present in cells, the histology or the origin of the cell

culture. However, in all of samples, the values obtained are largely consistent with exosomes derived from tumorsphere cultures (Figure 33).

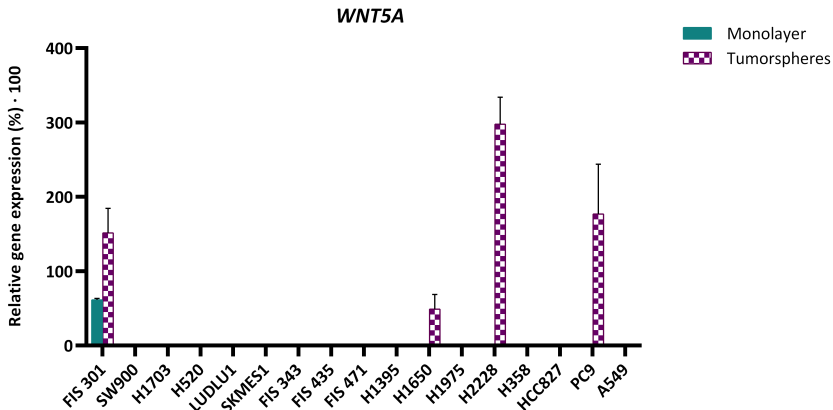


Figure 33. Validation of *WNT5A* expression in tumor-derived exosomes from 2D and 3D cell cultures. Error bars represent the standard error of the mean (SEM). Green bars correspond to 2D-derived exosomes while purple bars correspond to exosomes derived from 3D cultures. Mean with SD of de relative gene expression of *WNT5A* to reference genes *ACTB* and *GAPDH* analyzed in the complete group of cell cultures-derived exosomes.

To gain a deeper understanding of the role of these observed biomarkers in exosomes concerning the initiation and proliferation of tumors, it is crucial to contextualize certain scenarios. Tumor cells possess the capacity to adapt their nutrient metabolism and energy acquisition, even in low-energy conditions, with lipid metabolism playing a pivotal role in this adaptation. Metabolic substrates like cholesterol play a significant role in numerous biological processes and are used by these cells to support growth and survival [310–312]. Alterations in cholesterol biosynthesis are considered to be a hallmark of a variety of cancers [1] Therefore, enzymes involved in cholesterol

metabolism and related biomolecules, have recently attracted attention as potential targets for cancer therapies [311].

In particular, *FDFT1* (also known as squalene synthase, SQS) is a cholesterol biosynthesis enzyme. Some studies have reported that its upregulation is required for tumor progression, signal transduction, invasion and migration of cancer cells [313,314]. Specifically in lung cancer, a study published in 2014 showed that knockdown of *FDFT1* reduced cholesterol levels and inhibited invasion ability in cell lines [315]. Later, a study published by *Yang et al.* showed that *FDFT1* was the first cholesterol branch enzyme to be upregulated in highly invasive lung cancer cell lines. Overexpression of this squalene synthase promoted lung cancer invasion and metastasis *in vitro* and *in vivo*, which in turn enhanced cholesterol biosynthesis [316]. Regarding the presence of *FDFT1* in exosomes, the present work is the first to highlight this finding. Exosomes may be a great tool to consider the role of this marker in lung cancer. In addition, after the advance of immune checkpoint blockers, the implication of these type of EVs in the relationship between these tumors and the TME may also be noteworthy.

Another gene significantly expressed in 3D exosomes is *SNAIL1* (also called Snail), which is a zinc finger transcription factor that induces EMT [317]. *Snail* has been found to play a role in the pathogenesis of several malignancies, particularly by enhancing invasiveness and metastatic behaviour [318,319]. A few studies have suggested that *Snail* may also play a role in NSCLC tumor progression [320,321]. Regarding the presence of this biomarker in exosomes,

a study published in 2021 showed that *Snail* modifications in CRC cells towards a more invasive phenotype, also alter the microRNA load of released EVs [322].

Recent studies have shed light on the pivotal role of Snail in activating other cells within the TME, including CAFs, which are responsible for extracellular matrix remodeling. In CAFs, signaling through the platelet-derived growth factor (PDGF) receptor is a crucial functional determinant. While high expression of *SNAI1* and PDGF receptors has been linked to poor prognosis in cancer patients, the underlying mechanisms governing these associations remain unclear [323].

To go deeper into this mechanism, *You et al.* conducted a study focusing on the role of exosomes released by CAFs in promoting EMT in lung cancer cells. Interestingly, the level of *SNAI1* in exosomes secreted by CAFs exhibited a correlation with the expression of *SNAI1* in CAFs. Moreover, the level of *SNAI1* in these exosomes played a pivotal role in inducing EMT in lung cancer. The molecular mechanism underlying how CAFs induce EMT in cancer cells may involve the delivery of *SNAI1* to the recipient cancer cells through exosomes [324].

As discussed, in lung cancer, the presence of *SNAI1* in exosomes has been observed exclusively in EVs derived from CAFs. Our study presents a novel finding: exosomes from NSCLC tumor cells contain a substantial *SNAI1* content, particularly in 3D cultures where the growth conditions and activated

signaling pathways more closely resemble the *in vivo* tumor microenvironment.

Lastly, concerning the last of the markers emphasized in 3D exosomes, it is important to note that Wnt pathways are developmental signaling pathways with pivotal roles in the regulation of various cellular processes [325]. Furthermore, dysregulated Wnt signaling contributes to tumor development, increased CSC potential, and resistance to therapy for many cancers, including lung cancer [326].

However, a possible dual role of this marker in different cancers, acting as a suppressor [327–329] or promoter [330–333], has been highlighted in several studies. Specifically, in NSCLC a paper published in 2015 showed that elevated *WNT5A* expression was associated with poor prognosis in a cohort of patients (N=219) [334]. To date, there are no studies describing the presence of *WNT5A* in exosomes secreted by NSCLC cells. However, the role of this marker in microvesicles analyzed in various non-neoplastic lung diseases such as chronic obstructive pulmonary disease or pulmonary fibrosis has been described [335,336].

1.4.2. DIFFERENTIAL EXPRESSED GENES VALIDATION IN EXOSOMES FROM LUAD AND LUSC CULTURES

Using whole expression microarrays, *XAGE1B* continued to present a significantly ($p=0.01$) higher expression in LUAD-secreted exosomes (N=11,

Results & Discussion – Chapter 1

Figure 34a), while there was no expression of this gene in the LUSC group (N=6), except for the cell line SKMES-1, which exhibited low expression values (Figure 34b). On the other hand, RT-qPCR results for *CABYR* were also consistent with the transcriptomics findings. Expression of this gene was found in LUSC cell-derived exosomes, while no expression was detected in LUAD cells-secreted exosomes ($p < 0.001$) (Figure 34c-d).

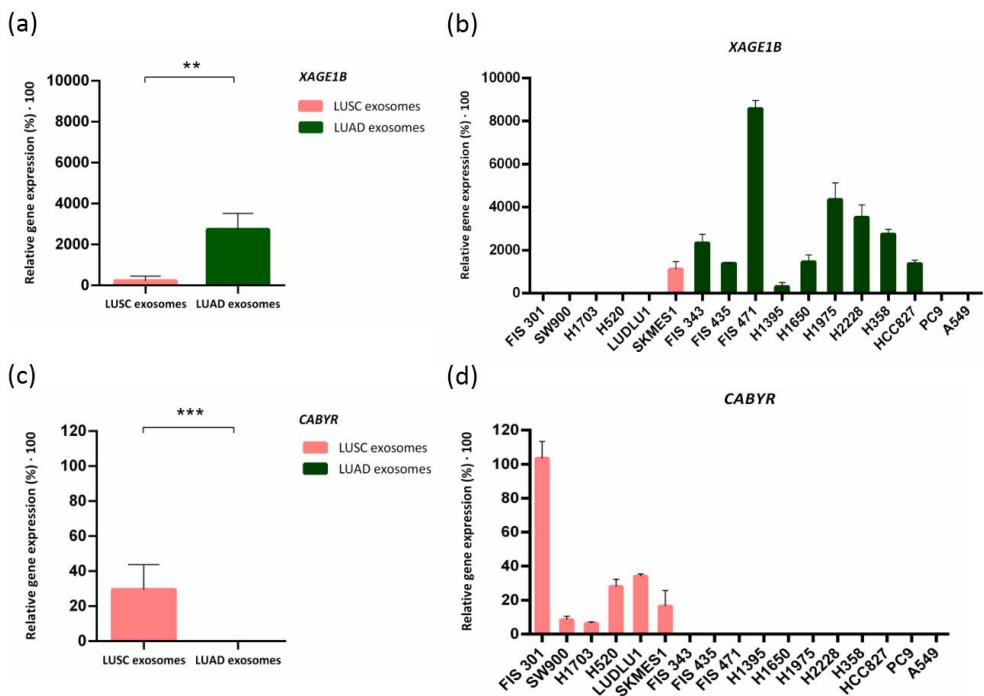


Figure 34. Validation of *XAGE1B* and *CABYR* expression in tumor-derived exosomes from 2D cell cultures. Median of relative gene expression of *XAGE1B* and *CABYR* measured by RT-qPCR in both histological groups (a-c). Mean with SD of de relative gene expression of *XAGE1B* and *CABYR* to reference genes *ACTB* and *GAPDH* analyzed in the complete group of cell cultures-derived exosomes (b-d). Error bars represent the standard error of the mean (SEM). Dark green bars correspond to LUAD-derived exosomes while pink bars correspond to exosomes derived from LUSC samples. Significance values were $**p \leq 0.01$, and $***p \leq 0.001$. LUAD: lung adenocarcinoma; LUSC: lung squamous cell carcinoma.

Both *XAGE1B* (also named *GAGED2a*) and *CABYR* are tumor-specific antigens of the Cancer Testis Antigens (CTA), which have attracted research attention as potential mediators of cancer cell recognition. CTAs are expressed in a variety of cancers, including lung cancer, while in normal tissues their expression is restricted to immune-privileged sites, such as the testis and placenta [337]. For this reason, they are considered ideal targets for cancer treatment due to their highly immunogenic and restricted expression in germ cells and malignancies [338,339].

However, when the expression of *TTF-1* (Figure 35a-b) and *SEPP1* (Figure 35c-d) was analyzed by RT-qPCR between LUAD and LUSC histologies, no significant differences in their expression were found ($p>0.05$). Although the *TTF-1* marker is widely used in the routine identification of LUAD [340,341], these results demonstrate that there is poor expression of this gene in NSCLC exosome samples, regardless of histology. This finding highlights the need to find new biomarkers that can better identify the different characteristics of lung cancer from a broader analytical approach such as liquid biopsies.

Results & Discussion – Chapter 1

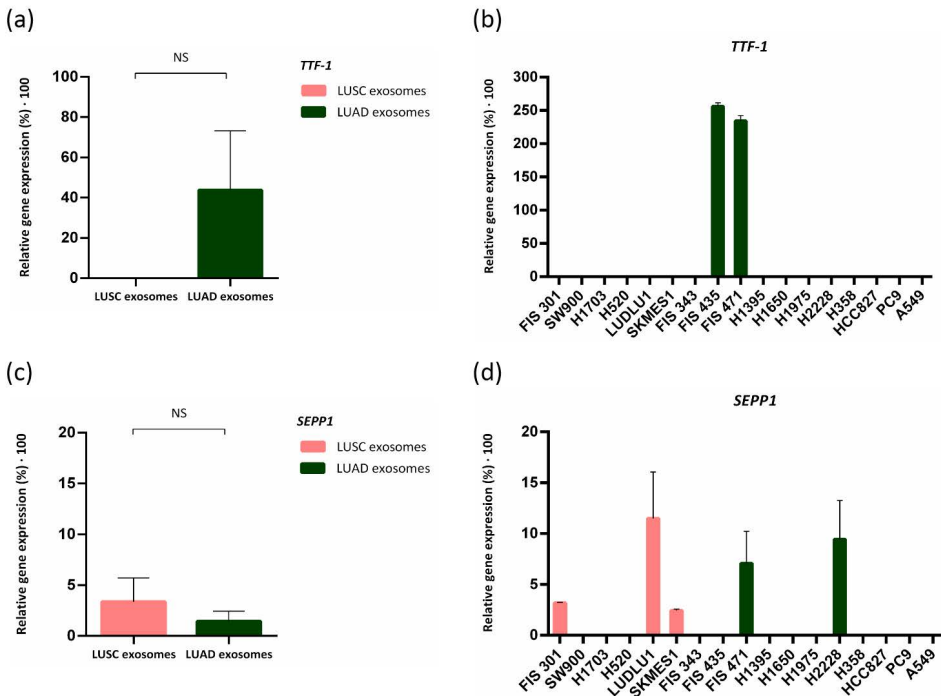


Figure 35. Analysis of *TTF-1* and *SEPP1* expression in tumor-derived exosomes from 2D cell cultures. Median of relative gene expression of *TTF-1* and *SEPP1* measured by RTqPCR in both histological groups (a-c). Mean with SD (standard deviation) of de relative gene expression of *TTF-1* and *SEPP1* to reference genes *ACTB* and *GAPDH* analyzed in the complete group of cell cultures-derived exosomes (b-d). Error bars represent the standard error of the mean (SEM). Dark green bars correspond to LUAD-derived exosomes while pink bars correspond to exosomes derived from LUSC samples. NS: non-significant; LUAD: lung adenocarcinoma; LUSC: lung squamous cell carcinoma.

Specifically, although the relative gene expression levels of *RIOK3* and *CAPRN1* do not reach a significant p-value ($p > 0.05$), there is a clear trend showing a higher expression of these 2 genes in the LUSC exosome group (Figure 36).

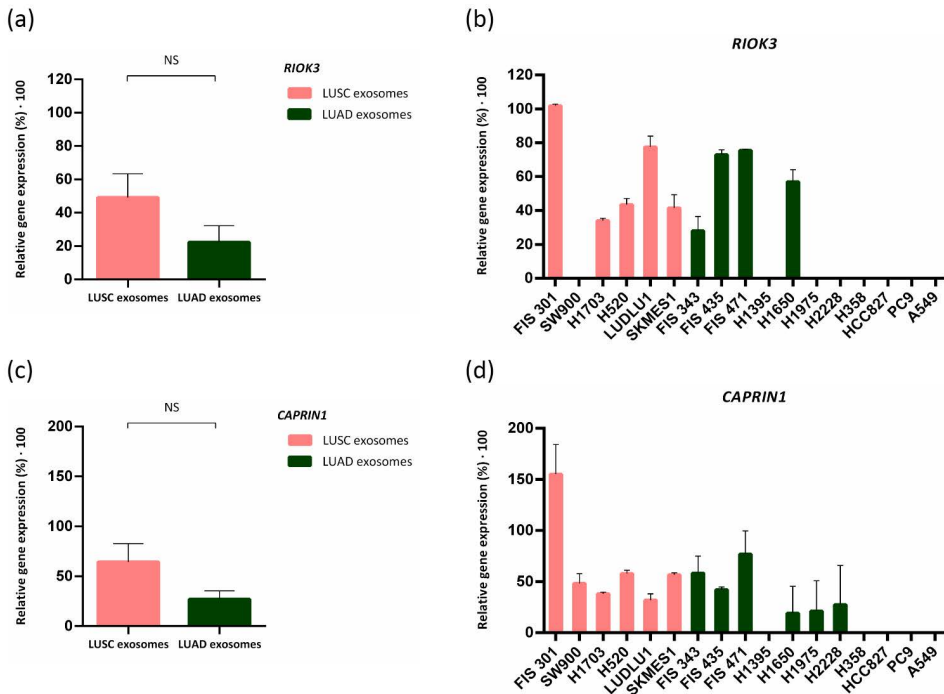


Figure 36. Analysis of *RIOK3* and *CAPRN1* expression in tumor-derived exosomes from 2D cell cultures. Median of relative gene expression of *RIOK3* and *CAPRN1* measured by RTqPCR in both histological groups (a-c). Mean with SD of de relative gene expression of *RIOK3* and *CAPRN1* to reference genes *ACTB* and *GAPDH* analyzed in the complete group of cell cultures-derived exosomes (b-d). Error bars represent the standard error of the mean (SEM). Dark green bars correspond to LUAD-derived exosomes while pink bars correspond to exosomes derived from LUSC samples. NS: non-significant; LUAD: lung adenocarcinoma; LUSC: lung squamous cell carcinoma.

SEPP1 gene is involved in selenium transport and the production of other selenoproteins. Previous studies have shown that *SEPP1* plays an important role in cancer through its function in mediating oxidative damage [342,343]. Moreover, there is evidence that *CAPRN-1* is involved during cell activation from a quiescent state, during cell division and is also required for cell growth [344]. In addition, *RIOK3* plays a key role in the synthesis of the 40S ribosomal

subunit in mammalian cells and in cytoskeletal organisation [345]. *RIOK3* also has been implicated in cell invasion, tumour growth and metastasis. However, previous research has limited the study of *RIOK3* to a few tumour types; and its mechanisms of action have not been well defined.[346] These observed markers such as *SEPP1*, *RIOK3* and *CAPRIN1* have been described for the first time in different exosomes samples through this work, so further analysis of these results in a NSCLC cohort would be of interest.

According to the cell culture models, transcriptomic differences were also observed in exosomes derived from 2D versus 3D cultures. PCA and hierarchical cluster analysis showed a distribution of the samples and two groups of differentially expressed genes according to the growth model used in cell cultures from which the exosomes were isolated (Figure 27). Interestingly, exosomes derived from LUAD cell cultures grown in 3D conditions (enriched in CSCs) showed a significant higher expression of *XAGE1B* ($p=0.013$) in comparison to 2D-monolayer (Figure 37). No differences were observed in the expression of the other genes analyzed for these two models. These results suggest that *XAGE1B* could be associated with a more aggressive tumor phenotype, or may even be related to the prognosis of NSCLC.

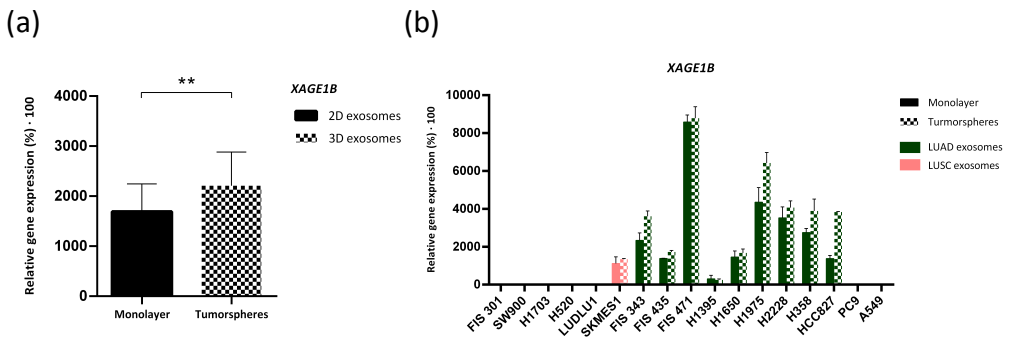
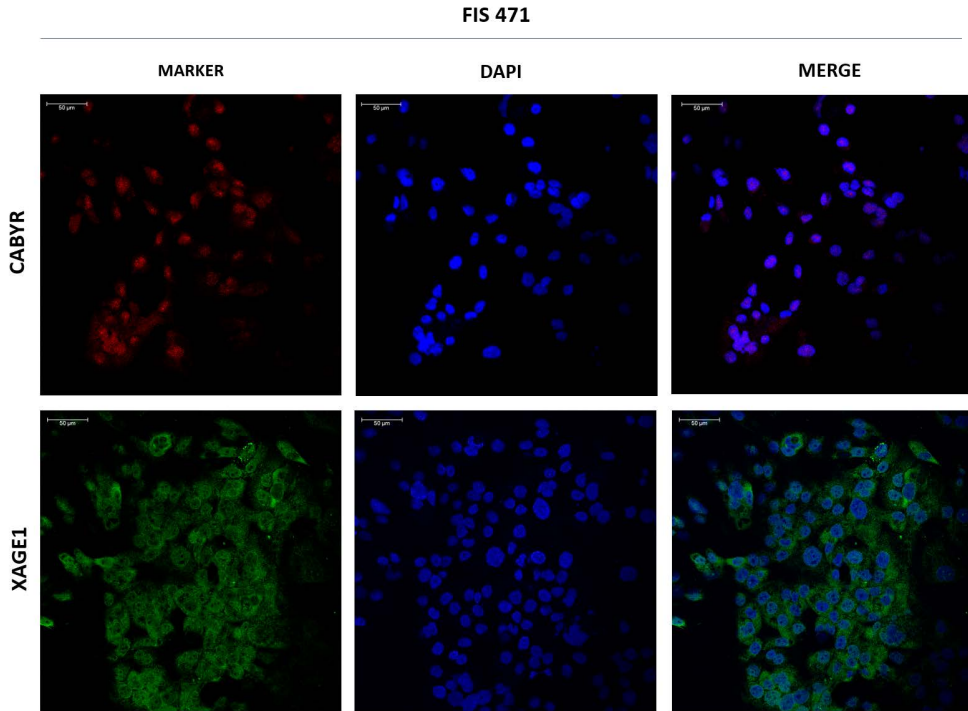


Figure 37. Validation of *XAGE1B* expression in cell cultures-derived exosomes from both models (2D-monolayer and 3D-tumorspheres). Median of relative gene expression of *XAGE1B* measured by RT-qPCR in both growth models of exosomes. Error bars represent the standard error of the mean (SEM). **(a)** Mean with SD of de relative gene expression of *XAGE1B* to reference genes *ACTB* and *GAPDH* analyzed in the complete group of cell cultures comparing to 2D vs 3D-derived exosomes. Dark green bars correspond to LUAD-derived exosomes while pink bars correspond to exosomes derived from LUSC samples **(b)**. Significant value was $**p \leq 0.01$. LUAD: lung adenocarcinoma; LUSC: lung squamous cell carcinoma.

Following the strong expression of *XAGE1* and *CABYR* in exosomes for LUAD and LUSC respectively, both markers were further investigated in the tumor cells of origin to check for possible differences with the secreted exosomes. For this purpose, protein analysis was performed by immunofluorescence (IF) in two primary cell cultures. As shown in Figure 38a, higher protein expression of *XAGE1B* was found in the cytosol of FIS 471 (LUAD), whereas FIS 301 (LUSC) showed higher expression of *CABYR* (Figure 38b), in agreement with transcriptomics and RT-qPCR results. However, both primary cultures showed basal expression of these two markers. Therefore, these results demonstrate that the analysis of these biomarkers in exosomes from tumor cells allows a clear histological classification with less ambiguity (Figure 34).

(a)



(b)

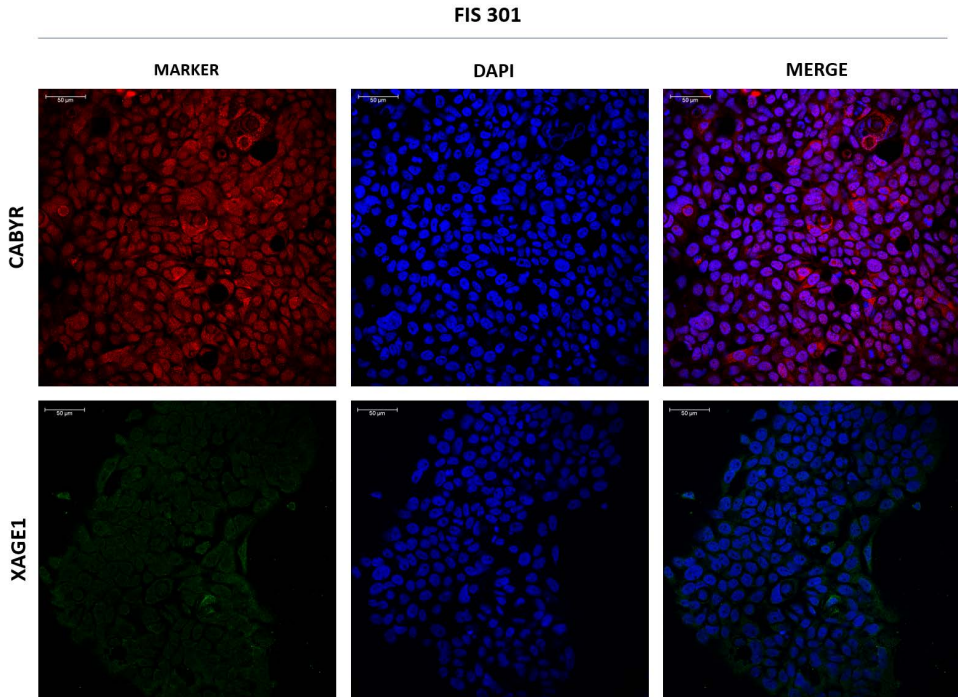


Figure 38. Immunofluorescent staining of CABYR and XAGE1 in primary cultures. Representative images of CABYR (red) and XAGE1B (green) in adherent-cultured cells from FIS 471 (LUAD) (a). Representative images of CABYR (red) and XAGE1B (green) in adherent-cultured cells from FIS 301 (LUSC) (b). Cell nuclei are stained with DAPI (blue). Scale bar represents 50 μm. **LUAD: lung adenocarcinoma; LUSC: lung squamous cell carcinoma.**

Interestingly, although previous studies have described the presence of *XAGE1* [347] and *CABYR* [348] in NSCLC tissues, our work demonstrates for the first time the presence of both biomarkers with robust overexpression within these lung cancer EVs.

The value of exosomes as prognostic biomarkers is not yet widely studied. One meta-analysis indicated that the expression level of exosomes was closely associated with the overall survival (OS) and disease-free survival (DFS) of patients with lung cancer, proposing that lung cancer exosomes are associated with poor prognosis [349]. The identification of these markers, among others, within components of liquid biopsy, particularly exosomes, presents a significant advantage in the management of NSCLC. The subsequent phase involves validating these findings within an independent cohort of NSCLC patients to establish the integration of exosomes as a forthcoming tool for biomarker assessment in clinical practice.

1.5. IN-SILICO VALIDATION OF EXOSOMAL BIOMARKERS IN NSCLC

In order to continue inquiring into the relevance of these previously described genes, we analyzed them in an independent cohort of NSCLC patients from the TCGA (The Cancer Genome Atlas Program). The clinicopathological characteristics of the patients included in this study are summarized in Table S5. Patients with post-surgical complications were excluded from the survival analysis. Of the 661 patients with resected NSCLC included in this subset, 208 (31.5%) had a recurrence and 261 (39.5%) died during follow-up. Only those patients who had at least 1 month of follow-up were included. However, information on recurrence was not available for 59

(8.9%) patients. The median follow-up was 23.08 months [range: 1.02-231.54].

The prognostic value of the different clinicopathological variables was assessed using the univariate Cox regression method for RFS and OS. This analysis showed that patients over 65, with more advanced stage (I vs. II vs. III) had shorter RFS and worse OS ($p < 0.05$) (Figure S2), which agrees with previously published results [350,351].

Also, a univariate Cox regression analysis was performed to determine whether the 3 most relevant biomarkers observed in exosomes from 3D cultures could be related to the prognosis of NSCLC patients. The results showed that high *SNAI1* levels were associated with worse RFS (HR:1.340; [1.081-1.660]; $p=0.007$) (Figure 39a) and OS (HR:1.350; [1.089-1.674]; $p=0.006$) (Figure 39b). Kaplan-Meier analyzes were carried out in order to obtain the survival plots (Figure 39). This relationship between *SNAI1* and prognosis in patients collected in the TCGA public database is consistent with data previously published by other authors in NSCLC [352,353], as well as in other cancer types [354,355]. In contrast, no significant association was found between *FDFT1* [OS: $p=0.170$; RFS: $p=0.20$] and *WNT5A* [OS: $p=0.80$; RFS: $p=0.40$] expression and patients' survival.

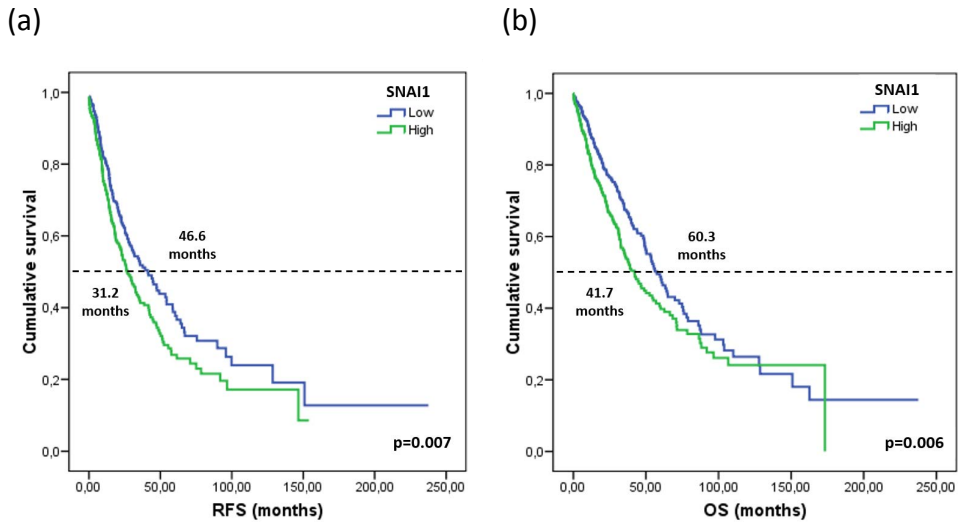


Figure 39. Prognostic value of *SNAI1* in the TCGA NSCLC cohort. Kaplan–Meier plot for RFS (a) and OS (b) according to the relative gene expression of *SNAI1*. Blue line represents patients with low expression levels, whereas green line represents patients with high expression. Cut-off values correspond to the median relative expression. P-values were calculated using the Kaplan–Meier test. RFS: relapse-free survival; OS: overall survival.

Moreover, a Mann-Whitney U test was performed in order to validate in this cohort, the exosomal biomarkers observed in the two most common histological types of NSCLC. These results indicated a relevant higher expression of *XAGE1B*, *SEPP1* and *TTF-1 (NKX2-1)* ($p < 0.001$) in the group of LUAD patients (N=328), compared to the LUSC group (Figure 40a-c).

Conversely, the expression of *CABYR* and *RIOK3* showed significantly higher values ($p < 0.001$) (Figure 40d-e), and with a minor difference *CAPRN1* ($p = 0.037$) in the group of patients with LUSC (N=316) compared with LUAD cohort (Figure 40f). No significant associations were found between the expression of this cluster of genes and patients' survival ($p > 0.05$).

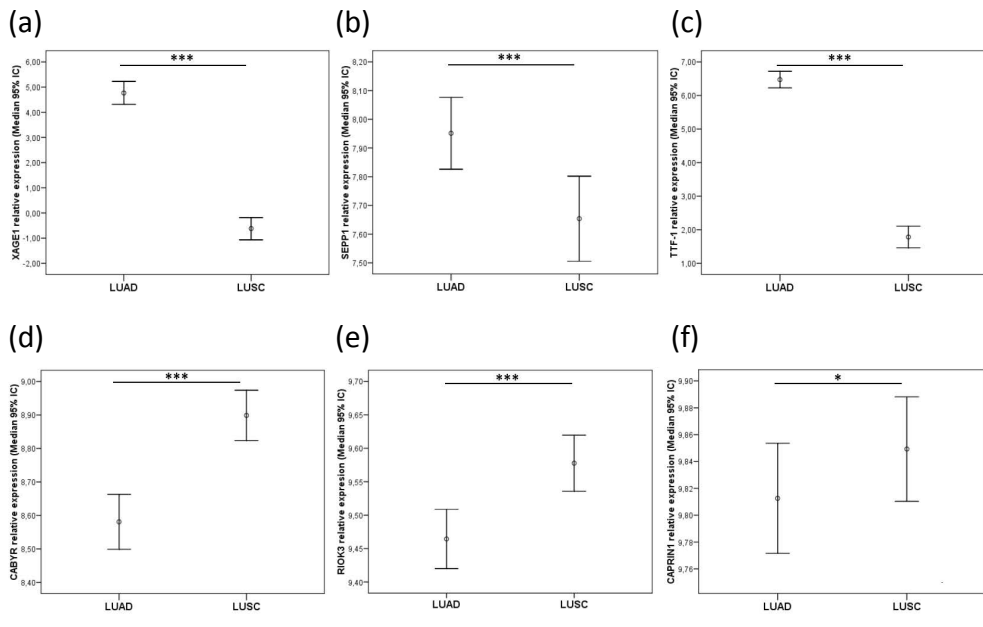


Figure 40. Mann–Whitney U-test of the histology-related biomarkers in TCGA cohort. *XAGE1* (a), *SEPP1* (b), *TTF-1* (c) relative expression in TCGA LUAD cohort and *CABYR* (d), *RIOK3*(e), *CAPRN1* (f) in LUSC cohort. Statistically significant differences were depicted: * $p < 0.05$, ** $p \leq 0.01$, and *** $p \leq 0.001$. IC: interval of confidence; LUAD: lung adenocarcinoma; LUSC: lung squamous cell carcinoma.

Although all these genes have been previously described in cancer [356–361], not all of them have been studied for their presence in NSCLC tumor cells, so their true role in this disease is still unknown. In addition, only *XAGE1* and *TTF-1* have been related to a specific histologic subtype. Meanwhile, the rest of the described markers have not yet been associated with a specific molecular pattern. Hence, the results described in this work may represent a relevant finding for the study of lung cancer biomarkers.

1.6. VALIDATION OF EXOSOMAL BIOMARKERS IN A RESECTED NSCLC COHORT

To further validate the potential value of the biomarkers seen in exosomes and validated in TCGA cohort, an independent cohort of patients with resected NSCLC tumors from HGUV was used. Of the 186 resected NSCLC patients included in this part of the study, 85 (45.7%) relapsed and 91 (48.9%) died during the follow-up. The median follow-up of the patients was 31.93 months [range: 1–161.7]. Clinicopathological characteristics of the resected patient's cohort are summarized in Table 10.

The prognostic value of the different clinicopathologic variables was assessed by univariate Cox regression for RFS and OS. Significant results obtained from the univariate Cox regression method were also analyzed using the Kaplan-Meier method (log-rank) to obtain survival plots. This univariate analysis showed that patients with more advanced disease stage had shorter RFS (HR:1.435; [1.147-1.794]; $p=0.002$) and OS (HR:1.436; [1.129-1.826]; $p=0.003$). In addition, smokers and former smokers also had shorter RFS (HR:2.074; [1.010-4.261]; $p=0.047$) (Figure S3).

Considering the significantly higher expression of markers found in exosomes belonging to 3D cultures and subsequently associated with survival of NSCLC patients in the TCGA cohort, we analyzed whether *SNAI1* expression could also be associated with prognosis of patients included in this new cohort.

Table 10. Clinicopathological characteristics of the patients included in HGUV NSCLC cohort.

Characteristics	Total	
	(N=186)	%
Age at surgery:	(median, range) 65 [26-85]	
Gender		
Male	158	84.95
Female	28	15.05
Smoking status		
Current	91	48.65
Former	74	39.78
Never	21	11.29
Stage		
I	96	51.61
II	55	29.57
IIIA	35	18.82
Histology		
Adenocarcinoma	79	42.48
Squamous cell carcinoma	90	48.38
Others	17	9.14
Relapse		
Yes	85	45.70
No	101	54.30
Exitus		
Yes	91	48.92
No	95	51.08
Mutations		
Yes	103	55.37
No	83	44.63

For this purpose, prognostic value of *SNAI1* was assessed using the univariate Cox regression method for RFS and OS. Gene expression level were dichotomized according to the median. No significant results were obtained for the entire cohort (RFS: HR=1.135; [0.768-1.676]; p=0.526) (OS: HR=1.210; [0.798-1.835]; p=0.368) (Figure 41a). Surprisingly, despite having observed *SNAI1* expression in most of the exosome samples analyzed (82%), univariate Cox regression analysis revealed that high levels of *SNAI1* were associated with worse OS in LUAD patients (HR:2.248 [1.092-4.629], p=0.024) (Figure 41b). Survival plot from Kaplan-Meier analysis is shown in Figure 41.

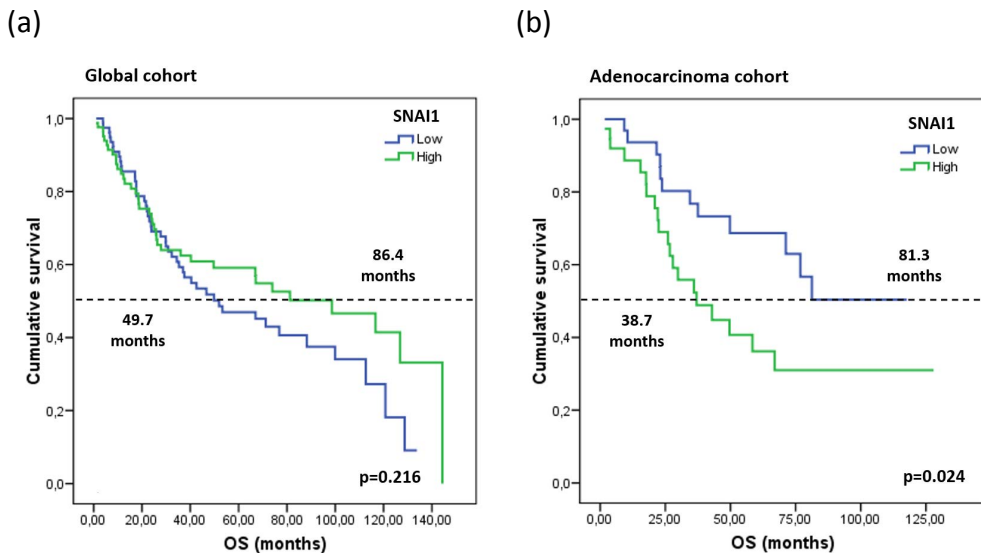


Figure 41. Kaplan–Meier plots for OS according to the relative expression of *SNAI1* in the global NSCLC HGUV cohort (a) and adenocarcinoma group (b). Blue lines represent patients with low levels of *SNAI1* expression, whereas green lines represent patients with high expression levels. Cut-off values correspond to the median relative expression. P-values were calculated using the Kaplan–Meier test. OS: overall survival.

Regarding LUSC patients, univariate Cox regression showed no associations between the expression of this gene and prognosis (RFS: HR=1.167; [0.696-1.954]; $p=0.558$) (OS: HR=0.982; [0.560-1.722]; $p=0.950$).

In addition, genes differentially expressed in exosomes and validated in the TCGA cohort as biomarkers for each of the main histologies of NSCLC were analyzed in this second cohort of patients. In this group of resected patients, analysis of TTF-1 expression was routinely performed by IHC at the Anatomical Pathology Department of the HGUV. All LUAD patients included in the cohort have been selected by this marker and by exclusion of other LUSC markers already established for this diagnosis in the department. Afterwards, we have analyzed the expression of the rest of the markers selected in the study by RT-qPCR, having previously extracted the genetic material from the same pieces of tumor tissue used for the formation of FFPE blocks for IHC analyzes.

Continuing with the LUAD group markers, only *XAGE1B* remain significant for this histology ($p<0.001$) showing a clear identification of the relative expression cut-off values to differentiate between LUAD and LUSC (Figure 42a), whereas in the relative expression of *SEPP1* great differences between both groups cannot be observed ($p>0.05$) (Figure S4a).

On the contrary, *CAPRN1* hardly showed differences in its expression between both histologies ($p>0.05$) (Figure S4b), meanwhile *CABYR* and *RIOK3* remain more expressed in LUSC patients ($p=0.003$ and $p=0.022$ respectively), showing no overlap in their relative expression cut-off values between groups (Figure 42b-c).

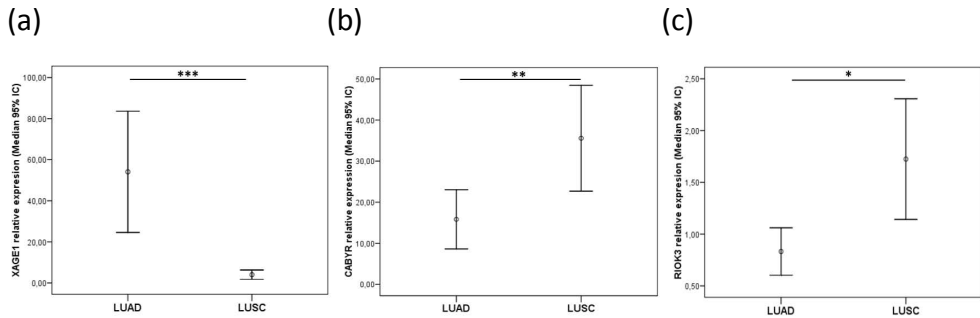


Figure 42. Mann–Whitney U-test of the histology-related biomarkers in HGUV cohort. *XAGE1* (a), *CABYR* (b) and *RIOK3* (c) relative expression in resected NSCLC adenocarcinomas and squamous cell carcinomas. Statistically significant differences were depicted: * $p < 0.05$, ** $p \leq 0.01$, and * $p \leq 0.001$. IC: interval of confidence; LUAD: lung adenocarcinoma; LUSC: lung squamous cell carcinoma.**

After observing the results previously obtained in this cohort, we selected only those markers that had presented very notable differences in relative expression cut-off values between both histology groups (*XAGE1B* and *CABYR*) ($p \leq 0.01$). Interestingly, Wilcoxon analysis of the resected NSCLC patients with paired samples revealed a higher presence of *XAGE1B* ($p = 0.003$) and *CABYR* ($p < 0.001$) in lung tumor tissue versus normal adjacent tissue (NAT) (Figure 43).

As previously mentioned, mRNA expression of different CTAs in healthy tissues is largely limited to testis, ovary, and placenta. So, as we can corroborate with these results, their expression in healthy lung tissue is very weak in many patients analyzed, compared to tumor tissue. The frequency of expression of an individual CTA is variable in different tumor types, as well as the frequency of expression of different CTA clusters in the same tumor [362].

The present work not only shows the presence of both cancer testis antigens (*XAGE1* and *CABYR*) in NSCLC tissues compared to healthy tissues, but also allows us to identify the histology of this type of cancer based on the expression ratios of both biomarkers. Moreover, these findings have been corroborated not only in tissue but also in microvesicles belonging to the tumor cells of origin, providing greater value of these markers in the study of NSCLC.

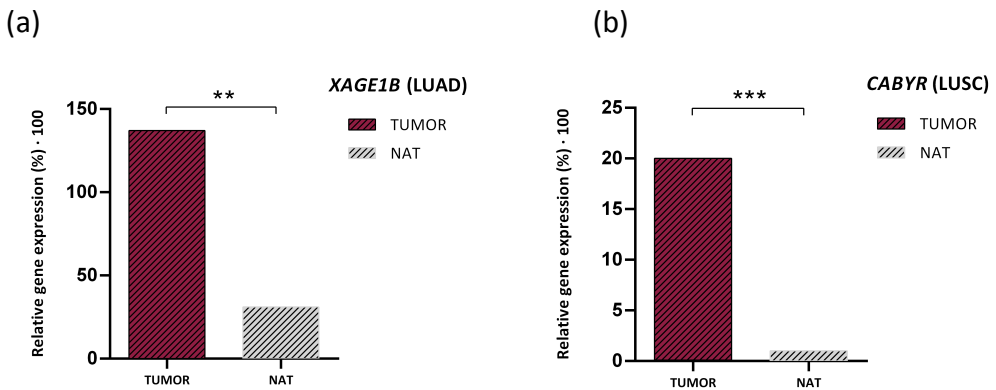
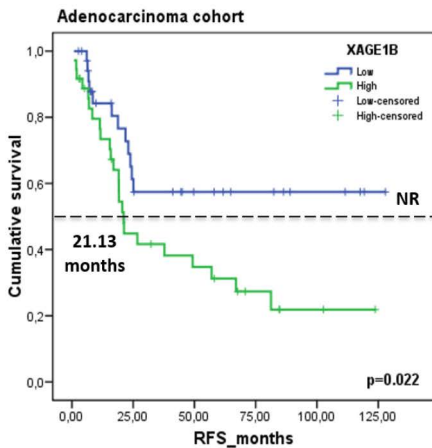


Figure 43. Median of relative expression of *XAGE1B* (a) and *CABYR* (b) in tumor tissue from HGUV NSCLC resected cohort vs. its expression in NAT (normal adjacent tissue) obtained by Mann-Whitney test. Statistically significant differences were depicted: ** $p \leq 0.01$, and *** $p \leq 0.001$. LUAD: lung adenocarcinoma; LUSC: lung squamous cell carcinoma.

Finally, upon confirming a significant expression of these two biomarkers in tumor tissue versus healthy tissue, we considered the role of these genes as possible prognostic factors. Kaplan–Meier analysis showed a significant association of *XAGE1B* with patient's prognosis (Figure 44). Patients with high expression of *XAGE1B* (>median) had shorter relapse-free survival (RFS: 21.13 vs NR months, HR: 2.16; [1.08-4.33]; $p=0.022$) (Figure 44a) and overall survival

(OS: 49.63 vs. not reached (NR) months, HR:2.69; [1.19-6.09]; $p=0.013$) (Figure 44b) in LUAD group (N=74).

(a)



(b)

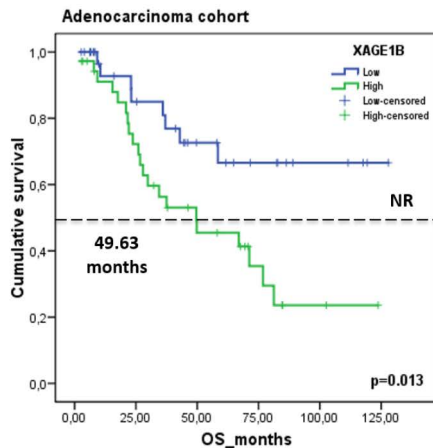


Figure 44. Prognostic value of *XAGE1B* in the HGUV NSCLC cohort. Kaplan–Meier plot for RFS (a) and OS (b) according to the relative gene expression to reference genes (*ACTB*, *GUSB*, *CDKN2A*) in the adenocarcinoma group. Blue line represents patients with low levels of *XAGE1B* expression, whereas green line represents patients with high expression levels. Cut-off values correspond to the median relative expression. P-values were calculated using the Kaplan–Meier test. RFS: relapse-free survival; OS: overall survival; NR: not reached.

In contrast, *CABYR* was not significantly correlated with RFS ($p=0.757$; HR: 1.08; [0.63-1.87]) or OS ($p=0.910$; HR: 1.03; [0.57-1.84]) in our hospital cohort (LUSC group) (Figure S5).

The results obtained in this first chapter reveal that exosomes from NSCLC tumor cells (under in vitro conditions) modulate the biological information present in their content according to the characteristics of the originating tumor cells. The presence of mRNAs and miRNAs in exosomes can provide relevant information about the tumor's histology, the different cellular subpopulations it comprises, and the multiple signaling pathways in which they are involved. Moreover, some of these biomarkers present in exosomes appear to be associated with the survival of NSCLC patients in the early stages of the disease. Furthermore, exosomes are proposed as a valuable tool for determining some of the most relevant molecular alterations in the clinical management of these patients.

CHAPTER 2: PLASMA

2.1. CHARACTERIZATION OF EXOSOMES DERIVED FROM NSCLC PLASMATIC SAMPLES

Following the isolation of microvesicles from plasma samples of NSCLC patients, the obtained samples underwent characterization to validate proper purification using a density gradient-based isolation kit. To ascertain the size of these vesicles, a subset of randomly chosen samples was subjected to NTA (Figure 45). The observed size range was between 99 and 140 nm, resembling the range observed in cell culture samples and aligning with sizes documented in literature corresponding to small extracellular vesicles (EVs) or exosomes.

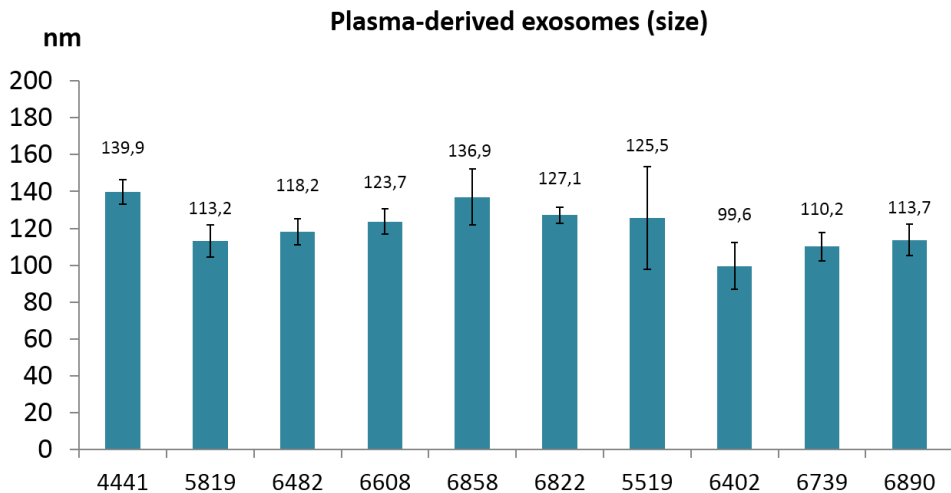


Figure 45. Plot of size distribution obtained using a NanoSight NS300 instrument in plasma-derived exosomes. Five measurements were taken five times over 60 seconds at 10 frames per second at room temperature. After all readings, mean size (nm) and standard deviation (SD) were calculated for exosome samples.

After this step, the size and morphology of the isolated exosomes were verified using TEM. As depicted in Figure 46, the structural analysis confirmed the typical spherical vesicles ('cupping') exhibiting well-defined and intact bilayer membranes, all measuring less than 200 nm in size.

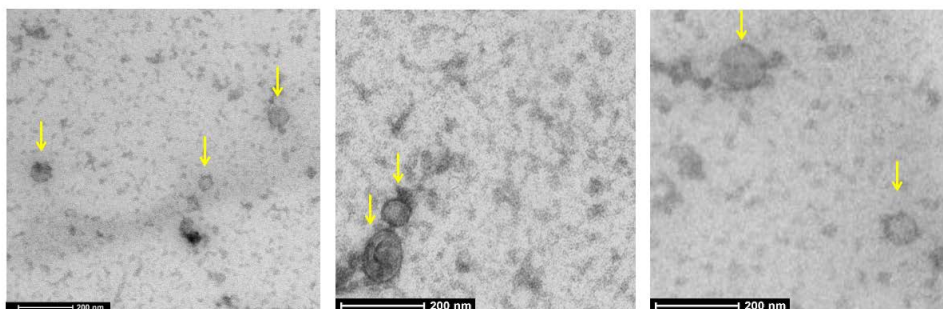


Figure 46. Representative TEM images of multiple exosomes isolated from NSCLC plasma samples. Small EVs are marked by yellow arrows. Scale bars to 200 nm.

Finally, to confirm the presence of surface markers, we conducted flow cytometry analysis using CD63 and CD81 antibodies. The results indicated the presence of these surface markers in the plasma exosome samples. Additionally, to validate the efficiency of the microvesicle isolation kit, we performed parallel labeling of both the obtained pellet and the resulting supernatant (Figure 47). The percentage of positivity observed between the supernatant of the samples and the exosome pellet obtained after isolation was quite remarkable. In the case of CD81 detection, we went from 0.15% positivity in the supernatant (Figure 47a) to 0.34% in the exosomal pellet (Figure 47b).

Results & Discussion – Chapter 2

On the other hand, the presence of CD63 was detected at 0.01% in the supernatant (Figure 47c), while the positivity of this marker increased to 0.15% in the obtained pellet (Figure 47d). This step allowed us to verify that the microvesicles were effectively precipitated under the sample-to-reactive ratio used in this isolation methodology.

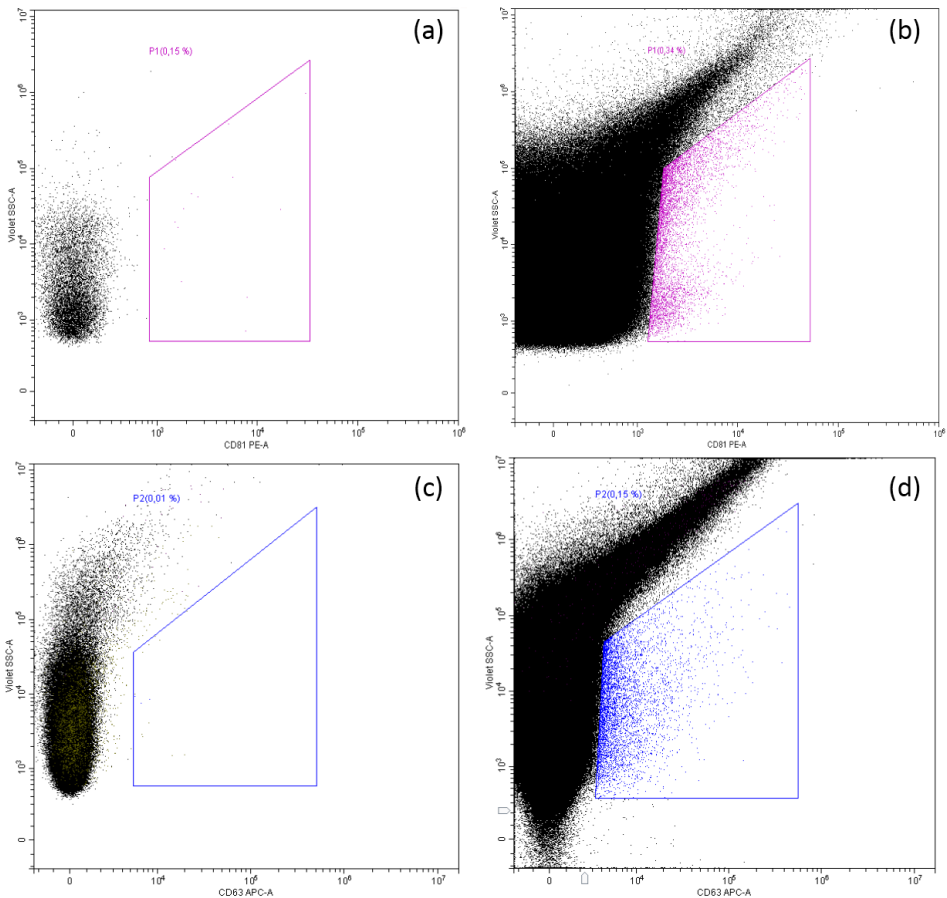


Figure 47. Flow cytometry analysis of the surface markers CD63 and CD81 in exosomes isolated from NSCLC patients' plasma. Supernatant of plasma samples after isolation of exosomes labeled for CD81 and CD63 (a, c). Pellet of exosomes isolated from plasma samples and labeled for CD81-PE (pink) and CD63-APC (blue) (b, d). The axes have a biexponential scale, where the Y-axis corresponds to side scatter (SSC), while the X-axis corresponds to forward scatter (FSC).

2.2. MUTATIONAL STATUS DETERMINATION VIA LIQUID BIOPSY ELEMENTS

To assess the capability of exosome-derived DNA detecting clinically relevant mutations, we conducted a comparison between cfDNA and exo-DNA analysis using NSCLC plasma samples. For cfDNA isolation, a sample volume of 2 ml was employed, following the established protocol for PCR-based methods. However, for the isolation of exo-DNA, a volume of 0.5-1 ml was used to assess its performance against the conventional gold standard.

Currently, digital PCR (dPCR) is one of the most robust and sensitive methods for determining DNA alterations [363]. In this work, we utilized different dPCR technologies, including BEAMing (beads, emulsion, amplification, and magnetics) dPCR and dPCR-3D (QuantStudio 3D Digital PCR System) (Thermo Fisher Scientific, USA), which are common and widely employed platforms in molecular biology laboratories.

As shown in Table 11, the DNA concentration obtained from isolated exosomes using 0.5 ml of plasma is comparable, if not more suitable, for the determination of these mutations by multiplex dPCR when compared to the ctDNA present in 2 ml of plasma. Furthermore, the comparison of these cases reveals that the percentage of the mutant fraction (MF) obtained in exosomes is similar or higher than the detected in ctDNA for several *KRAS* and *EGFR* mutations.

Table 11. Mutational analysis in cfDNA and exosomal DNA using different dPCR-based methods.

KRAS – G12V						
PATIENT	SAMPLE	PLASMA INPUT	CONCENTRATION	TECHNIQUE	MUTANT FRACTION	LOD
5519	cfDNA	2 ML	1.70 ng/μl	BEAMING	26 %	0.048
	cfDNA	2 ML	1.70 ng/μl	dPCR-3D	43.9 %	0.049
	EXOSOMES	0.5 ML	1.72 ng/μl	dPCR-3D	44.46 %	0.049
KRAS – G13D						
6402	cfDNA	2 ML	0.41 ng/μl	BEAMING	10 %	0.058
	cfDNA	2 ML	0.41 ng/μl	dPCR-3D	19.98 %	0.185
	EXOSOMES	0.5 ML	0.31 ng/μl	dPCR-3D	17.63 %	0.185
EGFR – L858R						
6858	cfDNA	2 ML	40.6 ng/μl	BEAMING	16.73 %	0.03
	cfDNA	2 ML	40.6 ng/μl	dPCR-3D	30.70 %	0.013
	EXOSOMES	0.5 ML	14.6 ng/μl	dPCR-3D	32.23 %	0.013
6890	cfDNA	2 ML	0.29 ng/μl	BEAMING	0.25 %	0.030
	cfDNA	2 ML	0.29 ng/μl	dPCR-3D	0 %	0.010
	EXOSOMES	0.5 ML	0.18 ng/μl	dPCR-3D	0 %	0.010
	EXOSOMES	1 ML	0.33 ng/μl	dPCR-3D	0.22 %	0.010
6739	cfDNA	2 ML	0.26 ng/μl	BEAMING	2.63 %	0.030
	cfDNA	2 ML	0.26 ng/μl	dPCR-3D	5.71 %	0.011
	EXOSOMES	0.5 ML	0.09 ng/μl	dPCR-3D	7.06 %	0.011
EGFR – T790M						
6739	cfDNA	2 ML	0.26 ng/μl	BEAMING	0.94 %	0.040
	cfDNA	2 ML	0.26 ng/μl	dPCR-3D	0.42 %	0.026
	EXOSOMES	0.5 ML	0.09 ng/μl	dPCR-3D	2.30 %	0.026

However, for patients with an extremely low MF, it was necessary to increase the volume of plasma used for exosome isolation to 1 ml before conducting the corresponding exo-DNA extraction (Table 11).

Results & Discussion – Chapter 2

In the case of patient 6890, the mutation was only detected in ctDNA using BEAMing (not detected by dPCR-3D), and it was also detected in exosomes (using dPCR-3D) after increasing the input volume (Figure 48).

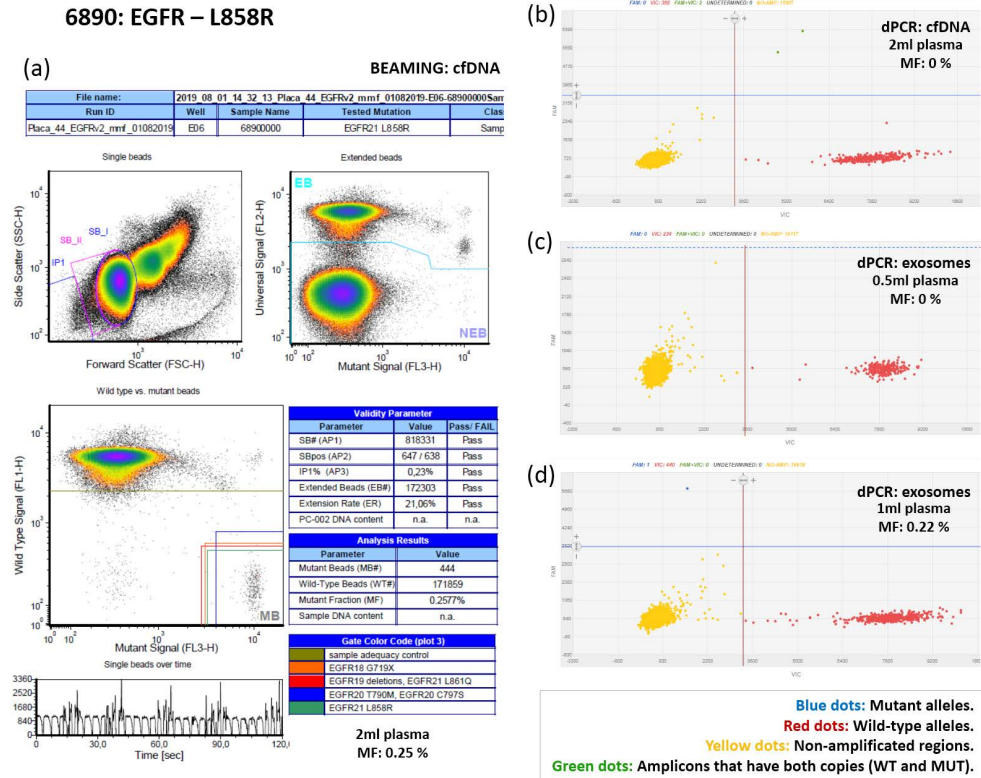


Figure 48. Comparison of different methods to detect EGFR alterations in a patient with a low mutant fraction. Results of ctDNA analysis were obtained by BEAMing (a) and dPCR-3D (b) from 2ml of plasma. Exo-DNA analysis was performed by dPCR-3D on 0.5ml (c) and 1ml of plasma (d). **dPCR: digital PCR; cfDNA: cell-free DNA; MB: mutant beads.**

Compared to other types of liquid biopsy biomarkers, exosome-based DNA tests are still in their early stages of development. However, they hold significant potential to enhance the analytical capabilities of more established diagnostic methods due to the greater stability of their genetic material when compared to cfDNA. While some studies suggest that microvesicle-based nucleic acid tests may exhibit slightly better performance than cfDNA tests, further comparative analyzes are required to determine the extent to which exosomes can surpass or complement cfDNA-based liquid biopsies [364,365].

Combining exo-DNA and cfDNA-based approaches has the potential to enhance disease information and improve both specificity and the limit of detection in tests. This is particularly valuable in scenarios such as the determination of certain tumor mutations known to be under-represented in some cases [366–369]. Moreover, due to the heterogeneity of EVs, multiplex assays that integrate DNA analysis with additional information on other biomolecules, such as miRNA, long non-coding RNA, and proteins, among others, have the potential to offer highly precise insights into the disease. This approach can significantly advance the prospects of personalized medicine [370].

There are also alternative biofluids, such as bronchoalveolar lavage fluid (BALF) from tumour sites, which show promising performance compared to blood-based assays due to their enrichment in tumour-specific EVs [371]. Notably, the reported average fragment length is longer in microvesicles

compared to cfDNA. Fragments of up to 4 kb are observed in exosome-derived DNA together with a nucleosome-associated pattern [372,373].

In liquid biopsies, the utilization of cfDNA has been considerably more prevalent than EV-DNA thus far. Nonetheless, it has been estimated that ctDNA may constitute as little as <0.01% of total cfDNA [374]. This ctDNA primarily originates from apoptosis, though its release kinetics can also be influenced by senescence and necrosis. Given its origin, ctDNA is highly fragmented nucleic acid, a factor to consider when designing amplicon sizes in PCR-based methodologies [375].

After identifying several mutations in NSCLC patients using various techniques (as shown in Table 11) for both cfDNA and exosomes isolated from plasma samples, the same mutations were also detected in exosomes from both serum and plasma samples. When comparing these results (see Table 12), it becomes evident that the concentration of exo-DNA isolated from serum is generally higher than that obtained from an equivalent amount of plasma sample. However, it's noteworthy that for most of the detected mutations, the mutant fraction (MF) is typically higher in plasma samples than in serum. In addition, in cases with a low percentage of MF, serum samples may give a questionable result where it is difficult to ensure the accuracy of the analysis (Figure 49).

Table 12. Comparative summary of exosomal DNA features isolated from NSCLC serum and plasma samples.

KRAS – G12V						
PATIENT	EXOSOMES SAMPLE	INPUT	CONCENTRATION	TECHNIQUE	MUTANT FRACTION	LOD
5519	PLASMA	0.5 ML	1.72 ng/μl	dPCR-3D	44.46 %	0.049
	SERUM	0.5 ML	30.6 ng/μl	dPCR-3D	1.02 %	0.049
EGFR – L858R						
6858	PLASMA	0.5 ML	14.6 ng/μl	dPCR-3D	32.23 %	0.013
	SERUM	0.5 ML	12.9 ng/μl	dPCR-3D	12.47 %	0.013
6890	PLASMA	1 ML	0.33 ng/μl	dPCR-3D	0.22 %	0.010
	SERUM	1 ML	1.20 ng/μl	dPCR-3D	0.27 %	0.010
6739	PLASMA	0.5 ML	0.09 ng/μl	dPCR-3D	7.06 %	0.011
	SERUM	0.5 ML	0.54 ng/μl	dPCR-3D	2.49 %	0.011
EGFR – T790M						
6739	PLASMA	0.5 ML	0.09 ng/μl	dPCR-3D	2.30 %	0.026
	SERUM	0.5 ML	0.54 ng/μl	dPCR-3D	2.29 %	0.026

Results & Discussion – Chapter 2

6890: EGFR – L858R

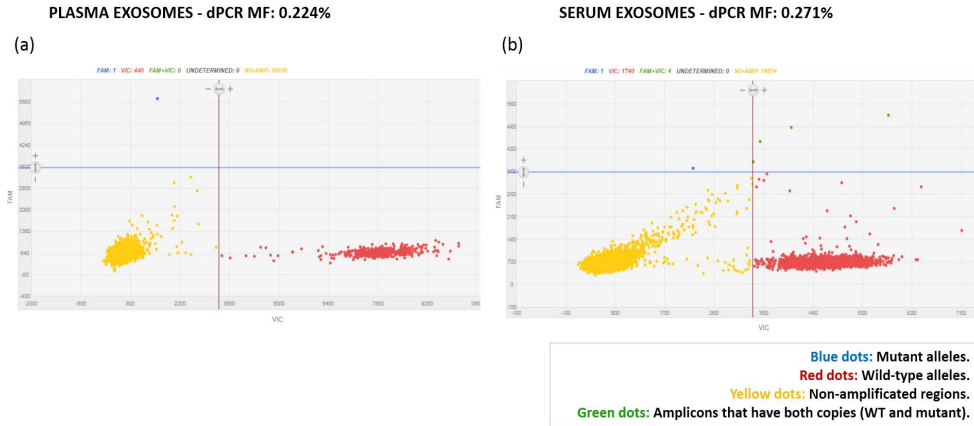


Figure 49. Comparison of dPCR-3D results on exosomal sample with low mutant fraction isolated from 1ml of plasma (a) and serum (b). Direct quantification of mutated and non-mutated sequences by dPCR-3D provides information on the percentage of mutated sequences. Samples are diluted and divided into many separate compartments that make up the chip, each containing one or zero copies of the target gene. PCR is performed on each compartment and the final fluorescence is measured to determine whether the compartment is positive or negative. This is followed by digital identification of the target gene in the sample. In cases where a mutant and WT copy (green dots) coincide in the same compartment, the result should be treated with caution and the total MF percentage should not be considered absolute. MF: mutant fraction; dPCR: digital PCR.

These findings in exosomes are consistent with a study conducted by Pittella-Silva and colleagues in 2020. In their research, they observed that the average total cfDNA concentration was 55% higher in serum samples, and longer DNA fragments were notably more prevalent in serum compared to plasma. Mutated nucleotides were detected in both sample types, but the proportion of mutated DNA was approximately half as much in serum compared to plasma. The authors suggested that this difference might be due to serum containing a higher dilution of non-cancerous DNA. In matched

samples from cancer patients, nearly 45% of mutations with low MF were not detected in serum samples, while concordance rates with somatic mutations identified in tissue biopsies at diagnosis were higher in plasma samples.[376]

Plasma and serum, the two primary types of blood supernatant, serve as sources of blood EVs, but it's still unclear if, how, and to what extent the choice between the two affects the results and interpretation of blood EV studies. Plasma and serum are collected using different methods, and it's well-known that this variance results in distinct protein and nucleic acid profiles [377,378].

Additionally, some studies suggest that serum-isolated EVs may contain additional vesicles released by platelets during clotting reactions, resulting in differences in EV profiles compared to plasma. Various factors, such as blood collection methods, hemolysis, selection between serum and plasma, use of anticoagulants, freeze/thaw cycles, storage duration/temperature, and EV isolation methods, are known or suspected to influence blood EV profiles. Therefore, it is essential to have a clear understanding of the study's objectives and always perform analyzes on the same type of sample to minimize potential variations [379,380].

2.3. ANALYSIS OF PLASMA EXO-mRNA FOR BIOMARKERS DETECTION

Exosomal RNAs were determined using the Agilent RNA Pico Chip. The small fragments were dominant in the exosomal RNAs (Figure 50). Unlike cells, microvesicle RNA does not contain the 18S and 28S ribosomal subunits. This approach helps us confirm the proper isolation of samples and the absence of contamination by cellular debris.

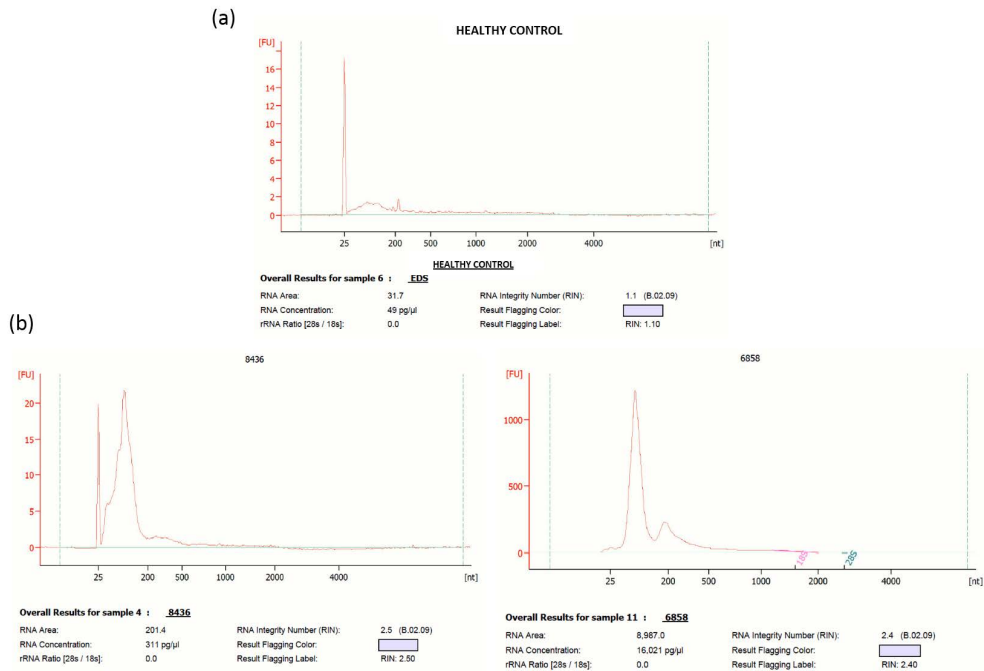


Figure 50. Quantification and integrity of RNA obtained from plasma exosomes by bioanalyzer. The upper panel graph corresponds to exo-RNA from a healthy individual (a), while the lower panel graphs correspond to exo-RNA from patients with NSCLC (b).

The pattern of integrity observed in exosomes from both healthy individuals and NSCLC patients is consistent with findings from other previously

published studies, in which exosomal RNA fragments were also found to be in the range of 30-200 nucleotides [381]. Furthermore, a significant difference in concentration and fragment size is also evident between exosomes from both types of samples. A study published in 2016 [382] analyzed oral fluid samples using NTA, revealing a significantly higher concentration of microvesicles in samples from patients with oral cancer compared to those from individuals without cancer. Previous studies have also demonstrated that various types of cancer cells, including lung cancer, tend to secrete elevated levels of exosomes compared to normal cells. These increased levels of exosomes in cancer are believed to facilitate intercellular communication and, consequently, tumor growth [383].

Until 2021, the nCounter platform had never been tested for mRNA analysis of plasma-derived EVs. However, *Bracht JWP et al.* [231] published a proof-of-concept study in which they optimized a workflow for EV enrichment, EV-mRNA purification, and subsequent gene expression analysis on the nCounter platform to develop biomarker assays. The methodology for exosomal RNA isolation and pre-amplification was optimized, resulting in a highly reproducible final workflow that can be completed in just three days. A significant finding was the binding of exo-DNA to the mRNA panel due to a probe design that did not span the intron, which requires the addition of a DNase step. In collaboration with this group, a custom human gene panel was designed with the goal of analyzing the gene expression of a set of biomarkers of interest in NSCLC exosomal plasma samples.

Out of the 30 probes included in the custom panel, only 23 finally yielded hybridization signals in more than one patient (3 probes corresponding to housekeeping genes were included). Although the design process aimed to include the same annotations as other genes previously analyzed (using microarrays) in exosomes from cell cultures, some of these probes (7 out of 30) did not produce expression values in the samples from this cohort.

Regarding this limitation, while NGS platforms are not always straightforward to implement in clinical practice, in this case, they might offer a more sensitive and accurate tool for biomarker discovery compared to the NanoString system, especially in terms of transcriptomic analysis of the content of these microvesicles. However, this is an interesting area that remains to be explored.

Out of the 36 plasmatic exosome samples from NSCLC patients (at baseline) intended for transcriptomic analysis, only 32 successfully completed the entire amplification, hybridization, and normalization process. The clinico-pathological characteristics of the patients included in this study are summarized in Table 13. Among the 32 patients in this subset, 26 (81.2%) experienced a recurrence, and 25 (78.1%) died during the follow-up. Only patients with at least 1 month of follow-up were included (96.8%). Additionally, information on recurrence was unavailable for one patient. The median follow-up duration was 12.23 months (range: 1.2-77.2). None of these variables showed a significant association with patient survival in univariate Cox regression analysis.

Table 13. Clinicopathological characteristics of the patients included in NSCLC plasma cohort.

Characteristics	Total	
	(N=32)	%
Age at surgery:	(median, range) 65 [51-82]	
Gender		
Male	24	75
Female	8	25
Stage		
III	5	16.3
IVa	20	62.2
IVb	7	21.5
Histology		
Adenocarcinoma	16	50
Squamous cell carcinoma	16	50
Mutations		
Yes	17	53.2
No	15	46.8
First Line Treatment		
Chemotherapy	15	46.9
Immunotherapy	10	31.2
Others	7	21.9

First, a hierarchical cluster analysis was conducted to obtain an overview of the global overexpression pattern of the markers analyzed in this cohort (Figure 51), followed by subsequent statistical analysis.

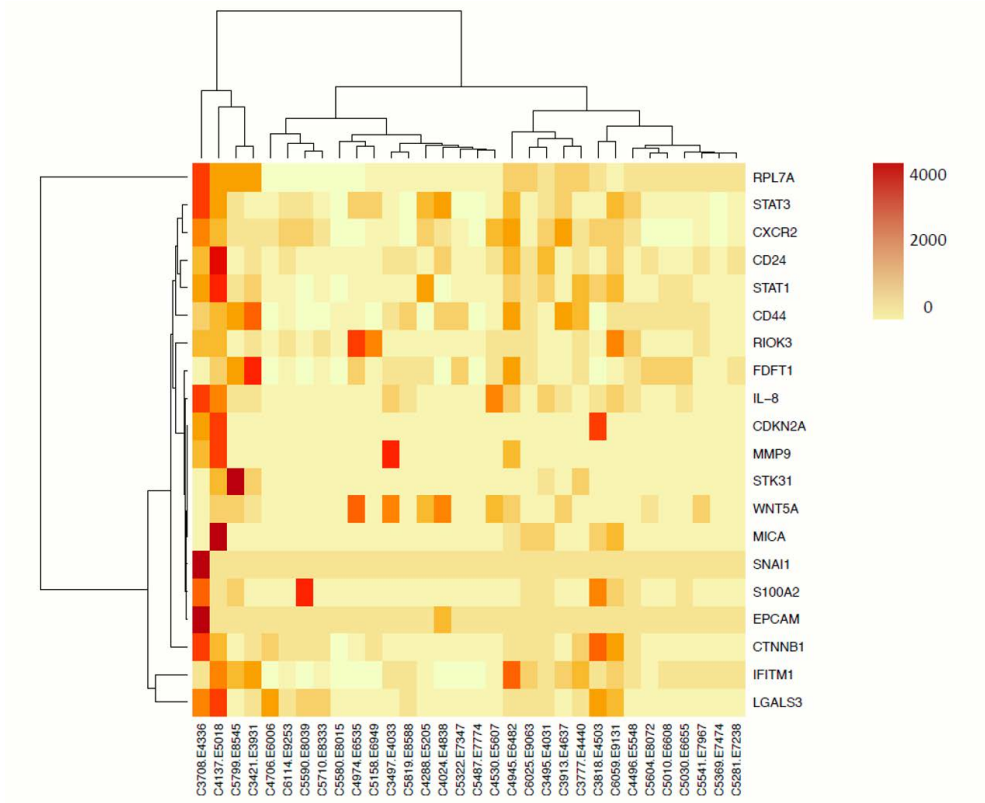


Figure 51. Hierarchical cluster analysis of probes that have amplified within the plasma exosome cohort. Light yellow corresponds to probes in which there has been no change in relative gene expression, while orange and red tones correspond to gradual overexpression.

After verifying that our data did not follow a normal distribution (Shapiro-Wilk test $p > 0.05$), as in the rest of the data analyzed previously, we proceeded to perform a Mann-Whitney U test to detect possible associations between the expression of these genes and some of the clinicopathological variables of our cohort (Figure 52).

Results & Discussion – Chapter 2

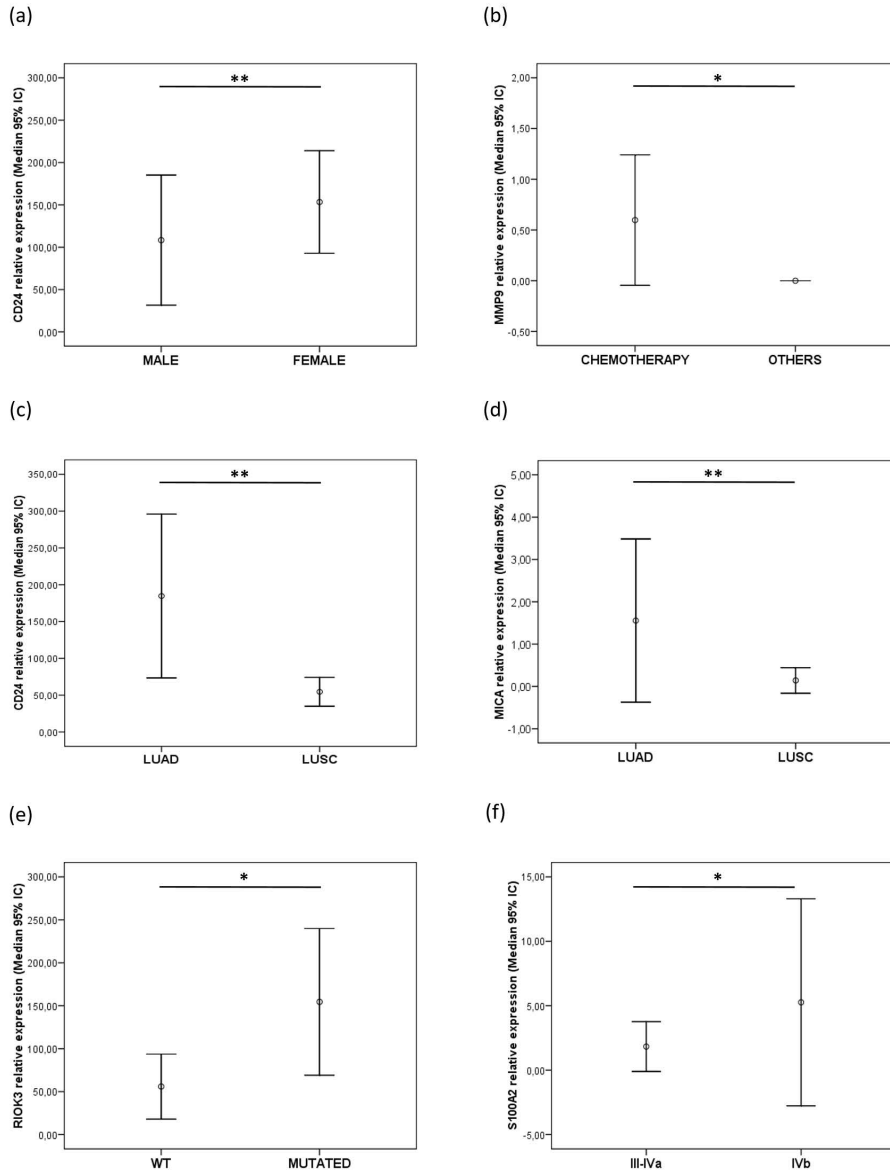


Figure 52. Mann–Whitney U-test of the exosomal biomarkers in plasma cohort. Relative expression of genes significantly associated with some of the clinicopathological variables such as gender **(a)**, treatment **(b)**, histology **(c-d)**, mutation status **(e)**, and stage **(f)**. Statistically significant differences were depicted: * $p < 0.05$, ** $p \leq 0.01$. IC: interval of confidence; LUAD: lung adenocarcinoma; LUSC: lung squamous cell carcinoma; WT: wild type.

Correlational analyzes revealed higher *MMP-9* expression in plasma exosomes from advanced NSCLC patients who received chemotherapy after diagnosis, as compared to those who underwent other types of therapy. Remarkably, several years ago, other authors demonstrated a close association between serum *MMP-9* concentrations in NSCLC cases during chemotherapy and the outcome of this treatment [384]. In addition, a study published a year later corroborated these same results in colorectal cancer [385]. A few years later, researchers reported combining serum *CD147* and *MMP-9* levels to predict the response to chemotherapy. Multivariate analysis demonstrated that variations in these markers could serve as independent factors for monitoring chemotherapy response in NSCLC patients, significantly improving predictive accuracy compared to using either protein alone [386].

Furthermore, the significant expression of *CD24* in the exosomes of LUAD patients is consistent with findings published by various authors that have linked *CD24* expression to this histology, and cancer-related mortality, suggesting an aggressive tumor behavior [387,388].

On the other hand, MHC Class I-Related Chain A (*MICA*) expression in exosomes also showed a significant relationship with the histology of the patients included in this cohort. As a tumour-associated antigen, it is widely expressed in a variety of neoplastic diseases [389–391].

It has previously been described in advanced NSCLC and its high expression was associated with a poor prognosis in these patients [391,392].

Additionally, plasma exosomal *RIOK3* expression was significantly associated with *EGFR*, *KRAS*, *ALK* or *PD-L1* positive tumours, as opposed to those with undetectable mutations. Previous evidence has shown that higher *RIOK3* expression in tumours, compared to healthy tissue, may be associated with the level of mismatch repair (MMR) gene mutations and DNA methyltransferase expression [360]. However, further analysis in a larger group of patients would be needed to determine whether there is a reliable association between *RIOK3* expression and the presence of molecular alterations.

Finally, the content of exosomes presents in NSCLC plasma samples showed an increased expression of the *S100A2* gene in patients with metastatic disease. The potential of this gene to induce metastasis has previously been described in mouse models [393]. There are evidences [393,394] demonstrating that *S100A2* is associated with poor survival in surgically resected NSCLC patients. Therefore, the presence of this marker in exosomes (obtained through liquid biopsy) could be a valuable tool for assessing the risk of relapse in early-stage patients and developing a more robust therapeutic strategy.

Moreover, regarding the potential association of the previously mentioned biomarkers with survival, the Cox regression analyzes conducted in this cohort did not reveal a significant association between these genes and the patients' RFS/OS ($p>0.05$). This lack of association could be attributed, at least in part, to the small number of individuals included in this cohort analyzed using this approach.

Finally, to determine whether the expression of any of these prominent markers in plasma exosomes might be associated with survival in early-stage NSCLC patients, a univariate analysis of these five genes was conducted in the TCGA cohort, which included 661 patients. The data did not show any significant association between these genes and RFS or OS in the overall cohort (Table S6).

However, when *CD24* and *MICA* genes were analyzed by histological subgroups, a lower significant RFS was observed in those LUSC patients with higher expression of *MICA* (HR:1.414; [1.005-1.988]; $p=0.045$) (Figure 53) (Table S7).

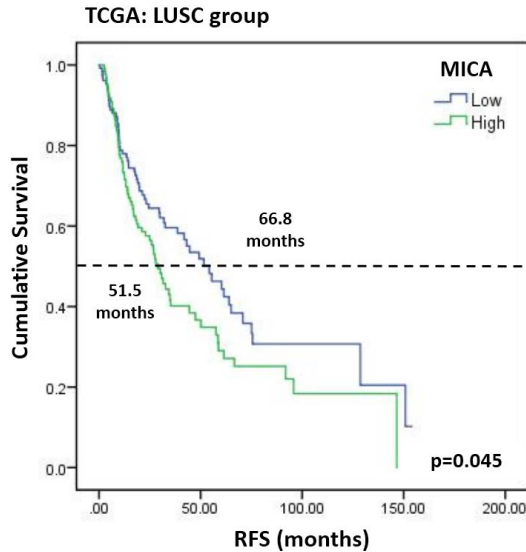


Figure 53. Kaplan-Meier plot for RFS according to *MICA* expression levels of the LUSC group (TCGA cohort). Blue line represents patients with low levels of *MICA* expression, whereas green line represents patients with high expression levels. Cut-off values correspond to the median relative expression. P-values were calculated using the Log-Rank test. **RFS: relapse-free survival; LUSC: lung squamous cell carcinoma.**

MICA is produced in response to viral infections and various forms of stress. *MICA* serves as a ligand for the *NKG2D* activating receptor, primarily found on natural killer (NK) and T cells. This interaction triggers the cytotoxicity of NK cells and plays a crucial role in immune surveillance, preventing the spread of pathogens and, in the context of cancer, impeding tumor progression [395].

However, in cancer patients with *MICA*-positive tumors, both systemic and tumor-infiltrating NK cells and CD8+ T cells frequently exhibit reduced *NKG2D* expression and diminished functionality. Tumor-associated matrix metalloproteinases (MMPs) can cut *MICA* at its transmembrane domain,

releasing soluble MICA proteins (sMICA) from tumor cells. As a result, this hinders the anti-tumoral actions of immune cells by reducing their ability to bind effectively to target cells [396,397].

It may be bewildering that the high expression of a molecule involved in alerting the immune response can, conversely, be associated with a tumor's immune evasion strategy. It is well-established that cellular transformation results in an increased expression of *NKG2D* (compared to baseline levels), turning these cells into specific targets for NK cell-mediated cytotoxicity [398,399]. Nevertheless, the elevated and maintained *MICA* expression can provide a selective advantage to tumor cells. This sustained expression may promote immunosuppression rather than immune activation, as the ongoing presence of *NKG2D* could desensitize NK cells and impair their function, ultimately contributing to tumor aggressiveness [400].

In relation to the results obtained from the TCGA database, there is no robust evidence confirming the relationship between patients' survival in the early stages of lung cancer and the overexpression of *MICA*. However, the association between this biomarker and poor prognosis in patients with advanced-stage lung cancer has been previously described [401,402].

The presence of *MICA* in tumor exosomes and its role in the immune evasion mechanism has already been described in some types of tumors [403–405]. Nevertheless, the results obtained in this thesis reveal, for the first time, the presence of *MICA* in exosomes derived from NSCLC.

This discovery could have significant implications for the development of new treatment strategies in lung cancer, with a focus on the role of these microvesicles in reshaping the tumor microenvironment and the immune system activation [406].

The results summarised in this final chapter demonstrate the great potential of exosomes as part of the liquid biopsy for the study and monitoring of this disease. Although there is still some way to go before standardisation of working protocols, exosomes have been shown to be an analyte that can be analysed using multiple approaches, starting with a small amount of sample obtained in a minimally invasive manner. However, many of the results obtained in this cohort of NSCLC patients need to be validated in a much larger number of patients. Given the complexity and relevance of the molecular information they contain; exosomes are a valuable tool that may represent a turning point in the clinical management of lung cancer.

V. INTEGRATION OF RESULTS

Integration of results

The present study has focused on the role of exosomes as elements of liquid biopsy for the study of NSCLC. To achieve this, exosomes from 4 primary cultures and 13 cell lines, as well as 50 peripheral blood samples from patients, were employed. Firstly, due to the lack of standardized protocols for the isolation of these microvesicles, a reliable and robust methodology was developed to obtain this analyte. Additionally, different cell culture methods were used, including 3D and 2D models.

The transcriptomic study of exosomes secreted by tumor cells *in vitro*, showed a significant expression differences between primary cultures vs. commercial cell lines, 3D and 2D cultures, and also in the classification of two of the most common histological subtypes in NSCLC (LUAD vs. LUSC). In these three comparative groups, a large number of differentially expressed mRNAs and miRNAs were observed.

In the group of samples from 3D-exosomes, it is worth highlighting notable genes, including *FDFT1*, *SNAI1*, and *WNT5A*, as some of them have been previously associated with CSCs. Enrichment analyzes conducted with the full set of differential mRNAs and miRNAs have identified various biological pathways closely related to the selected culture model, underscoring the importance of using 3D models enriched in CSCs to identify markers associated with malignant transformation, cell proliferation, or differentiation grade.

Additionally, a substantial number of genes present in exosomes were related to the histology of cell cultures. In the case of LUAD, *XAGE1B*, *SEPP1*,

Integration of results

and *TTF-1* stand out as notable biomarkers, while *CABYR*, *RIOK3*, and *CAPRIN1* are the most robust in the LUSC group. To investigate further the implication of these markers in NSCLC, the most prominent genes were analyzed using RT-qPCR in a set of exosomes from cell cultures larger than that used in the initial screening with arrays.

Our results reveal a robust expression of *FDFT1* and *SNAI1* in exosomes from 3D models. On the other hand, *XAGE1B* is significantly expressed in LUAD exosome samples, while *CABYR* emerges as a promising biomarker in LUSC.

Based on these findings, an *in silico* validation emphasized the correlation of *SNAI1* with the recurrence-free survival (RFS) and overall survival (OS) of 661 early-stage NSCLC patients from TCGA. High levels of this biomarker were associated with worse outcomes in individual survival analysis. In line with the previous results, Mann-Whitney tests revealed a significant association of *XAGE1B*, *SEPP1*, and *TTF-1* in LUAD patients, while *CABYR*, *RIOK3*, and *CAPRIN1* exhibited significant expression in LUSC. Additionally, the prognostic value of *SNAI1* was confirmed using an independent cohort of 186 patients from Hospital General Universitario de Valencia, showing that high levels of *SNAI1* were linked to worse OS in LUAD patients. Moreover, the role of *XAGE1B* as a prognostic biomarker in LUAD was reaffirmed in this cohort, and *CABYR* and *RIOK3* remained robust in LUSC.

Furthermore, the results demonstrated that *XAGE1B* and *CABYR* not only distinguished tumor histology in both tissue and exosomes from tumor cells but also exhibited higher expression in tumor tissue compared to weak

Integration of results

expression in healthy tissue, highlighting the significance of these markers in NSCLC research.

Continuing with the second chapter of this work, which is based on the study of exosomes derived from peripheral blood, a comprehensive characterization of the obtained samples was conducted. By analyzing various parameters such as morphology, size, concentration, and surface marker detection, the presence of these microvesicles was confirmed, corroborating the profile of NSCLC exosomes previously established from *in vitro* tumor samples. Furthermore, exo-DNA has allowed us to identify some of the most common molecular alterations in this pathology, including mutations in genes such as EGFR, KRAS, or ALK, which hold significant clinical relevance. This work highlights that a small volume of plasma can provide a sufficient amount of exo-DNA for reliable mutation detection, even in samples with a low mutant fraction.

Finally, the transcriptomic study of 36 exosome plasmatic samples from advanced-stage NSCLC patients made it possible to conduct multiplexed analysis in which significant associations between some markers (*CD24*, *MMP9*, *MICA*, *RIOK3*, and *S100A2*) and clinicopathological variables (such as histology, stage, presence of mutations, or subsequent treatment of these patients) were revealed.

In summary, the findings presented in this work underscore the pivotal role of exosomes in the study of lung cancer biology and also as a source of biomarkers assessment (Figure 54). The wide variety of genetic material

Integration of results

encapsulated within their lipid bilayer membrane allows us to construct a comprehensive understanding of the tumor's molecular characteristics and the mechanisms implicated in its progression. Certain exosomal markers may hold potential as therapeutic targets to modulate tumor behavior and its microenvironment. Validation of these results in larger number of NSCLC samples and the standardization of analytical methodologies are still necessary. However, in the near future, exosomes, along with other components of liquid biopsy, could serve as a complement to conventional tissue biopsies, especially in complex cases where they might become the primary diagnostic resource.

Integration of results

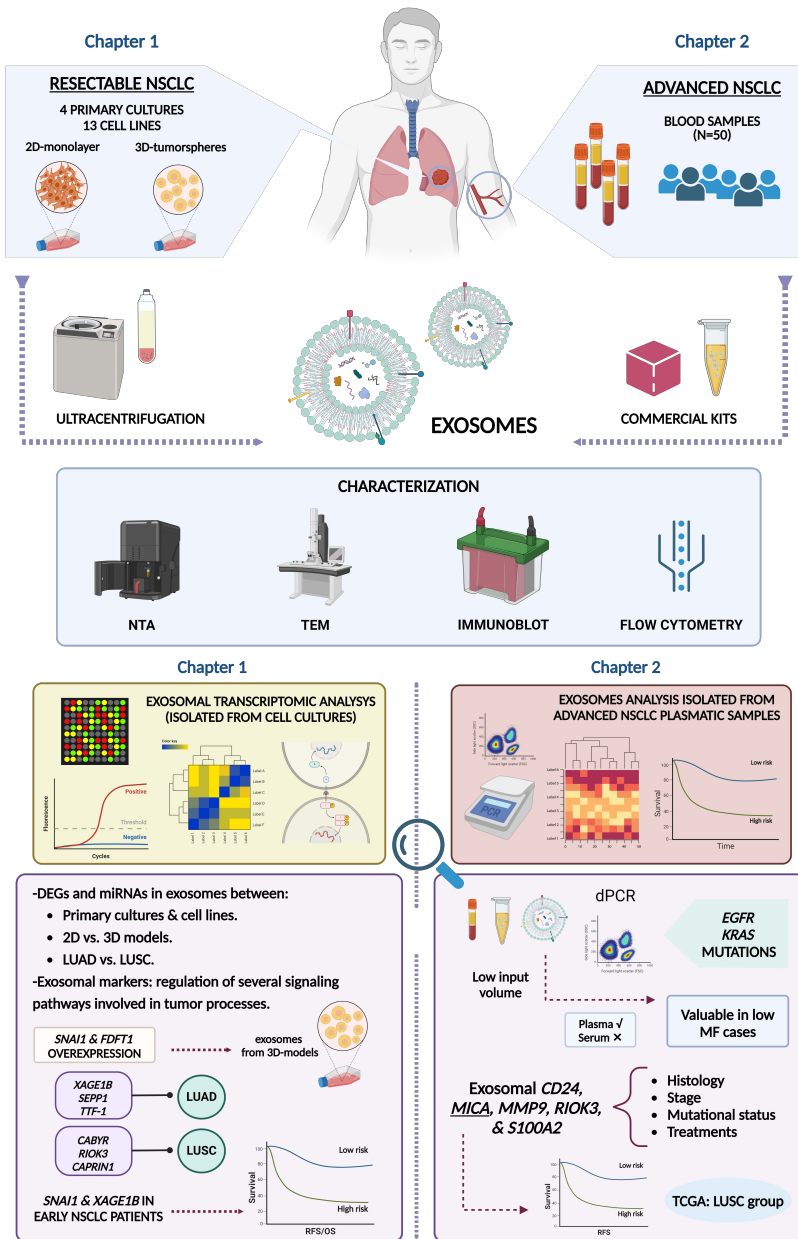


Figure 54. Integration of results encompassed in this thesis. (Own design created with BioRender.com) **LUAD:** lung adenocarcinoma; **LUSC:** lung squamous cell carcinoma; **NTA:** nanoparticle tracking analysis; **TEM:** transmission electron microscopy; **RFS:** relapse-free survival; **OS:** overall survival; **MF:** mutant fraction; **dPCR:** digital PCR; **TCGA:** The cancer genome atlas program.

VI. CONCLUSIONS

Conclusions

1. An optimal workflow has been developed for the isolation and subsequent quantification and characterization of exosomes secreted by cultured tumor cells, as well as those obtained from peripheral blood.

2. Several markers such as TSG-101, CD9, CD63, and CD81 were detected on the surface of microvesicles isolated from NSCLC, confirming the nature of the exosomes alongside the obtained size and morphology.

3. The use of different *in vitro* models such as primary cultures and 3D growth models is highly valuable for identifying biomarkers and signaling pathways involved in tumor processes in a more representative manner compared to conventional models.

3.1. Genes related to tumor progression, such as *FDFT1* and *SNAI1*, have shown significantly higher expression in exosomes from 3D models enriched in CSC populations.

3.2. According to gene expression analysis in both exosomes and tissue from early-stage NSCLC patients, the presence of certain markers can be used to predict histological subtypes: *XAGE1B*, *SEPP1*, and *TTF-1* in LUAD; while *CABYR*, *RIOK3*, and *CAPRIN1* were highly expressed in LUSC. Furthermore, *XAGE1B* and *CABYR* can be used to distinguish tumor tissue samples from adjacent healthy tissue.

4. In exosomes from plasma of advanced-stage NSCLC patients, markers like *CD24*, *MICA*, *MMP9*, *RIOK3*, and *S100A2* were significantly associated with clinicopathological variables such as histology, stage, mutational status, or response to therapeutic approaches.

Conclusions

4.1 The expression of markers selected from exosomal analysis (*SNAI1*, *XAGE1B* and *MICA*) in tissue samples has been shown to be related with the survival in early-stage NSCLC patients.

5. Mutations in clinically relevant genes (*EGFR*, *KRAS*, and *ALK*) can be reliably detected using nucleic acids extracted from microvesicles, even from small sample volumes and when dealing with a low percentage of mutant fraction.

6. The integration of these results establishes exosomes as highly valuable components for exploring the molecular characteristics of NSCLC, attainable through minimally invasive means throughout the course of the disease. The content encapsulated within these microvesicles emerges as a valuable asset for diagnosing, prognosis, and clinically managing patients with this condition.

VII. REFERENCES

References

1. Hanahan D, Weinberg RA. The Hallmarks of Cancer. *Cell*. 2000;100:57-70.
2. Fares J, Fares MY, Khachfe HH, Salhab HA, Fares Y. Molecular principles of metastasis: a hallmark of cancer revisited. *Sig Transduct Target Ther*. 2020;5(28).
3. Hanahan D, Weinberg RA. Hallmarks of Cancer: The Next Generation. *Cell*. 2011;144:646-674.
4. Hanahan D. Hallmarks of Cancer: New Dimensions. *Cancer Discov*. 2022;12(1):31-46.
5. Global Cancer Observatory. [web page] Accessed November 22, 2023. <https://gco.iarc.fr/>
6. Worldwide cancer data | World Cancer Research Fund International. [web page] Accessed November 22, 2023. <https://www.wcrf.org/cancer-trends/worldwide-cancer-data/>
7. SEOM: Sociedad Española de Oncología Médica - SEOM. [web page] Accessed November 22, 2023. <https://seom.org/>
8. Thandra K, A B, K S, JS A, A. B. Epidemiology of lung cancer. *Contemp Oncol (Pozn)*. 2021;25(1):45-52.
9. Sung H, Ferlay J, Siegel RL, et al. Global Cancer Statistics 2020: GLOBOCAN Estimates of Incidence and Mortality Worldwide for 36 Cancers in 185 Countries. *CA Cancer J Clin*. 2021;71(3):209-249.
10. Cui JW, Li W, Han FJ, Liu Y Di. Screening for lung cancer using low-dose computed tomography: Concerns about the application in low-risk individuals. *Transl Lung Cancer Res*. 2015;4(3):275-286.
11. Lancaster HL, Heuvelmans MA, Oudkerk M. Low-dose computed tomography lung cancer screening: Clinical evidence and implementation research. *J Intern Med*. 2022;292(1):68-80.
12. Remon J, Soria J c, Peters S, Guidelines Committeeclinicalguidelines E. Early and locally advanced non-small-cell lung cancer: an update of the ESMO Clinical Practice Guidelines focusing on diagnosis, staging, systemic and local therapy. *Ann Oncol*. 2021;32:1637-1642.
13. de Groot PM, Wu CC, Carter BW, Munden RF. The epidemiology of lung cancer. *Transl lung cancer Res*. 2018;7(3):220-233.

References

14. Gemine RE, Ghosal R, Collier G, et al. Longitudinal study to assess impact of smoking at diagnosis and quitting on 1-year survival for people with non-small cell lung cancer. *Lung Cancer*. 2019;129:1-7.
15. Tindle HA, Stevenson Duncan M, Greevy RA, et al. Lifetime Smoking History and Risk of Lung Cancer: Results From the Framingham Heart Study. *J Natl Cancer Inst*. 2018;110(11):1201-1207.
16. Rojewski AM, Tanner NT, Dai L, et al. Tobacco Dependence Predicts Higher Lung Cancer and Mortality Rates and Lower Rates of Smoking Cessation in the National Lung Screening Trial. *Chest*. 2018;154(1):110.
17. Greillier L, Cortot AB, Viguier J, et al. Perception of Lung Cancer Risk: Impact of Smoking Status and Nicotine Dependence. *Curr Oncol Rep*. 2018;20(18).
18. Sasco AJ, Secretan MB, Straif K. Tobacco smoking and cancer: A brief review of recent epidemiological evidence. *Lung Cancer*. 2004;45(SUPPL. 2).
19. Li Y, Hecht SS. Metabolism and DNA Adduct Formation of Tobacco-Specific N-Nitrosamines. *Int J Mol Sci*. 2022;23(9).
20. Pfeifer GP, Denissenko MF, Olivier M, Tretyakova N, Hecht SS, Hainaut P. Tobacco smoke carcinogens, DNA damage and p53 mutations in smoking-associated cancers. *Oncogene* 2002 2148. 2002;21(48):7435-7451.
21. Thun MJ, Henley SJ, Burns D, Jemal A, Shanks TG, Calle EE. Lung Cancer Death Rates in Lifelong Nonsmokers. *J Natl Cancer Inst*. 2006;98(10).
22. Sun S, Schiller JH, Gazdar AF. Lung cancer in never smokers — a different disease. *Nat Rev Cancer* 2007 710. 2007;7(10):778-790.
23. Torok S, Hegedus B, Laszlo V, et al. Lung cancer in never smokers. *Futur Oncol*. 2011;7(10):1195-1211.
24. Pelosof L, Ahn C, Gao A, et al. Proportion of Never-Smoker Non–Small Cell Lung Cancer Patients at Three Diverse Institutions. *JNCI J Natl Cancer Inst*. 2017;109(7).
25. Malhotra J, Malvezzi M, Negri E, La Vecchia C, Boffetta P. Risk factors for lung cancer worldwide. *Eur Respir J*. 2016;48(3):889-902.
26. Markowitz SB, Levin SM, Miller A, Morabia A. Asbestos, asbestosis, smoking, and lung cancer: New findings from the north american insulator cohort. *Am J Respir Crit Care Med*. 2013;188(1):90-96.

References

27. Clément-Duchêne C, Vignaud JM, Stoufflet A, et al. Characteristics of never smoker lung cancer including environmental and occupational risk factors. *Lung Cancer*. 2010;67:144-150.
28. Torres-Durán M, Ruano-Ravina A, Parente-Lamelas I, et al. Residential radon and lung cancer characteristics in never smokers. *Int J Radiat Biol*. 2015;91(8):605-610.
29. Corrales L, Rosell R, Cardona AF, Martín C, Zatarain-Barrón L, Arrieta O. Lung cancer in never smokers: The role of different risk factors other than tobacco smoking. *Crit Rev Oncol / Hematol*. 2020;148:102895.
30. Langevin SM, Kratzke RA, Kelsey KT. Epigenetics of Lung Cancer. *Transl Res*. 2015;165(1):74.
31. Amos CI, Wu X, Broderick P, et al. Genome-wide association scan of tag SNPs identifies a susceptibility locus for lung cancer at 15q25.1. *Nat Genet*. 2008;40(5):616.
32. Wang Y, Broderick P, Webb E, et al. Common 5p15.33 and 6p21.33 variants influence lung cancer risk. *Nat Genet*. 2008;40(12):1407.
33. Butkiewicz D, Rusin M, Enewold L, Shields PG, Chorazy M, Harris CC. Genetic polymorphisms in DNA repair genes and risk of lung cancer. *Carcinogenesis*. 2001;22(4):593-597.
34. Wenzlaff AS, Cote ML, Bock CH, et al. CYP1A1 and CYP1B1 polymorphisms and risk of lung cancer among never smokers: a population-based study. *Carcinogenesis*. 2005;26(12):2207-2212.
35. Li M, Li A, He R, et al. Gene polymorphism of cytochrome P450 significantly affects lung cancer susceptibility. *Cancer Med*. 2019;8:4892-4905.
36. Santillan AA, Camargo CA, Colditz GA. A meta-analysis of asthma and risk of lung cancer (United States). *Cancer Causes Control*. 2003;14:327-334.
37. Wang Y, Kuan PJ, Xing C, et al. Genetic Defects in Surfactant Protein A2 Are Associated with Pulmonary Fibrosis and Lung Cancer. *Am J Hum Genet*. 2009;84(1):52.
38. McNamee CJ, Adams A, Sugarbaker DJ. Overview of Anatomy and Pathophysiology of Lung Cancer. In: Sugarbaker DJ, Bueno R, Colson YL, et al., eds. *Adult Chest Surgery, Second Edition*. McGraw-Hill Education; 2015. <http://accesssurgery.mhmedical.com/content.aspx?aid=1105841950>

References

39. Gazdar AF, Brambilla E, Fourier J. Preneoplasia of lung cancer. *Cancer Biomarkers*. 2011;9(1-6):385-396.
40. National Cancer Institute. PDQ Adult Treatment Editorial Board. Non-Small Cell Lung Cancer Treatment (PDQ®): Health Professional Version. National Cancer Institute. Published 2020. [web page] Accessed December 29, 2022. <https://www.cancer.gov/types/lung/hp/non-small-cell-lung-treatment-pdq>
41. Walter FM, Rubin G, Bankhead C, et al. Symptoms and other factors associated with time to diagnosis and stage of lung cancer: a prospective cohort study. *Br J Cancer*. 2015;112(Suppl 1):S6.
42. Morgensztern D, Ng SH, Gao F, Govindan R. Trends in Stage Distribution for Patients with Non-small Cell Lung Cancer: A National Cancer Database Survey. *J Thorac Oncol*. 2010;5(1):29-33.
43. DR A, AM A, CD B, et al. Reduced lung-cancer mortality with low-dose computed tomographic screening. *N Engl J Med*. 2011;365(5):395-409.
44. Zhao YR, Xie X, De Koning HJ, Mali WP, Vliegenthart R, Oudkerk M. NELSON lung cancer screening study. *Cancer Imaging*. 2011;11(1A):S79.
45. Colella S, Vilmann P, Konge L, Clementsen PF. Endoscopic ultrasound in the diagnosis and staging of lung cancer. *Endosc ULTRASOUND*. 2014;3(4).
46. Munoz ML, Lechtzin N, Li QK, et al. Bronchoscopy with endobronchial ultrasound guided transbronchial needle aspiration vs. transthoracic needle aspiration in lung cancer diagnosis and staging. *J Thorac Dis*. 2017;9(7):2178.
47. Detterbeck FC, Boffa DJ, Kim AW, Tanoue LT. The Eighth Edition Lung Cancer Stage Classification. *Chest*. 2017;151(1):193-203.
48. Asamura H, Nishimura KK, Giroux DJ, et al. IASLC Lung Cancer Staging Project: The New Database to Inform Revisions in the Ninth Edition of the TNM Classification of Lung Cancer. *J Thorac Oncol*. 2023;18(5):564-575.
49. Goldstraw P, Chansky K, Crowley J, et al. The IASLC Lung Cancer Staging Project: Proposals for Revision of the TNM Stage Groupings in the Forthcoming (Eighth) Edition of the TNM Classification for Lung Cancer. *J Thorac Oncol*. 2016;11(1):39-51.
50. Lababede O, Meziane MA. The Eighth Edition of TNM Staging of Lung Cancer: Reference Chart and Diagrams. *Oncologist*. 2018;23(7):844-848.

References

51. Goldstraw P, Crowley J, Chansky K, et al. The IASLC Lung Cancer Staging Project: Proposals for the Revision of the TNM Stage Groupings in the Forthcoming (Seventh) Edition of the TNM Classification of Malignant Tumours. *J Thorac Oncol*. 2007;2(8):706-714.
52. Yang L, Wang S, Zhou Y, et al. Evaluation of the 7 th and 8 th editions of the AJCC/UICC TNM staging systems for lung cancer in a large North American cohort. *Oncotarget*. 2017;8(40):66784-66795.
53. Nicholson AG, Tsao MS, Beasley MB, et al. The 2021 WHO Classification of Lung Tumors: Impact of Advances Since 2015. *J Thorac Oncol*. 2022;17(3):362-387.
54. Travis WD, Brambilla E, Riely GJ. New pathologic classification of lung cancer: Relevance for clinical practice and clinical trials. *J Clin Oncol*. 2013;31(8):992-1001.
55. Gazdar AF, Bunn PA, Minna JD. Small-cell lung cancer: what we know, what we need to know and the path forward. *Nat Rev Cancer*. 2017;17(12):725-737.
56. Früh M, De Ruyscher D, Popat S, Crinò L, Peters S, Felip E. Small-cell lung cancer (SCLC): ESMO Clinical Practice Guidelines for diagnosis, treatment and follow-up. *Ann Oncol*. 2013;24(SUPPL.6):vi99-vi105.
57. Hamilton G, Rath B. Mesenchymal-epithelial transition and circulating tumor cells in small cell lung cancer. *Adv Exp Med Biol*. 2017;994:229-245.
58. Raso MG, Bota-Rabassedas N, Wistuba II. Pathology and Classification of SCLC. *Cancers* . 2021;13.
59. Godoy LA, Chen J, Ma W, et al. Emerging precision neoadjuvant systemic therapy for patients with resectable non-small cell lung cancer: current status and perspectives. *Biomark Res*. 2023;11(7):1-29.
60. Travis WD, Brambilla E, Nicholson AG, et al. The 2015 World Health Organization Classification of Lung Tumors: Impact of Genetic, Clinical and Radiologic Advances Since the 2004 Classification. *J Thorac Oncol*. 2015;10(9):1243-1260.
61. Travis WD, Brambilla E, Noguchi M, et al. International Association for the Study of Lung Cancer/American Thoracic Society/European Respiratory Society International Multidisciplinary Classification of Lung Adenocarcinoma. *J Thorac Oncol*. 2011;6(2):244.

References

62. Perez-Moreno P, Brambilla E, Thomas R, Soria JC. Squamous cell carcinoma of the lung: Molecular subtypes and therapeutic opportunities. *Clin Cancer Res.* 2012;18(9):2443-2451.
63. Travis WD. Lung tumours with neuroendocrine differentiation. *Eur J Cancer.* 2009;45(SUPPL. 1):251-266.
64. Konopka KE. Diagnostic Pathology of Lung Cancer. *Semin Respir Crit Care Med.* 2016;37(5):681-688.
65. Travis WD. Advances in neuroendocrine lung tumors. *Ann Oncol.* 2010;21(SUPPL. 7):vii65-vii71.
66. Peifer M, Fernández-Cuesta L, Sos ML, et al. Integrative genome analyses identify key somatic driver mutations of small cell lung cancer. *Nat Genet.* 2012;44(10):1104.
67. George J, Lim JS, Jang SJ, et al. Comprehensive genomic profiles of small cell lung cancer. *Nature.* 2015;524(7563):47.
68. Gridelli C, Rossi A, Carbone DP, et al. Non-small-cell lung cancer. *Nat Rev Dis Prim.* 2015;1.
69. Nakajima EC, Drezner N, Li X, et al. FDA Approval Summary: Sotorasib for KRAS G12C-Mutated Metastatic NSCLC. *Clin Cancer Res.* 2022;28(8):1482-1486.
70. Testa U, Castelli G, Pelosi E. Lung Cancers: Molecular Characterization, Clonal Heterogeneity and Evolution, and Cancer Stem Cells. *Cancers (Basel).* 2018;10(8).
71. Velizheva NP, Rechsteiner MP, Valtcheva N, et al. Targeted next-generation-sequencing for reliable detection of targetable rearrangements in lung adenocarcinoma-a single center retrospective study. *Pathol - Res Pract.* 2018;214:572-578.
72. Sasaki T, Rodig SJ, Chirieac LR, Jänne PA. The biology and treatment of EML4-ALK non-small cell lung cancer. *Eur J Cancer.* 2010;46(10):1773-1780.
73. McLaughlin J, Berkman J, Nana-Sinkam P. Targeted therapies in non-small cell lung cancer: present and future. *Fac Rev.* 2023;12.
74. Wu X, Zhang D, Shi M, Wang F, Li Y, Lin Q. Successful targeting of the NRG1 fusion reveals durable response to afatinib in lung adenocarcinoma: a case

References

- report. *Ann Transl Med.* 2021;9(19):1507-1507.
75. Heist RS, Sequist L V., Engelman JA. Genetic Changes in Squamous Cell Lung Cancer: A Review. *J Thorac Oncol.* 2012;7(5):924.
 76. Pikor LA, Ramnarine VR, Lam S, Lam WL. Genetic alterations defining NSCLC subtypes and their therapeutic implications. *Lung Cancer.* 2013;82(2):179-189.
 77. Salloum RG, Smith TJ, Jensen GA, Lafata JE. Survival among Non-Small Cell Lung Cancer Patients with Poor Performance Status after First Line Chemotherapy. *Lung Cancer.* 2012;77(3):545–549.
 78. Robinson CG, Dewees TA, El Naqa IM, et al. Patterns of Failure after Stereotactic Body Radiation Therapy or Lobar Resection for Clinical Stage I Non–Small-Cell Lung Cancer. *J Thorac Oncol.* 2013;8(2):192-201.
 79. Zaric B, Stojisic V, Tepavac A, et al. Adjuvant chemotherapy and radiotherapy in the treatment of non-small cell lung cancer (NSCLC). *J Thorac Dis.* 2013;5(S4):371-377.
 80. Rajeswaran A, Trojan A, Burnand B, Giannelli M. Efficacy and side effects of cisplatin- and carboplatin-based doublet chemotherapeutic regimens versus non-platinum-based doublet chemotherapeutic regimens as first line treatment of metastatic non-small cell lung carcinoma: A systematic review of randomized controlled trials. *Lung Cancer.* 2008;59(1):1-11.
 81. Ciuleanu T, Brodowicz T, Zielinski C, et al. Maintenance pemetrexed plus best supportive care versus placebo plus best supportive care for non-small-cell lung cancer: a randomised, double-blind, phase 3 study. *Lancet.* 2009;374(9699):1432-1440.
 82. Sandler A, Gray R, Perry MC, et al. Paclitaxel–Carboplatin Alone or with Bevacizumab for Non–Small-Cell Lung Cancer. *N Engl J Med .* 2006;355(24):2542-2550.
 83. Reck M, Von Pawel J, Zatloukal P, et al. Phase III trial of cisplatin plus gemcitabine with either placebo or bevacizumab as first-line therapy for nonsquamous non-small-cell lung cancer: AVAiL. *J Clin Oncol.* 2009;27(8):1227-1234.
 84. Garon EB, Ciuleanu TE, Arrieta O, et al. Ramucirumab plus docetaxel versus placebo plus docetaxel for second-line treatment of stage IV non-small-cell lung cancer after disease progression on platinum-based therapy (REVEL): a

References

- multicentre, double-blind, randomised phase 3 trial. *Lancet*. 2014;384(9944):665-673.
85. Reck M, Kaiser R, Mellemegaard A, et al. Docetaxel plus nintedanib versus docetaxel plus placebo in patients with previously treated non-small-cell lung cancer (LUME-Lung 1): a phase 3, double-blind, randomised controlled trial. *Lancet Oncol*. 2014;15(2):143-155.
 86. Pardoll DM. The blockade of immune checkpoints in cancer immunotherapy. *Nat Rev Cancer*. 2012;12(4):252.
 87. Planchard D, Popat S, Kerr K, et al. Metastatic non-small cell lung cancer: ESMO Clinical Practice Guidelines for diagnosis, treatment and follow-up †. *Ann ofOncology*. 2018;29.
 88. Yuan M, Huang LL, Chen JH, Wu J, Xu Q. The emerging treatment landscape of targeted therapy in non-small-cell lung cancer. *Signal Transduct Target Ther*. 2019;4(1).
 89. Chen R, Manochakian R, James L, et al. Emerging therapeutic agents for advanced non-small cell lung cancer. *J Hematol Oncol*. 2020;13(1).
 90. Chevallier M, Borgeaud M, Addeo A, Friedlaender A. World Journal of Clinical Oncology Oncogenic driver mutations in non-small cell lung cancer: Past, present and future Conflict-of-interest statement. *World J Clin Oncol*. 2021;12(4):217-237.
 91. Riudavets M, Sullivan I, Abdayem P, Planchard D. Targeting HER2 in non-small-cell lung cancer (NSCLC): a glimpse of hope? An updated review on therapeutic strategies in NSCLC harbouring HER2 alterations. *ESMO Open*. 2021;6(5):100260.
 92. Osmani L, Askin F, Gabrielson E, Li QK. Current WHO Guidelines and the Critical Role of Immunohistochemical Markers in the Subclassification of Non-Small Cell Lung Carcinoma (NSCLC). Moving from Targeted Therapy to Immunotherapy. *Semin Cancer Biol*. 2018;52(Pt 1):103.
 93. Yang CY, Yang JCH, Yang PC. Precision Management of Advanced Non–Small Cell Lung Cancer. *Annu Rev Med*. 2020;71:117-136.
 94. Olivares-Hernández A, Portillo EG del, Tamayo-Velasco Á, et al. Immune checkpoint inhibitors in non-small cell lung cancer: from current perspectives to future treatments—a systematic review. *Ann Transl Med*. 2023;11(10):354-354.

References

95. Marusyk A, Janiszewska M, Polyak K. Intratumor heterogeneity: the Rosetta stone of therapy resistance. *Cancer Cell*. 2020;37(4):471.
96. McGranahan N, Swanton C. Clonal Heterogeneity and Tumor Evolution: Past, Present, and the Future. *Cell*. 2017;168(4):613-628.
97. Li Y, Wang Z, Ajani JA, Song S. Drug resistance and Cancer stem cells. *Cell Commun Signal*. 2021;19(1).
98. Dick JE. Stem cell concepts renew cancer research. *Blood*. 2008;112(13):4793-4807.
99. Shackleton M, Quintana E, Fearon ER, Morrison SJ. Heterogeneity in cancer: cancer stem cells versus clonal evolution. *Cell*. 2009;138(5):822-829.
100. Safa AR, Saadatzadeh MR, Cohen-Gadol AA, Pollok KE, Bijangi-Vishehsaraei K. Glioblastoma stem cells (GSCs) epigenetic plasticity and interconversion between differentiated non-GSCs and GSCs. *Genes Dis*. 2015;2(2):152-163.
101. Luo J, Zhou X, Yakisich JS. Stemness and plasticity of lung cancer cells: paving the road for better therapy. *Onco Targets Ther*. 2014;7:1129.
102. Nowell PC. The Clonal Evolution of Tumor Cell Populations. *Science (80-)*. 1976;194(4260):23-28.
103. Kreso A, Dick JE. Evolution of the Cancer Stem Cell Model. *Cell Stem Cell*. 2014;14(3):275-291.
104. F. Quail D, J. Taylor M, Postovit LM. Microenvironmental Regulation of Cancer Stem Cell Phenotypes. *Curr Stem Cell Res Ther*. 2012;7(3):197-216.
105. Chaffer CL, Weinberg RA. How does multistep tumorigenesis really proceed? *Cancer Discov*. 2015;5(1):22.
106. Plaks V, Kong N, Werb Z. The Cancer Stem Cell Niche: How Essential is the Niche in Regulating Stemness of Tumor Cells? *Cell Stem Cell*. 2015;16:225-238.
107. Khan IN, Al-Karim S, Bora RS, Chaudhary AG, Saini KS. Cancer stem cells: a challenging paradigm for designing targeted drug therapies. *Drug Discov Today*. 2015;20(10):1205-1216.
108. Pisanti S, Lathia J, Wang R, et al. Role of Microenvironment on the Fate of Disseminating Cancer Stem Cells. *Front Oncol*. 2019;9:82.

References

109. Zhang S, Yang X, Wang L, Zhang C. Interplay between inflammatory tumor microenvironment and cancer stem cells. *Oncol Lett.* 2018;16(1):679.
110. Siolas D, Hannon GJ. Patient-Derived Tumor Xenografts: Transforming Clinical Samples into Mouse Models. *Cancer Res.* 2013;73(17):5315-5319.
111. Jilkova ZM, Kurma K, Decaens T. Animal Models of Hepatocellular Carcinoma: The Role of Immune System and Tumor Microenvironment. *Cancers (Basel).* 2019;11.
112. Maestri E. The 3Rs Principle in Animal Experimentation: A Legal Review of the State of the Art in Europe and the Case in Italy. *BioTech.* 2021;10(2).
113. Kapałczyńska M, Kolenda T, Przybyła W, et al. 2D and 3D cell cultures-a comparison of different types of cancer cell cultures. *Arch Med Sci.* 2018;14(4):910-919.
114. Cardoso BD, Castanheira EMS, Lanceros-Méndez S, Cardoso VF. Recent Advances on Cell Culture Platforms for In Vitro Drug Screening and Cell Therapies: From Conventional to Microfluidic Strategies. *Adv Healthc Mater.* 2023;12(18).
115. Herreros-Pomares A, Zhou X, Calabuig-Fariñas S, et al. 3D printing novel in vitro cancer cell culture model systems for lung cancer stem cell study. *Mater Sci Eng C.* 2021;122.
116. Chaicharoenaudomrung N, Kunhorm P, Noisa P. Three-dimensional cell culture systems as an in vitro platform for cancer and stem cell modeling. *World J Stem Cells.* 2019;11(12):1065-1083.
117. Bielecka ZF, Maliszewska-Olejniczak K, Safir IJ, Szczylik C, Czarnecka AM. Three-dimensional cell culture model utilization in cancer stem cell research. *Biol Rev Camb Philos Soc.* 2017;92(3):1505-1520.
118. Zanoni M, Piccinini F, Arienti C, et al. 3D tumor spheroid models for in vitro therapeutic screening: a systematic approach to enhance the biological relevance of data obtained. *Sci Rep.* 2015;6.
119. Drost J, Clevers H. Organoids in cancer research. *Nat Rev Cancer.* 2018;18(7):407-418.
120. Keller F, Bruch R, Schneider R, Meier-Hubberten J, Hafner M, Rudolf R. A Scaffold-Free 3-D Co-Culture Mimics the Major Features of the Reverse Warburg Effect In Vitro. *Cells.* 2020;9(8).

References

121. Ricci-Vitiani L, Lombardi DG, Pilozzi E, et al. Identification and expansion of human colon-cancer-initiating cells. *Nature*. 2006;445(7123):111-115.
122. Schöning JP, Monteiro M, Gu W. Drug resistance and cancer stem cells: the shared but distinct roles of hypoxia-inducible factors HIF1 α and HIF2 α . *Clin Exp Pharmacol Physiol*. 2017;44(2):153-161.
123. Ayob AZ, Ramasamy TS. Prolonged hypoxia switched on cancer stem cell-like plasticity in HepG2 tumourspheres cultured in serum-free media. *Vitr Cell Dev Biol - Anim*. 2021;57(9):896-911.
124. Loizzi V, del Vecchio V, Gargano G, et al. Biological Pathways Involved in Tumor Angiogenesis and Bevacizumab Based Anti-Angiogenic Therapy with Special References to Ovarian Cancer. *Int J Mol Sci*. 2017;18(9).
125. Semenza GL. Dynamic regulation of stem cell specification and maintenance by hypoxia-inducible factors. *Mol Aspects Med*. 2015;47-48:15-23.
126. Eguchi T, Sogawa C, Okusha Y, et al. Organoids with cancer stem cell-like properties secrete exosomes and HSP90 in a 3D nanoenvironment. *PLoS One*. 2018;13(2).
127. Calvet CY, André FM, Mir LM. The Culture of Cancer Cell Lines as Tumorspheres Does Not Systematically Result in Cancer Stem Cell Enrichment. *PLoS One*. 2014;9(2):89644.
128. Lee CH, Yu CC, Wang BY, Chang WW. Tumorsphere as an effective in vitro platform for screening anti-cancer stem cell drugs. *Oncotarget*. 2016;7(2):1215.
129. Weinfurtner K, Cho J, Ackerman D, et al. Variability in biopsy quality informs translational research applications in hepatocellular carcinoma. *Sci Reports*. 2021;11, 22763.
130. Fintelmann FJ, Troschel FM, Kuklinski MW, et al. Safety and Success of Repeat Lung Needle Biopsies in Patients with Epidermal Growth Factor Receptor-Mutant Lung Cancer. *Oncologist*. 2019;24(12):1570-1576.
131. Chouaid C, Dujon C, Do P, et al. Feasibility and clinical impact of re-biopsy in advanced non small-cell lung cancer: A prospective multicenter study in a real-world setting (GFPC study 12-01). *Lung Cancer*. 2014;86(2):170-173.
132. Calabuig-Fariñas S, Jantus-Lewintre E, Herreros-Pomares A, Camps C. Circulating tumor cells versus circulating tumor DNA in lung cancer—which

References

- one will win? *Transl Lung Cancer Res.* 2016;5(5):466.
133. Duréndez-Sáez E, Azkárate A, Meri M, et al. New insights in non-small-cell lung cancer: circulating tumor cells and cell-free DNA. *J Thorac Dis.* 2017;9(Suppl 13):S1332.
 134. Colombo M, Raposo G, Théry C. Biogenesis, Secretion, and Intercellular Interactions of Exosomes and Other Extracellular Vesicles. *Annu Rev Cell Dev Biol.* 2014;30:255-289.
 135. Doyle LM, Wang MZ. Overview of Extracellular Vesicles, Their Origin, Composition, Purpose, and Methods for Exosome Isolation and Analysis. *Cells.* 2019;8.
 136. Da Costa VR, Araldi RP, Vigerelli H, et al. Exosomes in the Tumor Microenvironment: From Biology to Clinical Applications. *Cells.* 2021;10(10).
 137. Théry C, Witwer KW, Aikawa E, et al. Minimal information for studies of extracellular vesicles 2018 (MISEV2018): a position statement of the International Society for Extracellular Vesicles and update of the MISEV2014 guidelines. *J Extracell Vesicles.* 2018;7(1).
 138. Johnstone RM, Adam M, Hammond JR, Orr L, Turbide C. Vesicle formation during reticulocyte maturation. Association of plasma membrane activities with released vesicles (exosomes). *J Biol Chem.* 1987;262(19):9412-9420.
 139. Frydrychowicz M, Kolecka-Bednarczyk A, Madejczyk M, Yasar S, Dworacki G. Exosomes – Structure, Biogenesis and Biological Role in Non-Small-Cell Lung Cancer. *Scand J Immunol.* 2015;81(1):2-10.
 140. Cordonnier M, Chanteloup G, Isambert N, et al. Exosomes in cancer theranostic: Diamonds in the rough Exosomes in cancer theranostic: Diamonds in the rough. *Cell Adhes Migr.* 2017;11:151-163.
 141. Benito-Martin A, Di Giannatale A, Ceder S, Peinado H, Sáenz-Cuesta M, Momma S. The new deal: a potential role for secreted vesicles in innate immunity and tumor progression. *Front Immunol.* 2015;6.
 142. Boukouris S, Mathivanan S. Exosomes in bodily fluids are a highly stable resource of disease biomarkers. *Proteomics Clin Appl.* 2015;9:358-367.
 143. Keller S, Ridinger J, Rupp AK, Janssen JWG, Altevogt P. Body fluid derived exosomes as a novel template for clinical diagnostics. *J Transl Med.* 2011;9(1):1-9.

References

144. Fu M, Gu J, Jiang P, Qian H, Xu W, Zhang X. Exosomes in gastric cancer: Roles, mechanisms, and applications. *Mol Cancer*. 2019;18(1):1-12.
145. Raposo G, Stoorvogel W. Extracellular vesicles: Exosomes, microvesicles, and friends. *J Cell Biol*. 2013;200(4):373.
146. Gurung S, Perocheau D, Touramanidou L, Baruteau J. The exosome journey: from biogenesis to uptake and intracellular signalling. *Cell Commun Signal*. 2021;19(1).
147. Wollert T, Hurley JH. Molecular Mechanism of Multivesicular Body Biogenesis by ESCRT Complexes. *Nature*. 2010;464(7290):864.
148. Babst M, Katzmann DJ, Snyder WB, Wendland B, Emr SD. Endosome-Associated Complex, ESCRT-II, Recruits Transport Machinery for Protein Sorting at the Multivesicular Body. *Dev Cell*. 2002;3:283-289.
149. Perez-Hernandez D, Gutiérrez-Vázquez C, Jorge I, et al. The Intracellular Interactome of Tetraspanin-enriched Microdomains Reveals Their Function as Sorting Machineries toward Exosomes. *J Biol Chem*. 2013;288(17):11649.
150. Stuffers S, Sem Wegner C, Stenmark H, Brech A. Multivesicular Endosome Biogenesis in the Absence of ESCRTs. *Traffic*. 2009;10(7):925-937.
151. Reclusa P, Sirera R, Araujo A, et al. Exosomes genetic cargo in lung cancer: a truly Pandora's box. *Transl lung cancer Res*. 2016;5(5):483-491.
152. Ostrowski M, Carmo NB, Krumeich S, et al. Rab27a and Rab27b control different steps of the exosome secretion pathway. *Nat Cell Biol*. 2009;12(1).
153. Yu X, Harris SL, Levine AJ. The regulation of exosome secretion: A novel function of the p53 protein. *Cancer Res*. 2006;66(9):4795-4801.
154. Thompson CA, Purushothaman A, Ramani VC, Vlodaysky I, Sanderson RD. Heparanase Regulates Secretion, Composition, and Function of Tumor Cell-derived Exosomes. *J Biol Chem*. 2013;288.
155. Messenger SW, Woo SS, Sun Z, Martin TFJ. A Ca²⁺-stimulated exosome release pathway in cancer cells is regulated by Munc13-4. *J Cell Biol*. 2018;217(8):2877.
156. Logozzi M, Mizzi D, Angelini DF, et al. Microenvironmental pH and Exosome Levels Interplay in Human Cancer Cell Lines of Different Histotypes. *Cancers (Basel)*. 2018;10(10).

References

157. Sheller-Miller S, Radnaa E, Arita Y, et al. Environmental Pollutant Induced Cellular Injury is Reflected in Exosomes from Placental Explants. *Placenta*. 2020;89:42.
158. To KKW, Cho WCS. Exosome secretion from hypoxic cancer cells reshapes the tumor microenvironment and mediates drug resistance. *Cancer Drug Resist*. 2022;5(3):577.
159. Laulagnier K, Motta C, Hamdi S, et al. Mast cell- and dendritic cell-derived exosomes display a specific lipid composition and an unusual membrane organization. *Biochem J*. 2004;380(Pt 1):161.
160. Llorente A, Skotland T, Sylvänne T, et al. Molecular lipidomics of exosomes released by PC-3 prostate cancer cells. *BBA - Mol Cell Biol Lipids*. 2013;1831:1302-1309.
161. Kowal J, Tkach M, Théry C. Biogenesis and secretion of exosomes. *Curr Opin Cell Biol*. 2014;29(1):116-125.
162. Becker A, Thakur BK, Weiss JM, Kim HS, Peinado H, Lyden D. Extracellular vesicles in cancer: cell-to-cell mediators of metastasis. *Cancer Cell*. 2016;30(6):836.
163. Li MY, Liu LZ, Dong M. Progress on pivotal role and application of exosome in lung cancer carcinogenesis, diagnosis, therapy and prognosis. *Mol Cancer*. 2021;20(1).
164. Reclusa P, Taverna S, Pucci M, et al. Exosomes as diagnostic and predictive biomarkers in lung cancer. *J Thorac Dis*. 2017;9(13):S1373-S1382.
165. Pucci M, Asiáin PR, Sáez ED, et al. Extracellular Vesicles As miRNA Nano-Shuttles : Dual Role in Tumor Progression. 2018;13(2):175-187.
166. Kumar Thakur B, Zhang H, Becker A, et al. Exosomes carry double-stranded DNA 766 Double-stranded DNA in exosomes: a novel biomarker in cancer detection. *Cell Res*. 2014;24:766-769.
167. Valadi H, Ekström K, Bossios A, Sjöstrand M, Lee JJ, Lötvall JO. Exosome-mediated transfer of mRNAs and microRNAs is a novel mechanism of genetic exchange between cells. *Nat Cell Biol*. 2007;9.
168. Chen F, Huang C, Wu Q, Jiang | Lili, Chen S, Chen | Liangyuan. Circular RNAs expression profiles in plasma exosomes from early-stage lung adenocarcinoma and the potential biomarkers. *J Cell Biochem*.

References

- 2020;121:2525-2533.
169. Konoshenko M, Sagaradze G, Orlova E, et al. Total Blood Exosomes in Breast Cancer: Potential Role in Crucial Steps of Tumorigenesis. *Int J Mol Sci.* 2020;21(19):1-18.
 170. Yu D, Li Y, Wang M, et al. Exosomes as a new frontier of cancer liquid biopsy. *Mol Cancer.* 2022;21(1).
 171. Kok VC, Yu CC. Cancer-Derived Exosomes: Their Role in Cancer Biology and Biomarker Development. *Int J Nanomedicine.* 2020;15:8019-8036.
 172. Wan Z, Gao X, Dong Y, et al. Exosome-mediated cell-cell communication in tumor progression. *Am J Cancer Res.* 2018;8(9):1661.
 173. Zhou W, Fong MY, Min Y, et al. Cancer-secreted miR-105 destroys vascular endothelial barriers to promote metastasis. *Cancer Cell.* 2014;25(4):501.
 174. Wang X, Pei X, Guo G, et al. Exosome-mediated transfer of long noncoding RNA H19 induces doxorubicin resistance in breast cancer. *J Cell Physiol.* 2020;235(10):6896-6904.
 175. Anderson NM, Simon MC. The tumor microenvironment. *Curr Biol.* 2020;30(16):R921-R925.
 176. Mulcahy LA, Pink RC, Carter DRF. Routes and mechanisms of extracellular vesicle uptake. *J Extracell Vesicles.* 2014;3(1).
 177. Chen F, Zhuang X, Lin L, et al. New horizons in tumor microenvironment biology: Challenges and opportunities. *BMC Med.* 2015;13(1).
 178. Kahlert C, Kalluri R. Exosomes in Tumor Microenvironment Influence Cancer Progression and Metastasis. *J Mol Med.* 2013;91(4):431.
 179. Whiteside TL. Tumor-Derived Exosomes and Their Role in Cancer Progression. *Adv Clin Chem.* 2016;74:103-141.
 180. Dang C Van, Zhao H, Yang L, et al. Tumor microenvironment derived exosomes pleiotropically modulate cancer cell metabolism. *Elife.* 2016;5.
 181. Huang TX, Guan XY, Fu L. Therapeutic targeting of the crosstalk between cancer-associated fibroblasts and cancer stem cells. *Am J Cancer Res.* 2019;9(9):1889-1904.
 182. Lee NK, Kumar Kothandan V, Kothandan S, Byun Y, Hwang SR. Exosomes and

References

- Cancer Stem Cells in Cancer Immunity: Current Reports and Future Directions. *Vaccines*. 2021;9.
183. Li X, Li X, Zhang B, He B. The Role of Cancer Stem Cell-Derived Exosomes in Cancer Progression. *Stem Cells Int*. 2022;2022.
184. Seo N, Akiyoshi K, Shiku H. Exosome-mediated regulation of tumor immunology. *Cancer Sci*. 2018;109(10):2998-3004.
185. Berchem G, Noman MZ, Bosseler M, et al. Hypoxic tumor-derived microvesicles negatively regulate NK cell function by a mechanism involving TGF- β and miR23a transfer Hypoxic tumor-derived microvesicles negatively regulate NK cell function by a mechanism involving TGF-b and miR23a transfer. *Oncoimmunology* . 2016;5(4).
186. Sobhani N, Tardiel-Cyril DR, Davtyan A, Generali D, Roudi R, Li Y. CTLA-4 in regulatory T cells for cancer immunotherapy. *Cancers (Basel)*. 2021;13(6):1-18.
187. Fernandes Ribeiro M, Zhu H, Millard RW, Fan GC. Exosomes Function in Pro- and Anti-Angiogenesis. *Curr Angiogenes*. 2013;2(1):54-59.
188. Whiteside TL. Exosomes and tumor-mediated immune suppression. *J Clin Invest*. 2016;126(4):1216-1223.
189. Watnick RS. The Role of the Tumor Microenvironment in Regulating Angiogenesis. *Cold Spring Harb Perspect Med*. 2012;2(12).
190. Zhang X, Yuan X, Shi H, Wu L, Qian H, Xu W. Exosomes in cancer: Small particle, big player. *J Hematol Oncol*. 2015;8(1).
191. Kalluri R. The biology and function of exosomes in cancer. *J Clin Invest*. 2016;126(4):1208-1215.
192. Maji S, Chaudhary P, Akopova I, et al. Exosomal Annexin A2 Promotes Angiogenesis and Breast Cancer Metastasis. *Mol cancer Res*. 2017;15(1):93.
193. Li I, Nabet BY. Exosomes in the tumor microenvironment as mediators of cancer therapy resistance. *Mol Cancer*. 2019;18(1):1-10.
194. Hoshino A, Costa-Silva B, Shen TL, et al. Tumour exosome integrins determine organotropic metastasis. *Nature*. 2015;527(7578):329-335.
195. Keklikoglou I, Cianciaruso C, Güç E, et al. Chemotherapy elicits pro-metastatic extracellular vesicles in breast cancer models. *Nat Cell Biol*.

References

- 2019;21(2):190-202.
196. Schillaci O, Fontana S, Monteleone F, et al. Exosomes from metastatic cancer cells transfer amoeboid phenotype to non-metastatic cells and increase endothelial permeability: Their emerging role in tumor heterogeneity. *Sci Rep.* 2017;7(1).
 197. Ye X, Brabletz T, Kang Y, et al. Upholding a role for EMT in breast cancer metastasis. *Nature.* 2017;547(7661):E1-E6.
 198. Wu M, Wang G, Hu W, Yao Y, Yu XF. Emerging roles and therapeutic value of exosomes in cancer metastasis. *Mol Cancer.* 2019;18(1).
 199. Zheng J. Energy metabolism of cancer: Glycolysis versus oxidative phosphorylation. *Oncol Lett.* 2012;4(6):1151-1157.
 200. Wang C, Xu J, Yuan D, et al. Exosomes carrying ALDOA and ALDH3A1 from irradiated lung cancer cells enhance migration and invasion of recipients by accelerating glycolysis. *Mol Cell Biochem.* 2020;469(1-2):77-87.
 201. Wang H, Wang L, Pan H, et al. Exosomes Derived From Macrophages Enhance Aerobic Glycolysis and Chemoresistance in Lung Cancer by Stabilizing c-Myc via the Inhibition of NEDD4L. *Front Cell Dev Biol.* 2021;8:620603.
 202. Lee JH, Kim C, Baek SH, et al. Capsazepine inhibits JAK/STAT3 signaling, tumor growth, and cell survival in prostate cancer. *Oncotarget.* 2017;8(11):17700.
 203. Nakagawa T, Oda G, Kawachi H, Ishikawa T, Okamoto K, Uetake H. Nuclear Expression of p-STAT3 Is Associated with Poor Prognosis in ER(-) Breast Cancer. *Clin Pract.* 2022;12(2):157-167.
 204. Kim DY, Cha ST, Ahn DH, et al. STAT3 expression in gastric cancer indicates a poor prognosis. *Gastroenterology.* 2008;24:646-651.
 205. Zhang Q, Liu RX, Chan KW, et al. Exosomal transfer of p-STAT3 promotes acquired 5-FU resistance in colorectal cancer cells. *J Exp Clin Cancer Res.* 2019;38(1).
 206. Paskeh MDA, Entezari M, Mirzaei S, et al. Emerging role of exosomes in cancer progression and tumor microenvironment remodeling. *J Hematol Oncol.* 2022;15(1).

References

207. Dorayappan KDP, Wanner R, Wallbillich JJ, et al. Hypoxia-induced exosomes contribute to a more aggressive and chemoresistant ovarian cancer phenotype: A novel mechanism linking STAT3/Rab proteins. *Oncogene*. 2018;37(28):3806.
208. Wu Q, Yang Z, Nie Y, Shi Y, Fan D. Multi-drug resistance in cancer chemotherapeutics: Mechanisms and lab approaches. *Cancer Lett*. 2014;347(2):159-166.
209. Lv M meng, Zhu X ya, Chen W xian, et al. Exosomes mediate drug resistance transfer in MCF-7 breast cancer cells and a probable mechanism is delivery of P-glycoprotein. *Tumor Biol*. 2014;35(11):10773-10779.
210. Corcoran C, Rani S, O'brien K, et al. Docetaxel-Resistance in Prostate Cancer: Evaluating Associated Phenotypic Changes and Potential for Resistance Transfer via Exosomes. *PLoS One*. 2012;7(12).
211. Mostafazadeh M, Samadi N, Kahroba H, Baradaran B, Haiaty S, Nouri M. Potential roles and prognostic significance of exosomes in cancer drug resistance. *Cell Biosci*. 2021;11(1).
212. Rabinowits G, Gerçel-Taylor C, Day JM, Taylor DD, Kloecker GH. Exosomal microRNA: A diagnostic marker for lung cancer. *Clin Lung Cancer*. 2009;10(1):42-46.
213. Wu Q, Yu L, Lin X, et al. Combination of serum miRNAs with serum exosomal miRNAs in early diagnosis for non-small-cell lung cancer. *Cancer Manag Res*. 2020;12:485-495.
214. Zhang Y, Zhang Y, Yin Y, Li S. Detection of circulating exosomal miR-17-5p serves as a novel non-invasive diagnostic marker for non-small cell lung cancer patients. *Pathol Res Pract*. 2019;215(8).
215. Li C, Lv Y, Shao C, et al. Tumor-derived exosomal lncRNA GAS5 as a biomarker for early-stage non-small-cell lung cancer diagnosis. *J Cell Physiol*. 2019;234(11):20721-20727.
216. Sandfeld-Paulsen B, Aggerholm-Pedersen N, Bæk R, et al. Exosomal proteins as prognostic biomarkers in non-small cell lung cancer. *Mol Oncol*. 2016;10(10):1595.
217. Jin X, Chen Y, Chen H, et al. Evaluation of tumor-derived exosomal miRNA as potential diagnostic biomarkers for early-stage non-small cell lung cancer using next-generation sequencing. *Clin Cancer Res*. 2017;23(17):5311-5319.

References

218. Gao J, Qiu X, Li X, et al. Expression profiles and clinical value of plasma exosomal Tim-3 and Galectin-9 in non-small cell lung cancer. *Biochem Biophys Res Commun*. 2018;498(3):409-415.
219. Wang Y, Niu X, Cheng Y, et al. Exosomal PD-L1 predicts response with immunotherapy in NSCLC patients. *Clin Exp Immunol*. 2022;208(3):316-322.
220. Dinh TKT, Fendler W, Chałubińska-Fendler J, et al. Circulating miR-29a and miR-150 correlate with delivered dose during thoracic radiation therapy for non-small cell lung cancer. *Radiat Oncol*. 2016;11(1):1-11.
221. Yuwen DL, Sheng BB, Liu J, Wenyu W, Shu YQ. Exosomal miR-146a-5p predicts cisplatin response of NSCLC. *Eur Rev Med Pharmacol Sci*. 2017;21:2650-2658.
222. Sandfeld-Paulsen B, Jakobsen KR, Bæk R, et al. Exosomal proteins as diagnostic biomarkers in lung cancer. *J Thorac Oncol*. 2016;11(10):1701-1710.
223. Zhang Y, Xu H. Serum exosomal miR-378 upregulation is associated with poor prognosis in non-small-cell lung cancer patients. *J Clin Lab Anal*. 2020;34(6).
224. Xian J, Zeng Y, Chen S, et al. Discovery of a novel linc01125 isoform in serum exosomes as a promising biomarker for NSCLC diagnosis and survival assessment. *Carcinogenesis*. 2021;42(6):831-841.
225. Dama E, Colangelo T, Fina E, et al. Biomarkers and lung cancer early detection: State of the art. *Cancers (Basel)*. 2021;13(15):3919.
226. Dragovic RA, Gardiner C, Brooks AS, et al. Sizing and phenotyping of cellular vesicles using Nanoparticle Tracking Analysis. *Nanomedicine*. 2021;7(6).
227. Malvern Panalytical. Applications of Nanoparticle Tracking Analysis (NTA) in Nanoparticle Research. Published online 2009. Accessed June 28, 2023. <https://www.azonano.com/article.aspx?ArticleID=2488>
228. Denis JA, Guillerme E, Coulet F, Larsen AK, Lacorte JM. The Role of BEAMing and Digital PCR for Multiplexed Analysis in Molecular Oncology in the Era of Next-Generation Sequencing. *Mol Diagnosis Ther*. 2017;21(6):587-600.
229. Huggett JF, Foy CA, Benes V, et al. The digital MIQE guidelines: Minimum information for publication of quantitative digital PCR experiments. *Clin Chem*. 2013;59(6):892-902.

References

230. Pfaffl MW. A new mathematical model for relative quantification in real-time RT-PCR. *Nucleic Acids Res.* 2001;29(9):0.
231. Bracht JWP, Gimenez-Capitan A, Huang CY, et al. Analysis of extracellular vesicle mRNA derived from plasma using the nCounter platform. *Sci Rep.* 2021;11(1):3712.
232. Waggott D, Chu K, Yin S, Wouters BG, Liu FF, Boutros PC. NanoStringNorm: An extensible R package for the pre-processing of nanostring mRNA and miRNA data. *Bioinformatics.* 2012;28(11):1546-1548.
233. Collisson EA, Campbell JD, Brooks AN, et al. Comprehensive molecular profiling of lung adenocarcinoma. *Nature.* 2014;511(7511):543-550.
234. Hammerman PS, Voet D, Lawrence MS, et al. Comprehensive genomic characterization of squamous cell lung cancers. *Nature.* 2012;489(7417):519-525.
235. Vlachos IS, Zagganas K, Paraskevopoulou MD, et al. DIANA-miRPath v3.0: deciphering microRNA function with experimental support. *Nucleic Acids Res.* 2015;43:W460-W466.
236. Kuleshov M V., Jones MR, Rouillard AD, et al. Enrichr: a comprehensive gene set enrichment analysis web server 2016 update. *Nucleic Acids Res.* 2016;44:W90-W97.
237. Bordanaba-Florit G, Madarieta I, Olalde B, Falcón-Pérez JM, Royo F. 3D Cell Cultures as Prospective Models to Study Extracellular Vesicles in Cancer. *Cancers (Basel).* 2021;13.
238. Baharvand H, Hashemi SM, Ashtiani SK, Farrokhi A. Differentiation of human embryonic stem cells into hepatocytes in 2D and 3D culture systems in vitro. *Int J Dev Biol.* 2006;50(7):645-652.
239. Nelson CM, Bissell MJ. Modeling dynamic reciprocity: Engineering three-dimensional culture models of breast architecture, function, and neoplastic transformation. *Semin Cancer Biol.* 2005;15(5):342.
240. Gurski LA, Petrelli NJ, Jia X, Farach-Carson MC. 3D Matrices for Anti-Cancer Drug Testing and Development. *Oncol Issues.* 2010;25(1):20-25.
241. Birgersdotter A, Sandberg R, Ernberg I. Gene expression perturbation in vitro-A growing case for three-dimensional (3D) culture systems. *Semin Cancer Biol.* 2005;15:405-412.

References

242. Kenny PA, Lee GY, Myers CA, et al. The morphologies of breast cancer cell lines in three-dimensional assays correlate with their profiles of gene expression. *Mol Oncol.* 2007;1(1):84.
243. Wu S, Luo M, To KKW, et al. Intercellular transfer of exosomal wild type EGFR triggers osimertinib resistance in non-small cell lung cancer. *Mol Cancer.* 2021;20(1).
244. Reclusa P, Taverna S, Pucci M, et al. Exosomes as diagnostic and predictive biomarkers in lung cancer. *J Thorac Dis.* 2017;9:S1373-S1382.
245. Van Veldhoven PP, Guan G, Shechter I, Claessens F, Verhoeven G, Swinnen J V. Squalene Synthase, a Determinant of Raft-associated Cholesterol and Modulator of Cancer Cell Proliferation. *J Biol Chem.* 2007;282(26):18777-18785.
246. Liu CW, Li CH, Peng YJ, et al. Snail regulates Nanog status during the epithelial-mesenchymal transition via the Smad1/Akt/GSK3 β signaling pathway in non-small-cell lung cancer. *Oncotarget.* 2014;5(11).
247. Yang J, Zhang K, Wu J, et al. Wnt5a increases properties of lung cancer stem cells and resistance to cisplatin through activation of Wnt5a/PKC signaling pathway. *Stem Cells Int.* 2016;2016.
248. Gene Ontology Resource. [web page] Accessed September 31, 2023. <https://geneontology.org/>
249. Banerjee S, Lo WC, Majumder P, et al. Multiple roles for basement membrane proteins in cancer progression and EMT. *Eur J Cell Biol.* 2022;101:151220.
250. Troussard AA, McDonald PC, Wederell ED, et al. Preferential Dependence of Breast Cancer Cells versus Normal Cells on Integrin-Linked Kinase for Protein Kinase B/Akt Activation and Cell Survival. *Cancer Res.* 2006;66(1):393-403.
251. Brognard J, Clark AS, Ni Y, Dennis PA. Akt/Protein Kinase B Is Constitutively Active in Non-Small Cell Lung Cancer Cells and Promotes Cellular Survival and Resistance to Chemotherapy and Radiation. *CANCER Res.* 2001;61:3986-3997.
252. Szymonowicz K, Oeck S, Malewicz NM, Jendrossek V. New insights into protein kinase B/Akt signaling: Role of localized akt activation and compartment-specific target proteins for the cellular radiation response. *Cancers (Basel).* 2018;10(3).

References

253. Garon EB, Chih-Hsin Yang J, Dubinett SM. The Role of Interleukin 1b in the Pathogenesis of Lung Cancer. *JTO Clin Res Reports*. 2020;1:1-11.
254. Short SM, Boyer JL, Juliano RL. Integrins regulate the linkage between upstream and downstream events in G protein-coupled receptor signaling to mitogen-activated protein kinase. *J Biol Chem*. 2000;275(17):12970-12977.
255. Scholz N. Cancer cell mechanics: Adhesion G Protein-coupled receptors in Action? *Front Oncol*. 2018;8:59.
256. Li M, Marin-Muller C, Bharadwaj U, Chow KH, Yao Q, Chen C. MicroRNAs: Control and Loss of Control in Human Physiology and Disease. *World J Surg*. 2009;33(4):667-684.
257. Salinas-Vera YM, Valdés J, Hidalgo-Miranda A, et al. Three-Dimensional Organotypic Cultures Reshape the microRNAs Transcriptional Program in Breast Cancer Cells. *Cancers (Basel)*. 2022;14(10).
258. Chiarella E, Aloisio A, Scicchitano S, Bond HM, Mesuraca M. Regulatory role of micrnas targeting the transcription co-factor znf521 in normal tissues and cancers. *Int J Mol Sci*. 2021;22(16).
259. Zhao X, Ren Y, Cui N, Wang X, Cui Y. Identification of key microRNAs and their targets in exosomes of pancreatic cancer using bioinformatics analysis. *Medicine*. 2018;97:39.
260. Preethi KA, Selvakumar SC, Ross K, Jayaraman S, Tsubira D, Sekar D. Liquid biopsy: Exosomal microRNAs as novel diagnostic and prognostic biomarkers in cancer. *Mol Cancer*. 2022;21(1).
261. Gurda GT, Zhang L, Wang Y, et al. Utility of five commonly used immunohistochemical markers TTF-1, Napsin A, CK7, CK5/6 and P63 in primary and metastatic adenocarcinoma and squamous cell carcinoma of the lung: a retrospective study of 246 fine needle aspiration cases. *Clin Transl Med*. 2015;4(1).
262. Derynck R, Turley SJ, Akhurst RJ. TGF β biology in cancer progression and immunotherapy. *Nat Rev Clin Oncol*. 2021;18(1):9-34.
263. Bruna A, Darken RS, Rojo F, et al. High TGFbeta-Smad activity confers poor prognosis in glioma patients and promotes cell proliferation depending on the methylation of the PDGF-B gene. *Cancer Cell*. 2007;11(2):147-160.

References

264. Tsushima H, Kawata S, Tamura S, et al. High levels of transforming growth factor beta 1 in patients with colorectal cancer: association with disease progression. *Gastroenterology*. 1996;110(2):375-382.
265. Domagała-Kulawik J, Hoser G, Safianowska A, Grubek-Jaworska H, Chazan R. Elevated TGF-beta1 concentration in bronchoalveolar lavage fluid from patients with primary lung cancer. *Arch Immunol Ther Exp*. 2006;54(2):143-147.
266. Hasegawa Y, Takanashi S, Kanehira Y, Tsushima T, Imai T, Okumura K. Transforming growth factor- β 1 level correlates with angiogenesis, tumor progression, and prognosis in patients with nonsmall cell lung carcinoma. *Cancer*. 2001;91(5):964-971.
267. Sato R, Imamura K, Semba T, et al. TGF β signaling activated by cancer-associated fibroblasts determines the histological signature of lung adenocarcinoma. *Cancer Res*. 2021;81(18):4751-4765.
268. Toonkel RL, Borczuk AC, Powell CA. TGF- β signaling pathway in lung adenocarcinoma invasion. *J Thorac Oncol*. 2010;5(2):153-157.
269. Kim BN, Ahn DH, Kang N, et al. TGF- β induced EMT and stemness characteristics are associated with epigenetic regulation in lung cancer. *Sci Rep*. 2020;10(1).
270. Miyashita N, Enokido T, Horie M, et al. TGF- β -mediated epithelial–mesenchymal transition and tumor-promoting effects in CMT64 cells are reflected in the transcriptomic signature of human lung adenocarcinoma. *Sci Rep*. 2021;11(1):22380.
271. Black CC, Turk MJ, Dragnev K, Rigas JR. Adenocarcinoma contains more immune tolerance regulatory T-cell lymphocytes (versus squamous carcinoma) in non-small-cell lung cancer. *Lung*. 2013;191(3):265-270.
272. Kinoshita T, Ishii G, Hiraoka N, et al. Forkhead box P3 regulatory T cells coexisting with cancer associated fibroblasts are correlated with a poor outcome in lung adenocarcinoma. *Cancer Sci*. 2013;104(4):409-415.
273. Usó M, Jantus-Lewintre E, Bremnes RM, et al. Analysis of the immune microenvironment in resected non-small cell lung cancer: the prognostic value of different T lymphocyte markers. *Oncotarget*. 2016;7(33):52849-52861.
274. Eilertsen M, Pettersen I, Andersen S, et al. In NSCLC, VEGF-A response to

References

- hypoxia may differ between squamous cell and adenocarcinoma histology. *Anticancer Res.* 2012;32(11):4729-4736.
275. Ma Z, Wei K, Yang F, et al. Tumor-derived exosomal miR-3157-3p promotes angiogenesis, vascular permeability and metastasis by targeting TIMP/KLF2 in non-small cell lung cancer. *Cell Death Dis.* 2021;12(9):1-13.
276. Li Q, Liu J, Jia Y, Li T, Zhang M. miR-623 suppresses cell proliferation, migration and invasion through direct inhibition of XRCC5 in breast cancer. *Aging.* 2020;12(11):10246-10258.
277. Ren F, Su H, Jiang H, Chen Y. Overexpression of miR-623 suppresses progression of hepatocellular carcinoma via regulating the PI3K/Akt signaling pathway by targeting XRCC5. *J Cell Biochem.* 2020;121(1):213-223.
278. Chen Y, Peng S, Cen H, et al. MicroRNA hsa-miR-623 directly suppresses MMP1 and attenuates IL-8-induced metastasis in pancreatic cancer. *Int J Oncol.* 2019;55(1):142-156.
279. Wei S, Zhang ZY, Fu SL, et al. Hsa-miR-623 suppresses tumor progression in human lung adenocarcinoma. *Cell Death Dis.* 2017;8(5):e2829-e2829.
280. Desi N, Teh V, Tong QY, et al. MiR-138 is a potent regulator of the heterogenous MYC transcript population in cancers. *Oncogene.* 2021;41(8):1178-1189.
281. Zeng D, Xu H, Ji N, et al. In situ measurement of miR-138 expression in oral squamous cell carcinoma tissue supports the role of this microRNA as a tumor suppressor. *J Oral Pathol Med.* 2019;48(10):911-918.
282. Ye Z, Fang B, Pan J, et al. MiR-138 suppresses the proliferation, metastasis and autophagy of non-small cell lung cancer by targeting Sirt1. *Oncol Rep.* 2017;37(6):3244-3252.
283. Wu J, Han X, Yang X, et al. MiR-138-5p suppresses the progression of lung cancer by targeting SNIP1. *Thorac cancer.* 2023;14(6):612-623.
284. Dar AA, Majid S, Rittsteuer C, et al. The Role of miR-18b in MDM2-p53 Pathway Signaling and Melanoma Progression. *JNCI J Natl Cancer Inst.* 2013;105(6):433-442.
285. Kumar Yadav A, Singh N, Kumar Yadav S, et al. Expression of miR-145 and miR-18b in Peripheral Blood Samples of Head and Neck Cancer Patients. *Indian J Clin Biochem.* 2013;38(4):528-535.

References

286. Yan Z, Sheng Z, Zheng Y, et al. Cancer-associated fibroblast-derived exosomal miR-18b promotes breast cancer invasion and metastasis by regulating TCEAL7. *Cell Death Dis.* 2021;12(12):1-14.
287. Gallach S, Jantus-Lewintre E, Calabuig-Fariñas S, et al. MicroRNA profiling associated with non-small cell lung cancer: next generation sequencing detection, experimental validation, and prognostic value. *Oncotarget.* 2017;8(34):56143-56157.
288. Liu XG, Zhu WY, Huang YY, et al. High expression of serum miR-21 and tumor miR-200c associated with poor prognosis in patients with lung cancer. *Med Oncol.* 2012;29(2):618-626.
289. Kim S, Choi MC, Jeong JY, et al. Serum exosomal miRNA-145 and miRNA-200c as promising biomarkers for preoperative diagnosis of ovarian carcinomas. *J Cancer.* 2019;10(9):1958.
290. Jiang Y, Ji X, Liu K, et al. Exosomal miR-200c-3p negatively regulates the migration and invasion of lipopolysaccharide (LPS)-stimulated colorectal cancer (CRC). *BMC Mol Cell Biol.* 2020;21(1):1-14.
291. Kawakubo-Yasukochi T, Morioka M, Hazekawa M, et al. miR-200c-3p spreads invasive capacity in human oral squamous cell carcinoma microenvironment. *Mol Carcinog.* 2017;57:295-302.
292. Tamagawa S, Beder LB, Hotomi M, et al. Role of miR-200c/miR-141 in the regulation of epithelial-mesenchymal transition and migration in head and neck squamous cell carcinoma. *Int J Mol Med.* 2014;33(4):879-886.
293. Wang YL, Chen C mei, Wang XM, Wang L. Effects of miR-339-5p on invasion and prognosis of hepatocellular carcinoma. *Clin Res Hepatol Gastroenterol.* 2016;40(1):51-56.
294. Wu ZS, Wu Q, Wang CQ, et al. MiR-339-5p inhibits breast cancer cell migration and invasion in vitro and may be a potential biomarker for breast cancer prognosis. *BMC Cancer.* 2010;10(542).
295. Zhou C, Liu G, Wang L, et al. MiR-339-5p regulates the growth, colony formation and metastasis of colorectal cancer cells by targeting PRL-1. *PLoS One.* 2013;8(5).
296. Trakunram K, Chaniad P, Geater SL, et al. Serum miR-339-3p as a potential diagnostic marker for non-small cell lung cancer. *Cancer Biol Med.* 2020;17(3):652.

References

297. Li P, Liu H, Li Y, Wang Y, Zhao L, Wang H. miR-339-5p inhibits lung adenocarcinoma invasion and migration by directly targeting BCL6. *Oncol Lett.* 2018;16(5):5785.
298. Sun Y, Mei H, Xu C, Tang H, Wei W. Circulating microRNA-339-5p and -21 in plasma as an early detection predictors of lung adenocarcinoma. *Pathol Res Pract.* 2018;214(1):119-125.
299. Xu K, Zhang C, Du T, et al. Progress of exosomes in the diagnosis and treatment of lung cancer. *Biomed Pharmacother.* 2021;134.
300. Lin G, Lin L, Lin H, et al. C1QTNF6 regulated by miR-29a-3p promotes proliferation and migration in stage I lung adenocarcinoma. *BMC Pulm Med.* 2022;22(1):1-14.
301. Pan J, Zhou C, Zhao X, et al. A two-miRNA signature (miR-33a-5p and miR-128-3p) in whole blood as potential biomarker for early diagnosis of lung cancer. *Sci Reports 2018 81.* 2018;8(1):1-12.
302. Li M, Liu T, Cheng W, Jin H, Wang X. A test of miR-128-3p and miR-33a-5p in serum exosome as biomarkers for auxiliary diagnosis of non-small cell lung cancer. *J Thorac Dis.* 2023;15(5):2616-2626.
303. Li YJ, Sun YX, Hao RM, et al. miR-33a-5p enhances the sensitivity of lung adenocarcinoma cells to celastrol by regulating mTOR signaling. *Int J Oncol.* 2018;52(4):1328-1338.
304. Davenport ML, Echols JB, Silva AD, et al. miR-31 Displays Subtype Specificity in Lung Cancer. *Cancer Res.* 2021;81(8):1942-1953.
305. Xu R, Liu T, Zuo L, et al. The high expression of miR-31 in lung adenocarcinoma inhibits the malignancy of lung adenocarcinoma tumor stem cells. *Biochem Biophys Reports.* 2021;28.
306. Yu F, Liang M, Huang Y, Wu W, Zheng B, Chen C. Hypoxic tumor-derived exosomal miR-31-5p promotes lung adenocarcinoma metastasis by negatively regulating SATB2-reversed EMT and activating MEK/ERK signaling. *J Exp Clin Cancer Res.* 2021;40(1):1-15.
307. Ren J. Intermittent hypoxia BMSCs-derived exosomal miR-31-5p promotes lung adenocarcinoma development via WDR5-induced epithelial mesenchymal transition. *Sleep Breath.* 2023;27(4):1399-1409.
308. Jiang Y, Zhao J, Zhang Y, et al. Establishment of lung cancer patient-derived

References

- xenograft models and primary cell lines for lung cancer study. *J Transl Med.* 2018;16(1):1-18.
309. Kodack DP, Farago AF, Dastur A, et al. Primary Patient-Derived Cancer Cells and Their Potential for Personalized Cancer Patient Care. *Cell Rep.* 2017;21(11):3298-3309.
310. Kuzu OF, Noory MA, Robertson GP. The role of cholesterol in cancer. *Cancer Res.* 2016;76(8):2063.
311. Ding X, Zhang W, Li S, Yang H. The role of cholesterol metabolism in cancer. *Am J Cancer Res.* 2019;9(2):219.
312. Simons K, Toomre D. Lipid rafts and signal transduction. *Nat Rev Mol Cell Biol.* 2000;1(1):31-39.
313. Visca P, Sebastiani V, Botti C, et al. Fatty Acid Synthase (FAS) is a Marker of Increased Risk of Recurrence in Lung Carcinoma. *Anticancer Res.* 2004;24(6):4169-4174.
314. Li FF, Zhang H, Li JJ, Cao YN, Dong X, Gao C. Interaction with adipocytes induces lung adenocarcinoma A549 cell migration and tumor growth. *Mol Med Rep.* 2018;18(2):1973-1980.
315. Yang YF, Jan YH, Liu YP, et al. Squalene synthase induces tumor necrosis factor receptor 1 enrichment in lipid rafts to promote lung cancer metastasis. *Am J Respir Crit Care Med.* 2014;190(6):675-687.
316. Yang YF, Chang YC, Jan YH, Yang CJ, Huang MS, Hsiao M. Squalene synthase promotes the invasion of lung cancer cells via the osteopontin/ERK pathway. *Oncog* 2020 98. 2020;9(8):1-12.
317. Cano A, Pérez-Moreno MA, Rodrigo I, et al. The transcription factor snail controls epithelial-mesenchymal transitions by repressing E-cadherin expression. *Nat Cell Biol.* 2000;2(2):76-83.
318. Usami Y, Satake S, Nakayama F, et al. Snail-associated epithelial-mesenchymal transition promotes oesophageal squamous cell carcinoma motility and progression. *J Pathol.* 2008;215(3):330-339.
319. Kudo-Saito C, Shirako H, Takeuchi T, Kawakami Y. Cancer metastasis is accelerated through immunosuppression during Snail-induced EMT of cancer cells. *Cancer Cell.* 2009;15(3):195-206.

References

320. Dohadwala M, Yang SC, Luo J, et al. Cyclooxygenase-2-dependent regulation of E-cadherin: prostaglandin E(2) induces transcriptional repressors ZEB1 and snail in non-small cell lung cancer. *Cancer Res.* 2006;66(10):5338-5345.
321. Zhuo W, Wang Y, Zhuo X, Zhang Y, Ao X, Chen Z. Knockdown of Snail, a novel zinc finger transcription factor, via RNA interference increases A549 cell sensitivity to cisplatin via JNK/mitochondrial pathway. *Lung cancer.* 2008;62(1):8-14.
322. Papiewska-Pajak I, Przygodzka P, Krzyżanowski D, et al. Snail Overexpression Alters the microRNA Content of Extracellular Vesicles Released from HT29 Colorectal Cancer Cells and Activates Pro-Inflammatory State In Vivo. *Cancers (Basel).* 2021;13(2):172.
323. Herrera A, Herrera M, Guerra-Perez N, et al. Endothelial cell activation on 3D-matrices derived from PDGF-BB-stimulated fibroblasts is mediated by Snail1. *Oncogenesis.* 2018;7(9):1-15.
324. You J, Li M, Cao LM, et al. Snail1-dependent cancer-associated fibroblasts induce epithelial-mesenchymal transition in lung cancer cells via exosomes. *QJM.* 2019;112(8):581-590.
325. Anastas JN, Moon RT. WNT signalling pathways as therapeutic targets in cancer. *Nat Rev Cancer.* 2013;13(1):11-26.
326. Takebe N, Miele L, Harris PJ, et al. Targeting Notch, Hedgehog, and Wnt pathways in cancer stem cells: clinical update. *Nat Rev Clin Oncol.* 2015;12(8):445-464.
327. Dejmek J, Dejmek A, Säfholm A, Sjölander A, Andersson T. Wnt-5a protein expression in primary dukes B colon cancers identifies a subgroup of patients with good prognosis. *Cancer Res.* 2005;65(20):9142-9146.
328. Cheng R, Sun B, Liu Z, et al. Wnt5a suppresses colon cancer by inhibiting cell proliferation and epithelial-mesenchymal transition. *J Cell Physiol.* 2014;229(12):1908-1917.
329. Jiang W, Crossman DK, Mitchell EH, Sohn P, Crowley MR, Serra R. WNT5A Inhibits Metastasis and Alters Splicing of Cd44 in Breast Cancer Cells. *PLoS One.* 2013;8(3):e58329.
330. Bo H, Zhang S, Gao L, et al. Upregulation of Wnt5a promotes epithelial-to-mesenchymal transition and metastasis of pancreatic cancer cells. *BMC Cancer.* 2013;13(1):1-11.

References

331. Pukrop T, Binder C. The complex pathways of Wnt 5a in cancer progression. *J Mol Med*. 2008;86(3):259-266.
332. Lee GT, Kang DI, Ha YS, et al. Prostate cancer bone metastases acquire resistance to androgen deprivation via WNT5A-mediated BMP-6 induction. *Br J Cancer*. 2014;110:1634-1644.
333. Kanzawa M, Semba S, Hara S, Itoh T, Yokozaki H. WNT5A is a key regulator of the epithelial-mesenchymal transition and cancer stem cell properties in human gastric carcinoma cells. *Pathobiology*. 2013;80(5):235-244.
334. Lu C, Wang X, Zhu H, Feng J, Ni S, Huang J. Over-expression of ROR2 and Wnt5a cooperatively correlates with unfavorable prognosis in patients with non-small cell lung cancer. *Oncotarget*. 2015;6(28):24912.
335. Feller D, Kun J, Ruzsics I, et al. Cigarette Smoke-Induced Pulmonary Inflammation Becomes Systemic by Circulating Extracellular Vesicles Containing Wnt5a and Inflammatory Cytokines. *Front Immunol*. 2018;9.
336. Martin-Medina A, Lehmann M, Burgy O, et al. Increased Extracellular Vesicles Mediate WNT5A Signaling in Idiopathic Pulmonary Fibrosis. *Am J Respir Crit Care Med*. 2018;198(12):1527-1538.
337. Simpson AJG, Caballero OL, Jungbluth A, Chen YT, Old LJ. Cancer/testis antigens, gametogenesis and cancer. *Nat Rev Cancer*. 2005;5(8):615-625.
338. Yokoe T, Tanaka F, Mimori K, et al. Efficient identification of a novel cancer/testis antigen for immunotherapy using three-step microarray analysis. *Cancer Res*. 2008;68(4):1074-1082.
339. Caballero OL, Chen YT. Cancer/testis (CT) antigens: potential targets for immunotherapy. *Cancer Sci*. 2009;100(11):2014-2021.
340. Yatabe Y, Mitsudomi T, Takahashi T. TTF-1 expression in pulmonary adenocarcinomas. *Am J Surg Pathol*. 2002;26(6):767-773.
341. Schilsky JB, Ni A, Ahn L, et al. Prognostic impact of TTF-1 expression in patients with stage IV lung adenocarcinomas. *Lung Cancer*. 2017;108:205-211.
342. Tian G, Lin XX, Zhang XM, He Z, Hu ZL. Helicase lymphoid-specific and selenoprotein P1 are potential candidate genes in the progression and prognosis of lung adenocarcinoma. *Transl Cancer Res*. 2019;8(6):2380-2388.

References

343. Jablonska E, Raimondi S, Gromadzinska J, et al. DNA damage and oxidative stress response to selenium yeast in the non-smoking individuals: a short-term supplementation trial with respect to GPX1 and SEPP1 polymorphism. *Eur J Nutr.* 2016;55(8):2469-2484.
344. Okano F, Saito T, Minamida Y, et al. Identification of Membrane-expressed CAPRIN-1 as a Novel and Universal Cancer Target, and Generation of a Therapeutic Anti-CAPRIN-1 Antibody TRK-950. *Cancer Res Commun.* 2023;3(4):640-658.
345. Baumas K, Soudet J, Caizergues-Ferrer M, et al. Human RioK3 is a novel component of cytoplasmic pre-40S pre-ribosomal particles. *RNA Biol.* 2012;9(2):162-174.
346. Singleton DC, Rouhi P, Zois CE, et al. Hypoxic regulation of RIOK3 is a major mechanism for cancer cell invasion and metastasis Europe PMC Funders Group. *Oncogene.* 2015;34(36):4713-4722.
347. Sato S, Noguchi Y, Ohara N, et al. Identification of XAGE-1 isoforms: predominant expression of XAGE-1b in testis and tumors. *Cancer Immun.* 2007;7(1):5.
348. Luo C, Xiao X, Liu D, et al. CABYR is a novel cancer-testis antigen in lung cancer. *Clin Cancer Res.* 2007;13(4):1288-1297.
349. Xiang H, Li F, Luo J, et al. A meta-analysis on the relationship of exosomes and the prognosis of lung cancer. *Medicine (Baltimore).* 2021;100(15):e25332.
350. Tas F, Ciftci R, Kilic L, Karabulut S. Age is a prognostic factor affecting survival in lung cancer patients. *Oncol Lett.* 2013;6(5):1507.
351. Bitenc M, Cufer T, Kern I, et al. Real-life long-term outcomes of upfront surgery in patients with resectable stage I-IIIa non-small cell lung cancer. *Radiol Oncol.* 2022;56(3):346-354.
352. Herreros-Pomares A, de-Maya-Girones JD, Calabuig-Fariñas S, et al. Lung tumorspheres reveal cancer stem cell-like properties and a score with prognostic impact in resected non-small-cell lung cancer. *Cell Death Dis* 2019 109. 2019;10(9):1-14.
353. Wang Q, Wu M, Li H, et al. Therapeutic targeting of glutamate dehydrogenase 1 that links metabolic reprogramming and Snail-mediated epithelial-mesenchymal transition in drug-resistant lung cancer. *Pharmacol*

References

- Res. 2022;185.
354. Xu H, Xu WH, Ren F, et al. Prognostic value of epithelial-mesenchymal transition markers in clear cell renal cell carcinoma. *Aging (Albany NY)*. 2020;12(1):866-883.
 355. Fang J, Ding Z. SNAI1 is a prognostic biomarker and correlated with immune infiltrates in gastrointestinal cancers. *Aging (Albany NY)*. 2020;12(17):17167.
 356. Nakagawa K, Noguchi Y, Uenaka A, et al. XAGE-1 Expression in Non-Small Cell Lung Cancer and Antibody Response in Patients. *Clin Cancer Res*. 2005;11(15):5496-5503.
 357. Gresner P, Gromadzinska J, Jablonska E, Kaczmarek J, Wasowicz W. Expression of selenoprotein-coding genes SEPP1, SEP15 and hGPX1 in non-small cell lung cancer. *Lung cancer*. 2009;65(1):34-40.
 358. Moldvay J, Jackel M, Bogos K, et al. The role of TTF-1 in differentiating primary and metastatic lung adenocarcinomas. *Pathol Oncol Res*. 2004;10(2):85-88.
 359. Qian Z, Li M, Wang R, et al. Knockdown of CABYR-a/b Increases Chemosensitivity of Human Non-Small Cell Lung Cancer Cells through Inactivation of Akt. *Cell Death Surviv*. 2014;12(3):35-347.
 360. Li J, Sun R, He L, et al. A systematic pan-cancer analysis identifies RIOK3 as an immunological and prognostic biomarker. *Am J Transl Res*. 2022;14(6):3750-3768.
 361. Wang B, David MD, Schrader JW. Absence of caprin-1 results in defects in cellular proliferation. *J Immunol*. 2005;175(7):4274-4282.
 362. Scanlan MJ, Gordon CM, Williamson B, et al. Identification of cancer/testis genes by database mining and mRNA expression analysis. *Int J cancer*. 2002;98(4):485-492.
 363. Tanaka J, Nakagawa T, Harada K, et al. Efficient and accurate KRAS genotyping using digital PCR combined with melting curve analysis for ctDNA from pancreatic cancer patients. *Sci Rep*. 2023;13:3039.
 364. Allenson K, Castillo J, San Lucas FA, et al. High Prevalence of Mutant KRAS in Circulating Exosome-derived DNA from Early Stage Pancreatic Cancer Patients. *Ann Oncol*. 2017; 28(4):741-747.

References

365. Möhrmann L, Huang HJ, Hong DS, et al. Liquid Biopsies Using Plasma Exosomal Nucleic Acids and Plasma Cell-Free DNA Compared with Clinical Outcomes of Patients with Advanced Cancers. *Clin cancer Res.* 2018;24(1):181-188.
366. García-Silva S, Gallardo M, Peinado H. DNA-Loaded Extracellular Vesicles in Liquid Biopsy: Tiny Players With Big Potential? *Front cell Dev Biol.* 2021;8.
367. Krug AK, Enderle D, Karlovich C, et al. Improved EGFR mutation detection using combined exosomal RNA and circulating tumor DNA in NSCLC patient plasma. *Ann Oncol.* 2018;29(3):700-706.
368. Castellanos-Rizaldos E, Grimm DG, Tadigotla V, et al. Exosome-Based Detection of EGFR T790M in Plasma from Non-Small Cell Lung Cancer Patients. *Clin cancer Res.* 2018;24(12):2944-2950.
369. Castellanos-Rizaldos E, Zhang X, Tadigotla VR, et al. Exosome-based detection of activating and resistance EGFR mutations from plasma of non-small cell lung cancer patients. *Oncotarget.* 2019;10(30):2911.
370. Yu W, Hurley J, Roberts D, et al. Exosome-based liquid biopsies in cancer: opportunities and challenges. *Ann Oncol.* 2021;32(4):466-477.
371. Hur JY, Lee JS, Kim IA, Kim HJ, Kim WS, Lee KY. Extracellular vesicle-based EGFR genotyping in bronchoalveolar lavage fluid from treatment-naive non-small cell lung cancer patients. *Transl lung cancer Res.* 2019;8(6):1051-1060.
372. Vagner T, Spinelli C, Minciocchi VR, et al. Large extracellular vesicles carry most of the tumour DNA circulating in prostate cancer patient plasma. *J Extracell vesicles.* 2018;7(1).
373. Lázaro-Ibáñez E, Lässer C, Shelke GV, et al. DNA analysis of low- and high-density fractions defines heterogeneous subpopulations of small extracellular vesicles based on their DNA cargo and topology. *J Extracell vesicles.* 2019;8(1).
374. Pantel K, Alix-Panabières C. Liquid biopsy and minimal residual disease - latest advances and implications for cure. *Nat Rev Clin Oncol.* 2019;16(7):409-424.
375. Rostami A, Lambie M, Yu CW, Stambolic V, Waldron JN, Bratman S V. Senescence, Necrosis, and Apoptosis Govern Circulating Cell-free DNA Release Kinetics. *Cell Rep.* 2020;31(13).

References

376. Pittella-Silva F, Chin YM, Chan HT, et al. Plasma or Serum: Which Is Preferable for Mutation Detection in Liquid Biopsy? *Clin Chem*. 2020;66(7):946-957.
377. Ayache S, Panelli MC, Byrne KM, et al. Comparison of proteomic profiles of serum, plasma, and modified media supplements used for cell culture and expansion. *J Transl Med*. 2006;4.
378. Foye C, Yan IK, David W, et al. Comparison of miRNA quantitation by Nanostring in serum and plasma samples. *PLoS One*. 2017;12(12).
379. Zhang X, Takeuchi T, Takeda A, Mochizuki H, Nagai Y. Comparison of serum and plasma as a source of blood extracellular vesicles: Increased levels of platelet-derived particles in serum extracellular vesicle fractions alter content profiles from plasma extracellular vesicle fractions. *PLoS One*. 2022;17(6).
380. Palviainen M, Saraswat M, Varga Z, et al. Extracellular vesicles from human plasma and serum are carriers of extravesicular cargo-Implications for biomarker discovery. *PLoS One*. 2020;15(8).
381. Bryzgunova OE, Zaripov MM, Skvortsova TE, et al. Comparative Study of Extracellular Vesicles from the Urine of Healthy Individuals and Prostate Cancer Patients. *PLoS One*. 2016;11(6):e0157566.
382. Zlotogorski-Hurvitz A, Dayan D, Chaushu G, Salo T, Vered M. Morphological and molecular features of oral fluid-derived exosomes: oral cancer patients versus healthy individuals. *J Cancer Res Clin Oncol*. 2016;142(1):101-110.
383. Rosell R, Wei J, Taron M. Circulating MicroRNA Signatures of Tumor-Derived Exosomes for Early Diagnosis of Non-Small-Cell Lung Cancer. *Clin Lung Cancer*. 2009;10(1):8-9.
384. Qiao X, Zhai X, Wang J, et al. Sequential measurements of serum matrix metalloproteinase 9 to monitor chemotherapy responses in patients with advanced non-small-cell lung cancer. *Onco Targets Ther*. 2016;9:3299-3305.
385. Yang XZ, Cui SZ, Zeng LS, et al. Overexpression of Rab1B and MMP9 predicts poor survival and good response to chemotherapy in patients with colorectal cancer. *Aging (Albany NY)*. 2017;9(3):914-931.
386. Qiao X, Gu Y, Yu J, et al. The Combination of CD147 and MMP-9 Serum Levels Is Identified as Novel Chemotherapy Response Markers of Advanced Non-Small-Cell Lung Cancer. *Dis Markers*. 2020;2020.

References

387. Kristiansen G, Schlüns K, Yongwei Y, Denkert C, Dietel M, Petersen I. CD24 is an independent prognostic marker of survival in nonsmall cell lung cancer patients. *Br J Cancer*. 2003;88(2):231-236.
388. Lee HJ, Choe G, Jheon S, Sung SW, Lee CT, Chung JH. CD24, a novel cancer biomarker, predicting disease-free survival of non-small cell lung carcinomas: a retrospective study of prognostic factor analysis from the viewpoint of forthcoming (seventh) new TNM classification. *J Thorac Oncol*. 2010;5(5):649-657.
389. Madjd Z, Spendlove I, Moss R, et al. Upregulation of MICA on high-grade invasive operable breast carcinoma. *Cancer Immun*. 2007;7:17.
390. Espinoza I, Agarwal S, Sakiyama M, et al. Expression of MHC class I polypeptide-related sequence A (MICA) in colorectal cancer. *Front Biosci - Landmark*. 2021;26(10):765-776.
391. Li JJ, Pan K, Gu MF, et al. Prognostic value of soluble MICA levels in the serum of patients with advanced hepatocellular carcinoma. *Chin J Cancer*. 2013;32(3):141.
392. Chen Y, Lin G, Guo Z qing, Zhou Z feng, He Z yong, Ye Y bin. Effects of MICA expression on the prognosis of advanced non-small cell lung cancer and the efficacy of CIK therapy. *PLoS One*. 2013;8(7).
393. Bulk E, Sargin B, Krug U, et al. S100A2 induces metastasis in non-small cell lung cancer. *Clin Cancer Res*. 2009;15(1):22-29.
394. Wang H, Zhang Z, Li R, et al. Overexpression of S100A2 protein as a prognostic marker for patients with stage I non small cell lung cancer. *Int J cancer*. 2005;116(2):285-290.
395. Bauer S, Groh V, Wu J, et al. Activation of NK cells and T cells by NKG2D, a receptor for stress-inducible MICA. *Science*. 1999;285(5428):727-729.
396. Groh V, Wu J, Yee C, Spies T. Tumour-derived soluble MIC ligands impair expression of NKG2D and T-cell activation. *Nature*. 2002;419(6908):734-738.
397. Jinushi M, Takehara T, Tatsumi T, et al. Impairment of natural killer cell and dendritic cell functions by the soluble form of MHC class I-related chain A in advanced human hepatocellular carcinomas. *J Hepatol*. 2005;43(6):1013-1020.

References

398. Raulet DH, Guerra N. Oncogenic stress sensed by the immune system: role of NK cell receptors. *Nat Rev Immunol*. 2009;9(8):568.
399. Nausch N, Cerwenka A. NKG2D ligands in tumor immunity. *Oncogene*. 2008;27(45):5944-5958.
400. Oppenheim DE, Roberts SJ, Clarke SL, et al. Sustained localized expression of ligand for the activating NKG2D receptor impairs natural cytotoxicity in vivo and reduces tumor immunosurveillance. *Nat Immunol*. 2005;6(9):928-937.
401. Zhao Y, Chen N, Yu Y, et al. Prognostic value of MICA/B in cancers: a systematic review and meta-analysis. *Oncotarget*. 2017;8(56):96384-96395.
402. Xing S, Zhu Y, Sun Y. Serum sMICA as biomarker in detection of non-small-cell lung carcinoma. *Br J Biomed Sci*. 2018;75(1):50-52.
403. López-Cobo S, Campos-Silva C, Moyano A, et al. Immunoassays for scarce tumour-antigens in exosomes: Detection of the human NKG2D-Ligand, MICA, in tetraspanin-containing nanovesicles from melanoma. *J Nanobiotechnology*. 2018;16(1):1-12.
404. Clayton A, Mitchell JP, Court J, Linnane S, Mason MD, Tabi Z. Human tumor-derived exosomes down-modulate NKG2D expression. *J Immunol*. 2008;180(11):7249-7258.
405. Shi C, Li H, Couturier JP, et al. Allele Specific Expression of MICA Variants in Human Fibroblasts Suggests a Pathogenic Mechanism. *Open Rheumatol J*. 2015;9(1):60-64.
406. Moloudizargari M, Asghari MH, Mortaz E. Inhibiting exosomal MIC-A and MIC-B shedding of cancer cells to overcome immune escape: new insight of approved drugs. *DARU J Pharm Sci*. 2019;27:879-884.

VIII. ANNEXES

A. SUPPLEMENTARY MATHERIAL

Table S1. The definition of descriptors of the TNM Classification System 8th Edition.

T – Primary Tumor		
Category	Subcategory	Descriptors
TX	Primary tumor cannot be assessed, or tumor proven by the presence of malignant cells in sputum or bronchial washings but not visualized by imaging or bronchoscopy.	
T0	No evidence of primary tumor.	
Tis	Carcinoma in situ: Tis(AIS): adenocarcinoma. Tis(SCIS): squamous cell carcinoma.	
T1	Tumor dimension ≤ 3 cm, surrounded by lung or visceral pleura, without bronchoscopic evidence of invasion more proximal than the lobar bronchus.	
	T1mi	Minimally invasive adenocarcinoma.
	T1a	Tumor dimension ≤ 1 cm.
	T1b	Tumor dimension >1 cm but not >2 cm.
	T1c	Tumor dimension >2 cm but not >3 cm.
T2	Tumor dimension >3 cm but not >5 cm; or tumor with any of the following features. <ul style="list-style-type: none"> • Involves main bronchus regardless of distance to the carina, but without involving the carina. • Invades visceral pleura. 	
	T2a	Tumor dimension >3 cm but not >4 cm.
	T2b	Tumor dimension >4 cm but not >5 cm.
T3	Tumor dimension >5 cm but not >7 cm or one that directly invades any of the following: parietal pleura (PL3), chest wall (including superior sulcus tumours), phrenic nerve, parietal pericardium; or associated separate tumor nodule(s) in the same lobe as the primary.	

Annexes

T4	Tumors >7 cm or one that invades any of the following: diaphragm, mediastinum, heart, great vessels, trachea, recurrent laryngeal nerve, esophagus, vertebral body, carina; separate tumor nodule(s) in a different ipsilateral lobe to that of the primary.	
N – Regional Lymph Nodes		
NX	Regional lymph nodes cannot be assessed.	
N0	No regional lymph node metastasis.	
N1	Metastasis in ipsilateral peribronchial and/or ipsilateral hilar lymph nodes and intrapulmonary nodes, including involvement by direct extension.	
N2	Metastasis in ipsilateral mediastinal and/or subcarinal lymph node(s).	
N3	Metastasis in contralateral mediastinal, contralateral hilar, ipsilateral or contralateral scalene, or supraclavicular lymph node(s).	
M- Distant Metastasis		
M0	No distant metastasis.	
M1	Distant metastasis.	
	M1a	Separate tumor nodule(s) in a contralateral lobe; tumor with pleural nodules or malignant pleural or pericardial effusion.
	M1b	Single extrathoracic metastasis in a single organ and involvement of a single distant (non-regional) node.
	M1c	Multiple extrathoracic metastases in one or several organs.

Annexes

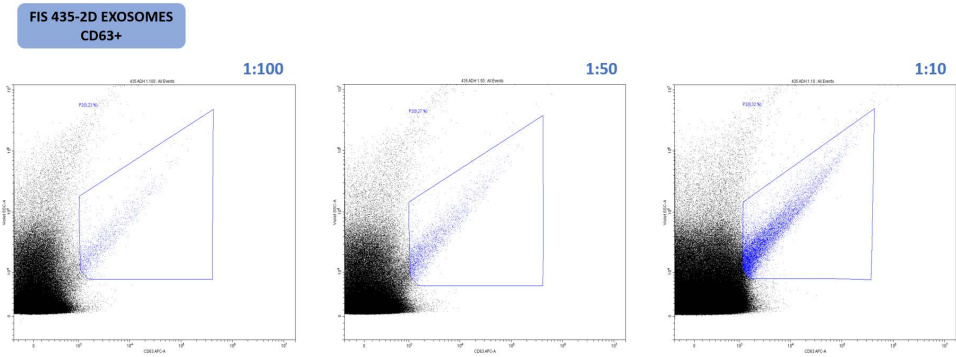


Figure S1. Flow cytometry control serial dilutions for validation of signal detection in exosome samples. The axes have a biexponential scale, where the Y-axis corresponds to side scatter (SSC), while the X-axis corresponds to forward scatter (FSC) CD63-APC (blue).

Table S2. Molecular alterations detected in cell cultures-derived exosomes with different histologies.

SW900	H1975	H358	PC9	H1650	A549	HCC827	H2228	FIS 435
LUSC	LUAD	LUAD	LUAD	LUAD	LUAD	LUAD	LUAD	LUAD
KRAS p.G12V	EGFR p.L858R + p.T790M	KRAS p.G12S	EGFR p.E746_ A750del	EGFR p.E746_ A750del	KRAS p.G12S	EGFR p.E746_ A750del	EML4- ALK fusion	KRAS p.G12C

LUSC: squamous cell lung cancer; LUAD: adenocarcinoma cell lung cancer.

Annexes

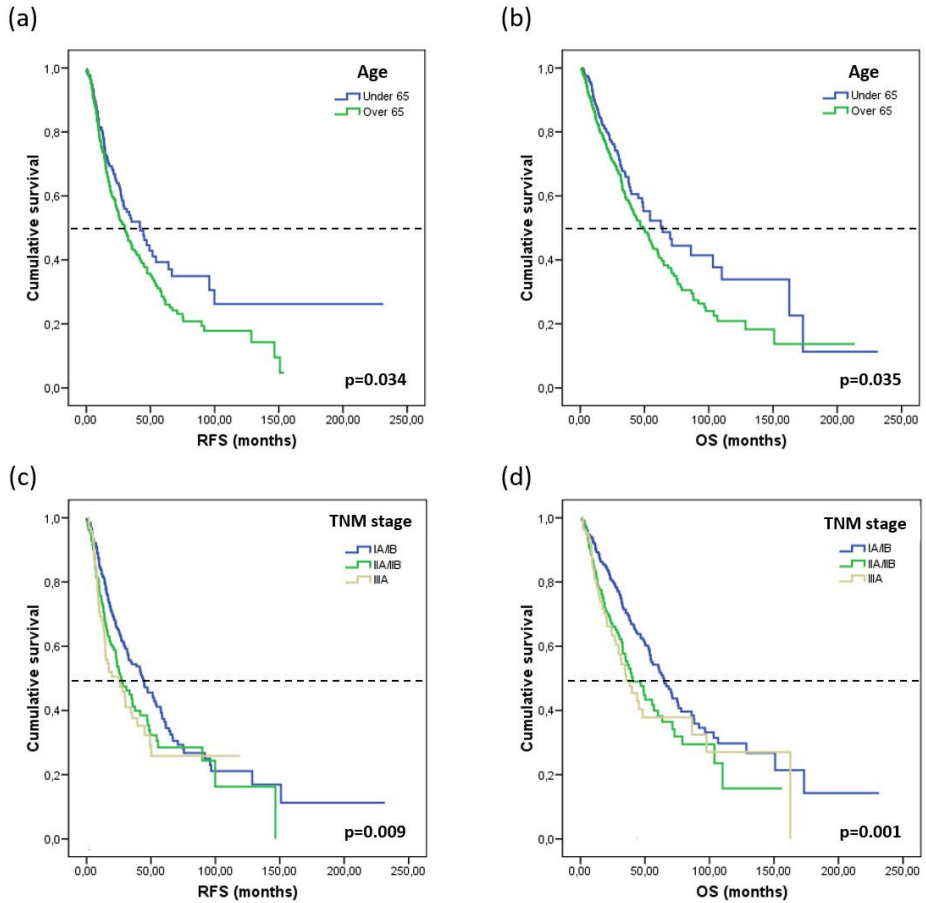


Figure S2. Kaplan-Meier plots for survival according to clinicopathological variables for the TCGA cohort. Significant RFS (HR:1.305; [1.020-1.671]; $P=0.034$) and OS (HR:1.327; [1.019-1.727]; $P=0.036$) for age (a-b) and RFS (HR:1.252 [1.081-1.450] $P=0.009$) and OS (HR:1.312; [1.125-1.529]; $P=0.001$) for TNM stage (c-d).

Table S3. Enrichment of GOBP categories according to the target genes of exo-miRNAs secreted from 2D and 3D cell cultures.

GOBP categories enrichment	Cell culture model overlap
Chromatin remodeling	3D-Target genes
Regulation of cellular macromolecule biosynthetic process	3D & 2D-Target genes
Platelet aggregation	3D-Target genes
Homotypic cell-cell adhesion	3D-Target genes
Modification-dependent protein catabolic process	3D-Target genes
Positive regulation of cell morphogenesis involved in differentiation	3D-Target genes
Protein ubiquitination	3D-Target genes
Regulation of transcription, DNA-templated	3D & 2D-Target genes
Cellular response to interleukin-6	2D-Target genes
Protein phosphorylation	2D-Target genes
Cellular response to cytokine stimulus	2D-Target genes
Negative regulation of translation	2D-Target genes
Vesicle fusion	2D-Target genes
Cellular response to decreased oxygen levels	2D-Target genes
Regulation of transcription from RNA polymerase II promoter	3D & 2D-Target genes
Regulation on gene expression	3D & 2D-Target genes

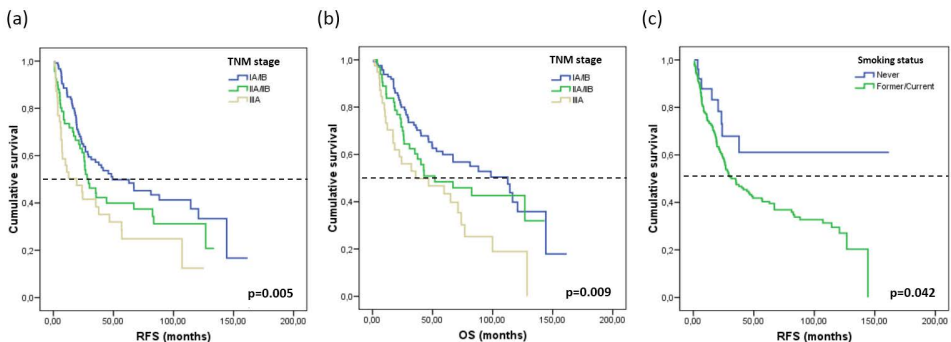


Figure S3. Kaplan-Meier plots for survival according to clinicopathological variables for the HGU cohort. Significant RFS and OS for TNM stage (P-values <0.01) (a-b) and RFS for smoking status (P-value <0.05) (c).

Annexes

Table S4. Enrichment analysis of pathological processes and its associated pathways based on the number of DEGs overlapped.

Process name	Hallmarks of Cancer	p-value	JSI	Overlap
G0/G1 Cell Cycle Phase Transition Activation in Cancer	Sustaining Proliferative Signaling	1.30x10 ⁵	0.007	10
TGFβ Signaling activation by Blocking of Tumor Suppressors	Evading Growth Suppressors	3.85x10 ⁵	0.008	11
Treg Cells Promote Immunosuppression in Cancer Immune Escape	Evading Immune Destruction	7.25x10 ⁵	0.006	9
TGFβ Family in Epithelial to Mesenchymal Transition in Cancer	Activating Invasion and Metastasis	1.57x10 ⁴	0.007	11
VEGF Independent Angiogenesis in Cancer	Inducing Angiogenesis	2.43x10 ⁴	0.006	8
ANGPT/TEK Stimulates Endothelial Cell Migration in Cancer	Inducing Angiogenesis	3.49x10 ⁴	0.005	7
Vascular Smooth Muscle Cell/Pericyte Migration and Proliferation	Inducing Angiogenesis	2.16x10 ³	0.005	8
CDH2 Activation Promotes Cancer Cell Migration and Survival	Activating Invasion and Metastasis	2.27x10 ³	0.005	8
Glioma Invasion Signaling	Activating Invasion and Metastasis	4.97x10 ³	0.005	8
ROS in Triggering Vascular Inflammation	*Toxicity Induced Pathways	7.02x10 ³	0.005	8
IDO1 in Cancer Immune Escape	Evading Immune Destruction	0.01	0.005	7
Integrins in Cancer Cell Motility, Invasion and Survival	Activating Invasion and Metastasis	0.02	0.006	9
Acetylases Inhibition in Histone Deacetylation in Cancer	Genome Instability	0.03	0.003	4

*Toxicity Induced Pathways is not a Hallmark of Cancer; JSI: Jaccard similarity index.

Annexes

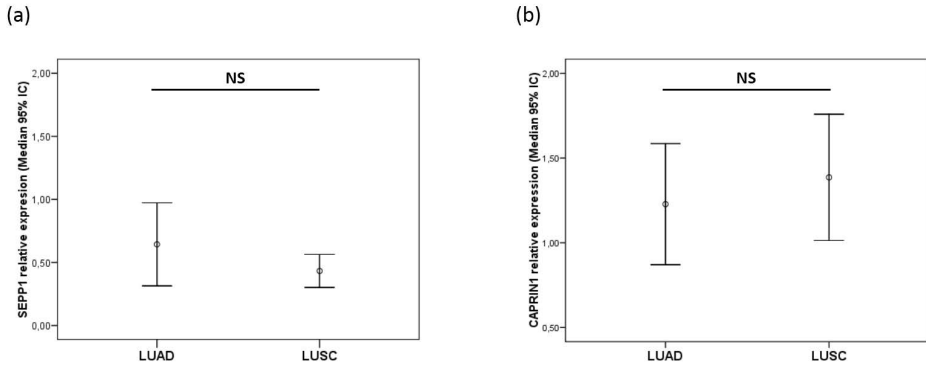


Figure S4. Mann–Whitney U-test in HGUV cohort. Non-significant (NS) p-values for *SEPP1* (a) and *CAPRN1* (b).

Table S5. Clinicopathological characteristics of the patients included in the *in silico* cohort (TCGA database).

Characteristics	Total (N=661)	%
Age at surgery:	(median, range) 66 [38-88]	
Gender		
Male	395	59.76
Female	266	40.24
Smoking status		
Current	165	24.96
Former	382	57.79
Never	114	17.25
Stage		
IA	152	22.99
IB	223	33.74
IIA	63	9.53
IIB	116	17.55
IIIA	107	16.19
Histology		
Adenocarcinoma	345	52.19
Squamous cell carcinoma	316	47.81
Exitus		
Yes	261	39.49
No	400	60.51

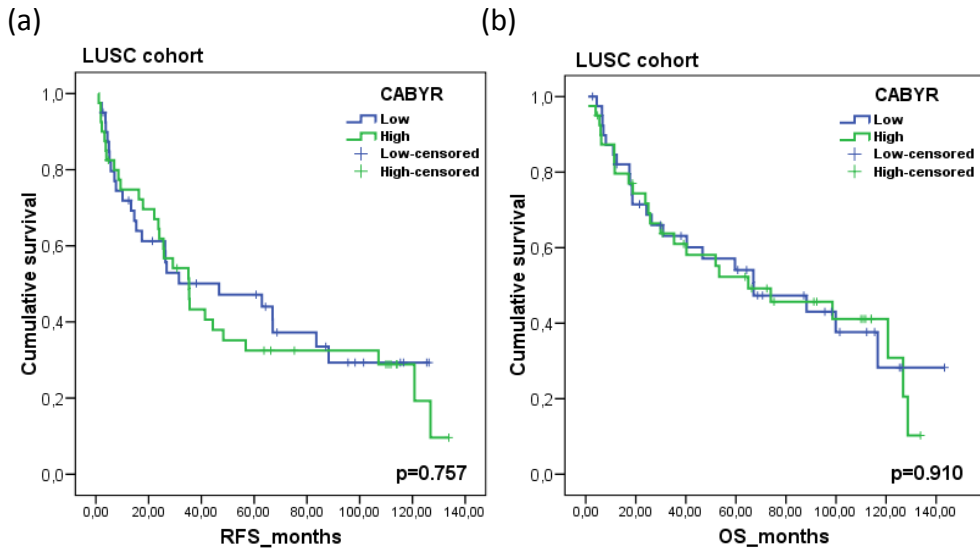


Figure S5. Prognostic value of *CABYR* in the HGUV NSCLC cohort. Kaplan–Meier plot for RFS (a) and OS (b) according to the relative gene expression to reference genes (*ACTB*, *GUSB*, *CDKN2A*) in the LUSC group. Blue line represents patients with low levels of *CABYR* expression, whereas green line represents patients with high expression levels. Cut-off values correspond to the median relative expression. P-values were calculated using the Log–Rank test.

Table S6. Results of survival analysis in the TCGA validation cohort, based on the expression of exosomal biomarkers found in plasma cohort.

GENE	RFS			OS		
	HR	95% CI	P-value	HR	95% CI	P-value
CD24	0.913	0.725-1.150	0.438	0.876	0.685-1.120	0.290
MICA	1.098	0.817-1.384	0.428	1.045	0.818-1.334	0.727
MMP9	1.127	0.896-1.1419	0.308	1.054	0.826-1.344	0.672
RIOK3	0.947	0.752-1.193	0.646	0.996	0.781-1.269	0.972
S100A2	1.228	0.975-1.547	0.080	1.107	0.868-1.412	0.413

Gene expression levels of each gene were dichotomized as high and low according to their medians. The results were obtained using the univariate Cox regression method. * $p < 0.05$. CI: confidence interval; HR: hazard ratio; OS: overall survival; RFS: relapse-free survival.

Annexes

Table S7. Results of survival analysis in the TCGA validation cohort, based on exosomal expression of CD24 and MICA (previously detected in plasma cohort).

GENE	RFS			OS		
	HR	95% CI	P-value	HR	95% CI	P-value
CD24						
LUAD GROUP	0.827	0.603-1.135	0.239	0.834	0.574-1.211	0.340
LUSC GROUP	0.998	0.712-1.400	0.992	0.928	0.669-1.289	0.657
MICA						
LUAD GROUP	0.855	0.622-1.173	0.332	0.854	0.589-1.239	0.406
LUSC GROUP	1.414	1.005-1.988	0.047*	1.182	0.851-1.640	0.318

Gene expression levels of each gene were dichotomized as high and low according to their medians. The results were obtained using the univariate Cox regression method. * $p < 0.05$. CI: confidence interval; HR: hazard ratio; OS: overall survival; RFS: relapse-free survival.

B. FUNDINGS

This thesis was supported by the following Spanish institutions:

- Asociación Española Contra el Cáncer (AECC Valencia)
Beca predoctoral para jóvenes investigadores
- Centro de Investigación Biomédica en Red Cáncer (CIBERONC).
Project CB16/12/00350.
- Fondo de Investigación Sanitaria-Fondo Europeo de Desarrollo Regional.
Project PI18/00266.
- Generalitat Valenciana
GV/2018//026

C. COMMUNICATIONS TO NATIONAL AND INTERNATIONAL CONGRESSES

“Exosomes analysis in non-small cell lung cancer for the identification of new biomarkers”.X Educational Symposim of the Spanish Lung Cancer Group. Oral communication. Madrid, España. 2020. Grupo Español de Cancer de Pulmón.

E. Duréndez-Sáez; S. Calabuig-Fariñas; C. Suarez; M. Ferrero-Gimeno; M. Mosqueda; A. Moreno; S. Torres-Martinez; A. Herreros-Pomares; S. Gallach; E. Escorihuela; A. Blasco Cordellat; F.D.A. Aparisi Aparisi; E. Serna; J. Paramio; E. Jantus-Lewintre; C. Camps.

“Identification of new biomarkers in Non-Small Cell Lung Cancer (NSCLC) by analysing exosomes cargo”. IASLC 2020 Lung Cancer Hot Topic: Liquid Biopsy. Oral Poster. Madrid, España. 2020. International association for the study of lung cancer (IASLC).

E. Duréndez; S. Calabuig-Fariñas; C. Suarez; M. Ferrero Gimeno; M. Mosqueda; A. Moreno-Manuel; S. Torres Martinez; A. Herreros Pomares; S. Gallach; M. Nuñez

Annexes

Abad; A. Blasco Cordellat; F.D.A. Aparisi Aparisi; E. Serna; J.M. Paramio; E. Jantus-Lewintre; C.J. Camps Herrero.

“Exosomes cargo analysis as an approach to identify new biomarkers in NSCLC”.

ESMO Virtual Congress 2020. Poster. Madrid, España. 2020. European Society of Medical Oncology (ESMO).

E. Duréndez; S. Calabuig-Fariñas; C. Suarez; M. Ferrero Gimeno; M. Mosqueda; A. Moreno-Manuel; S. Torres Martinez; A. Herrerros Pomares; S. Gallach; M. Nuñez Abad; A. Blasco Cordellat; F.D.A. Aparisi Aparisi; E. Serna; J.M. Paramio; E. Jantus-Lewintre; C.J. Camps Herrero.

“Exosomes in NSCLC as a new tool for biomarkers searching”.

V Simposio de Biopsia Líquida. Oral communication. Santiago de Compostela, Galicia, España. 2020. Instituto de Investigación Sanitaria de Santiago de Compostela (IDIS).

Elena Durendez-Saez; Silvia Calabuig-Fariñas; Cristian Suarez; Marais Mosqueda; Alexandre de la Fuente; Laura Muinelo-Romay; Eva Serna; Jesus M. Paramio; Eloisa Jantus-Lewintre; Carlos Camps Herrero.

“Exosomes as a valuable tool for biomarkers searching in NSCLC”.

II Encuentro de Jóvenes Investigadores. Poster. Madrid, España. 2019. CIBERONC

Elena Durendez-Saez; Silvia Calabuig-Fariñas; Cristian Suarez; Marais Mosqueda; Alexandre de la Fuente; Laura Muinelo-Romay; Eva Serna; Jesús M. Paramio; Eloisa Jantus-Lewintre; Carlos Camps.

“Exosomes as a valuable tool for biomarkers searching in NSCLC”.

13th Congress on Lung Cancer. Poster. 2019. Grupo Español de Cancer de Pulmón. Valencia, España.

Elena Durendez-Saez; Silvia Calabuig-Fariñas; Cristian Suarez; Marais Mosqueda; Alexandre de la Fuente; Laura Muinelo-Romay; Eva Serna; Jesús M. Paramio; Eloisa Jantus-Lewintre; Carlos Camps.

“Exosomes in NSCLC: a valuable tool for the search of biomarkers”.

5th GEIVEX Symposium. Oral communication. Granada, España. 2019. Grupo Español de Innovación e Investigación en Vesículas Extracelulares (GEIVEX).

Annexes

Elena Durendez-Saez; Silvia Calabuig-Fariñas; Cristian Suarez; Marais Mosqueda; Andrea Moreno; Ernesto de la Cueva; Eva Serna; Jesus M. Paramio; Eloisa Jantus-Lewintre; Carlos Camps Herrero.

“Exosomas en cáncer de pulmón no microcítico como herramienta para la búsqueda de biomarcadores”. Congreso SEOM 2019. Poster. 2019. Sociedad Española de Oncología Médica (SEOM). Pamplona, España

Elena Duréndez Sáez; Silvia Calabuig Fariñas; Cristian Suarez Cabrera; Marais Mosqueda; Andrea Moreno Manuel; Ernesto de la Cueva; Eva Serna; Jesús M Paramio González; Eloisa Jantus Lewintre; Carlos Camps Herrero.

“Exosomes in NSCLC as a source of biomarkers”. ESMO CONGRESS 2019. Poster. Barcelona, España. 2019. European Society of Medical Oncology (ESMO)

E. Duréndez; S. Calabuig-Fariñas; C. Suarez; M. Mosqueda; A. Moreno-Manuel; S. Torres Martinez; A. Herreros Pomares; S. Gallach; E. Escorihuela; E. de la Cueva; A. Martinez-Romero; E. Serna; J.M. Paramio; E. Jantus-Lewintre; C.J. Camps Herrero.

“Exosomes in NSCLC: Analysis of its cargo as a source of biomarkers”. European Lung Cancer Congress (ELCC). Poster. Ginebra, Suiza. 2019.

Elena Duréndez-Sáez; Silvia Calabuig-Fariñas; Cristian Suarez; Marais Mosqueda; Sandra Gallach; Eva Escorihuela; Andrea Moreno; Ning Dong; Alejandro Herreros-Pomares; Ernesto de la Cueva; Alicia Martínez-Romero; Eva Serna; Jesús M Paramio; Eloísa Jantus-Lewintre; Carlos Camps."Annals of Oncology 30 (Supplement_2)".

“Exosomes in NSCLC: a valuable tool for the search of biomarkers”. II Valencian Vesicles Workshop (Valensicles). Poster. Valencia, España. 2019

E. Duréndez; S. Calabuig-Fariñas; C. Suarez; M. Mosqueda; A. Moreno-Manuel; S. Torres Martinez; A. Herreros Pomares; S. Gallach; E. Escorihuela; E. de la Cueva; A. Martinez-Romero; E. Serna; J.M. Paramio; E. Jantus-Lewintre; C. Camps Herrero.

“Exosomes in NSCLC: study of its cargo for the search of biomarkers”. IV Simposio Biopsia Líquida.Poster. Santiago de Compostela, España. 2019

Annexes

Duréndez, Elena; Calabuig, Silvia; Suarez, Cristian; Mosqueda, Marais; Gallach, Sandra; de la Cueva, Ernesto; Serna, Eva; Paramio, Jesús M; Jantus, Eloisa; Camps, Carlos.

“Study of exosomes in NSCLC for biomarkers searching”. 2019 World Conference on Lung Cancer. Oral communication. Barcelona, España. 2019. IASLC (International Association for the Study of Lung Cancer).

E. Durendez-Saez; S. Calabuig-Fariñas; C. Suarez; M. Mosqueda; S. Gallach; E. Escorihuela; A. Moreno; S. Torres; A. Herreros-Pomares; Á. González; E. De La Cueva; E. Serna; J. Paramio; E. Jantus Lewintre; C. Camps.

“Exosomal miRNA profile in NSCLC: differential cargo between 2D and 3D cultures”. 16th ASEICA International Congress. Oral communication. Valencia, España. 2018
Elena Duréndez-Sáez; Silvia Calabuig-Fariñas; Cristian Suarez; Marais Mosqueda; Sandra Gallach; Ernesto de la Cueva; Alicia Martínez-Romero; Jesús M Paramio; Eloisa Jantus-Lewintre; Carlos Camps.

D. AWARDS

- Primer Premio Mejor Comunicación Oral en el X Educational Symposim of the Spanish Lung Cancer Group. Grupo Español de Cancer de Pulmón. 2020.
- Premio Mejor Comunicación Oral en el V Simposio de Biopsia Líquida Instituto de Investigación Sanitaria de Santiago de Compostela (IDIS). 2020.

E. PUBLICATIONS

“Soluble galectin-3 as a microenvironment-relevant immunoregulator with prognostic and predictive value in lung adenocarcinoma”. Susana Torres-Martínez; Silvia Calabuig-Fariñas; Andrea Moreno-Manuel; Giulia Bertolini; Alejandro Herreros-Pomares; Eva Escorihuela; Elena Duréndez-Saéz; Ricardo Guijarro; Ana Blasco; Luca Roz; Carlos Camps; Eloisa Jantus-Lewintre. *Molecular Oncology* (John Wiley). 2023. ISSN 1574-7891. DOI: 10.1002/1878-0261.13505.

“Analysis of Exosomal Cargo Provides Accurate Clinical, Histologic and Mutational Information in Non-Small Cell Lung Cancer”. Duréndez-Sáez, E.; Calabuig-Fariñas, S.; Torres-Martínez, S.; Moreno-Manuel, A.; Herreros-Pomares, A.; Escorihuela, E.; Mosqueda, M.; Gallach, S.; Guijarro, R.; Serna, E.; Suárez-Cabrera, C.; Paramio, J.M.; Blasco, A.; Camps, C.; Jantus-Lewintre, E. *Cancers (Basel)* (MDPI). 2022; 14 - 13, pp. 3216.

“Analysis of the Gut Microbiota: An Emerging Source of Biomarkers for Immune Checkpoint Blockade Therapy in Non-Small Cell Lung Cancer”. Feiyu Zhang; Macarena Ferrero; Ning Dong; Giuseppe D'Auria; Mariana Reyes-Prieto; Alejandro Herreros-Pomares; Silvia Calabuig-Fariñas; Elena Duréndez; Francisco Aparisi; Ana Blasco; Clara García; Carlos Camps; Eloisa Jantus-Lewintre; Rafael Sirera. *Cancers (Basel)* (MDPI). 2021, 13 - 11, pp. 2514.

“Lung tumorspheres reveal cancer stem cell-like properties and a score with prognostic impact in resected non-small-cell lung cancer”. Herreros-Pomares A; de-Maya-Girones JD; Calabuig-Fariñas S; Lucas R; Martínez A; Pardo-Sánchez JM; Alonso S; Blasco A; Guijarro R; Martorell M; Escorihuela E; Chiara MD; Duréndez E; Gandía C; Forteza J; Sirera R; Jantus-Lewintre E; Farràs R; Camps C. *Cell Death & Disease (Nature)*. 2019; 10 - 9, pp. 660. ISSN 2041-4889

Annexes

“Exosomal microRNAs in non-small cell lung cancer”. E. Duréndez-Sáez; S. Torres; S. Calabuig-Fariñas; M. Meri-Abad; M. Ferrero-Gimeno; C. Camps. *Transl Cancer Res (AME)*. 2021; 10(6): 3128–3139. DOI: 10.21037/tcr-20-2815

“Extracellular vesicles as miRNA nano-shuttles: Dual role in tumor progression”. Pucci M; Reclusa Asiáin P; Duréndez Sáez E; Jantus-Lewintre E; Malarani M; Khan N; Fontana S; Naing A; Passiglia F; Raez LE; Rolfo C; Taverna S. *Targeted Oncology (EUROPE PMC)*. 2018, 13(2):175-187

“Exosomes as diagnostic and predictive biomarkers in lung cancer”. Reclusa P; Taverna S; Pucci M; Durendez E; Calabuig S; Manca P; Serrano MJ; Sorber L; Pauwels P; Russo A; Rolfo C. *J Thorac Dis (AME)*. 2017; 9(Suppl 13): S1373–S1382.

“Exosomes in semen: opportunities as a new tool in prostate cancer diagnosis”. Pucci M; Taverna S; Reclusa; Pinto JA; Durendez E; Jantus-Lewintre E; Mahafarin M; Zito G; Rolfo C. *Transl Cancer Res (AME)*. 2017;6(Suppl 8):S1331-S1333

“New insights in non-small-cell lung cancer: circulating tumor cells and cell-free DNA”. Duréndez-Sáez E; Azkárate A; Meri M; Calabuig-Fariñas S; Aguilar-Gallardo C; Blasco A; Jantus-Lewintre E; Camps C. *J Thorac Dis (AME)*. 2017; 9(Suppl 13): S1332–S1345.



Consorcio Hospital General Universitario de Valencia

Comité Ético de Investigación Clínica

APROBACIÓN PROYECTOS DE INVESTIGACIÓN

- ANEXO 11 -

Este CEIm tras evaluar en su reunión de 29 de Junio de 2017 el Proyecto de Investigación:

Título:	Biopsia líquida en cáncer de pulmón no microcítico análisis molecular de los exosomas para la búsqueda de biomarcadores		
I.P.:	Silvia Calabuig Fariñas	Servicio/Unidad	Laboratorio Oncología Molecular

Acuerda respecto a esta documentación:

Que se cumplen los requisitos éticos y metodológicos y la Hoja de Información al Paciente y Consentimiento Informado presentado reúnen las condiciones exigidas por este CEIC, por tanto se decide su APROBACIÓN.

COMPOSICIÓN DEL CEIm

Presidenta:

Dra. Elena Rubio Gomis (Unidad de Farmacología Clínica)

Vocales:

Dr. Ernesto Bataller Alonso (Gerencia del CHGUV)
 Dr. Alberto Berenguer Jofresa (Servicio de Cardiología)
 Dra. Ana Blasco Cordellat (Servicio de Oncología)
 Dra. Pilar Blasco Segura (Servicio de Farmacia)
 Dr. Julio Cortijo Gimeno (Unidad de Docencia e Investigación)
 Dña. Encarna Domingo Cebrián (Servicio de Estomatología)
 Dña. María Teresa Jareño Roglán (Unidad de Reanimación Cardíaca)
 Dr. Gustavo Juan Samper (Servicio de Neumología)
 Dra. Goltzane Marcalda Benito (Servicio de Análisis Clínicos)
 Dr. Antonio Martorell Aragonés (Unidad de Alergología)
 Dr. Javier Milara Payá (Servicio de Farmacia)
 D. Alejandro Moner González (Gerencia CHGUV – Asesoría Jurídica)
 Dr. Enrique Ortega Gonzalez (Gerente CHGUV)
 Dr. Pedro Polo Martín (Pediatra Att Primaria)



Consorcio Hospital General Universitario de Valencia

Comité Ético de Investigación Clínica

Dr. Aurelio Quesada Dorador (Servicio de Cardiología)
Dra. M^a José Safont Aguilera (Servicio de Oncología)
Dña. Carmen Sarmiento Cabañes (Miembro independiente de la organización asistencial)

Secretario:

Dr. Elías Ruiz Rojo (Servicio de Farmacia – Atención Primaria)

El CEIm del Consorcio Hospital General Universitario de Valencia, cumple con las normas de BPC (CPMP/ICH/135/95) tanto en su composición como en sus procedimientos y con la legislación vigente que regula su funcionamiento, y que la composición del CEIm es la indicada en el anexo I, teniendo en cuenta que en el caso de que algún miembro participe en el ensayo o declare algún conflicto de interés no habrá participado en la evaluación ni en el dictamen de la solicitud de autorización del ensayo clínico

Lo que comunico a efectos oportunos:

Valencia a 03 de julio de 2017

Fdo. Dra Elena Rubio Gomis
(Presidenta CEIC CHGV)



CONSORCIO HOSPITAL GENERAL UNIVERSITARIO
DE VALENCIA
COMITÉ ÉTICO DE INVESTIGACIÓN CLÍNICA

Annexes



Consorcio Hospital General Universitario de Valencia

Comisión de Investigación

APROBACIÓN PROYECTO DE INVESTIGACIÓN

Esta Comisión tras evaluar en su reunión de 29 de Marzo de 2017 el Proyecto de Investigación:

Título:	Biopsia líquida en cáncer de pulmón no microcítico análisis molecular de los exosomas para la búsqueda de biomarcadores		
I.P.:	Silvia Calabuig Fariñas	Servicio/Unidad	Laboratorio Oncología Molecular

Acuerda respecto a esta documentación:

- Que cumple con los requisitos exigidos por esta Comisión para su realización, por tanto se decide su APROBACIÓN.

Los miembros que evaluaron esta documentación:

	Presente	Ausente	Disculpa
Presidente Dr. José Vte Bagan Sebastian	x		
Dr. Carlos Camps Herrero	x		
Dra. Goltzane Marcaida Benito			x
Dr. Carlos Sánchez Juan	X		
Dña. Anna Martí Monros	x		
Dr. Emilio López Alcina	x		
Dr. Rafael Paya Serrano	X		
Dr. Miguel Garcia del Toro	x		
Dr. Jose Luis Sanchez Carazo	x		
Dr. Francisco Ridocci Soriano	X		
Dra. Empar Lurbe Ferrer			x
Dª Amparo Muñoz Izquierdo	x		
Dra. Amparo Esteban Rebol	x		
Dr. Enrique Zapater Latorre	x		
Secretario Dra. Dolores Lopez Alarcón	x		

Lo que comunico a efectos oportunos a jueves,
30 de marzo de 2017:

Fdo. Dr. Jose vte Bagan Sebastian
Presidente de la Comisión de Investigación:



DOCUMENTO DE INFORMACION AL PACIENTE Y CONSENTIMIENTO INFORMADO

DONANTE: _____

ACERCA DE LA DONACIÓN VOLUNTARIA DE MUESTRAS BIOLÓGICAS PARA LÍNEAS DE INVESTIGACIÓN BIOMÉDICA OBTENIDAS EN EL CURSO DE PROCEDIMIENTOS QUIRÚRGICOS, TERAPÉUTICOS O DIAGNÓSTICOS.

LÍNEA DE INVESTIGACIÓN	Oncología Molecular
INVESTIGADOR PRINCIPAL	Dr. Carlos Camps
CENTRO	Servicio de Oncología Médica (SOM) del Consorcio Hospital General Universitario de Valencia (CHGUV) y Laboratorio de Oncología Molecular de la Fundación para la Investigación del Hospital General Universitario de Valencia (FIHGUUV)
EQUIPO INVESTIGADOR	Facultativos del SOM, personal de la Unidad de Investigación Clínica del SOM, y del laboratorio de Oncología Molecular, miembros de los servicios quirúrgicos involucrados (Cirugía Torácica, Cirugía General), facultativos del servicio de Anatomía Patológica.

1. DESCRIPCIÓN GENERAL: La línea de investigación de "Oncología Molecular" centra sus esfuerzos en la comprensión de la patogénesis de los eventos genéticos y moleculares implicados en el origen y la progresión del cáncer. Uno de los aspectos de mayor interés en esta línea de investigación es la búsqueda de biomarcadores que puedan ser usados en la clínica y ayuden a la individualización del tratamiento del cáncer.

PROPÓSITO DE LA LÍNEA DE INVESTIGACIÓN: Analizar en diferentes tipos de muestras, factores que puedan ser importantes en el diagnóstico, pronóstico y en la respuesta del cáncer a los tratamientos empleados, así como en la aparición de efectos tóxicos asociados a dichos tratamientos. Si bien la constitución genética de los seres humanos es muy similar, existen pequeñas diferencias entre las personas que, en algunos casos podrían asociarse con el desarrollo o evolución de diferentes enfermedades. Por otra parte, los tumores también presentan diferencias a nivel genético que necesitan seguir siendo estudiadas. Por lo tanto, para poder llevar a cabo esta línea de investigación, es necesario disponer de muestras biológicas para poder realizar estos estudios genéticos. También es necesario recoger datos sobre su historial médico para obtener información que pudiera tener relevancia para nuestros estudios.

2. IDENTIFICACIÓN Y DESCRIPCIÓN DEL PROCEDIMIENTO: Durante la intervención quirúrgica o la prueba diagnóstica a la que va a ser sometido en las instalaciones del CHGUV se tomarán muestras de sus tejidos y/o sangre. El procedimiento que se le propone consiste en donar voluntariamente una parte de la muestra biológica sobrante de la intervención o prueba a una colección de muestras que se usará con fines de investigación biomédica, que esto suponga ningún riesgo añadido para su salud ni comprometa el correcto diagnóstico y tratamiento de su enfermedad. También es posible que le recojamos muestras biológicas que no requieran un procedimiento invasivo, como orina, heces, saliva etc. o que el procedimiento de obtención sea mínimamente invasivo como una extracción de sangre. Las muestras que done se almacenarán en una colección de muestras que corresponden a una Línea de Investigación sobre Oncología Molecular, que se encuentra en las instalaciones de la FIHGUUV y que cumple con los requerimientos establecidos en la normativa vigente.

Sus muestras solo podrán ser utilizadas en proyectos de investigación avalados científicamente y que hayan sido evaluados y aprobados por el CEIC, en los que participen miembros del equipo investigador que forma parte de esta línea de investigación.

3. OBJETIVO: El Centro Sanitario en el que usted está siendo atendido/tratado, dispone de investigadores que desean recoger y almacenar sus muestras biológicas para poder realizar proyectos de investigación biomédica en el área de la Oncología. Los resultados de dichos proyectos de investigación pueden derivar en el descubrimiento de nuevos métodos para el mejor diagnóstico, pronóstico y tratamientos.



4. BENEFICIOS ESPERADOS: Por su participación no percibirá ninguna compensación económica o de otro tipo por las muestras donadas. Sin embargo, si las intervenciones que se pudieran realizar tuvieran éxito, podrían ayudar en el futuro a pacientes que tienen la misma enfermedad o padecen otras enfermedades similares.

Las muestras de los tejidos y/o sangre no serán vendidas o distribuidas a terceros con fines comerciales.

La donación de muestras no impedirá que usted o su familia puedan hacer uso de ellas siempre que estén disponibles, cuando por razones de salud puedan ser necesarias.

5. CONSECUENCIAS PREVISIBLES DE SU REALIZACIÓN: Sólo si usted lo desea, existe la posibilidad de que pueda ser contactado en el futuro para completar o actualizar la información con la que contamos relacionada con su enfermedad.

Es posible, que los estudios realizados sobre sus muestras aporten información relevante para su salud o la de sus familiares. Tiene derecho tanto a ser informado como a que no se le informe de los datos obtenidos en la investigación. A estos efectos se entenderá que no desea recibir tal información salvo que manifieste lo contrario, utilizando para ello el formulario que se adjunta al presente documento.

6. CONSECUENCIAS PREVISIBLES DE SU NO REALIZACIÓN Y DERECHO DE REVOCACIÓN DEL CONSENTIMIENTO. La decisión de donar muestras biológicas es totalmente voluntaria, pudiendo negarse a donarlas e incluso pudiendo revocar su consentimiento en cualquier momento, sin tener que dar ninguna explicación y sin que ello tenga ninguna repercusión en la atención médica que recibe en el Centro.

Si decidiera revocar el consentimiento que ahora presta, la parte de las muestras que no se hayan utilizado en la investigación, será destruida o anonimizada. Tales efectos, no se extenderán a los datos resultantes de las investigaciones que ya se han llevado a cabo una vez haya revocado su consentimiento.

7. RIESGOS. El procedimiento que se le propone no supone ningún riesgo añadido para su salud ni compromete el correcto diagnóstico y tratamiento de su enfermedad, puesto que se trata de muestras sobrantes de la intervención, muestras invasivas obtenidas durante los procedimientos de diagnóstico, o muestras de sangre extra que se han obtenido para ser utilizadas en investigación. En este último caso, la extracción de sangre, apenas tiene efectos secundarios, lo más frecuente es la aparición de pequeños hematomas en la zona de punción que desaparecen transcurridos 1 o 2 días. En el caso de las muestras que requieren procedimientos más complejos o invasivos, estos sólo se realizarán si forman parte del procedimiento habitual que debe realizarse para su correcto diagnóstico o tratamiento de su enfermedad.

8. PROTECCIÓN DE DATOS PERSONALES Y CONFIDENCIALIDAD. Sus datos personales y de salud serán incorporados y tratados en una base de datos de la que es responsable el Investigador del Proyecto, que debe estar inscrita en un registro nacional dependiente del Instituto de Salud Carlos III y que debe cumplir con todos los requisitos legales. Sólo el INVESTIGADOR RESPONSABLE podrá relacionar estos datos con usted, siendo responsable de custodiar el documento de consentimiento y de garantizar el cumplimiento de su voluntad en relación al uso de la muestra biológica que usted cede para investigación. La información será procesada durante el análisis de los datos obtenidos y aparecerá en los informes y/o memorias de los proyectos derivados de la Línea de Investigación, aunque en ningún caso será posible identificarle, asegurando en todo momento el cumplimiento de la Ley Orgánica 15/1999, de 13 de diciembre, de Protección de Datos de Carácter Personal.

La cesión de muestras así como de la información contenida en las bases de datos vinculadas a las mismas, solo se realizará si forman parte de la línea de investigación en la cual participan miembros del equipo investigador, realizándose un procedimiento de codificación previo, que consiste en desligar la información que le identifica sustituyéndola por un código.

Asimismo, el titular de los datos personales podrá ejercitar los derechos de acceso, rectificación, cancelación y oposición al tratamiento de datos de carácter personal, incluir alguna restricción sobre el uso de sus muestras, y ejercer los derechos de revocación del consentimiento (en este último caso, conforme al formulario que figura en el apartado 11) en los términos previstos en la normativa aplicable, dirigiendo al titular del centro el escrito correspondiente firmado por Ud. y copia de un documento acreditativo de su identidad.



9. DESTINO DE LAS MUESTRAS TRAS FINALIZACION DE LA LÍNEA DE INVESTIGACION. En el supuesto de finalización de la línea de investigación, es posible que existan muestras sobrantes. En relación a las mismas, se le ofrecen las siguientes opciones: a) la destrucción de la muestra sobrante, b) su utilización en otros proyectos de investigación biomédica, para lo cual, se le ofrece la opción de donar la muestra excedente al Biobanco del CHGUV (en el siguiente apartado le explicamos de manera resumida en que consiste un biobanco y cuáles son sus objetivos). En este caso, deberá marcar esta opción en el consentimiento incluido en este documento. En dicho consentimiento usted podrá escoger si desea que esta donación se haga codificada de forma que usted pueda conocer si lo desea los resultados de las investigaciones que se lleven a cabo, o anonimizada, si usted prefiere que nunca nadie pueda recobrar la relación entre sus muestras y su persona.

10. BIOBANCO. DEFINICIÓN Y OBJETIVOS. El Biobanco del CHGUV es un establecimiento público, sin ánimo de lucro, que acoge una colección organizada de muestras biológicas. Estas muestras almacenadas en el biobanco, tienen por finalidad ser utilizadas en proyectos de investigación biomédica que hayan sido aprobados por los comités ético y científico a los que esté adscrito el biobanco. Los resultados de las investigaciones realizadas con estas muestras pueden derivar en el descubrimiento de nuevos métodos para el mejor diagnóstico de las enfermedades o en nuevas formas de tratamientos de las mismas. Sus muestras seguirán almacenadas en el biobanco hasta el fin de las existencias si no existe una revocación del presente consentimiento.



11. DECLARACIONES Y FIRMAS.

Declaración del donante:

D./Dña _____ de _____ años de edad, con domicilio en _____ DNI _____ y nº de SIP _____

D./Dña _____ de _____ años de edad, con domicilio en _____ DNI _____ en calidad de representante (en caso de minoría legal o incapacidad) del paciente _____ con DNI _____ y nº de SIP _____

DECLARO

Que he sido informado por el profesional de salud abajo firmante:

- Sobre las ventajas e inconvenientes del procedimiento
- Sobre el lugar de obtención, almacenamiento y proceso que sufrirán los datos personales y las muestras.
- Que mis muestras y datos personales serán tratados de acuerdo a la legislación vigente.
- Que en cualquier momento puedo revocar mi consentimiento y solicitar la eliminación o anonimización de todos mis datos personales y muestras que permanezcan almacenadas. Esta eliminación no se extendería a los datos resultantes de las investigaciones que ya se hubieran llevado a cabo
- Que en cualquier momento, yo, mi representante legal, o tutor, de conformidad con lo establecido en el artículo 4, punto 5 de la Ley 14/2007, de 3 de Julio, puedo solicitar información sobre los datos que se obtengan a partir del análisis de las muestras donadas.
- Que he comprendido la información recibida y he podido formular todas las preguntas que he creído oportunas

CONSIENTO

- Que el CHGUV y la FIHUV, a través de los miembros del equipo investigador de la Línea de Investigación: "Oncología Molecular", utilicen mis datos y las muestras, incluyendo la información sobre mi salud, para investigaciones biomédicas dentro del marco de la línea de investigación antes mencionada, manteniendo siempre la confidencialidad de mis datos.
- Libre y voluntariamente en la donación voluntaria de: (márquese con una cruz lo que proceda)

<input type="checkbox"/> Mis tejidos excedentarios	<input type="checkbox"/> Muestra de heces, orina o saliva
<input type="checkbox"/> Muestra de sangre	<input type="checkbox"/> Muestras obtenidas en procedimientos que sean necesario para el diagnóstico)
- Yo, mi representante legal o tutor, accedo (márquese sí o no) a que los miembros del equipo investigador puedan contactarme en el futuro en el caso de que se estime oportuno añadir nuevos datos a los recogidos.

<input type="checkbox"/> Sí
<input type="checkbox"/> No
- Que en el supuesto de finalización de la línea de investigación, mis muestras sean (márquese con una cruz lo que proceda)

<input type="checkbox"/> destruidas
<input type="checkbox"/> cedidas al Biobanco del CHGUV y anonimizadas
<input type="checkbox"/> cedidas al Biobanco del CHGUV codificada, junto a los datos clínicos asociados.

D. Dña : _____ FIRMA: _____

En _____, a _____ de _____ de 20____

DECLARACIÓN DEL PROFESIONAL DE SALUD:

He informado debidamente al donante:

Nombre facultativo: _____ DNI _____ Colegiado Nº _____

FIRMA : _____

En _____, a _____ de _____ de 20____



12. REVOCACIÓN DEL CONSENTIMIENTO.

Yo, D./Dña _____, con DNI _____ revoco el consentimiento prestado en fecha _____ de _____ de 20_____ y no deseo proseguir la donación voluntaria, que doy con esta fecha por finalizada.

Fdo: _____

En _____, a _____ de _____ de 20_____

Yo, D./Dña _____, con DNI _____ como representante legal de D./ Dña _____, con DNI _____ revoco el consentimiento prestado en fecha _____ de _____ de 20_____ y no deseo proseguir la donación voluntaria, que doy con esta fecha por finalizada.

Fdo: _____

En _____, a _____ de _____ de 20_____

Annexes



SOLICITUD DE INFORMACION DE DATOS O RESULTADOS DERIVADOS DE LAS INVESTIGACIONES

LÍNEA DE INVESTIGACIÓN	Oncología Molecular
------------------------	---------------------

PACIENTE: _____

D./Dña _____, de ____ años de edad, con domicilio en _____, DNI _____ y nº de SIP _____
D./Dña _____, de ____ años de edad, con domicilio en _____, DNI _____ _____ en calidad de representante (en caso de minoría legal o incapacidad) del paciente _____, con DNI _____ y nº de SIP _____

SOLICITO

Ser informado/a del resultado de las investigaciones realizadas con la/las muestra/s donada/s de manera voluntaria en fecha _____ de _____ de 20____ si éstas afectan a mi salud o a la de mi representado.

Fdo.: _____

En _____, a _____ de _____ de 20____